SNOW AVALANCHE RELEASE

A thesis presented for the degree of doctor of philosophy in Chemical engineering in the University of Canterbury.

By

Howard Conway

1985.

ABSTRACT.

Avalanche occurrence is closely related to the local meteorological conditions which may be quite variable in mountain topography. To investigate these conditions, and to provide information for avalanche forecasting, we designed and built a weather station which is currently relaying information to a base station from a remote site.

Most field tests of snow do not adequately describe the engineering properties. In this study, we wanted to design some tests which would measure such properties and also provide an estimate of snow slope stability.

Our tests of shear and tensile strength of snow were designed to simulate as closely as possible conditions expected in a naturally occurring snow slab, and were made in-situ using large samples. We describe several sets of measurements made across crownwalls after avalanche release. Such measurements typically showed considerable spatial variability and in 4 cases out of 5, a probabilistic approach combined with a simple force balance provided a satisfactory indication of the likelihood of failure. From the results of this analysis, we proposed a new field test to estimate stability. This test requires only a snow saw and is simple and quick to complete.

It is well known that the strength of materials depends on strain-rate, and we made some measurements using a strain gauge in conjunction with the simple field tests. Although the rates applicable during snow avalanche release are uncertain, investigations of such properties provides an insight into release mechanisms.

A device to measure air permeability of snow in the field was designed and built. Results from measurements showed that air permeability gave a good measure of snow structure which is related to stength.

We think most of the variability of snow strength originates from air-flow patterns above the slope during storms, and further studies concerning these patterns could define the location of weak zones within a snow pack. Such information would enhance understanding of release mechanisms, and also improve avalanche forecasts.

TABLE OF CONTENTS.

ACKNOWLEDGEMENTS.

Almost all the papers and reports resulting from this study are jointly authored and this is a reflection of the support I have had from many people.

Of particular note is the support of John Abrahamson who firstly accepted the supervision of the project, and has since provided positive encouragement and ideas. I am particularly grateful to John for his perspective throughout the study.

All of the technical staff of the Chemical and Process Engineering department have at some stage been involved in building equipment, and although much of it did not operate for very long, it was through no fault of the manufacturing. The continued operation of the weather station particularly is a reflection of the skill of the staff, and also Peter Squires who with Warwick Earl and Gordon Grey designed the telemetry link.

Friends who assisted with field measurements and made the whole project possible include: Martin Heine, Lisle Irwin, Barrie Thomas, Teabags, Ray Slater, Rob Young, Bert Youngman, Digger Blue and Whist - the dirty dogs quit early, Ding, Jane Pearson, Bob Munroe, Colin and Betty Monteath, Jos Lang, Stu Allan, Suzie Snowpit, Kevin Bochault, and Kem Johnstone. To all these people and many others who helped along the way - thanks. Thanks too to Tasman saddle hut who often provided shelter from a storm.

The Department of Lands and Survey (Wellington, New Zealand), University of Canterbury (Christchurch, New Zealand), Mountain Safety Council of New Zealand, and the Mt. Hutt Ski Company provided financial support for the study. Mt. Cook Airlines provided transport to the field area, and assistance from Mt. Cook National Park staff was invaluable. We are grateful to all these people for their assistance.

1.1 INTRODUCTION.

Perla (1980) reported that in North America, approximately 10000 avalanches are reported annually to the US Forest Service, but only about 1% of these cause structural damage or casualties. Charlie Douglas, an early explorer in New Zealand was quoted as saying: ".... avalanches are like wild pigs - they are only dangerous if you foolishly get in their road.....".

In New Zealand, approximately one half of the total land area is above tree-line in elevation, and the mountain areas are increasingly used for recreation. Clearly, the interaction of people and mountains poses a threat to people from avalanches, and there is an increasing demand for safety from this hazard both in this country and in any mountainous country (see for example Conway,1983b and Dingwall,1976).

Although avalanche frequency decreases rapidly with increasing avalanche size, relatively small avalanches triggered by people are the cause of most avalanche casualties. An avalanche starts in the so called fracture or starting zone. The amount of fractured snow (ie.the total volume given by the fracture depth and fracture area) is directly related to the destructive power and area of influence of the avalanche. Often the area of fractures at a particular location is fairly uniform from one event to the next because the surrounding topography and geometry control the snow distribution. The change with time in the destructive power of a particular slide path therefore depends on the fracture depth of each event (Salm, [Buser et al., 1985]). After flowing through the so called avalanche-path or track, the avalanche comes to rest in the relatively flat terrain of the run-out zone.

In a snowpack, homogeneous snow exists in layers originating from uniform snowfall periods. The individual layers have different physical and mechanical properties, depending largely on a variety of meteorological conditions at the time of deposition. The layering results in discontinuities in snow properties, and the interfaces between

individual layers, or between the ground and a layer, play an important part in snow stability, (Conway,1983a, Salm,[Buser et al.,1985]). Perla (1980) described a potential slab avalanche as a relatively stiff slab of snow overlying a weak layer (or weak interface between layers).

In general terms, avalanche forecasting is closely related to weather forecasting, but release mechanisms for individual avalanches are still unclear. The main focus of this study has been directed towards understanding the release mechanisms for individual avalanches, and in particular, we have attempted to provide some guidelines for field measurements in assessing snowslope stability.

As previously mentioned, the most common method of avalanche forecasting is to interpret snow stability from past and future weather expectations. This is also the most indirect type of observation, and is further complicated by mountain topography causing "local" weather conditions which may be significantly different from the overall weather pattern. One aspect of our work has been to develop and build a weather station which can be located at remote sites and transmit weather information to a base station. We have located such a weather station at the head of the Tasman glacier (2320m asl) in the Mount Cook National Park, and information about windspeed, wind direction, air temperatures and snow accumulation is transmitted to the Mount Cook village some 35kms away. This information provides a powerful input to the avalanche forecast which is compiled daily at the Park Headquarters.

In an effort to understand bonding mechanisms, snow structure and time dependent properties of snow, we built four instruments:

(a) simple shear and tensile testing equipment.

(b) an air permeability device which we found gave a good indication of snow crystal structure. We are still unclear how this measurement relates to snow strength (see Conway and Abrahamson,1982b,1984b).

(c) a tensile testing device in which we froze two end

plates to a sample of snow and applied traction across the sample. We could also measure strain and a good estimate of strain-rate across a sample with this instrument (Conway and Abrahamson,1982a).

(d) a strain gauge designed to be used in conjunction with the simple shear tests (described by Conway and Abrahamson,1984c) and which gave a measure of shear strains across a snow sample.

These instruments are described in more detail in subsequent sections.

The most direct method of predicting avalanches involves measurements related to mechanical strength. In order to provide some guidelines for field observations regarding snowslope stability we developed field tests which measured shear and tensile strengths in a way which we thought simulated conditions in a snowpack (see Conway and Abrahamson,1982a,1983,1984a). We have made these types of measurements across and down the boundaries of some avalanched slopes (often slopes we had released ourselves), at the head of the Tasman glacier.

Because only a few tens of measurements of various snow parameters (in particular those related to strength) can be made in a practical time, and because there is an inherent variation in the measured values, we have chosen to model a snowslope by applying probability theory to a capacity/demand (or limit equilibrium) approach. By using simplified models, we can relate the measurements made in the field to slope stability. These methods and models are discussed more fully in a subsequent section and also in Conway and Abrahamson (1985).

We think wind transport and wind deposition of snow may cause much of the variability of strength we have measured in snowpacks. Section 4 includes some measurements and observations of wind-affected-snow and suggests how they might relate to snow strength properties.

During studies at Mount Cook, we recorded snowpit stratigraphy (including crystal type, hardness, particle diameter, snow temperatures and density) at many sites and some of these are summarised in the appendices. Because neither the mechanics of metamorphic processes nor the dependence of snow strength on snow morphology are known quantitatively, these measurements are only indirectly useful in assessing snowslope stability. Also recorded in the appendices are some of our reports and papers resulting from the study.

1.2 REFERENCES.

Buser, O., Fohn, P., Good, W., Gubler,H., and Salm, B.:(1985) "Different methods for the assessment of avalanche danger". Cold Regions Science and Technology, Vol.10, p199-218.

*Conway, H.:(1983a) "Mountain avalanche forecasting using meteorological data from Mount Cook village". Unpublished report.

Conway, H.:(1983b) "Aspects of avalanche forecasting in New Zealand". New Zealand Alpine Journal, Vol.36, p164-69.

Conway, H. and Abrahamson, J.:(1982a) "Insitu tests of large volumes of snow". Unpublished report.

*Conway, H. and Abrahamson, J.:(1982b) "Air permeability as a measure of snow structure". Unpublished report.

*Conway, H. and Abrahamson, J.:(1983) "A summary of weather and snow conditions at the Tasman saddle area during the winters of 1980-1982". Unpublished report.

*Conway, H. and Abrahamson, J.:(1984a) "Snow stability index". Journal of Glaciology, Vol.30, No.106, p321-327.

*Conway, H. and Abrahamson, J.:(1984b) "Air permeability as a textural indicator of snow". Journal of Glaciology, Vol.30, No.106, p328-333.

*Conway, H. and Abrahamson, J.:(1984c) "Snow and avalanche research at Tasman saddle - a progress report of the winter 1984.

*Conway, H. and Abrahamson, J.:(1985) "Snow slope stablity - a probabilistic approach". Submitted to Journal of Glaciology.

Dingwall, P.R.:(1976) "Coping with the avalanche hazard in New Zealand". New Zealand Alpine Journal, Vol.29, p77-83.

Perla, R.I.:(1980) "Avalanche release motion and impact". In Dynamics of Snow and Ice Masses, (S.Colbeck, ed.), chapter 7, p397 -462, Academic Press, New York.

*Young, R., and Conway, H.,:(1983) "Comparisons of weather between the Tasman saddle area and Mount Cook village - winter 1983". Unpublished report.

* References marked thus are included in the appendices of this thesis.

2.1 INTERPRETATION OF SNOW STABILITY FROM METEOROLOGICAL CONDITIONS.

Snow stability is directly related to past and present meteorological conditions, and often avalanche forecasts are formulated by combining this past information with future weather forecasts. Buser et al.(1985) reviewed different methods for the assessment of avalanche danger and emphasised the problems of attempting to forecast avalanche occurrence using weather forecasts. Weather is strongly influenced by topography, and so mountains will cause weather conditions to vary considerably both with time and location. This makes it difficult to forecast for specific locations from another location, especially as rapid changes of factors such as temperature, precipitation, wind speed and direction, may also occur during a storm affecting precipitation rates and crystal morphology. The added uncertainty of the relationship between snow strength and snow morphology is considered in a later section.

Young and Conway (1983) compared weather data recorded at the head of the Tasman glacier with that observed at Mount Cook village. They compared daily windruns, precipitation and temperatures and found poor correlation between the sets of data. Furthermore, Conway and Abrahamson (1983) for different locations on the Tasman neve, measured snow accumulation variation of factors up to 2.5 within an area of $100m^2$, depending mainly on the aspect of the slope and the prevailing wind direction. It is well known that mountain ridges cause uneven snow distribution (see for instance, Fohn and Meister,1983).

However, because snow avalanches commonly involve failure of the more recent snow layers, and typically occur in response to a storm period of heavy precipitation, snow stability assessment using meteorological data is a reasonable, although indirect method of general forecasting. Conway (1983a) noted that for a more specific assessment of slope stability, fairly continuous weather measurements recorded close to the avalanche starting zones would greatly

improve a forecast.

2.2 THE REMOTE WEATHER STATION.

To fulfill this requirement we designed and built a weather station. Several conditions were imposed on the design of the instrument:

(a) it needed to make measurements of meteorological data which could be used for avalanche forecasting, and allow immediate access of the data.

(b) it needed to be semi-portable for two reasons (1) access to the Tasman neve is generally by ski-equipped aircraft or helicopter, and so the weather station needed to be easily dismantled for transportation by these means; (2) because the Tasman neve is a zone of snow accumulation, periodically the weather station would need to be dug out of the snow and raised. Typically two people would be available for this task, so we required that the instrument be capable of being shifted at least short distances by two people.

(c) it needed to be robustly built to withstand extreme weather conditions such as temperatures of -15°C, blowing snow, and hourly average wind-speeds of up to 180km/hr.

(d) it needed to be able to operate using a battery power supply.

(e) it needed to have low cost.

We mounted the weather recording instruments on a tripod made from 50mm diameter aluminium tubing. Each leg could be unscrewed into two sections, each 1.5m long and a 400mm diam plate was attached at the base of each leg to anchor the tripod base to the snow (see plate 1).

Air temperature was measured by a downward pointing thermocouple. We found it necessary to shield the thermocouple from heating by radiation, and so the thermocouple was mounted within a white open ended double tube, which also allowed free air circulation. This double tube also swung on a bearing about the thermocouple, with a vane to align it with the wind.

Plate 1: The weather station at Tasman Saddle.

In order to make measurements of new snow depth increments, we adapted a Polaroid ultrasonic rangefinder. The modifications and design of the instrument are descibed by Earl et al.(1985). By mounting the instrument at the top of the tripod we could measure the distance to the snow surface. During times of storms or blowing snow, a scatter of data was recorded either because of reflection of the signal off drifting snow between the sensor and the ground, or because the wind increased the length of the signal path. The scatter enabled us to determine the duration of the storm, and at the end, a measure the new increment of snow was available. It is possible that further information such as fluctuations in transport rates could be obtained from the scatter of the depth data during storms.

Windspeed was measured using a robust Munroe cup anemometer which gave an electrical count. We designed and built a wind direction vane which was mounted on a viscous damped oil bearing within 16 reed switches arranged to give a step-wise resistance read-out.

A 12 volt lead acid battery with high specific gravity acid was used as a power supply and kept charged with a solar panel capable of charging about 600mA at 16v. Because the instrument shuts down between transmissions, this power supply has been found to be sufficient.

Initially the information was recorded on a small data logger (built by Solid State Equipment Ltd., NZ), which was left at the tripod. This was unsatisfactory for several reasons: (a) the information was only available after the data had been retrieved from the memory (using a magnetic tape at the site) and then processed on a computer in Christchurch. This meant the information was not readily available each day; (b) the data records were often not continuous, and we suspect that either static electricity (which is common during conditions of blowing snow) erased the memory of the data logger, or the retrieval of the data onto the tape was not satisfactory.

For the winter of 1985, a telemetry system capable of transmitting via the normal voice-link radio network already installed throughout the Mount Cook Park, was designed by Peter Squires (Department of Electrical Engineering, University of Canterbury), and this enabled transmission of the data to the Mount Cook village. The information at present is recorded on hard copy and used for input for the local avalanche forecast which is compiled daily. The information is also relayed daily to the Meteorological department at Christchurch airport and used by Mt. Cook Airlines for assessing flying conditions. The station can be programmed from the base to transmit at intervals varying from 1 to 60min but the faster rate of transmissions may be limited by the available power supply.

Further refinements to the weather station might include:

(a) storage of the data on a disc at the base station to enable further processing and analysis of the data.

(b) other instrumentation such as humidity, solar radiation, or a measure of snow drifting rates may be useful.

(c) a measure of the minute by minute fluctuations or standard deviations associated with each measurement would be valuable.

(d) although icing and riming of the instrument is not a bad problem at the Tasman neve location, at some locations this could be a problem. The usual way of de-icing is by providing propane, electrical heaters or using an anti-freeze fluid.

All of these modifications would add to the power requirements and cost of the instrument.

2.3 REFERENCES.

Buser, O., Fohn, P., Good, W., Gubler,H., and Salm, B.:(1985) "Different methods for the assessment of avalanche danger". Cold Regions Science and Technology, Vol.10, p199-218.

*Conway, H.:(1983a) "Mountain avalanche forecasting using meteorological data from Mount Cook village". Unpublished report.

*Conway, H. and Abrahamson, J.:(1983) "A summary of weather and snow conditions at the Tasman saddle area during the winters of 1980-1982". Unpublished report.

*Earl, W.M., Grey, G.R., Conway, H. and Abrahamson, J.:(1985) "Remote sensing of snow accumulation". Cold Regions Science and Technology, Vol.11, p199-202.

Fohn, P.M.B. and Meister, R.:(1983) "Distribution of snow drifts on ridge slopes: measurements and theoretical approximations". Annals of Glaciology, Vol.4, p52-57.

*Young, R., and Conway, H.:(1983) "Comparisons of weather between the Tasman saddle area and Mount Cook village - winter 1983". Unpublished report.

* References marked thus are included in the appendices

3. MECHANICAL PROPERTIES OF SNOW.

3.1 INTRODUCTION.

For understanding avalanche release mechanisms, we are particularly interested in those properties of snow which might be related to snow strength and, for practical use, those which can be easily measured in the field.

On a microscopic scale, these properties can be characterised by snow grains (shape, dimensions, orientation of the crystals), the mean number of bonds per grain, and the spatial arrangement of chains formed by several grains. Measurements commonly made in the field include snow depths, density, relative hardness, snow temperatures, grain diameter and type, and an assessment of the degree of bonding between, as well as within, layers.

LaChapelle and Ferguson (1980) gathered snowpit information from various locations, and then asked several different avalanche forecasters to make an interpretation of the snow stability. Their study emphasised the subjective nature of stability assessment, and they suggested that a better quantitative definition of the parameters related to snow stability would improve stability evaluation. Most techniques developed recently to describe snow structure rely on thin section analysis. For example, methods developed by Good (1975) and Kry (1975a,1975b) provide an insight into bonding mechanisms and snow structure but are difficult to perform in the field. One measure which can quantify snow structure somewhat is that of air permeability. We designed and built an air permeability device for use in the field which is discussed later.

Sommerfeld (1973,1974,1980) and Gubler (1978a,1978b) described snow strength using statistical models by considering the snow bonds to consist of either (a) elements of force conducting material in series (Weibull theory) or (b) elements in parallel (Daniels theory). For snow Sommerfeld suggested that a combination of these models would be realistic, and he applied the models to interpret snow slab

properties (in particular strengths) from strength tests made on small samples. We wanted to make strength measurements in the field on relatively large samples of snow with minimum sample disturbance. We also wanted to simulate as closely as possible the stress conditions which occur in the snowpack. Our tests are described later in this section.

3.2 POWDER MODELS AND APPLICATIONS TO SNOW.

Bonding forces acting between contacting particles cause cohesive behaviour of solid materials. Molerus (1982) described the simplest model for a cohesive material. If a sample is subjected to a sliding stress S, and normal stress σ, over an area A, then for slip within the material (assuming Coulomb friction), the limiting equation is:

$$\mu = \tan\rho = S/(\sigma+T_0) \qquad (1)$$

for the coefficient of friction μ and the angle of friction ρ respectively. T_0 is the isostatic tensile force and represents the cohesive forces acting at the contacts of the powder when it is unconsolidated.

Combination of the slip equation (eqn.1) with the Mohr circle representation of stress, yields the condition that slip will occur if the largest Mohr circle touches the yield locus.

Often the cohesive forces T_0 are not constant but depend on the previous compressive normal force. The behaviour of a bulk powder can be described by three parameters: (a)the adhesive force T_0 at the contacts in an unconsolidated powder, (b)a constant κ, which describes the increase in adhesive forces between particles due to consolidation, and (c)the angle of internal friction ρ, which describes the frictional behaviour at inter particle contacts. A family of yield loci can be experimentally derived at different consolidation forces for a particular powder.

Under normal conditions, particularly for fine-grained materials, van der Waals forces dominate bonding between particles. However, several other factors may contribute to the adhesive forces (Molerus, 1982): (1) solid or liquid bridges in the powder, (2) sintering at temperatures close to

the melting point of the material, (3) electrostatic forces.

The different bonding mechanisms and the fact that the shear may not be strictly according to the Coulomb approximation (there also may be bulk volume changes see fig. 3.1), cause the yield locus to be non-linear for most materials. Furthermore, it is easy to see how conditions within a powder may change with time and the yield locus can be thought of as time dependent. Non linearity of the yield locus for snow was particularly evident in the measurements made by Haefeli [Bader et al.,1954]. Many laboratory studies note the change of strength of snow with time and also changes of characteristics with test rate during the experiment (for example, Singh and Smith,1980 and Narita,1980,1983 making tensile tests, and McClung,1977 and de Montmollin,1982 making shear tests). Most snow is relatively compressible and close to its melting point so such behaviour is not unexpected.

Pure coulomb friction without volume change.

Homogeneous shearing throughout the sample.

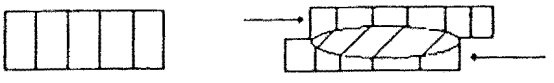

A combination of coulomb friction and volume changes.

Figure 3.1. Idealised shear behaviour in granular materials.

It is well known that the strength of a material of the same chemical composition increases as the grain size decreases. Load is transmitted through bonds between grains, and the number of contacts between grains increases for materials of smaller size. Perla and Martinelli (1976) also note that snow consisting of large sized crystals fails more easily than snow consisting of small sized crystals .

3.3 THE AIR PERMEABILITY DEVICE.

Measurements of air permeability of snow were first made by Bader [Bader et al.,1954]. He thought because air permeability was related to the void space and structure, it might give an unambiguous measure of some snow properties. We also thought it might be well correlated with tensile strength and strain history so we designed and built two air permeability devices. These two devices together with our measurements are discussed fully in Conway and Abrahamson (1982b,1984b). In these papers we concluded that air permeability gave a useful indication of snow texture, but the relationship with our strength measurements was less clear. In general terms, we found that a decrease of air permeability over a period of time on similar snows was a stabilizing trend (due to formation of bonds and a tendency to equilibrium crystal forms), and an increase of air permeability over a period of time was indicative of decreasing stability (either due to bond elongation and stretching from tensile strain, and/or kinetic growth of crystals).

3.4 SHEAR TESTS - STRAIN SOFTENING OF MATERIALS.

Schwedes (1975) noted that most shear tests made on materials are a combination of: (a) pure Coulomb friction with no volume change; (b) homogeneous shear which occurs throughout the sample together with volumetric changes (see fig.3.1).

Schwedes also showed using a tri-dimensional condition diagram (derived by Roscoe) that a "critical state" line exists which divides the states of a material into two regions: "looser than critical" - or unconsolidated, and "denser than critical" - or over consolidated. A shear stress

vs shear strain graph for the conditions is shown in fig.3.2.

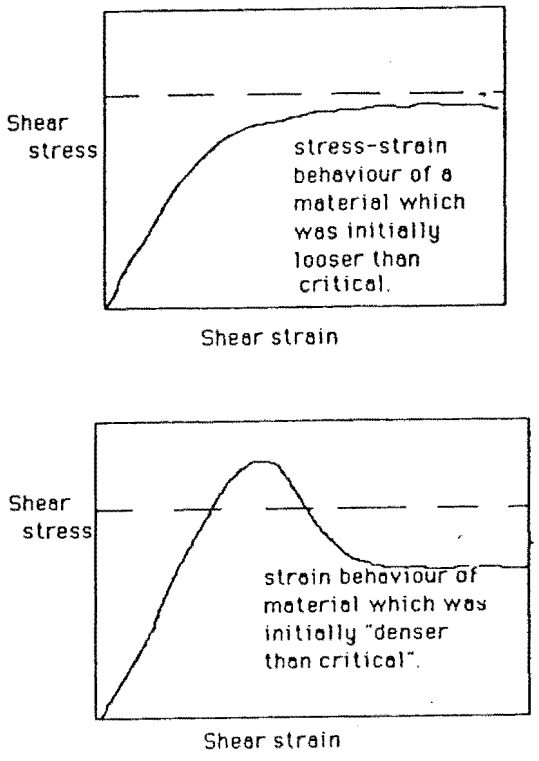

Figure 3.2
Shear stress-strain for different initial material conditions.

Roscoe (1970) summarized experimental investigations of soils noting that the void ratio in a sample changed dramatically with strain. If a material was more dense than critical, it expanded and then softened after a peak stress was reached. The ratio of the peak stress to the softened "residual" strength increased as the initial density of the sample increased. While the material existed in a condition between peak and critical states, it was unstable and would tend to fail in thin zones or bands. If a material was loose initially, it contracted up until the critical state line was reached and then the sample would continue to undergo shear distortion without further changes of density or stress.

Skempton (1985) suggested that the post peak drop in the shear strength of some (drained) over-consolidated soils could be thought of as occurring in two stages: (1) the drop to the critical state strength (with associated material dilatancy); (2) at larger displacements particles reorient and the

strength drops to a residual value.

Experiments by McClung (1977) showed that snow also could exhibit both types of behaviour, and suggested that the softening characteristics depended not only on whether the sample was initially more or less dense than critical but also on the rate of loading. We also measured such behaviour in tests of snow shear strength, and these measurements are recorded in Conway and Abrahamson (1984c).

Palmer and Rice (1973) first modelled the progression of a shear failure in a thin band by equating the gravitational work input from the slab when extending the band, with that required to deform the material in the slab plus the frictional losses. McClung (1979a) applied these fracture models to snow, and although he did not deal with the initiation of the shear fracture, he showed how a failure might progress at stresses less than peak values. We think these concepts are particularly important when considering failure progression through a snow slab (Conway and Abrahamson,1985). Some of our strain softening measurements as well as our simple shear tests are discussed later.

3.5 TENSILE TESTING.

The fracture face of a tensile fracture is not plane, but rather follows the surface of the particles where the forces of adhesion have been exceeded by the tensile stresses in the sample. These adhesive forces have different values at different elongations for almost every material, and for fine-grained particles, the ratio of the maxima of the force/elongation curves at different strains can be as much as 100:1.

Schubert (1975) outlined various models for tensile failure of materials with inter-particle forces at contact points. These models related tensile strength to factors such as density, porosity, particle surface area, inter-particle forces, particle diameter, and other form fitting parameters, many of which were difficult to measure and quantify. Materials which have other bonding mechanisms may require different models.

Two common methods of testing tensile strengths of powders are: (a) the adhesive method in which two end plates are bonded to the sample and then pulled apart; (b) the split plate or traction table method.

Of particular interest is the split-plate method of tensile testing because this method closely resembles conditions that might apply in a snow slab overlaying a thin weak layer (see fig.3.3).

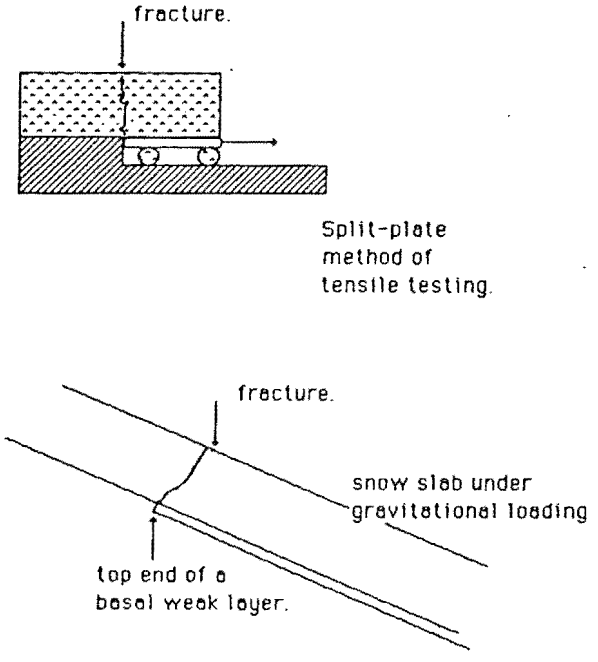

Figure 3.3

Split-plate method of tensile testing and a snow slab overlying a weak layer in a snowpack.

Schubert (1975) measured the dependence of tensile strength on the height of the sample. Because a powder may deform in shear, the tensile strain would be greatest in the vicinity of the slit in the plate and would decrease towards the surface of the material. For large sample depths, the tensile stress would decrease near the surface. Part of the sample above a certain height, therefore has lower than breaking stress values when the lower material breaks. As the height of a sample increased, Schubert found smaller tensile forces per unit area were required to fracture the sample. He

found for a particular height, the ratio of the measured to actual value of strength depended on the elastic and plastic behaviour of the material and the conditions of cohesion between the material and the supporting split-plate.

Applying these arguments to snow slabs, we would expect a deep slab to fail at lower apparent values of tensile strength than those expected for that area. Also, since a snow slab consists of layers of different types of snow (and varying Young's modulii), the stresses would be concentrated in layers which were (a) close to the basal weak layer, and (b) of high Young's modulus.

3.6 STRESS-STRAIN RELATIONSHIPS.

Schubert (1975) used a model of spheres to describe a stress/strain relationship in powders, and noted that for most agglomerates the strains at failure (defined to be the position the stress-strain curve became unstable) were usually quite small (order of 10^{-3}). For dry powders and agglomerates with solid bridges, the strains may be even smaller. For all but the slowest strain-rates, Narita (1980) found the tensile stress of snow became unstable after strains of about 0.5-1%. Because of the sensitivity of powders, including snow, to small strains, we suspect minor disturbances may cause at least local ruptures in snow slabs.

Schubert et al., (1975) found that if the fracture strain (ie. the strain at maximum load) was small, a powder would be more sensitive to cracking than materials which exhibited large fracture strains even though both may have the same tensile strength. They suggested that knowledge of the strain behaviour helped clarify the various bonding mechanisms within the powder. For example, dry powders have a markedly smaller fracture strain than moist powders (with liquid bridges) and tend to exhibit brittle behaviour. Furthermore, under conditions of loading and unloading, they observed hysteresis of the tensile stress-strain curve. It followed that deformation even at the start of stress was not purely elastic but also had a plastic component. Brown et al.(1973) recognised this type of behaviour in snow subjected to

torsional stresses.

Although some stress-strain measurements have been made in the laboratory, little is known about strain-rates applicable during slab failure. In an attempt to gather more information about such rates, we built a strain gauge similar to that described by Sommerfeld (1975,1979), and this is discussed later.

3.7 SIMPLE SHEAR AND TENSILE TESTS DESIGNED FOR THE FIELD.

LaChapelle and Ferguson (1980) found that identification of potential sliding surfaces from inspection of snowpit stratigraphy was often based on subjective judgement. Because most slab failure models assume a weak basal layer (Perla,1980), a method of finding such weak layers and assessing their strength would be a primary consideration for stability predictions. A shear frame first used by Roch (1966) has been used by many to study the strength of layers, but this technique relies on the operator either identifying the weakest layer, or finding the layer by many trials. A tilt test described by Perla and Martinelli (1976) in which a snow sample is tilted until failure occurs somewhere within the sample, overcomes this problem. However this cannot be easily applied in a snow slab because of the difficulty in placing a sample on the tilting surface without disturbance. The "shovel test" is a popular field technique for finding potential sliding surfaces (see Sommerfeld,1984). The "wedge test" developed by LaChapelle and Ferguson (1980), used a technique similar to that incorporated in the ram penetrometer to drive a wedged-shaped block behind a column of snow to transfer compressive stress to the block, and hence shear stress along different layer surfaces. The wedge appeared to quantify the shovel test somewhat.

Our shear tests were designed to simulate stress conditions that might occur in a snow slab and are fully described in Conway and Abrahamson(1984a,1985). The shovel, wedge and our shear tests have advantages over other tests in that (a) the normal loading conditions on a particular slope are not altered during the test, (b) detailed analysis of the

snow stratigraphy is not required, and the weak layers (if they exist) are easily identified. However our test did subject the snow to a bending moment which would not normally occur under natural loading.

The strength of the slab overlying the weak basal layer is often not considered in field tests of snow stability. Our simple tensile tests were designed to attempt to simulate conditions which might occur in a snow slab, and are discussed in our papers Conway and Abrahamson(1984a,1985). In these papers we have discussed the importance of viewing these measurements as strength indices rather than absolute values, because of factors such as; (a) the rate of strain during an avalanche may be quite different to the rate during the test, and (b) size effects of the test compared with the scale of the avalanche as discussed by Sommerfeld(1980) or Gubler(1978b).

We also found considerable spatial variability in the values of the measurements and this is discussed in more detail in a later section as well as in Conway and Abrahamson (1984,1985). Sommerfeld (in prep.) has also recorded spatial variability of shear strength measurements.

3.8 TIME DEPENDENT MEASUREMENTS.

A) Strain measurements over a slab.

Sommerfeld (1979) measured strain rates in a snowpack near an avalanche starting zone. Using a 3m strain gauge, he measured between two positions straddling the eventual fracture, sharply increased strain rates for almost 5 hours preceeding an avalanche, and suggested that this could be used as an indicator of instability. Strain rates thus measured in the field were about 1.5 orders of magnitude lower than those measured by Narita (1980), using samples 125mm long in the laboratory. Because of this, Sommerfeld suggested that the strain might be concentrated and that snow fails over localised areas. This proposal is also supported by the laboratory measurements made by Singh and Smith (1980) and Narita (1980).

Another explanation might be that discussed earlier in which strain in the slab would be unevenly distributed, and most likely concentrated near the shear layer (about 0.44m below the strain gauge used by Sommerfeld during his measurements).

In order to further investigate some of these properties, we built a strain gauge similar to that built by Sommerfeld (1975,1979). By measuring change in resistance of a potentiometer with movement, we planned to estimate strains and strain rates on a snow slab. We found that a rotary wire-wound potentiometer was not sufficiently accurate to measure the expected magnitude of strain rates in a slab of snow (10^{-6} to 10^{-4} per hour) and so we used a linear potentiometer made from conducting plastic with a total travel of 75mm. At no time were we able to locate the instrument on an unstable slope during critical periods, and we were wary of leaving the instrument on slopes during storms. Typically high snow accumulation occurs with each storm period and so the likelihood of losing the instrument was high, because often during storms it was not possible to visit the slopes. We also found, especially for low density snows and over long periods of time (hours), the pads attaching the instrument to the snow would creep, thus masking the creep we were trying to measure.

B) Shear stress-strain measurements.

Because of the difficulties described above in obtaining strain measurements on slopes, we decided to apply a shear stress to a large sample (300mm x 300mm) and measure the shear strain. The methods are described in Conway and Abrahamson (1984c), together with some measurements made. We had no control over strain rate, and the stress was applied using a calibrated spring over a period of 5-10 seconds. Because the spring did not unload immediately after small displacements, we could not use the device to measure stress/strain characteristics after peak stresses had been reached. We could however measure the residual strength by disconnecting the strain gauge and further stressing the sample (see Conway and Abrahamson,1984c). A further major disadvantage of this

test was that we could not separate the component of shear movement in the weak layer from that due to the deformation of the slab. Slab deformation may be small in hard slabs, but measurements of the slip at the weak layer may be masked by deformation of the slab especially in soft slabs.

We think shear strain softening of snow (measured by McClung,1977, and Conway and Abrahamson,1984c), might control propagation of failures during avalanche events, and so we developed a further simple field test to measure the peak and residual shear stresses. The technique (described in Conway and Abrahamson,1984c) was to first stress the sample to failure using the frame, and then repeat the test (with the same sample). It was assumed that the first stress value might be an indication of average normal strength and the second, a residual strength index.

As with the other tests, rates of failure were not considered, but measurements tabled in Conway and Abrahamson (1984c) suggest that different crystal structures exhibit different degrees of strain softening, and probably the degree relates to the strength of the initial bonds (ie. either over or under consolidated). For instance some new, unmetamorphosed, low density (50 kg/m^3), snow did not strain soften, while some graupel crystals were observed to soften to a value of 12% of the average normal value. This consideration plays an important role in our criteria for propagation of failure in assessment of slope stability from field tests and is discussed in a later section and in Conway and Abrahamson (1985).

C) Tensile stress-strain measurements.

In 1981 we built a tensile tester theoretically capable of straining large samples of snow (up to 300x300x600mm). For various reasons we have had only limited success in obtaining measurements using the tester, and some of these reasons are discussed by Conway and Abrahamson (1982a). Probably the major limitation when using the device was the lack of control over environmental conditions, especially for those tests over extended time periods. For instance changes in temperature

often meant that creep near the end plates contributed significantly to our measurements of strain, and wind frequently eroded our samples. We have described some measurements made with the device, but we have only managed to complete a few tests which we can regard as successful (see Conway and Abrahamson,1982a). We do not draw any conclusions from these tests concerning tensile stress-strain relationships, but further tests with this instrument would be possible if made in a colder environment or a cold laboratory.

3.9 MODELS OF SLOPE FAILURE.

Typically, failure criteria are formulated in terms of maximum stress, strain or energy capacities of a material. However it is well known that for most engineering materials, the tensile stresses required to cause a fracture by crack propagation are very much smaller than the ultimate tensile strength of the material. In order to improve a fracture model, materials are often considered to contain flaws at which stress concentrations occur. A failure criterion may be based on a comparison of the yield strength and the maximum stress calculated at the tip of a crack, or more commonly, a balance of energy requirements and energy released during extension of a crack. Such models can be fairly easily extended to materials exhibiting plastic as well as elastic behaviour, and for complex stress fields or inclined cracks (see for example, Jayatilaka,1979 or Liebowitz,1971).

McClung (1979a) modeled propagation of a basal shear crack in snow using these concepts and there is good evidence of tensile modes of failure in snow. Narita (1980,1983) observed cracking in laboratory tensile tests, and we have observed tensile cracking in natural snow packs. Furthermore, strain-rates measured by Sommerfeld (1979) in the field just prior to an avalanche, were much lower than those required to fracture laboratory samples which suggests strain was concentrated over small regions. For these reasons, we think a model which considered the extension of cracks or flaws could be usefully applied to failure of snow slabs (a tensile stress causing an opening type of failure).

3.10 CONCLUSIONS.

The material discussed above outlines some of the difficulties in measuring (and applying) strengths of snow in the field. In applying these strengths to snow slope stability, we have used methods to determine average stresses, and then considered equilibrum conditions around a snow slice (see Conway and Abrahamson,1985). It is clear that any model of failure would be greatly improved by knowledge of relationships between stress, strain and strain-rates. If characteristics of snow properties which vary with time, stress history and strain-rates can be determined with simple measurements in the field, and then related to rates of failure and stress history on slopes, the stability estimate would be greatly improved.

3.11 REFERENCES.

Bader, H., Haefeli, R., Bucher, E., Neher, J., Eckel, O., and Thams, Chr.:(1954) Translation: In "Snow and its metamorphism", 313pp, illus. Snow, Ice and Permafrost Res. Estab., Transl. 14. Corps Eng., U.S. Army, Wilmette, Ill.

Brown, R.L., Lang, T.E., St. Lawrence, W.F. and Bradley, C.C.:(1973) "A failure criterion for snow". Journal of Geophysical Research, Vol.78, No.23, p4950-58.

Buser, O., Fohn, P., Good, W., Gubler, H. and Salm, B.:(1985) "Different methods for the assessment of avalanche danger". Cold Regions Science and Technology, Vol. 10, p199-218.

Conway, H.:(1984d) "Variations of basal shear strength". The Avalanche Review,Vol.3, No.1, p5.

Conway, H. and Abrahamson, J.:(1982a) "Insitu tests of large volumes of snow". Unpublished report for Mountain Safety Council.

*Conway, H. and Abrahamson, J.:(1982b) "Air permeability as a measure of snow structure". Unpublished report for Mountain Safety Council.

*Conway, H. and Abrahamson, J.:(1983) "A summary of weather and snow conditions at the Tasman saddle area during the winters of 1980-1982". Unpublished report for Dept. of Lands and Survey.

*Conway, H. and Abrahamson, J.:(1984a) "Snow stability index". Journal of Glaciology, Vol. 30, No. 106, p321-7.

*Conway, H. and Abrahamson, J.:(1984b) "Air permeability as a textural indicator of snow". Journal of Glaciology, Vol. 30, No. 106, p328-33.

*Conway, H. and Abrahamson, J.:(1984c) "Snow and avalanche research at Tasman saddle - a progress report of the winter 1984". Unpublished report for Dept. of Lands and Survey.

*Conway, H. and Abrahamson, J.:(1985) "Snow slope stability - a probabilistic approach". Submitted to Journal of Glaciology.

Fohn, P.M.B. and Meister, R.:(1983) "Distribution of snow drifts on ridge slopes: measurements and theoretical approximations". Annals of Glaciology, Vol.4, p52-57.

Good, W.:(1975) "Numerical parameters to identify snow structure". IAHS-AISH publication No.114, p91-102.

Gubler, H.:(1978a) "Determination of the mean number of bonds per snow grain and of the dependence of the tensile strength of snow on stereological parameters". Journal of Glaciology, Vol. 20, No. 83, p329-341.

Gubler, H.:(1978b) "An alternate statistical interpretation of the strength of snow". Journal of Glaciology, Vol. 20, No. 83, p343-357.

Jayatilaka, A. de S.:(1979) In "Fracture of Engineering Brittle Materials". Applied Science Publishers Ltd. London.

Kry, P.R.:(1975a) "Quantitative stereological analysis of grain bonds in snow". Journal of Glaciology, Vol. 14, No. 72, p467-477.

Kry, P.R.:(1975b) "The relationship between the visco-elastic and structural properties of fine-grained snow". Journal of Glaciology, Vol. 14, No. 72, p479-500.

LaChapelle, E.R. and Ferguson, S.A.:(1980) "Snowpack structure: stability analysed by pattern-recognition techniques". Journal of Glaciology, Vol.29, No.94, p506-511.

Liebowitz, H.(editor):(1971) In "Fracture - an advanced treatise" Vol.3, Academic Press, New York.

McClung, D.M.:(1977) "Direct simple shear tests on snow and their relation to slab avalanche formation". Journal of

Glaciology, Vol. 19, No. 81, p101-109.

McClung, D.M.:(1979a) "Shear fracture precipitated by strain softening as a mechanism of dry slab release". Journal of Geophysical Research, Vol. 84, No. B7, p3519-3526.

McClung, D.M.:(1979b) "In-situ estimates of the tensile strength of snow utilizing large sample sizes". Journal of Glaciology, Vol. 22, No. 87, p321-29.

Mellor, M.:(1975) "A review of basic snow mechanics" IAHS AISH Publ. 114, p251-291.

Molerus, O.:(1982) "Invited Review: Flow behaviour of cohesive materials". Chem. Eng. Commun. Vol.15, p257-289.

Montmollin, V. de:(1982) "Shear tests on snow explained by fast metamorphism". Journal of Glaciology, Vol. 28, No. 98, p187-198.

Narita, H.:(1980) "Mechanical behaviour and structure of snow under uniaxial tensile stress". Journal of Glaciology, Vol 26, No. 94, p275-282.

Narita, H.: (1983) "An experimental study on tensile fracture of snow". Contrib. No.2625 from the Inst. of Low Temp. Science, Series A, No.32, Hokkaido Uni., Sapporo, Japan, p1-37.

Palmer, A.C. and Rice, J.R.:(1973) "The growth of slip surfaces in progressive failure of over-consolidated clay". Proc. Royal Society London, Ser. A, No. 332, p527-548.

Perla, R.I.:(1980) "Avalanche release, motion and impact". In Dynamics of Snow and Ice Masses, (S. Colbeck, ed.), Chapter 7, p397-462, Academic Press, New York.

Perla, R.I., and Martinelli Jr., M. :(1976) "Avalanche Handbook" US Department of Agriculture Forest Service. Agriculture Handbook No.489.

Roch, A.:(1966) "Les decenchements d'avalanches". International Symposium of Scientific Aspects of Snow and Ice Avalanches. International Association of Hydrological Sciences Publication, No. 69, p182-195.

Roscoe, K.H.:(1970) "The influence of strain in soil mechanics". Geotechnique, Vol.20, p129-170.

Schubert, H.:(1975) "Tensile strength of agglomerates", Powder technology, Vol.11, p.107-119.

Schubert, H., Herrmann, W. and Rumpf, H.:(1975)

"Deformation behaviour of agglomerates under tensile stress". Powder Technology, Vol.11, p121-131.

Schwedes, J.:(1975) "Shearing behaviour of slightly compressed cohesive granular materials". Powder technology, Vol.11, p59-67.

Singh, H. and Smith, F.W.:(1980) "Constant strain-rate tensile testing of natural snow (abstract)". Journal of Glaciology, Vol.26, No.94, p519.

Skempton, A.W.:(1985) "Residual strengths of clays in landslides, folded strata and the laboratory". Geotechnique, Vol.35, No.1, p3-18.

Sommerfeld, R.A.:(1973) "Statistical problems in snow mechanics". U.S. Dept. of Agriculture, Forest Service General Report, RM-3, p29-36.

Sommerfeld, R.A.:(1974) "A Weibull prediction of the tensile strength-volume relationship in snow". Journal of Geophysical Research, Vol. 79, No. 23, p3353-3356.

Sommerfeld, R.A.:(1975) "Continuous measurements of deformations on an avalanche slope", IAHS-AISH, No. 114, (Snow mechanics symposium, 1974), p293-7.

Sommerfeld, R.A.:(1979) "Accelerating strain preceeding an avalanche". Journal of Glaciology, Vol. 22, No. 87, p402-404.

Sommerfeld, R.A.:(1980) "Statistical models of snow strength". Journal of Glaciology, Vol. 26, No. 94, p217-223.

Sommerfeld, R.A.:(1984) "Instructions for using the 250cm2 shear frame to evaluate the strength of a buried snow surface". USDA Rocky Mountain Forest and Range Experiment Station, Research note RM-446, 6pps.

Sommerfeld, R.A.:(in prep.) "Spatial variation of shear strengths of avalanche sliding surfaces".

* References marked thus are included in the appendices.

4. INFLUENCES OF WIND ON SNOW DISTRIBUTION AND AVALANCHING.

4.1 INTRODUCTION.

When snow is transported by wind (especially when transport is not fully developed), it is well known that complex patterns of drift occur behind discontinuities or obstacles, between obstacles and below cliffs. Our measurements over slopes exhibit spatial variability, not only in depths of snow layers but also in strengths of layers and between layers. We think the spatial variability is caused in part by wind and wind redistribution of snow, and suspect a relationship exists between the depositional characteristics of snow and the patterns of fluctuation of the strength. Identification of such a relationship would be a valuable tool for characterising snow properties on a snow slope and for subsequent slope stability estimates.

We can consider a potential slab avalanche to consist of some relatively stiff snow layers separated by a weak layer. We are particularly interested in ways in which the wind might affect the stability of a snow pack. Some of these are outlined below and discussed in more detail later:

1) Wind-transported particles are generally smaller and more rounded than the original precipitating crystals, and so tend to form dense well-bonded layers such as those expected in a slab. As a result of uneven snow distribution, stress concentrations develop may develop at positions where sharp changes occur in the depth of the slab. If the downslope component of the gravitational load is sufficiently high, the stress concentrations may be sufficient to cause slope instability.

2) Discontinuities in the thickness of a buried weak layer may cause variability of basal shear strength, and in such cases the size of the weak area is important for determining whether a local fracture can propagate and become an avalanche (see Conway and Abrahamson, 1984,1985). Often shear planes we have observed consist of very thin layers of snow or occur at boundaries between layers, and this has been also noted by others (eg. Sommerfeld, in prep.). Such shear layers would be strongly affected by the roughness of the

surfaces of the adjacent snows. Bridgewater (1980) for example suggested a specific layer thickness was required for shearing to occur in non-cohesive and non-deforming particles. If the snow surrounding the weak layer had been rippled by winds, the shear layer might show a pattern of large scale, regular fluctuations of strength, corresponding to positions where the layer thickness changed. If the shear layer was very thin, fast random fluctuations of strength might occur when grains from adjacent layers protrude through the weak layer. On the other hand, if the snow surrounding the shear plane was not protruding through the weak layer, less variation in values of strength would be expected.

For surface snow with low cohesive strength, the threshold wind velocity for wind transport may be very low. This may cause redistribution of a potential weak layer such as surface hoar before burial by subsequent snowfalls. Furthermore, the light winds may not drastically alter the crystal structure but sweep the weak crystals into areas which would be determined by the surface topography. After snowfalls, such conditions may result in pockets of weakness separated by stable regions (which had been eroded before the snowfall).

3) Buried weak layers often consist of large unbroken crystals which have fragile bonds, and a low wind-speed appears to be a necessary condition during the time of deposition of such crystals. We expect the variation of strength due to the random distribution of crystal bonds to be on a smaller scale than that which we are measuring.

4.2 AIR-FLOW STUDIES.

Airflow patterns vary considerably, especially when the flow is not steady, and mathematical modeling of such flows is difficult. We suspect wind could strongly affect snow strength by causing transfer not only of snow particles, but also of heat and moisture.

Our model of slope stability indicated that low strength values over areas of only $1m^2$ may be sufficient to cause an avalanche (see Conway and Abrahamson, 1985). Hence we are interested in small scale as well as larger scale effects of the wind especially in locations behind topographic obstacles near avalanche starting zones. We do not attempt a comprehensive study of wind parameters under such conditions, but list below a few recent studies which have some relevance to our problem.

It is well known that windspeeds and directions are quite variable over a mountainside, and terrain obstacles exert drag forces that disturb smooth flow of free air. An important feature of air-flow over and around obstacles is flow separation and reattachment. Separation occurs when the pressure field is sufficient to stop the air-flow near the ground surface. Scorer (1972) noted that although the windspeed is zero along lines of separation, this may be caused by two opposing air-flows and strong shear zones and vortices may occur at such positions. The position and size of an eddy between the separation and reattachment regions depends among other things, on the shape and slope of the topography and may vary rapidly with changing windspeed.

Recently in an attempt to gather more knowledge of the details of turbulent flow, several studies have been made around large scale obstacles. Mason and King (1984) for example measured flow across a steep (about 32°) ridge and valley system. When the flow across the ridge separated, the size of the separated region was found to be sensitive to flow direction (flow directions within about ±60° to perpendicular caused flow separation), and varied from almost filling the whole valley system to just a small region on the lee slope. On the ridge crests, they found (at heights of 2m and 12m above the summit) that apart from a small increase in the lateral component of turbulent energy, the turbulence levels and stress ratios were broadly similar to those measured over level terrain. In contrast to these measurements, observations in the valley showed standard deviations of the velocity fluctuations could exceed the local mean flow speed,

and the turbulence level was much higher than that measured on the summit. Using a two dimensional model to simulate flow, Mason and King found they could adequately describe the mean flow but not the spatial distribution and levels of turbulence in the valley. They did find if they decreased the "mixing length" parameter in the model (effectively allowing the flow to become unsteady), that their field observations were more closely simulated by the model. However they note that no theoretical ideas or observations existed to justify decreasing the "mixing length".

Measurements and observations around an island (about 1km diam, 330m altitude with slope angles of 30°-45°) showed a distinct region of reversed flow on the lee slope and a strong local speed-up of flow over the summit (Jenkins et. al.,1981). High windspeeds were measured around the sides of the island and they found a well defined flow pattern showing two singular points: a nodal point of separation just downstream of the summit, and a saddle point just downstream of the island. They were uncertain whether the saddle point represented a point of separation or one of reattachment, but found the turbulence energy around the side of the island to be much higher than in undisturbed flows. Furthermore using measurements from aircraft flights, they found a single trailing vortex downstream of the island. The vortex had its axis oriented close to the upstream wind direction with circulation velocities of similar magnitude to the undisturbed horizontal speed. The direction of vortex rotation depended on the incident wind direction, and they suggested the assymmetry of the island contributed to the generation of the vortex. A similar type of vortex was also observed by Cook et. al.,(1978) during measurements in a wind tunnel model study of flow around the Rock of Gibralta.

Recently several studies of turbulent flow have also been made on a smaller scale in wind tunnels. One such study (Trout et. al.,1984) used the motion of a turbulent boundary layer of air over a two-dimensional downstream-facing step to produce a flow field. The step height was large compared with the up-stream boundary layer thickness and the flow separated

immediately and reattached further downstream (at a distance of about seven step-heights). Before the reattachment region, they observed pairs of vortices above the separation line. Downstream of the reattachment region, although the vortices retained their structure, they were not paired. The marked reduction of turbulence energy after reattachment was attributed to the disappearance of the paired vortices and they suggested the slow readjustment to bounded flow after reattachment could be caused by the large-scale (but unpaired) vortices.

Streamwise vortices have also been observed in several studies, and it is thought that such vortices may enhance deposition from two-phase flow. Winoto et. al.,(1979) observed such vortices in a laminar boundary layer of water flowing in a curved channel. The vortices have also been observed in turbulent boundary layers (eg.Meroney and Bradshaw,1975; Tani,1962). Most of these studies describe the so-called "Gortler" vortices resulting from centrifugal instability on concave surfaces. Using measurements made by others in the developing region of flow over flat plates, Blackwelder (1979) described the occurrence of different streamwise vortices, triggered after a two-dimensional perturbation had been introduced to a flow. He suggested the perturbation initially produced "Tollmein-Schlichting" type waves which generated pairs of counter-rotating streamwise vortices. Because of their periodic nature, the vortices would cause a "pumping" type action, resulting in zones of unstable and localised shear. The resulting velocity profile would be unsteady and not directly related to the usual boundary layer parameters.

Uncertainty in knowing the values of wind parameters is typical of studies of turbulent flow. Computer models and statistical models have been used (for example Taylor,1984 and Maeda and Adachi,1983), but although estimates of mean flows are in good agreement with measured flows, simulation of turbulence is characteristically poor. If turbulence and snow strengths are related, we expect a simulation of the precise spatial location of areas of weak snow, would also be

difficult.

4.3 BLOWING AND DEPOSITS OF SNOW.

Schmidt (1982) reviewed recent literature related to blowing snow. He noted that various particle properties such as size, shape and density dictate fall velocities. He also noted that most literature studied flow over plane surfaces, and relatively few studies related to more complex problems of snow transport around obstacles.

A) Flow over plane surfaces.

Few transport processes consider transport of cohesive particles, but it is useful to separate transport processes which occur near the bed-surface (either by saltation or rolling of the particles), from those of particles which are suspended further up in the flow. The flow process can be categorised into either "upper" or "lower" flow regime, depending on the level of turbulence of the flow. The level is determined by a number of factors, and dimensionless combinations are a useful way to describe the process. For example, a Froude number (μ/gh for a mean velocity μ and depth of flow h), and various Reynolds numbers (for example the mean flow Reynolds number $\mu h/\upsilon$, where υ is the kinematic fluid viscosity) are two such combinations. Furthermore several authors have described turbulent flow as a random process and then applied theories of probability to describe the flow. Some of these methods have been discussed and summarised by Yalin (1976).

In two-dimensional flow three basic linear structures are recognised. These are: antidunes, dunes and ripples, and the processes which cause these features to form are still unclear. For three-dimensional flow, as might be expected in the atmosphere (Peterka et. al.,1985), these linear structures become truncated, and if spheroidal eddies occurred, barchan or crescent shaped features might form. In such cases the thickness of the boundary layer is an important parameter for defining the wave-length of the features. Because the thickness may vary considerably with time the wavelength of dunes would also vary.

Considerable experimental studies were carried out by Simons et. al.,(1964) using an alluvial channel. They found ripples and dunes formed when flow was in a "lower regime", and initially the ripples had uniform shape and spacing, but as the flow continued, the spacing became more irregular. When flow was such that resistance to bulk flow was small and sediment transport large (ie. "upper flow regime"), they observed features such as plane-bedding, antidunes, chutes and pools. When the flow was neither upper nor lower regime (ie. "transition flow"), dunes were commonly scoured out, and erratic and variable structures were commonly observed.

Bagnold (1941) observed sand ripples and dunes normal to a local wind direction. He found these either had a periodic distribution or were short and irregular, depending on the particle density of the transported medium.

For snow, Dyunin (1967) and Kobayashi (1979) have recorded periodic fluctuations in transport rates. At low windspeeds, Kobayashi observed formation of ripples which had wavalengths of the order of 10-100mm. At speeds greater than about 7m/s (measured at a height 1m above the snow surface), "transverse waves" formed. The wavelength of these features (which typically varied from 3-15m) was found to vary inversely with the mean windspeed, and approached zero as the wind velocity at 1m increased beyond 15m/s. For higher speeds, features which were transverse to the wind direction were replaced by ones which were longitudinal. These types of deposits could well be formed by the paired rolling vortices ("Gortler" vortices or "Tollmein-Schlichting" waves) discussed earlier. Because the transport rates depend not only on windspeed but also on various other parameters discussed earlier, we expect these threshold velocities controlling the formation of each type of feature to differ somewhat for each snow type and condition.

B) Flow around large obstacles.

As previously mentioned, large scale terrain obstacles typically cause flow to separate and cause reverse eddies in the wake region. Bagnold (1941) for instance observed

longitudinal drift patterns of sand caused by wind channelling between irregularities along a cliff top, and explained the drifts by "lee eddying". Tabler (1980) using measurements collected over many years, found that snow drifts behind fences had characteristic lengths and cross-sectional areas which were proportional to the height of the fence. Presumably the geometry of the drifts reflect the size of the wake behind the fence (see for example, Humphries and Vincent,1978). Tabler (1980) also noted an increase in snow density behind the fences which he attributed to densification due to the increased snow depth. Schmidt (1980) pointed out that transported snow was also likely to have a small grain size (and therefore be more dense) and to develop strong bonds almost immediately after deposition. He suggested this might contribute to the relative stability of drifts behind obstacles and that transport could stop either because the wind velocity decreased or if the frequency between maximum gusts increased (thus enabling rapid bonding during periods between gusts). These factors would suggest that such drifts would be more conducive to slab formation in a snowpack rather than deposition of weak layers.

On a larger scale, we are particularly interested in the measurements made by Fohn (1980) and Fohn and Meister (1983) concerning the distribution of snow drifts down slopes behind ridge crests. Fohn (1980) found the drift flux profile to be humped over a ridge crest for reasonably high velocities (7-10m/s), and the maximum drift flux was measured at 1-1.5m above the ridge crest. Fohn and Meister (1983) modelled snow distribution down the lee side of a ridge using a combination of plume and potential models in conjunction with the slope geometry. The resulting deposition was approximated by a damped sine wave whose amplitude and wavelength was a function of the ridge size and crest sharpness. The model fitted their experimental measurements very well. For three-dimensional situations when the plume may not be adequately described by a two-dimensional Gaussian distribution, they suggested a more complex model might be appropriate..

4.4 SNOW WAVES AND SNOW STRENGTH - SOME OBSERVATIONS.

It is easy to imagine that features such as ripples, dunes and antidunes as well as drifts behind topographic discontinuities or ridges could strongly affect snow strength. Clearly the statistical characteristics of a process describing the features must depend on whether they are ripples, dunes or antidunes and whether they are superimposed on drift patterns of a larger scale such as those measured by Fohn and Meister (1983) or Bagnold (1941). As well as changing with time, we also expect the formation of the features to depend strongly on the snow type, and so each process would be unique.

In a similar way in which we have described snow strength (Conway and Abrahamson,1985), the distribution of snow waves may be thought of as a randomly varying process and so be described by parameters defining the mean, standard deviation and correlation between the values of wave height. If snow strength is somehow related to the spacing and height of snow waves, we should find some similarities between the processes which describe the two variables. We do not have sufficient measurements of size and standard deviations of snow waves so for this study we consider only the correlation between spacing of wave peaks, and compare it with the correlation between measurements of snow strength.

We derived a "scale of fluctuation" describing the correlation between measurements of snow strength (see section 5 and Conway and Abrahamson,1985), and use of the approach outlined by Vanmarcke (1977a,1983) may also be applied to snow-wave measurements. Vanmarcke showed how the "scale of fluctuation" (δ), was related approximately to the average distance between "mean crossings" (ie. one half of the average wavelength, λ), in fact to a first approximation:

$$\lambda/2 = (\pi/2)^{1/2}\delta$$
$$= 1.25\delta \qquad (1)$$

$\lambda/2$ is a measure of the length the process is expected to be above (or below) the mean value,and for snow stability estimates, we are particularly interested to determine whether λ is short or long.

1) Short period snow waves.

Although we are not sure of the details of formation of transverse snow waves, we know that the process involves a combination of erosion and deposition of snow. In some instances, we have observed migration of such features at rates up to 2mm/s when large conglomerates (1-4mm diam) of crystals were being rolled along the snow surface. On other occasions, typically after periods of high snowfalls of soft, low-density snow (60-100kg/m^3), large features which measured up to 0.6m in relief between troughs and crests were formed. Often these features had steep sides (40-60°) facing into the local wind direction.

It is not surprising that we commonly found the snow stratigraphy (in particular snow thickness) beneath such surface features had also been influenced by the erosion/deposition processes, and often varied with the same period. Therefore although a weak layer may have been deposited under conditions of low wind speeds and be fairly uniformly distributed over a surface, any subsequent wind would be likely to disturb this layer. Figure 4.1 is a sketch of one such observation. This process may happen over a short time span during storms.

Because ripple formation is strongly dependent on wind and snow conditions and these may vary rapidly, it is unlikely that the features observed on the surface will reflect the atmospheric and snow conditions at the time a weak layer was deposited in the snowpack. However observations of the surface features can give an insight into the range of conditions which might be expected during storms.

For surface features which had formed probably transverse to the local wind direction, we measured wavelengths varying from very small values (order of 10mm) up to 13m, and commonly, the larger features were spaced at about 5m or less. These observations (made over several years near the head of the Tasman glacier) are similar to those reported by Kobayashi (1979) who measured transverse features with wavelengths up to 15m.

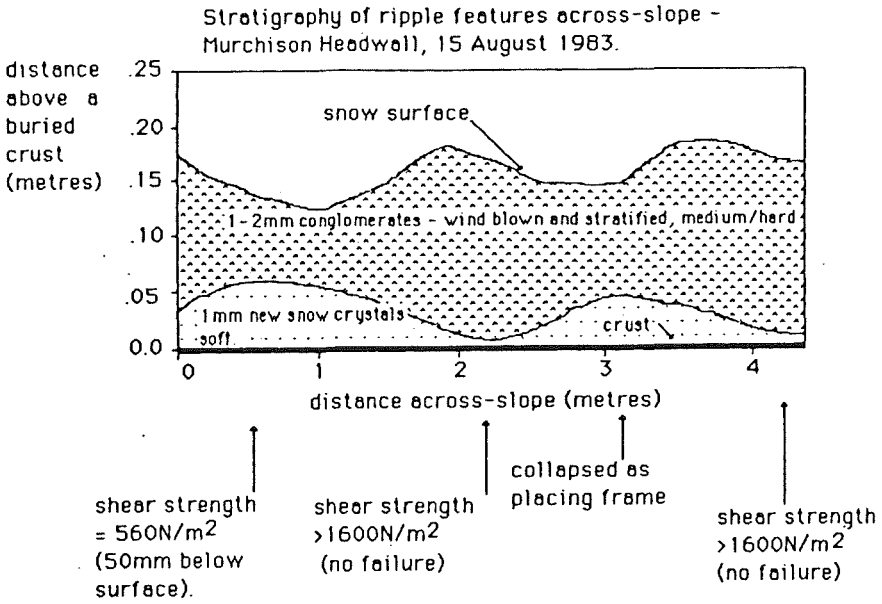

Figure 4.1.

Surface ripples influence basal snow layers.

Eqn.1 indicates that for wavelengths less than about 5m, the "scale of fluctuation" associated with the snow waves would be less than about 2m, and for wavelengths of 15m, the scale would be about 6m. In our paper on snow slope stability (Conway and Abrahamson,1985) all the calculated "scales of fluctuation" for both strength and slab depth measurements were within this range. These measurements are summarised in table 4. 1. The scales describing strength measurements varied from 0.13m to 2.1m and those associated with slab depth varied from 0.18m to 2.58m. The slab depth measurements are likely to be the sum of several superimposed snow waves and so we suspect the fluctuations of such measurements to be smaller and more closely spaced than those originating from a single wave pattern. The tensile strength of a snow slab might also exhibit these same characteristics and have a similar "scale of fluctuation". We only have one set of tensile strength measurements across a slope (see table 1 and appendices), and it is interesting to note that the scale of fluctuation of the tensile strength measurements (0.45m) was almost the same as

that for the slab depth measurements (0.44m). We are not certain whether this would be typical for all slopes.

TABLE 4.1

Strength and slab depth measurements on six slopes.

	av. basal shear(N/m^2)	δ (m)	av. slab depth(m)	δ (m)
1)	549±345	2.1	.43±.09	1.18
2)	1840±722	.24	.93±.10	2.58
3)	1111±397	.22	.43±.16	.57
4)	271±158	1.12	.18±.03	1.0
5)	559±273	.13	.25±.08	2.0
	av. tensile ($N/m^{\wedge 2}$)	δ (m)	av. slab depth(m)	δ (m)
6)	2780 ± 834	.45	.22±.02	.44

On the otherhand, the basal shear strength is likely to be affected over a relatively short period of time and have a scale of fluctuation which reflected the conditions close to the time the weak layer formed. It is not surprising therefore, that for particular slopes, although the range of the "scales of fluctuation" associated with the basal shear strength and slab depth were similar, the magnitudes were different (see table 1).

2) Longer period snow waves.

Examples of how snow depth might fluctuate slowly are when snow is deposited in the form of a damped sine wave below a ridge crest (as measured by Fohn and Meister,1983), or a series of drift patterns behind large obstacles or discontinuities in terrain as observed by Bagnold (1941) or Tabler (1980). Transported snow may be deposited rapidly immediately to the lee of obstacles or discontinuities (in the "wake" region), because the airflow is light or reversed. For instance the Cornicewall (a lee slope to the prevailing

westerly wind which sweeps across the Tasman neve), typically accumulates about 2.5 times the depth of snow on the neve (Young and Conway, 1983).

Such rapid accumulations of snow may increase the stresses within a snowpack sufficiently to cause avalanching. The size and location of the drift is controlled by the size and location of the wake. This may provide an explanation for the position of some avalanche crownwalls which occur at places other than at the maximum slope angle. This position may be close to the "point of separation" of the flow where a discontinuity in snow depth would be expected to occur.

In our paper on snow stability (Conway and Abrahamson,1985), we defined and evaluated safety margins across slopes. One of the assumptions for the estimates was that the snow was statistically homogeneous and the mean safety margin did not change significantly, at least within the area of interest. Large fluctuations of snow accumulation are likely to cause significant changes to the mean value of the safety margin. In order to satisfy the assumptions, a slope would then need to be subdivided into zones which could be treated as homogeneous within themselves. As noted in our paper, if such conditions are suspected, clusters of measurements within each zone would be required to properly evaluate the strength characteristics of the entire slope.

Plates 2 to 5 show some typical features we have observed.

4.5 OPTIMUM SAMPLING POSITIONS.

Vanmarcke (1983) showed that optimal sampling intervals may be expected to be proportional to the scale of fluctuation and for nearly error free interpolation (using a linear combination of observations) the process should be sampled at lengths of one half the scale of fluctuation.

1) Estimates of short wavelength processes.

From the preceeding discussion and observations, for a good estimate of the parameters describing snow waves, sampling distances should be at the most 3m and generally

Plate 2: Extensive waves across-slopes caused by drifting snow. The Cornicewall is the slope in the background.

Plate 3: Surface snow waves on Hochstetter Dom Shoulder.

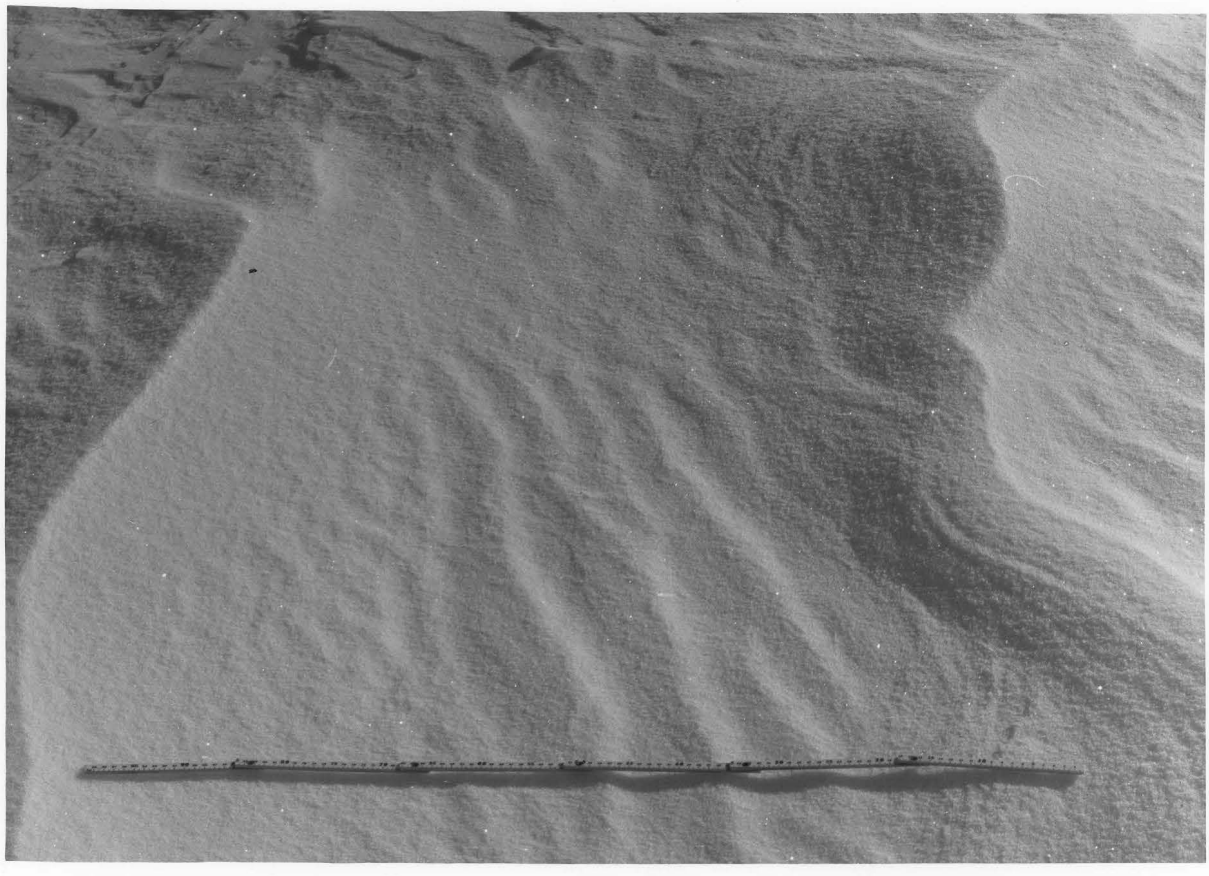

Plate 4: Waves of short wavelength superimposed on waves of larger wavelength. 1 m rule for scale.

Plate 5: Multiple pits across the Murchison Headwall to measure spatial characteristics of strength.

smaller. If as suggested snow waves and snow strength are closely related, this sampling distance would also apply when measuring snow strength. We think a weak area of about 1m x 1m may be sufficient to initiate an avalanche, and because the fluctuations are commonly of the same order of size, a cluster of measurements side by side would best describe a rapidly fluctuating process (practically, our measurements have a minimum spacing of 0.6m).

2) Estimates of long wavelength processes.

As previously mentioned, if the snow properties show distinct lateral trends, the simplest way to estimate the parameters of the process is to divide the slope into subsections which have relatively homogeneous properties. A cluster of contiguous measurements would then best describe the process of each section.

Some of the places where gradual changes in snow properties occur may show obvious surface features such as drifts behind outcrops or a change in snow texture down a slope and so be easily recognised. We are also interested in the areas where the property change is very gradual but less obvious from surface features. Picking out such an area is particularly difficult when considering basal shear strength which may not vary in a manner which is related to the surface features. In Conway, Abrahamson, and Young (1985), we suggest some ways of testing snow quickly which may aid field assessment of slope stability as well as provide understanding of factors which might influence snow strength.

4.6 CONCLUSIONS.

The turbulent nature of airflow appears to cause both short and long wavelength variations in snow properties. The short wavelength variations appear to be oriented mainly perpendicular to the direction of airflow, and the longer wavelength variations occur in areas of reduced flow (wake regions) where transported snow is more readily deposited. At least for our measurements, the range of the scale of these fluctuations appears to be similar to those describing our measurements of snow strength. However, because airflow

velocities (and hence snow transport rates) change rapidly during storms, the scale of the fluctuations are also expected to vary considerably (within limits). This means that although snow wave formation may have influenced the shear strength under a slab of snow close to the time of deposition, the fluctuations associated with the slab (slab depth for instance) may not necessarily be the same as those associated with the basal shear strength.

The short scale of the fluctuations does mean that in order to obtain a good estimate of the mean and standard deviation of snow strength, a cluster of closely spaced measurements would be required. If the mean strength changed dramatically across or down a slope, clusters of measurements at several positions over the slope would be appropriate.

4.7 REFERENCES:

Bagnold, R.A.:(1941) "The Physics of Blown Sand and Desert Dunes". London, Methuen and Co., Ltd.

Blackwelder, R.F.:(1979) "Boundary layer transition". Physics of Fluids, Vol.23, No.3, p583-84.

Bridgewater, J.:(1980) "On the width of failure zones". Geotechnique, Vol.30, No.4, p533-536.

Cook, N.J., Coulson, R.H. and McKay, W.:(1978) "Wind conditions around the Rock of Gibralta". Journal of Wind Engineering and Industrial Aerodynamics, Vol.2, p289-309.

*Conway, H. and Abrahamson, J.:(1984a) "Snow stability index". Journal of Glaciology, Vol.30, No.106, p321-327.

*Conway, H.:(1984c) "Snow and avalanche research at Tasman saddle - a progress report of the winter 1984". Unpublished progress report for Dept. of Lands and Survey.

*Conway, H., and Abrahamson, J.:(1985)"Snow slope stability - a probabilistic approach". Submitted to Journal of Glaciology.

*Conway, H., Abrahamson, J. and Young, R.:(1985)"A field test to assess snow slope stability". Submitted to Journal of Glaciology.

Dyunin, A.K.:(1967) "Fundamentals of the mechanics of snow storms". (In Oura, H., ed. Physics of Snow and Ice: International conference on low temperature

science.....1966.....proceedings, Vol.1, pt.2, [Sapporo], Institute of Low Temperature Science, Hokkaido University, p1065-73.

Fohn, P.M.B.:(1980) "Snow transport over mountain crests". Journal of Glaciology, Vol.26, No.94, p469-80.

Fohn, P.M.B. and Meister, R.:(1983) "Distribution of snow drifts on ridge slopes: measurements and theoretical approximations". Annals of Glaciology, Vol.4, p52-57.

Humphries, W. and Vincent, J.H.:(1978) "The transport of airborne dusts in the rear wake of bluff bodies". Chemical Engineering Science, Vol.33, p1141-46.

Jenkins, G.J., Mason, P.J., Moores, W.H. and Sykes, R.I.:(1981) "Measurements of the flow structure around Ailsa Craig, a steep, three-dimensional, isolated hill". Quart. J. R. Met. Soc., Vol.107, p833-51.

Kobayashi, D.:(1972) "Studies of snow transport in low-level drifting snow". Low Temp. Sci. Ser.A, No.24, p1-58.

Kobayashi, S.:(1979) "Studies on interaction between wind and dry snow surface". Low Temp. Sci. Contib. No.2184.

Maeda, J. and Adachi, K.:(1983) "On the spatial structures of longitudinal wind velocities near the ground in strong winds". Journal of Wind Engineering and Industrial Aerodynamics, Vol.15, p197-207.

Mason, P.J. and King, J.C.:(1984) "Atmospheric flow over a succession of nearly two-dimensional ridges and valleys". Quart. J. R. Met. Soc., Vol.110, p821-845.

Meroney, R.N. and Bradshaw, P.:(1975) "Turbulent boundary-layer growth over a longitudinally curved surface". AIAA Journal, Vol.13, p1448-53.

Peterka, J.A., Meroney, R.N. and Kothari, K.M.:(1985) "Windflow patterns about buildings". Journal of Wind Engineering and Industrial Aerodynamics, Vol.21, p21-38

Schmidt, R.A.:(1980) "Threshold wind-speeds and elastic impact in snow transport". Journal of Glaciology, Vol.26, No.94, p453-67.

Schmidt, R.A.:(1982) "Properties of blowing snow". Reviews of Geophysics and Space Physics, Vol.20, No.1, p39-44.

Scorer, R.:(1972) "Clouds of the World". Lothian

Publishing Co. (PTY) Ltd., Melbourne, David and Charles, Newton Abbot.

Simons, D.B., Richardson, E.V. and Nordin Jr., C.F.:(1964) "Sedimentary structures generated by flow in alluvial channels". Report CER 64 DBS-EVR-CFN15, Colorado State University, Fort Collins, Colorado.

Tabler, R.D.:(1980) "Geometry and density of drifts formed by snow fences". Journal of Glaciology, Vol.26, No.94, p405-19.

Tani,I.:(1962) "Production of longitudinal vortices in the boundary layer along a concave wall". Journal of Geophysical Research, Vol.67, p3075-80.

Taylor, P.A.:(1983) "Windflow over conical hills: computer model results". Journal of Wind Engineering and Industrial Aerodynamics, Vol.16, No.1, p119-124.

Troutt, T.R., Scheelke, B. and Norman, T.R.:(1984) "Organised structures in a reattaching separated flow field". Journal of Fluid Mechanics, Vol.143, p413-427.

Vanmarcke, E.H.:(1977a) "Probabilistic modeling of soil profiles". Journal of Geotechnical Engineering Division, ASCE Vol.103, No.GT111, Proc. Paper 13364, p1227-1246.

Vanmarcke, E.H.:(1983) "Random Fields - analysis and synthesis". MIT Press, Cambridge, Massachusetts.

Winoto, S.H., Durao, D.F.G. and Crane, R.I.:(1979) "Measurements within Gortler vortices". Journal of Fluids Engineering, Vol.101, p517-520.

Yalin, M.S.:(1976) "Mechanics of Sediment Transport". 2nd edition, Pergamon Press Ltd., Oxford OX3,OBW, England.

*Young, R. and Conway, H.:(1983) "Comparisons of weather between the Tasman saddle area and Mount Cook village - winter 1983". Unpublished report for Mount Cook National Park.

* References marked thus are included in the appendices.

5. SLOPE STABILITY AND PROBABILILITY THEORY.

5.1 INTRODUCTION.

Slope stability is often described by a sliding equilibrium model. Typically a factor of safety or safety margin is evaluated as some function of predicted resistance and predicted load on a slope, and failure will occur when the resistance is exceeded by the load.

A probabilistic method can be used to complement the above deterministic model. Probability theory recognises that the magnitude of some quantity is not exactly fixed and may vary, and a probability distribution describes the relative likelihood that a random variable will have a particular value. A safety margin which varies across a slope is itself composed of numerous variables, each of which may be described as a stochastic "process", and so the safety margin may also be described as such a process, and its first- and second-order statistics can be evaluated. This provides the basis for our paper "Snow slope stability - a probabilistic approach".

Statistical independence is often assumed between successive values and although this assumption simplifies the representation and analysis, in many cases it is not justified. Often, the value of a variable at one position will be influenced to some extent by the variable at an adjacent position. The degree of influence is reflected in the second-order statistics describing the process, and is commonly represented by a correlation function or by its Fourier transform (the spectral density function). Recently Vanmarcke (1975, 1977a,1977b,1983) proposed a new approach which makes evaluation of the pattern of correlation more attractive than these representations.

5.2 ESTIMATION PROBLEMS.

The Central limit theorem states that under general conditions, the distribution of the sum of random variables converges to the normal distribution as the number of variables in the sum becomes large. Although the Central limit theorem does not require complete independence between

variables, it does require that no single effect (or subset of effects) causes a dominant fraction of the total variance of the variables. Because of this theorem, random variables are often assumed to take a Gaussian or normal distribution.

Commonly we want to estimate the continuous, spatially varying properties of a process from a finite number of "point" observations. For example, for a process which varies in two-dimensions, a "best" estimate of the process at each of a number of locations may be determined by linearly combining the observations at a number of other locations. The criteria for making the estimates are that the prediction be unbiased and the mean square of the prediction error be minimised. Krige (1966) applied these methods to geological phenomena, and subsequently these techniques have been used for many applications (see for example Matheron,1967 or Delhomme,1983)

Given the first- and second-order statistics of a random process, a computer simulation method can also be used to generate the random variables. A commonly used method is a Monte-Carlo simulation which determines the distribution of a function of random variables by performing repeated computations using randomly selected point estimates for the component variables. The random variables are selected to conform with the assumed distribution of each variable. For example Nguyen and Chowdhury (1985) used a simulation process to generate a probability distribution for water draw-down in a soil. They assumed the individual variables followed a normal distribution and a joint normal distribution existed between correlated variables. The computer simulation used an equation of the form:

$$X = \sigma Y + \mu$$

where Y was a standardised variate corresponding to the variable X with mean μ and standard deviation σ. Y takes values between 0 and 1, and is randomly selected. Simulation techniques have not yet been extended to model spatial variability of a process.

5.3 SCALE OF FLUCTUATION.

Vanmarcke (1975,1977a,1977b,1983) introduced a method of

describing the autocorrelation between values of a spatially varying process, which remained tractable even when the process varied in two-dimensions. The basis of his model was to study the behaviour of the spatial average of the original process which could be described as a new process in which the microscale fluctuations were smoothed and the variance was less. As the averaging size increased, more fluctuations cancelled. Vanmarcke described the decay of the variance in terms of a "scale of fluctuation". The scale defines the size at which increased averaging commences to have a significant influence on the variance. He showed how a function using this scale was equivalent to a correlation or spectral density function, especially for the larger averaging sizes.

For processes with no long term memory, the scale tends towards zero, and the variables are essentially uncorrelated. On the other hand, for broad-band processes, the components of the function may be complex, and because of the way in which the variance decays, the scale contains information about low as well as high frequency content of the process. The variance decay and scales for some measurements of strength we have made across slopes are discussed later in this section.

5.4 EXTREME VALUES OF A RANDOM PROCESS.

For slope stability estimates we are particularly interested when the safety margin takes values less than a threshold level and failure results (ie. less than zero). This type of event has been studied extensively, mainly with respect to time-series processes. (for example, Rice,1944, Cramer and Leadbetter,1976, Crandall, Chandiramani and Cook,1966, and Vanmarcke,1975,1983). Typically the crossings of such a threshold are modelled by considering the crossings/no-crossings to be a binary random series, and therefore described by a binomial distribution. If the threshold level is far away from the mean value of the process, the crossings become increasingly rare, and may be considered to be independent. In such cases, the binomial distribution converges to a Poisson distribution, which simplifies the mathematics of solving the probability distribution. This was the basis of the work done by Rice

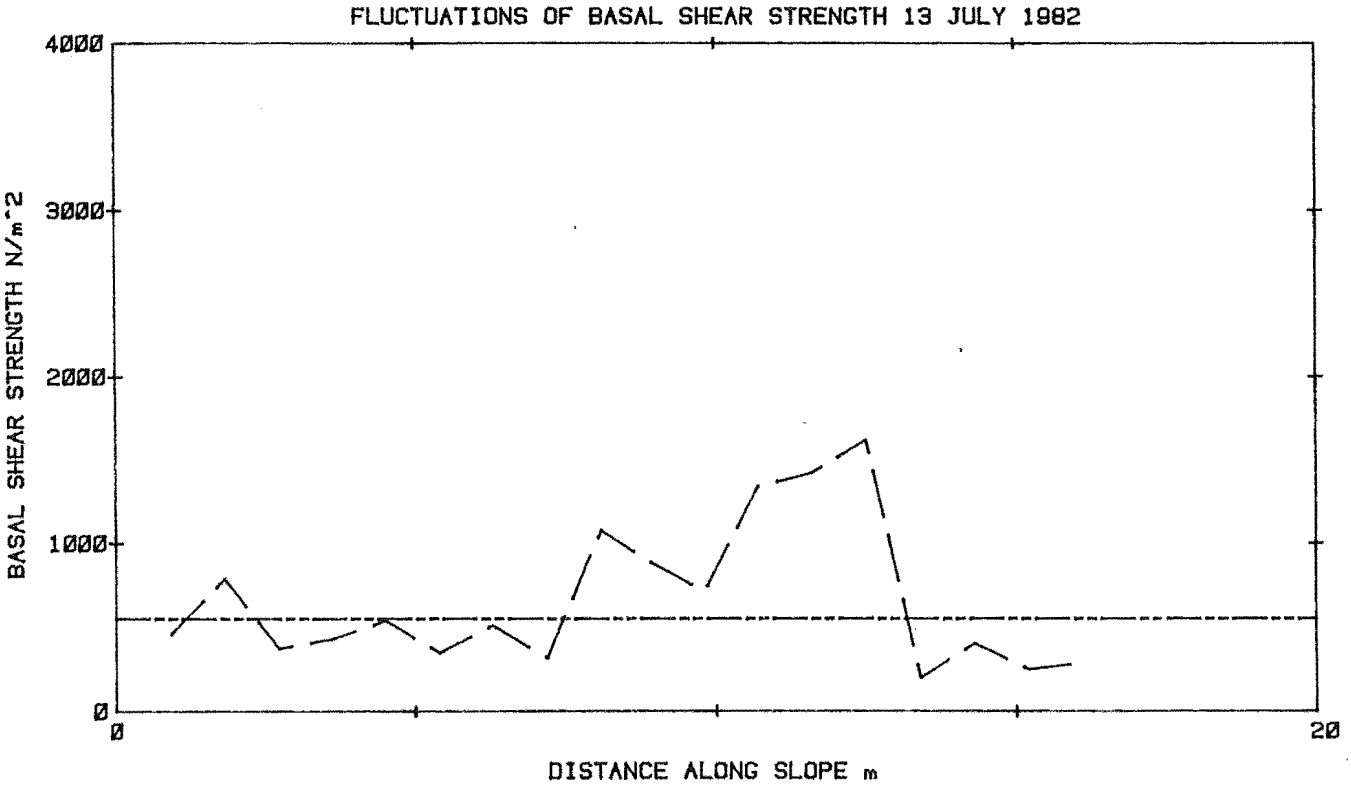

Figure 5.1

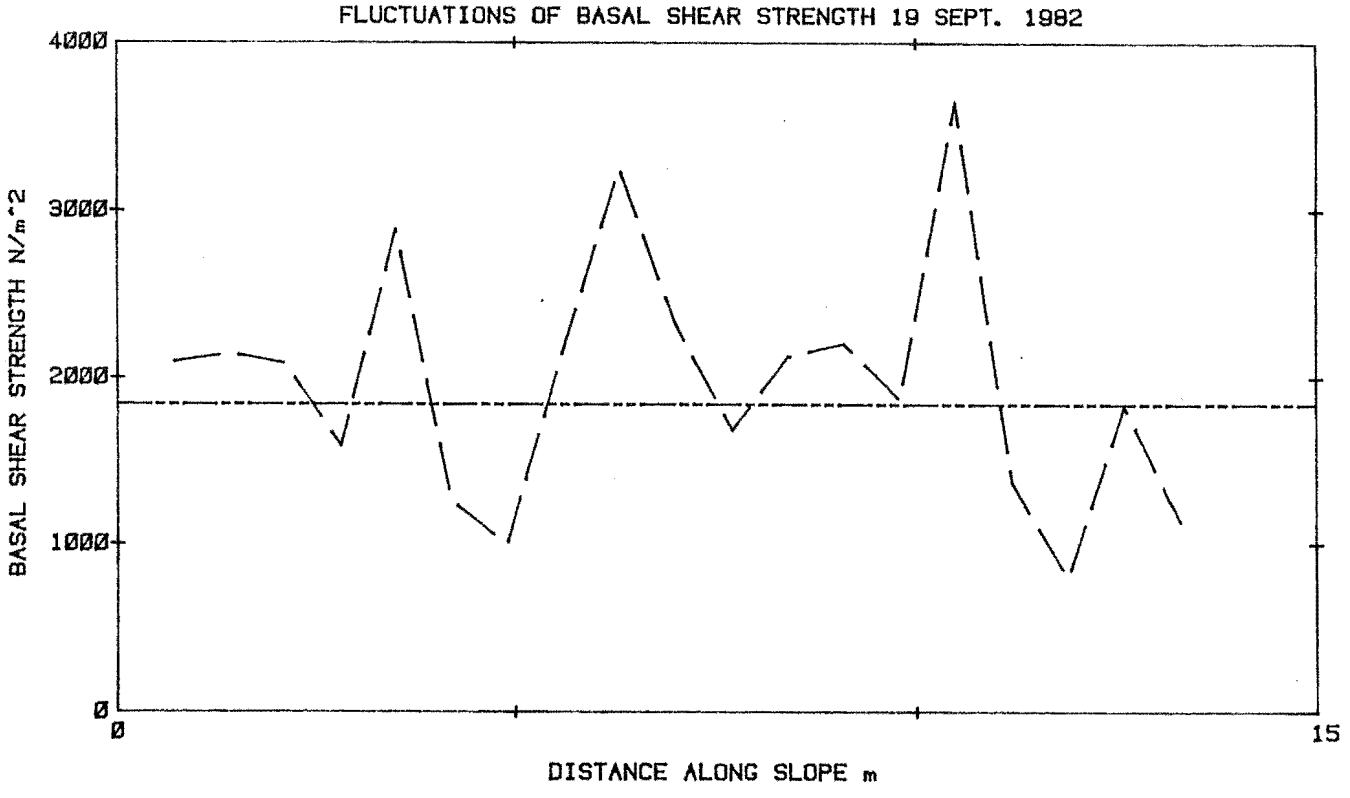

Figure 5.2

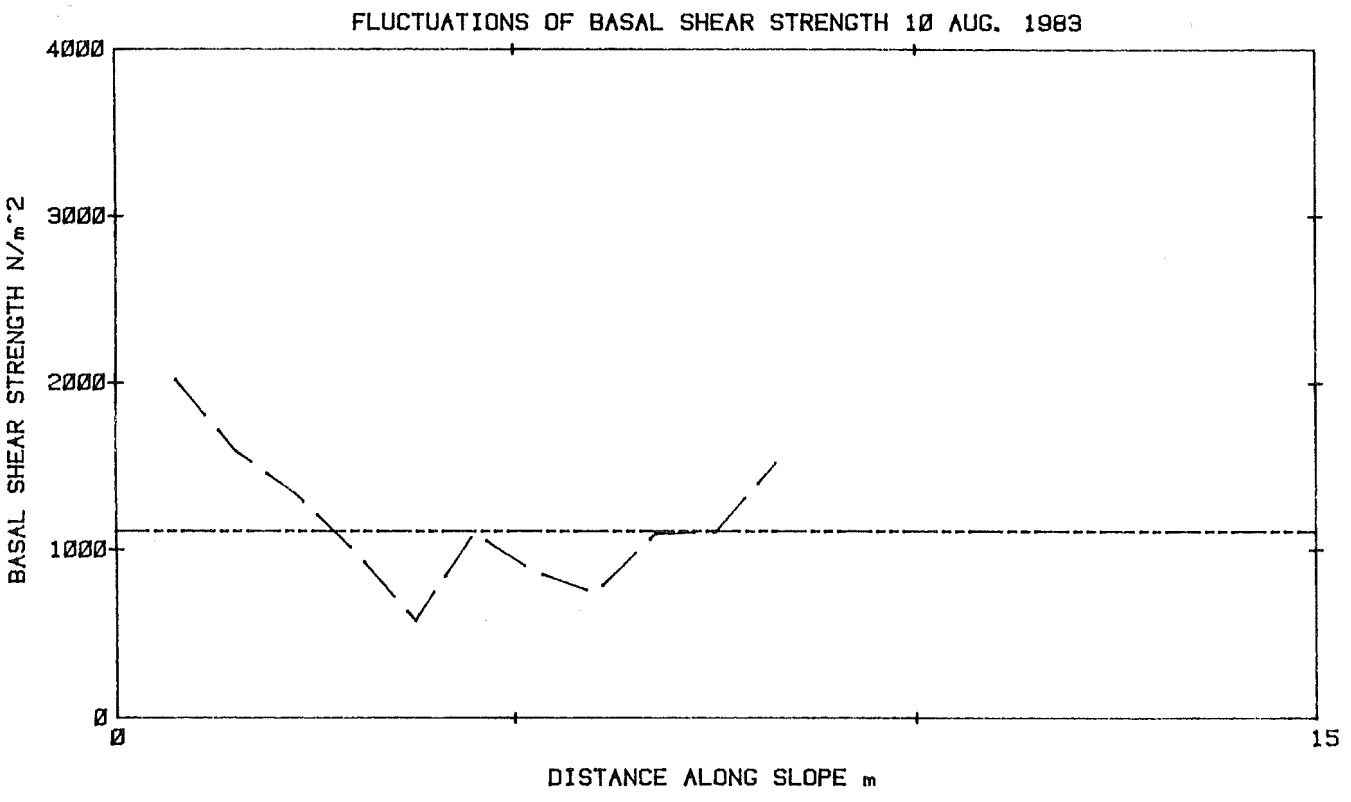

Figure 5.3

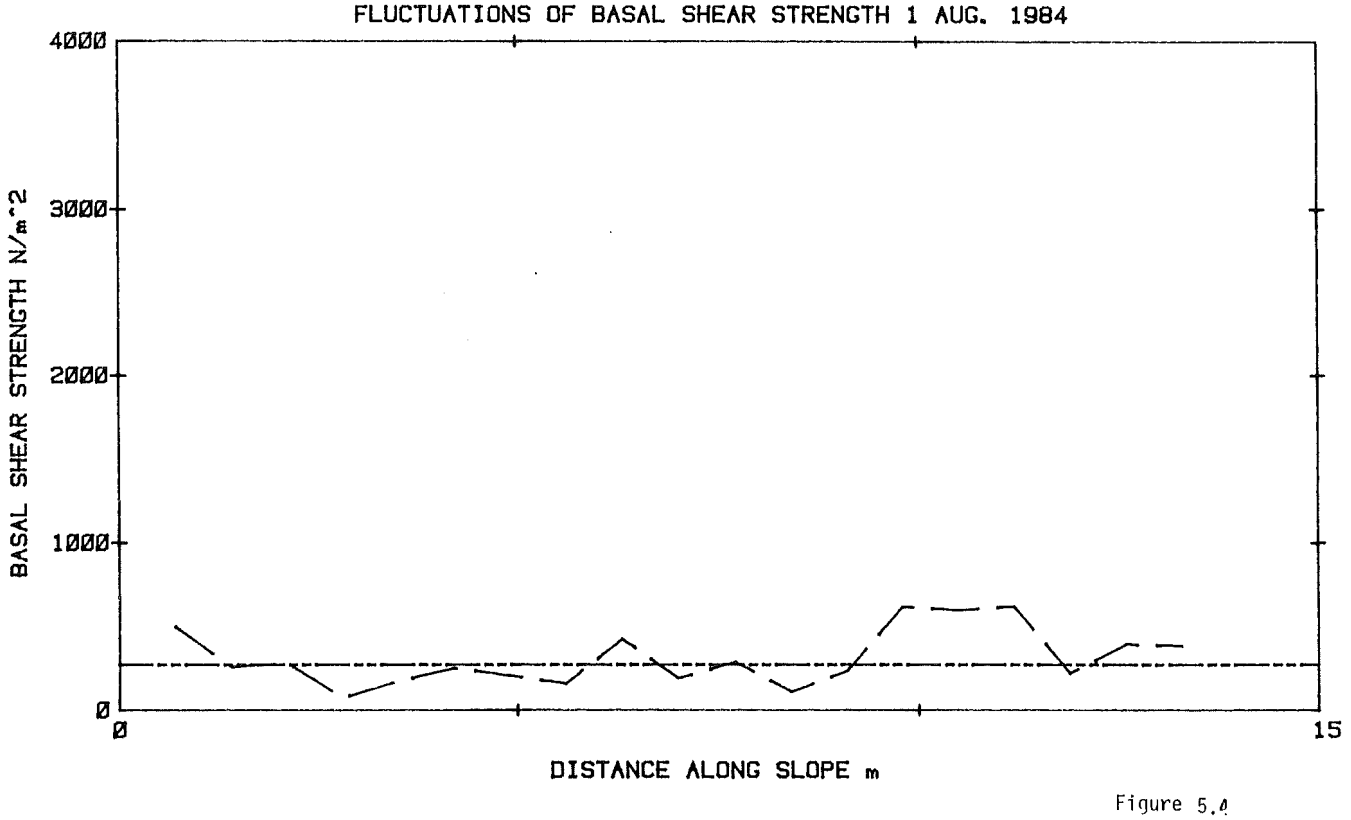

Figure 5.4

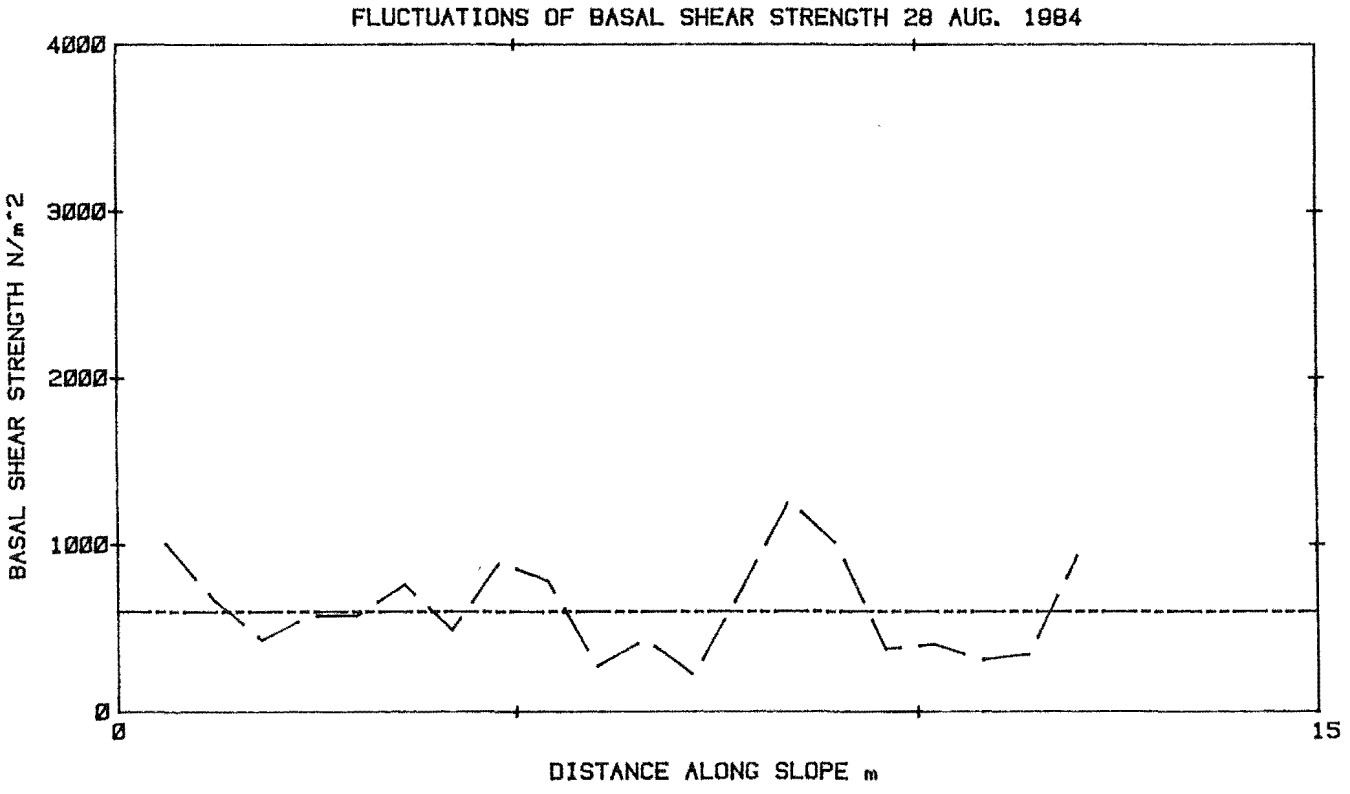

figure 5.5

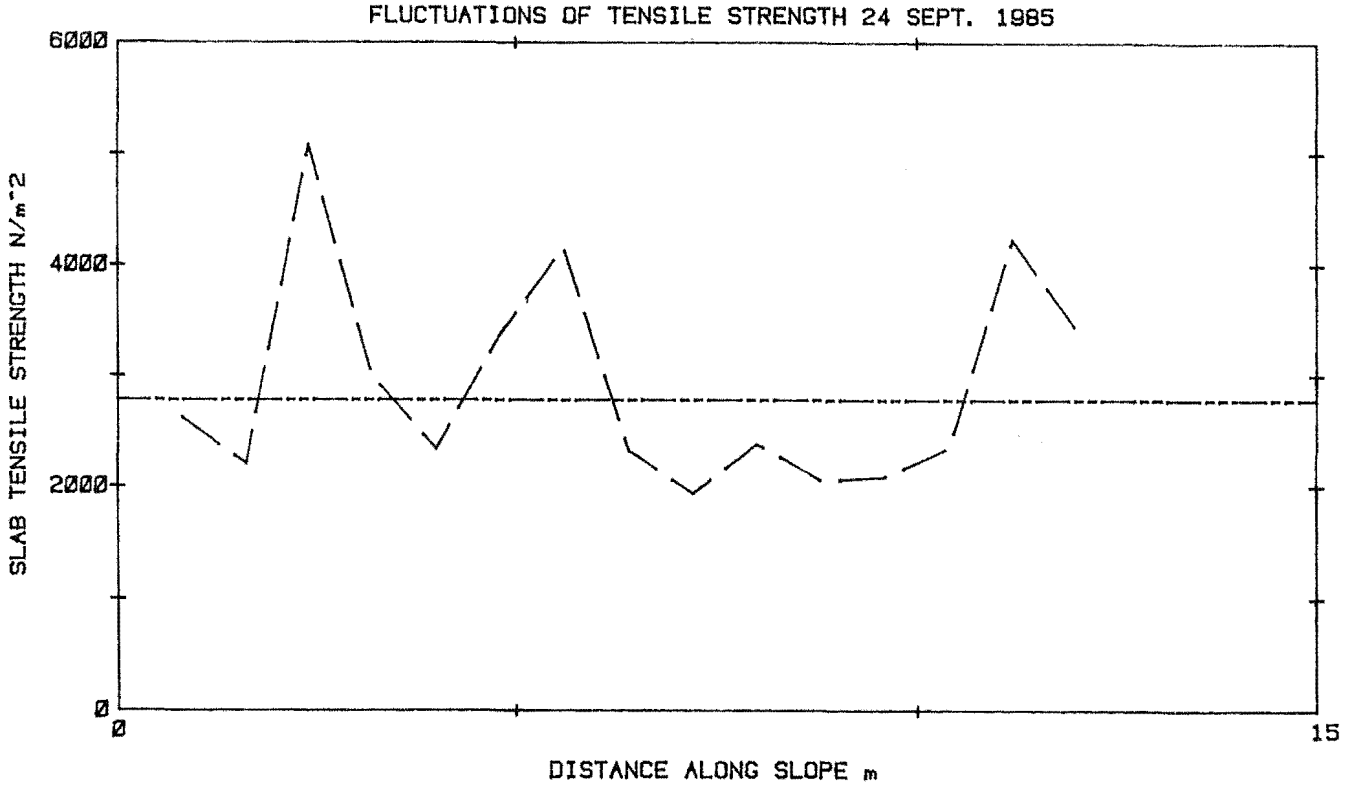

Figure 5.6

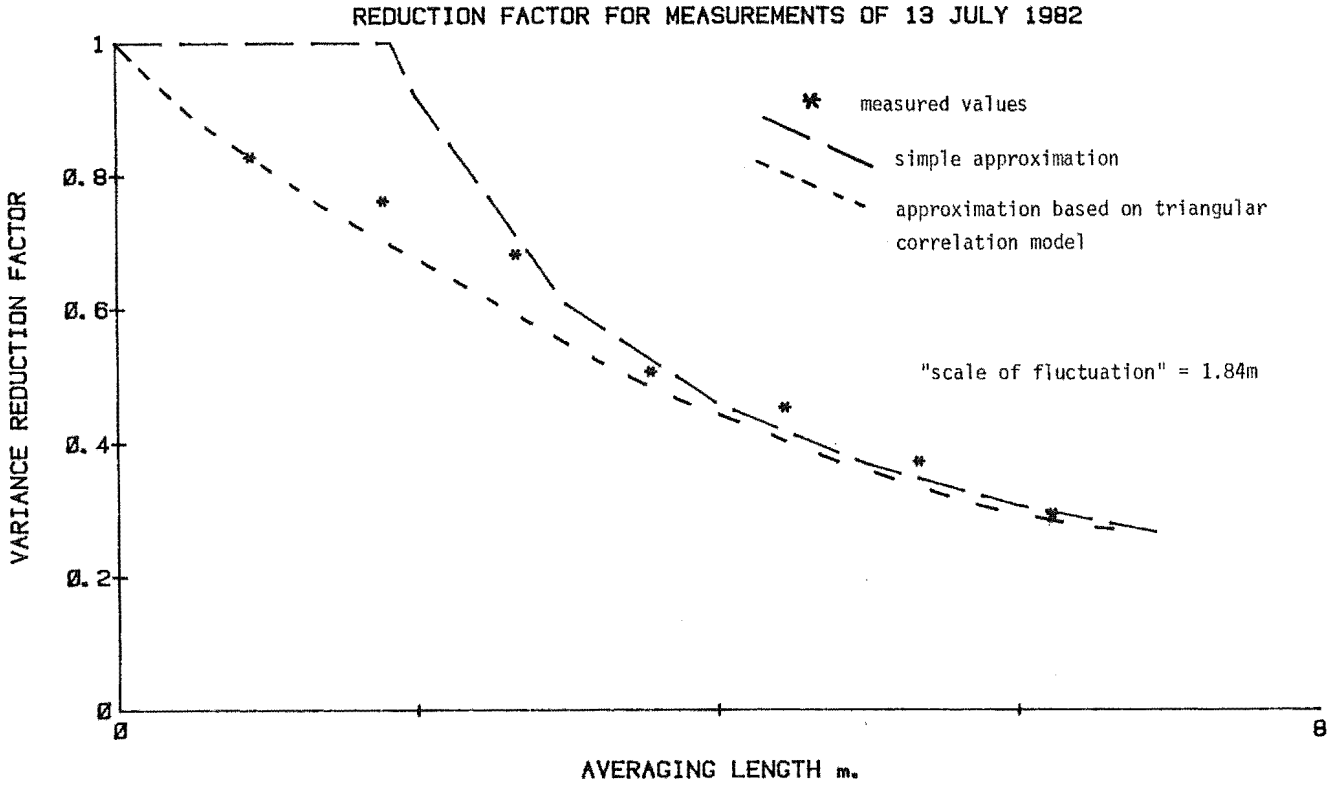

Figure 5.7

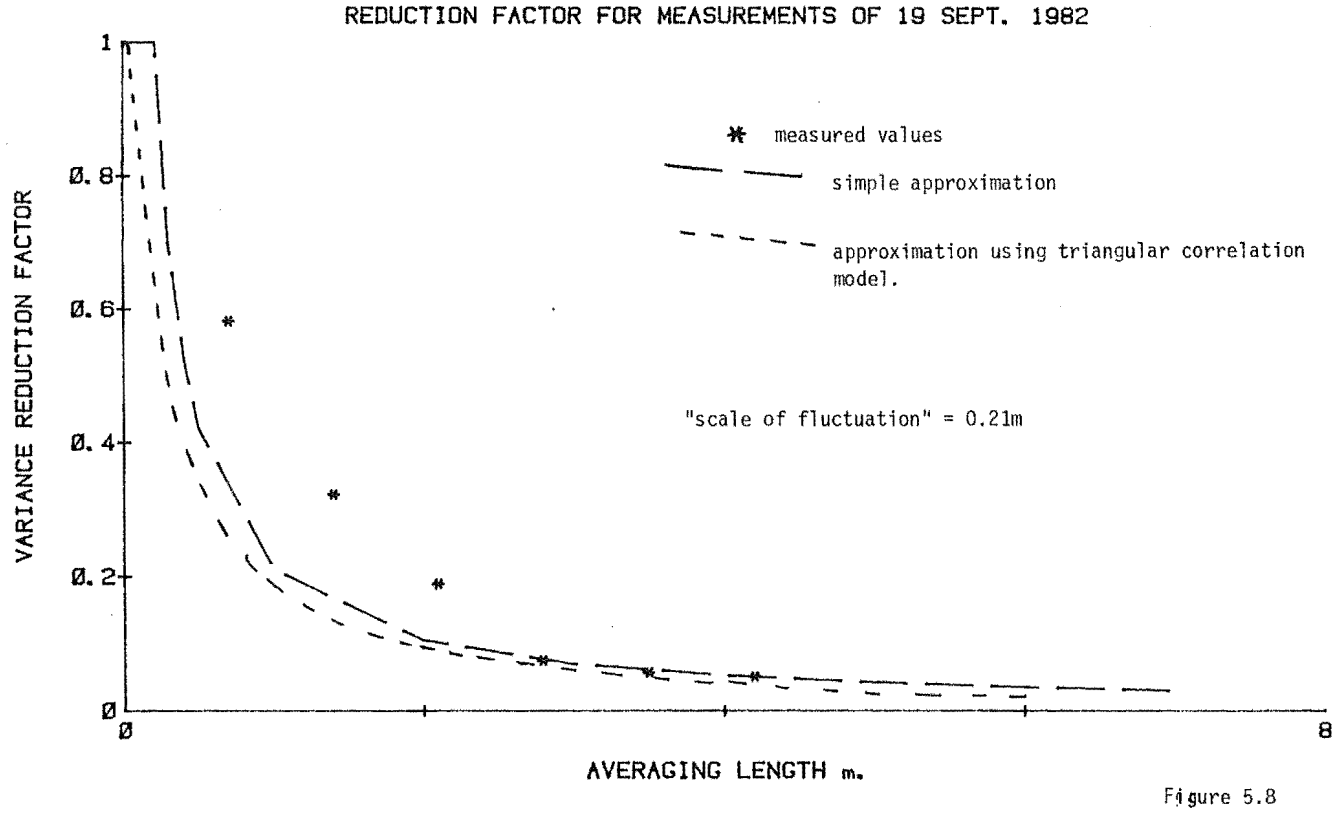

Figure 5.8

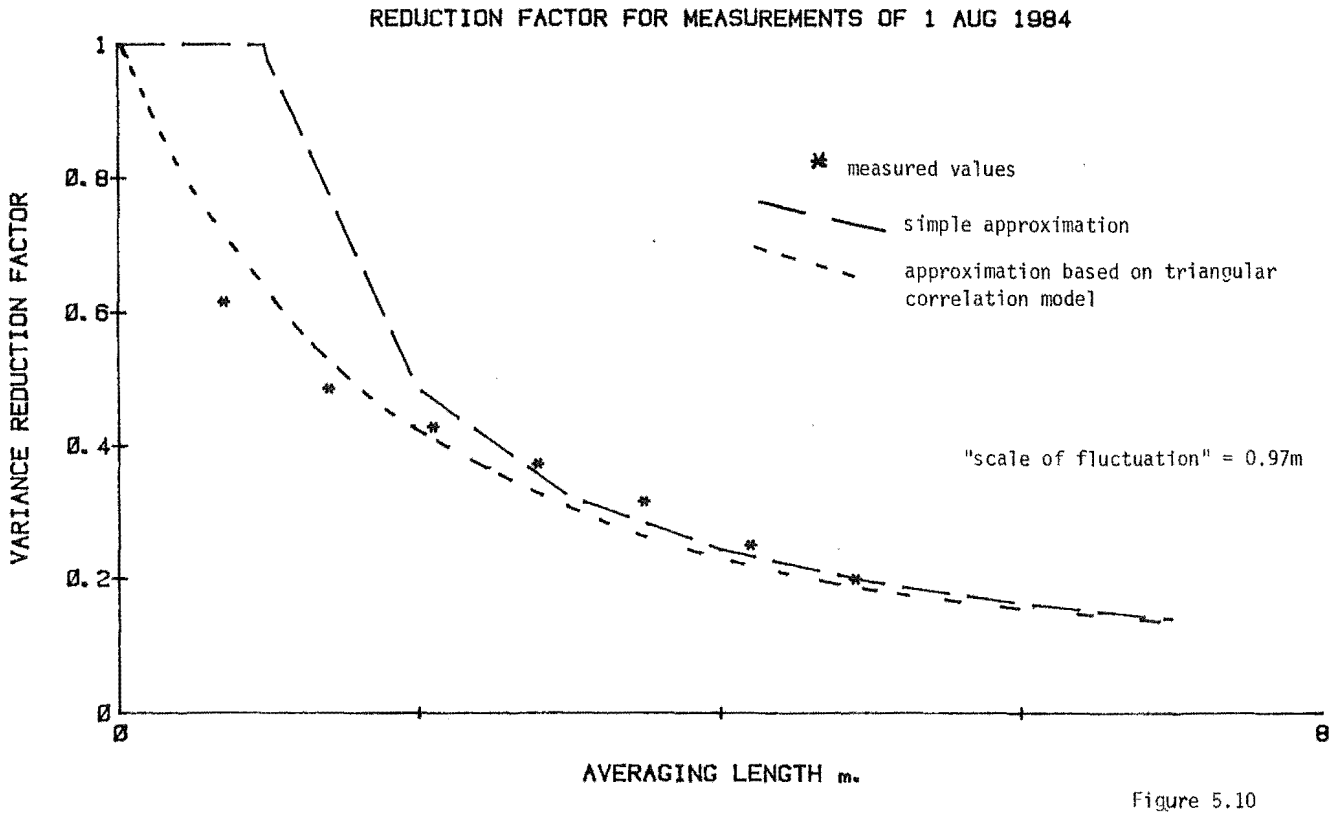

Figure 5.10

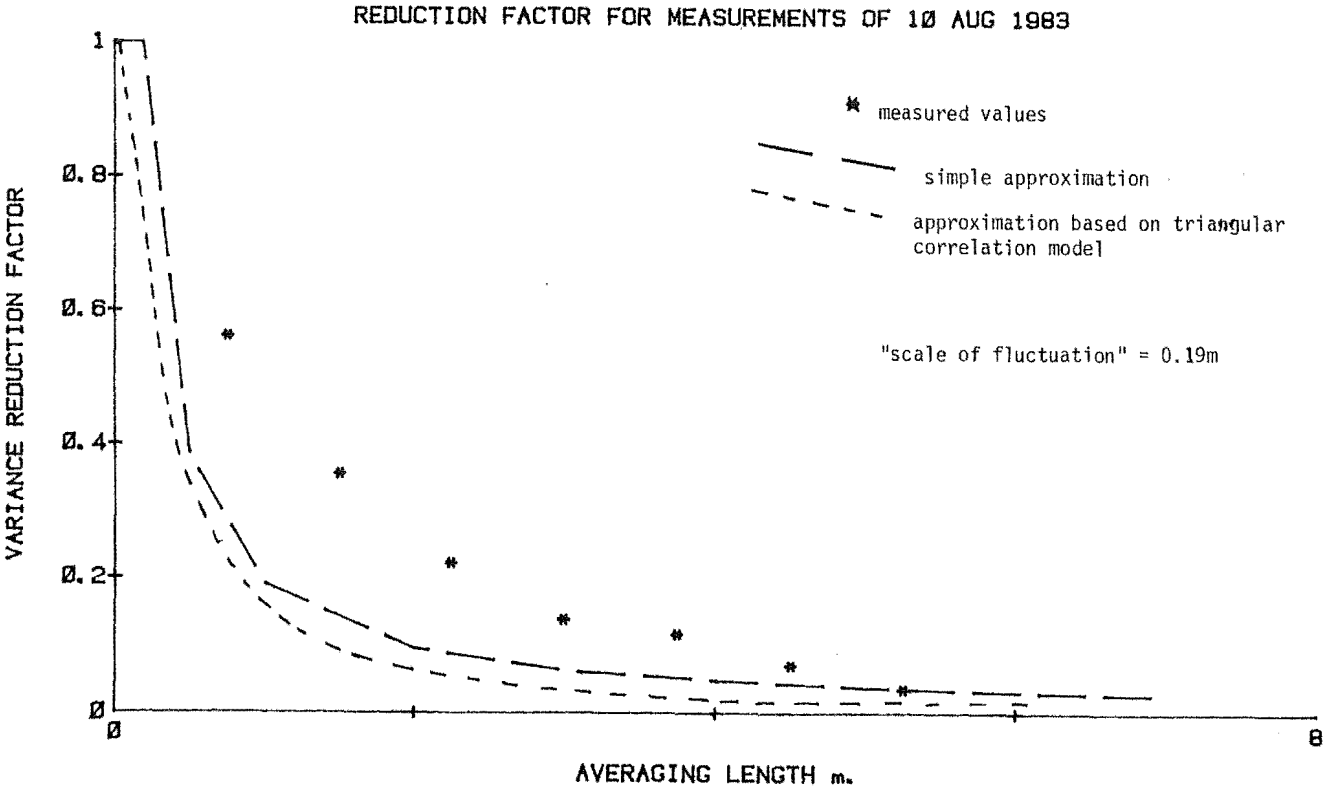

Figure 5.9

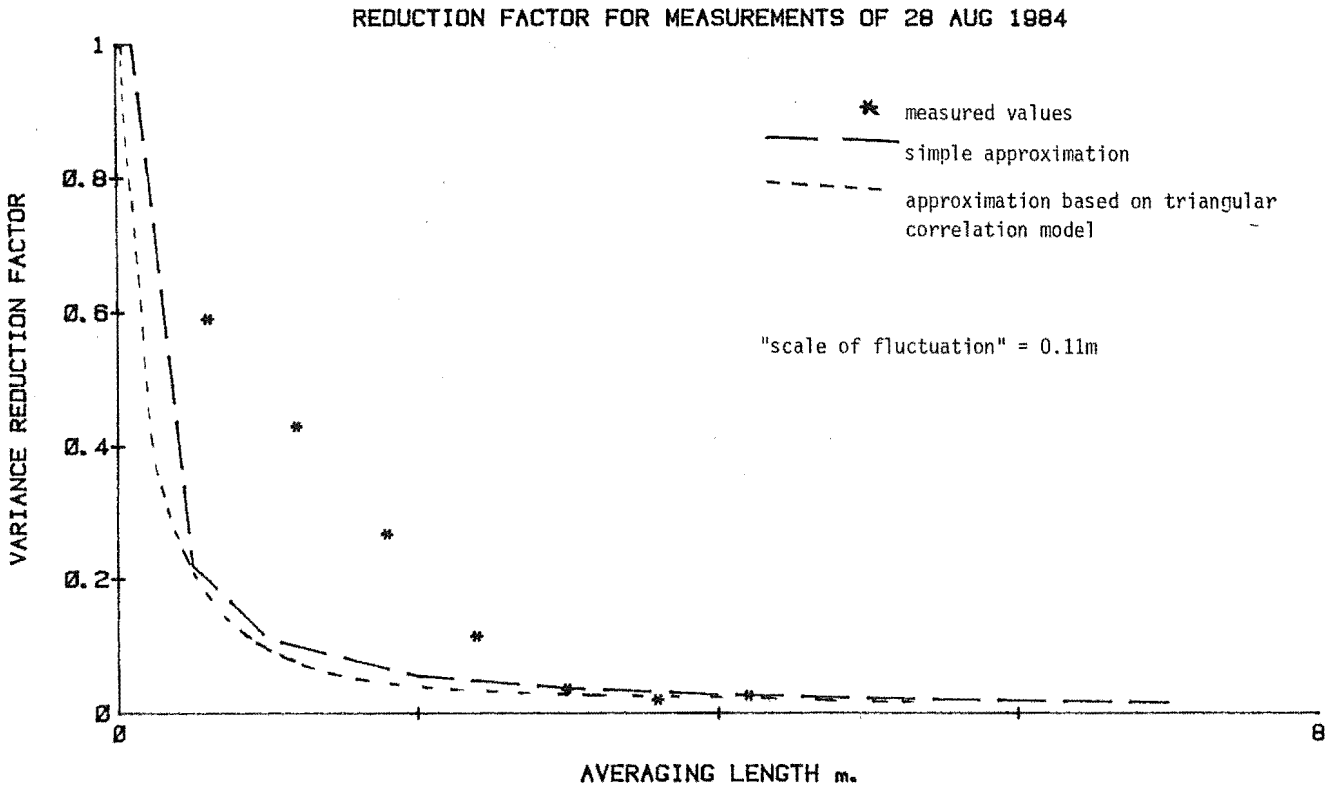

Figure 5.11

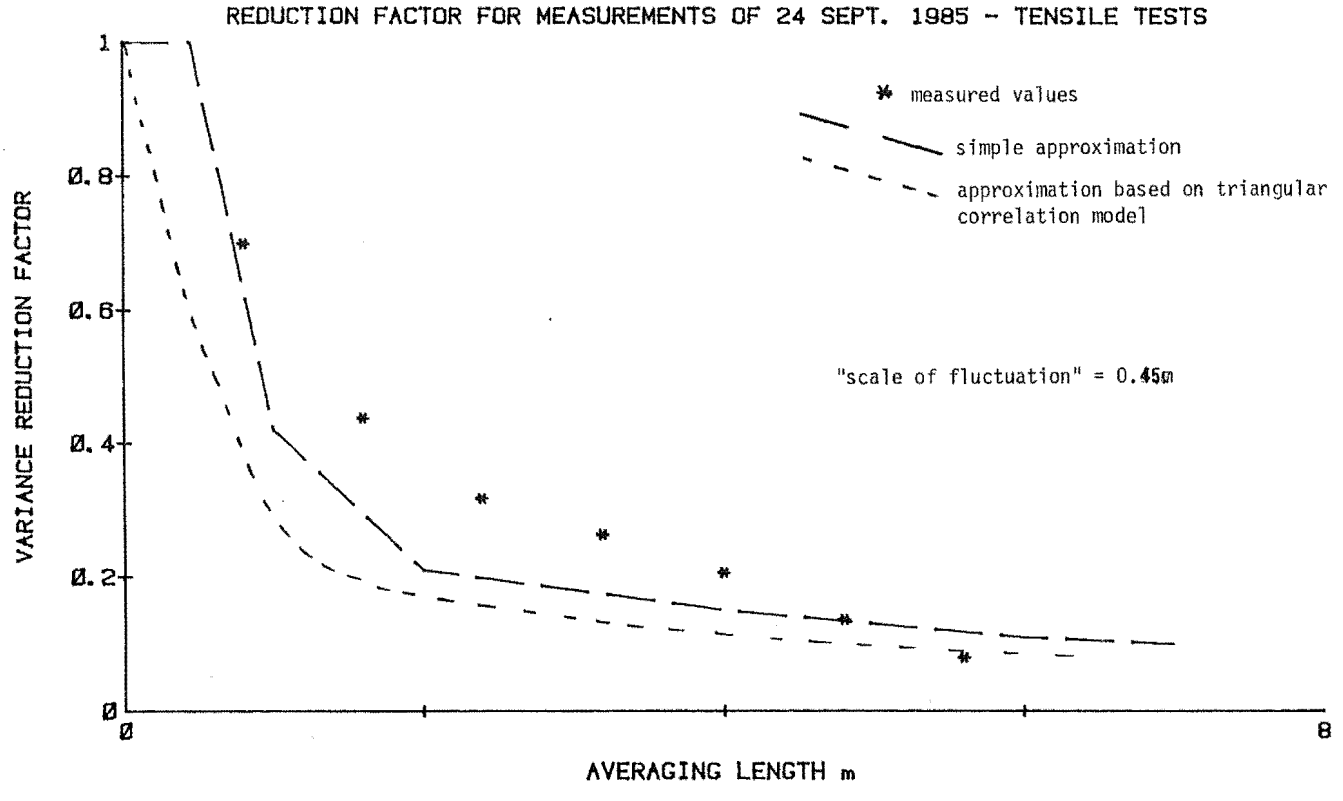

Figure 5.12

(1944), who derived an expression for the mean rate of crossings of an arbitary level by a one-dimensional random process.

If the crossings cannot be considered to be independent (for example if the threshold level for the process is not high), the Poisson distribution may not adequately describe the crossings, and Vanmarcke (1983) showed how it was possible to allow for "clumping" of values. "Clumping" refers to conditions when the crossings are clustered, and more than one peak occurs during each crossing of the threshold level. In these cases, the period spent above (or below) the threshold increases, and the interval between crossings also increases. Vanmarcke (1983) showed how the Poisson distribution could still be used to model the "clump arrivals", provided a reduced "mean rate of crossing" was used in the calculations.

Vanmarcke (1977a,1977b) applied the "moving average" approach to the equation derived by Rice (1944), and used the model to describe soil properties, in particular strength. In Conway and Abrahamson (1985), we have used Vanmarcke's approach, and adapted the techniques to model snow slope stability. Below, we present further analysis of some measurements, in particular those of strength across slopes.

5.5 SPATIAL MEASUREMENTS OF SNOW PROPERTIES.

For stability assessment we are interested in knowing the existance of extremely low values of snow strength, and the likely spatial distribution of these values. The method of making the tests has been described elsewhere (Conway and Abrahamson,1984a).

Following Vanmarcke (1977a,1983), the decay of variance when averaging over a process over lengths b, can be described by a variance function:

$$\Gamma^2 = Var(u_b)/Var(u_0) \qquad (1)$$

where $Var(u_0)$ is the variance of "point" values of the process, and $Var(u_b)$ is the variance of measurements which have been averaged over a length b.

For many cases, the analytical model

$$\Gamma^2 = 1 \qquad b<\delta \qquad (2)$$

$= \delta/b \qquad b>\delta$

provides a reasonable approximation of the true variance function, especially when b exceeds about 2δ. This approximaton implies the correlation function:

$\rho(\tau) = 1 \qquad |\tau|<\delta$

$= 0 \qquad |\tau|>\delta$

where $\rho(\tau)$ is the correlation function for the process.

A triangular correlation function improves the representation, and takes the form,

$\rho(\tau) = 1 - |\tau|/\delta \qquad |\tau|<\delta$

$= 0 \qquad |\tau|>\delta$

The corresponding variance function is

$\Gamma^2 = 1 - b/3\delta \qquad b<\delta \qquad (3)$

$= (\delta/b)(1 - \delta/3b) \qquad b>\delta$

We have made five sets of shear strength measurements at regular spacings, and one set of tensile strength measurements.These are listed in the appendices. We programmed a computer to manipulate the data.

Figs.1-6 show plots of the spatial variations of "point" values (ie single measurements) across each slope studied. These plots consistantly show a pattern of short-scaled fluctuations about a mean. Under spatial averaging, on most slopes the mean changed less than 12%, which suggests the assumption of statistical homogeneity is suitable. The mean of the data from 13 July 1982 changed by 30% under averaging, which suggests the mean strength may have been slowly changing, and statistical homogeneity may only apply over small lengths. Again for this analysis, as a first approximation, we consider all our measurements to be statistically homogeneous.

Figs.7-12 show the decrease of variance with spatial averaging of each set of measurements. Comparison of the experimental variance function with the simplest analytical model (eqn.2), in most cases shows good agreement, especially when $b>2\delta$. For measurements made on 13 July 1982 and 1 August 1984, use of a model based on a triangular correlation function (eqn.3) improved the representation of experimental

data in the lower range. We think failure initiates over small areas of the order of $1m^2$ (Conway and Abrahamson,1985), and so are particularly intersted in the strength characteristics over these small areas. In that paper, we described the variance decay using experimental values (eqn.1).

Over the distances sampled, for four sets of measurements, the scale of fluctuation was in theory less than the sampling interval. This means these random series were uncorrelated, and the "scale" was taken to be equal to the sampling distance. The other two sets of measurements showed some correlation (1.84m on 13 July 1982, and 0.97m on 1 August 1984), but these scales were also relatively small.

A scale of fluctuation is related to the wavelength λ of a variable considered as a periodic function, and Vanmarcke (1977a,1983) showed an approximate relation to be

$$\lambda = 2.5\delta \qquad (4)$$

The maximum δ calculated from our strength measurements was 1.84m (13 July 1982), and using this length in eqn.4 shows the expected average wavelength to be less than 4.6m. This pattern of typically short-scaled fluctuations of strength is confirmed by the graphic representations in figs.1-6. Although most of these measurements were of shear strength, we do have one set of tensile strength measurements, and the pattern was found to be typical also of snow depth measurements.

In the section ("Influences of wind on snow distribution") and also Conway and Abrahamson (1985), we discussed the possible causes of the short-scaled fluctuations, and the effect of such fluctuations on a safety margin and slope stability. Further, a short scale determines that for a good estimate of strength, the sampling interval should also be short. We proposed a new "saw test" to enable rapid sampling of snow strength (see "A simple field test of snowslope stability" Conway, Abrahamson and Young,1985).

5.6 CONCLUSIONS.

We applied the probabilistic approach suggested by Vanmarcke (1975,1977a,1977b,1983) to snow strength. Spatial measurements of strength show that values typically fluctuate over short scales. For stability assessment, we found areas most likely to fracture were often about $1m^2$, and for many slopes, strengths over areas of this size could be considered to be uncorrelated. Although this assumption may not be strictly correct, it simplifies analysis of stability. On the other hand, the small likely fracture areas, combined with large variations (about 50% standard deviation for shear strength data) over short scales, requires multiple sampling at close intervals to ascertain the strength characteristics.

Our proposed "saw test" described elsewhere, partially fulfils these requirements.

5.7 REFERENCES.

Chowdhury, R.N.: (1978) "Propagation of failure surfaces in natural slopes". Journal of Geophysical Research. Vol.83, No.B12, p5983-88.

Chowdhury, R.N. and A-Grivas, D.:(1982) "A probabilistic model of progressive failure of slopes". Journal of Geotechnical Engineering Division, ASCE, Vol. 108, No. GT6, p803-819.

*Conway, H. and Abrahamson, J.:(1984a) "Snow stability index". Journal of Glaciology, Vol. 30, No. 106, p321-7.

*Conway, H. and Abrahamson, J.:(1985) "Snow slope stability - a probabilistic approach".

*Conway, H., Abrahamson, J. and Young, R.:(1985) "A field test to assess snow stability".

Crandall, S.H., Chandiramani, K.L. and Cook, R.G.:(1966) "Some first-passage problems in random vibration". Journal of Applied Mechanics, Vol.33, trans. ASME, Vol.88, series E, p532-538.

Delhomme, J.P.:(1983) In "Flow through Porous media" (G.F. Pinder, ed.), Computational Mechanics, Great Britain.

Harr, M.E.:(1977) "Mechanics of Particulate Media". Chapter 11, p403-54, McGraw-Hill, New York, N.Y.

Lomnitz, C. and Rosenbleuth, E.:(1976)" Seismic risk and engineering decisions" Elsevier, The Netherlands.

Matheron, G.:(1967) "Kriging or polynomial interpolation procedures".Canadian Inst. of Mining Bulletin, Vol.60, p1041.

Morla Catalan, J. and Cornel, C.A.:(1976) "Earth slope reliability by a level crossing method". Journal of Geotech. Eng. Div., ASCE, Vol.102, No.GT6, p591-604.

Nguyen, V.U. and Chowdhury, R.N.:(1985) "Simulation of risk analysis". Geotechnique, Vol.35, No.1, p47-58.

Vanmarcke, E.H.:(1975) "On the distribution of the first-passage time for normal stationary random processes". Journal of Applied Mechanics, trans. ASME, Vol.42,p215-220.

Vanmarcke, E.H.:(1977a) "Probabilistic modeling of soil profiles". Journal of Geotech. Eng. Div., ASCE, Vol. 103, No. GT11, p1227-1246.

Vanmarcke, E.H.:(1977b) "Reliability of earth slopes". Journal of Geotech. Eng. Div., ASCE, Vol. 103, No. GT11, p1247-1265.

Vanmarcke, E.H.:(1980) "Probabilistic stability analysis of earth slopes". Engineering Geology. Vol.16, No. 1, p29-50.

Vanmarcke, E.H.:(1983) "Random Fields, analysis and synthesis". MIT Press, Cambridge, Massachusetts.

Whitman, R.V.:(1984) "Calculated risk in Geotechnical engineering". Journal of Geotech. Eng. Div., ASCE, Vol. 110, No. 2, p145-188.

* References marked thus are included in the appendices.

6.1 CONCLUSIONS AND FURTHER STUDIES.

We have estimated shear and tensile strengths from simple tests, and made measurements over slopes. The measurements were characterised by large variability over short distances. and we attributed most of this variability to effects of wind transport and deposition of snow.

The strength measurements were then used in a deterministic model which balanced forces over a slice of snow. A failure would occur if the forces driving the slice down-slope exceeded the restraining forces. Probability theories are useful to describe variability of a property and, in conjunction with a deterministic approach, a powerful technique for assessing slope stability. We applied these techniques using measurements from several slopes to determine a slope reliability index. We were able to correctly assess stability in four out of five slopes (see "Snow slope stability - a probabilistic approach").

A model which considered stress-strain relationships and the temporal as well as the spatial variability, should yield an improved representation of stress conditions in the snow. Our tensile and shear tests which incorporated a strain gauge to measure movement, were an attempt to gather such data.

Because we could not control stress- and/or strain-rates, the tests were only partly successful and further work developing a test with better control of rate is required. Parameters obtained from such tests could then be used as input into a more sophisticated model. It is well known that the stress required to fracture by crack propagation is generally smaller than the yield stress, and fracture mechanics studies which determine the stress field in the vicinity of a crack tip might best represent snow slope failure. Such models are commonly based on an energy balance, and may also incorporate non-linear strain expected during slow failures.

Continued application of powder models may help to identify the effect of crystal structure on strength and the mechanics of bonding and fracture. Our air permeability device did give an indication of snow structure, but we are have not adequately related the permeability to strength. More permeability tests in conjunction with measurements of strength may help to clarify such a relationship, if in fact one does exist.

The most important outcome from this study has been the recognition of spatial variability of strength over short distances. Further, we have shown how variability can strongly influence slope stability, and have proposed a new field test to assess stability ("A field test to assess snow stability").

If the patterns of fluctuations can be attributed to the influence of wind on snow, further study of this phenomenom may enable one to spatially locate a critical weak area without extensive testing of strength. Such knowledge would improve not only estimates of stability at particular sites, but also provide a firmer base for forecasting avalanches from weather observations.

APPENDICES.

(1) Snow slope stability - a probabilistic approach.

(2) A field test to assess snow slope stability.

(3) Remote sensing of snow accumulation.

(4) Snow stability index.

(5) Air permeability as a textural indicator of snow.

(6) Snow and avalanche research at Tasman Saddle - a progress report of the winter,1984.

(7) Mountain avalanche forecasting using meteorological data from Mt Cook village.

(8) Comparisons of weather between the Tasman Saddle area and Mt Cook village, Winter 1982.

(9) A summary of weather and snow conditions at the Tasman Saddle area during the winters of 1980-1982.

(10) Tasman Saddle snow studies, 1981. Insitu tests of large volumes of snow.

(11) Tasman Saddle snow studies, 1981. Weather data report, winter 1981.

(12) Tasman Saddle snow studies, 1981. Air permeability as a measure of snow structure.

(13) Summary of measurements of snow properties.

SNOW SLOPE STABILITY - A PROBABILISTIC APPROACH

By H. Conway and J.Abrahamson,
(Department of Chemical and Process Engineering, University of Canterbury, Private Bag, Christchurch, New Zealand.)

ABSTRACT.

An analysis of the likelihood of snow slope fracture has been made using a probabilistic description of snow properties. Measurements made across a number of slopes have been used in a deterministic model which considers the downslope components of forces on a snow slab, giving a failure when the driving forces exceed the resisting forces. The use of probability theory in conjunction with such a limit equilibrium model recognises variations in the values of the driving and resisting terms, and allows an estimation of the reliability of a slope.

Analysis of five cases (four avalanche events and one non-avalanched slope) by these methods indicate that avalanches initiate from small local failures (about $1m^2$ area) before propagating across other areas. The criteria for propagation are considered to be more crucial for estimating slope stability than those for the initiation of the local failure.

INTRODUCTION.

Limit equilibrium models.

Limit equilibrium models applied to slopes consider the mass of a section of slope as a free body with external boundaries including a lower boundary along a discontinuity or slip surface. The free body is subjected to the action of a driving force (in this case, the gravitational weight), and a resisting force (the resultant of stresses on the boundaries). On each body, a safety margin can be defined:

SM = [Sum of resisting forces - Sum of driving forces] (1)

By definition, a local failure will occur when the sum of driving forces exceeds the sum of resisting forces, ie. SM<0.

Limit equilibrium analyses have been applied extensively to classical soil mechanics problems for many years (eg Bishop,1955; Morgenstern and Price,1965; Spencer,1967). Although development of numerical techniques such as finite element and finite difference methods have enabled rigorous analysis of stress within bodies, the simplified limit equilibrium concepts can still be used successfully in practical problems (Chowdhury,1980).

Probability theories using limit equilibrium analysis.

There is generally an uncertainty in the values of the resisting forces and the driving forces. If one takes them as random variables, the safety margin is also a random variable (see for example Harr,1977 or Whitman,1984).

The safety margins across a slope may be described by a stationary random process. The correlation structure of such a process is commonly represented either by its correlation function or by its Fourier transform, but Vanmarcke (1975,1977a,1977b,1980,1983) has proposed a new approach somewhat more attractive for assessing slope stability. He has used a "moving average" approach to describe correlation, and this has suited stability calculations very well. For a specific area, a safety margin and its standard deviation can be evaluated by considering the driving and resisting forces. As the size of the averaging area increases, although the mean safety margin (per unit area) would not change significantly, fluctuations around the mean tend to cancel each other. Thus the variance of the mean safety margin per unit area diminishes as the averaging area increases.

For processes varying in one dimension Vanmarcke defined simple functions characterised by a "scale of fluctuation" δ, which describe the decay of the variance with spatial averaging over a larger length (b), and showed how this variance decay was related to the correlation function of a process. His simplest function was:

$$\Gamma^2 = \mathrm{Var}(u_b)/\mathrm{Var}(u_0)$$

$$=1 \qquad b<\delta \qquad (2)$$

$$=\delta/b \qquad b\geq\delta$$

where $Var(u_o)$ and $Var(u_b)$ are respectively, the variances of the "point" values, and values which have been averaged over length b.

Vanmarcke also showed how these techniques could easily be extended to processes which varied in more than one dimension. For each specific area, a probability distribution can be used to describe the likelihood that a safety margin will take a particular value. The risk of failure for that area is the probability that the safety margin will be less than zero, ie., $p_f = p[SM<0]$. As the averaging area increased, this probability at first increased because of the decreasing mean safety margin (body weight growing faster than the resisting forces) and then diminished because of the reduced standard deviation. A critical failure area was defined to be the area at which the probability of failure was maximised.

By calculating failure probabilities from values of strength that had been averaged, highly localised extremely low strength values which would not affect the system as a whole, could essentially be ignored. If on the other hand the area of low strength was sufficiently large, slope stability would be affected.

For slope stability, we are particularly concerned when the safety margin becomes negative. Such an occurrence can be descibed by a binomial probability distribution, with the probability of failure in each of N "critical failure" areas assumed equal. If each failure can be considered to be statistically independent, it is easy to show the probability of a failure occurring somewhere on the slope is (Harr,1977):

$$P = [1 - (1-p_f)^N] \qquad (3)$$

where p_f is the probability of failure of an area.

More likely, the safety margins of neighbouring areas will not be independent, and will be correlated. It is then convenient to use a "first crossing" technique to determine the probability that the safety margins will become negative. Rice (1944) derived an expression for the mean rate of crossings of an arbitary level by a one-dimensional random

process. He assumed the process was Gaussian and the crossings were rare and therefore independent (ie.the threshold level was far from the mean and the crossing probability small), and so could be described by a Poisson distribution.

Vanmarcke applied the "moving average" approach to Rice's equation, and derived an expression which was tractable, even for processes which varied in more than one dimension. By applying the methods to slope stability, for a particular sized slope Vanmarcke (1977b) calculated the probability of a failure occurring somewhere on the slope.

Progressive failure using limit equilibrium analysis.

Using the previous analysis, one can determine (a) the most likely size of local failure and (b) the probability of occurrence somewhere over a slope. The effect of a local failure will be to cause transfer of stress from one section to another. Therefore an important consideration for slope stability is the probability of the local failure progressing to other areas. Law and Lumb (1978) applied a limit equilibrium method to analyse failure progression in soil slopes. They divided the slope into slices, and suggested that a local failure of a slice caused the basal shear strength to drop to a residual value (the slip layer was strain-softened). This would cause a redistribution of interslice forces which might lead to further failure. They worked down a slope evaluating interslice forces on each of the upslope sidewalls, and determined whether the slice would fail or remain stable.

APPLICATIONS TO SNOW.

If a potential avalanche is thought of as a relatively strong slab of snow overlying a weaker layer then especially for the stronger slabs, the strengths of the vertical boundaries of the slab as well as that at the base of the slab must contribute to slope stability. In this paper, we divide a slope into rectangular slices of relatively small, and equal size, and balance the downslope static resisting and driving forces acting on each slice. We have assumed the spatial

distribution of snow strength in the down-slope direction (see appendix). This can then be repeated for slices of varying dimensions.

The three-dimensional stress distribution over a rectangular slice of snow with a mixture of boundary conditions is complex, especially as snow may exhibit both elastic and plastic properties which themselves are expected to vary within the slab and with stress. The yield strengths (relevant to the particular strain rates), combined with the directions and magnitudes of the principal stresses determine the location and most likely mode of the initial failure. Typical properties of snow suggest the following order of slab failure: (1) tensile, (2)sideshear, (3) compressive slab failure (see appendix 1). Furthermore, finite element analyses show that stresses vary by only about 10% over the slab depth (near an expected crownwall), and so for a first approximation, we have used stress values which have been averaged both over the depth and along each boundary of a particular sized slice of snow (see appendix 1 and Perla,1975,1980).

Over a slice of snow of average density ρ, inclined at an angle of θ to the horizontal, of dimensions B_x, B_y and h deep, the driving force is defined to be (fig.1):

$$D = \rho g h \sin\theta B_x B_y + EW\sin\theta$$

where EW is any extra vertically applied load on the slope (such as a skier, cornicefall, or explosion etc).

The resisting forces on a slice consist of the sum of the sideshear, compressive, tensile and basal boundary forces (fig.1). We assume a "local" failure (proceeding downslope) when the driving force on a slice exceeds the resistance at the basal, tensile and sideshear regions. This assumes that the failure will occur in these regions before the compressive region and takes no account of any compressive stress support occurring before failure of the other regions (neglect of this counterbalances somewhat the neglect of places of higher than average stress within the slice).

The force resisting the failure is therefore:

$R = \sigma_b B_x B_y + ThB_x + 2ShB_y$

where T=tensile strength of the slab, S=sideshear strength of the slab, and σ_b=basal shear strength under the slab.

The safety margin SM defined above is then:

$SM = [\sigma_b B_x B_y + ThB_x + 2ShB_y] - [\rho g h B_x B_y \sin\theta + EW\sin\theta]$ (4)

Again, a failure is assumed if SM becomes negative.

A probability density function describing a set of safety margins can be evaluated and for a Gaussian distribution, the probability that the safety margin will be less than zero can be described by the standard normal variate or "reliability ratio":

$\beta = (\bar{SM} - 0)/\tilde{SM}$ (5)

$\bar{SM}$ is the mean value of the safety margin, and $\tilde{SM}$ is its standard deviation.

We have preferred to use a reliability ratio derived from a "safety margin" rather than from a "safety factor" (the ratio of the resisting to the driving term) because of the relative ease with which the uncertainty of the driving term can be added to that of the resisting term for calculating the standard deviation of the safety margin.

We have made measurements of basal shear and tensile strengths, densities and depths across slopes (Conway and Abrahamson,1984a,1984b). In this paper we use these and some unpublished measurements to evaluate average safety margins and their standard deviations for different sized areas across the slopes. Vanmarcke (1977b) assumed the variation in basal strength was the only contributing factor to the uncertainty, but for snow we have also included important contributions from variations of slab depth, slab density, and slab boundary strengths as well as basal shear strength.

The assumptions and methods used to estimate the safety margin and variance are outlined in appendix 2a and 2b.

Determination of the most likely fracture area.

The safety margin defined by eqn.4 may have a complex

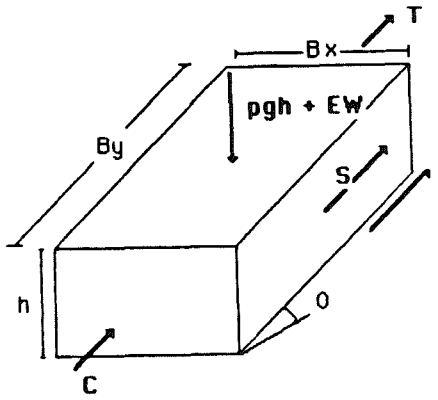

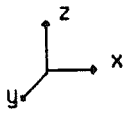

p = slab density
h = slab depth
0 = bed surface angle
g = gravitational accel.
= basal shear strength
T = tensile strength
S = side shear strength
C = compressive strength
EW = extra loading

Safety Margin SM
= BxBy + TBxh +2SByh - (EWsin0 +pghsin0BxBy)

Fig. 1: Forces acting on a slice of snow.

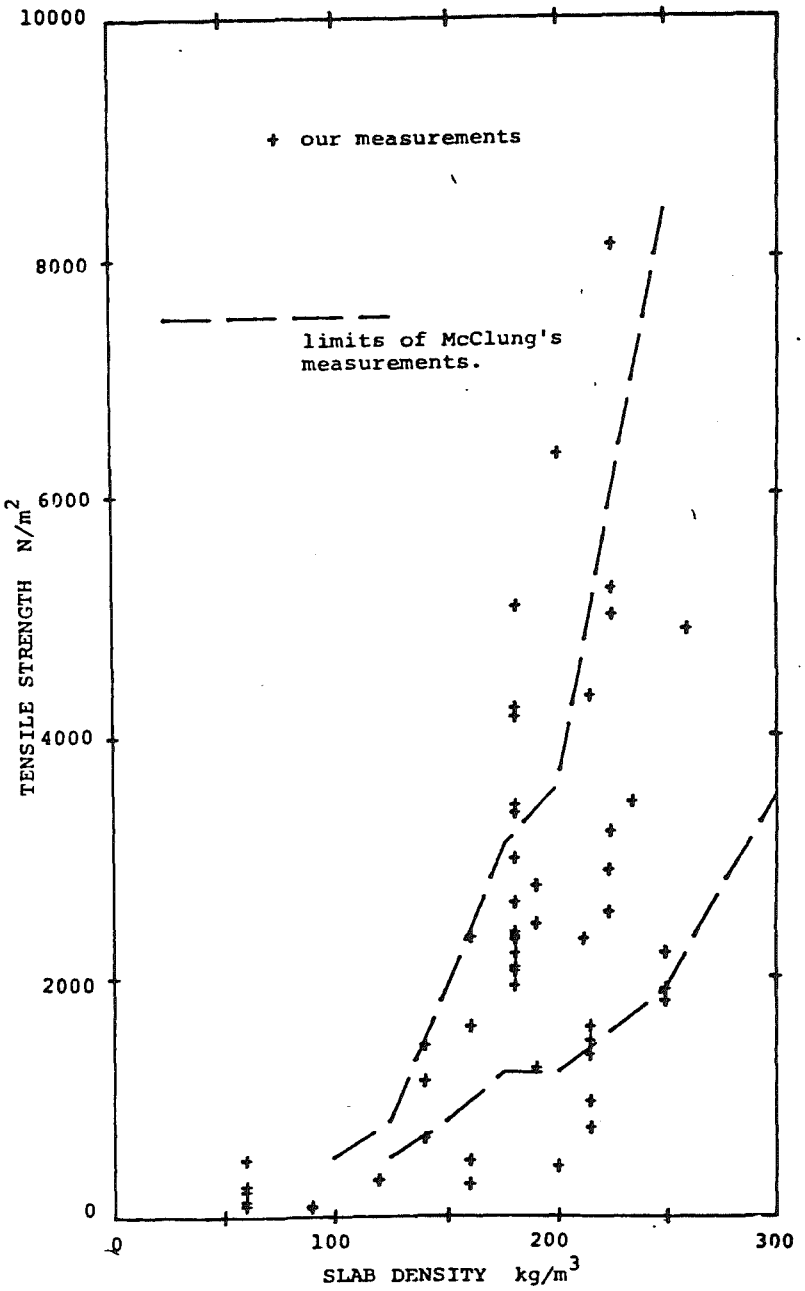

Fig 2: Relationship between tensile strength and density.

probability density function governed by the composite parameters and their relative contributions. To simplify the calculations and because of the Central Limit theorem, we have assumed a Gaussian distribution.

The reliability ratio, β (eqn.5) is a measure of the distance between the mean safety margin, and its failure threshold (zero), in units of the standard deviation of the safety margin. In our calculations of β we allowed the length as well as the width of the slice of snow to vary until a minimum β was found. This gave the dimensions of the area which maximised the probability of a local failure.

The local failure probability (p_f) could then be obtained from entering probability tables for normal distributions with the minimum β value..

Probability of a local fracture occurring on a slope.

Once the size of the most likely failure has been established, we are interested in determining the likelihood of such a fracture on a particular slope.

Each adjacent most probable failure area is considered to be a "component", and if the local failures are statistically independent, then eqn.3 can be used to estimate the probability of failure somewhere on the slope. However when adjacent components are correlated, eqn.3 gives an unconservative estimate, and such cases are best modelled by "first crossing" methods.

We have allowed the safety margin to vary both across and down slopes. By separating the components in each direction (with corresponding scales of fluctuation δ_x and δ_y), Vanmarcke (1983) derived an expression for the mean rate of crossings, υ of a zero threshold level (ie.SM$\leq$0):

$$\upsilon = \{[\beta \exp(-\beta^2/2)]/[\pi^{3/2}(2\delta_x\delta_y A_c)^{1/2}]\} \quad (6)$$

where A_c is the area most likely to fail, and β is the minimum reliability ratio.

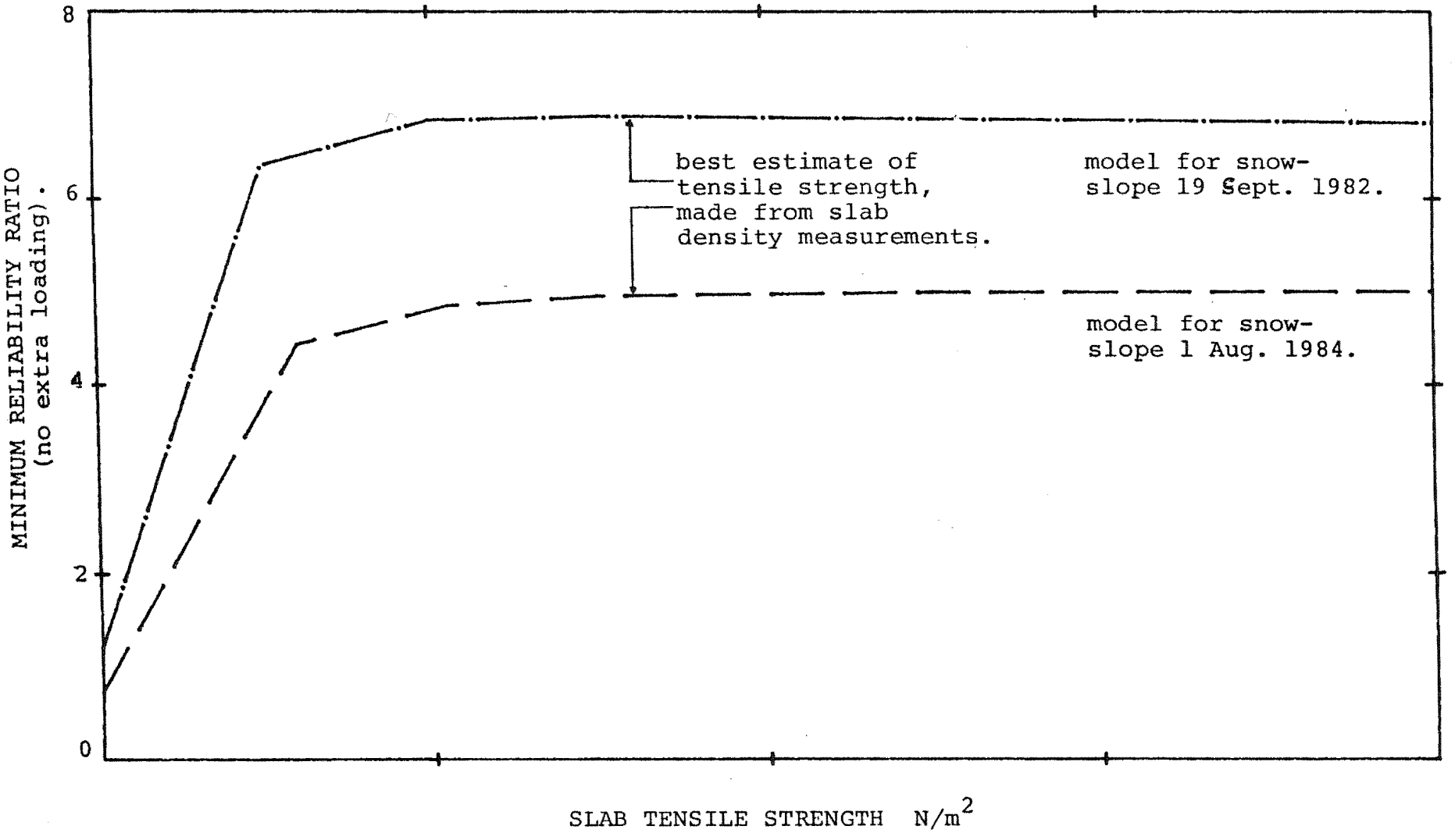

Fig.3: Change in the minimum calculated reliability ratio with tensile strength.

The probability of one such crossing occurring within a circular area A is (Vanmarcke,1983):

$$P = 1-(1-p_f)\exp\{-\upsilon A\}$$
$$= 1-(1-p_f)\exp\{-\beta/\pi^{3/2}[A_c/(2\delta_x\delta_y)]^{1/2}N\exp[-\beta^2/2]\} \quad (7)$$

Where N is the number of "components" in the total area A [ie. $N=A/A_c$] and p_f is the associated probability of failure.

For narrow band processes or those where the crossing level is not far from the mean, ($\beta<2$), rather than one minimum occurring during each crossing (as has been assumed by using the Poisson distribution), several might occur. Vanmarcke (1975,1983) showed that clustering of crossings would cause the crossing rate to be slower than that predicted by eqn.6. In such cases, a safety margin is likely to be less than zero over larger areas, thus increasing the probability of progressive failure.

From eqn.3 or eqn.7, the risk of a failure somewhere on the slope is shown to be dependent on the number of "components" (which is determined mainly by the size of the slope), as well as on the magnitude of the minimum reliability ratio.

Progression of failure.

McClung (1977) showed with experiments how some snows do strain soften, and we have also observed such behaviour (Conway and Abrahamson,1984b). When failure occurs, energy is released. If the energy can be absorbed elastically, the failure is confined and ceases, but if there is an excess, work will be done extending the fracture. McClung (1979a) applied to snow a model suggested by Palmer and Rice (1973), and showed using an energy balance how a shear failure can propagate along the base of a slab leaving a strain-softened region where failure has occurred. Although he did not deal with initiation of the fracture, McClung did show how shear failure might progress when applied stresses were less than peak shear strength valuess.

In the preceeding sections of this paper we have used a force balance together with a method of statistics of extreme values, and have shown how a failure of a particular size might occur somewhere on a slope. In order to determine whether this initial fracture might progress across the rest of the slope, we now use a limit force balance, similar to that used by Law and Lumb (1978), rather than an energy balance.

By considering typical values of both the displacement required for snow to strain-soften, and shear deformation of a slab of snow, McClung (1979a) established that the "endzone" of a slab over which the basal shear stress might drop from peak to residual values was about 0.5 to 1m in length. To simplify our calculations, we have assumed that once a local failure has occurred, the basal shear resistance under the failed slice drops abruptly to a residual value. Furthermore for a fracture progressing down-slope, the tensile resistance at the adjacent unfailed slice is removed and the extra driving force available from the failed slice results in a redistribution of stresses, provided the compressive strength between the two slices is sufficient to support the additional weight. If the compressive strength is not sufficient to support the extra load, a "loose" rather than "slab" avalanche might occur. Once a local failure has occurred, the stresses in the slab change, and this may change the calculated size of the most likely failure area. For this analysis however, the area most likely to fail (ie. the standard "component" of area A_c) has been assumed to remain unchanged and we consider redistribution of forces onto slices which are the same size as the initial failed slice.

The additional component of the load, IL_i, available from the ith failed slice is:

$$IL_i = [(\rho g h \sin\theta)_i - \sigma_{ri}] * A_c$$

where A_c is the area over which the slice has failed, and σ_{ri} is the residual basal shear strength under the failed slice.

The total load from i slices is $\Sigma_i IL_i$ and is transferred to the $(i+1)^{th}$ unfailed slice, which takes a new safety margin

because of the stress redistribution (additional load and zero tensile strength):

$$SM_{(i+1)} = [\sigma_b A_c + 2ShB_y] - [\rho g h A_c \sin\theta + EW\sin\theta + \Sigma_i IL_i] \quad (8)$$

where σ_b is the peak basal shear strength under the unfailed slice.

The analysis can be extended down a slope, increasing the number of failed slices. In the same way as described earlier, a reliability ratio and failure probability can be evaluated for each unfailed slice immediately below a number of failed slices. A slightly different model could be used to predict the probability of progression of failure across or up a slope. Progression up a slope is seen to be less likely because compressive strength is normally larger than the tensile strength (most powders have ratios of these two, of 2 to 4. We have taken a ratio of 2 in this work). The probability of failure progression is a conditional probability that all of the slices will fail and is the product of the individual slice failure probabilities:

$$P_{tot.} = \prod_{i=1}^{n} p_i \quad (9)$$

Either from the "first crossing" or the independent series probability model, the probability p_f for a failure initiating somewhere on the slope has already been estimated, and so the probability of such a failure occurring and then progressing would be:

$$P_{slope} = p_f \prod_{i=1}^{n} p_i \quad (10)$$

BACK ANALYSIS USING LIMIT EQUILIBRIUM.

In a previous paper, (Conway and Abrahamson,1984a) we described how sequential basal shear strength measurements were made either across or down slopes, many of these being around the peripheries of avalanches. We also described how tensile strength measurements of a snow slab could be made. Using this data and further unpublished measurements, we have tested the above limit equilibrium models. The measurements had been made on slopes at the head of the Tasman glacier (2130m) in New Zealand, and most of the avalanches tested were small (300 - 1500m^2 area). Because of high snow accumulation

and glacial movement, the shape of the Cornicewall (where most measurements were made) often changes. For this reason, none of the sets of measurements were in exactly the same position. Appendix 3 summarises data collected on five different occasions. Of the five, one (19 September 1982) had avalanched naturally about 12 hours prior to making the measurements, three (13 July 1982, 1 August 1984, 28 August 1984) avalanched only after a skier had jumped near the crownwall, and the other (1 August 1983) failed locally after ski-jumping, but did not avalanche.

Most spatial sequences measured were of basal shear strength and depth of the snow slab (because these are the easiest to make). Appendix 3 also lists the "scales of fluctuation" derived from these measurements. We have one set of spatially distributed tensile strength measurements across a slope (appendix 3). For these measurements the "scale of fluctuation" (0.45m) relating to the tensile strengths was found to be less than the spacing between samples (0.8m). Although we did not make shear strength tests on the same snow slab, this inequality is also typical for shear data so the assumption that similar patterns of variation occur for both shear and tensile strength measurements on a slope seems reasonable for a first approximation. We have in fact made this assumption in our analysis (appendix 1). It is also interesting to note that the "scale of fluctuation" describing the depth measurements on the same snow slab (0.44m) is closely similar to that of the tensile strength. Because both the depth and tensile strength measurements are summations over the different layers making up the slab depth, the variations (reflected by the scale of fluctuation) might be expected to be similar. Again, we have used the assumption that the respective scales are equal.

On many of the slopes, we did not have time to measure tensile strength and have used an estimate based on slab density measurements. For the estimate, we used measurements from other occasions, in conjunction with the limits suggested by McClung (1979b) graphed in fig.2. Our tensile strength/density data fit generally within McClung's envelope,

even although our measurements have averaged vertically slabs of snow which often consisted of several different layers. We used an average snow density to estimate strength, but suspect in some cases that a relatively thin strong layer may dominate the characteristics of a slab.

We have made a total of 54 tensile tests, and by pooling all of these measurements for a particular snow density, the best estimate of the standard deviation of a single measurement was found to be 27%.

For calculations of the safety margin (using eqn.4), we have taken the strengths in the sideshear and compressive regions to be respectively, equal, and twice that determined for the tensile region. These assumptions together with those listed in app.2 and app.3, enabled estimates of reliability ratios, and most likely "local" failure areas. These values have been listed in table 1, and indicate that the expected failure areas were small ($0.7m^2$ to $7.1m^2$), and generally became smaller when a slope was "point" loaded (over $1m^2$), with a skier ($.98m^2$ to $1.6m^2$). These areas are much smaller than the avalanche areas observed on the slopes ($88 - 10^4 m^2$).

Because slab boundary effects have been included, the correlation between safety margin values cannot be described by simple multiplication of two one-dimensional processes. The correlation structure of the safety margin will change somewhat when the boundary strengths are included, but for a first approximation, we calculated the correlation structure based on the shear strength values, using assumptions outlined in appendix 2b.

For three of the five cases studied (19 September 1982, 10 August 1983, 28 August 1984) the "scale of fluctuation" derived from the shear measurements (<0.21m) was smaller than the distance between samples (<0.75m), and so at least on this scale, the values of shear strength were essentially uncorrelated. Hence for these cases, the probability of a local failure somewhere on a slope (shown in table 1), can be estimated from eqn.3 for statistically independent events. The assumption of independence simplifies the mathematics of

TABLE 1.

INITIATION OF FRACTURE.

1) min. reliability ratio, [β]
2) prob. of a local failure, [p_f]
3) most likely "local" failure size [A_c]
4) size of slope for one failure (90% prob.) [A]
5) min. reliability ratio when only the basal resisting forces are considered [β_0]
6) observed area and occurrence of avalanches

		no load	+280kg
13 July 1982 mean tensile strength $=1073 N/m^2$ (triggered by a skier)		$\beta=2.81$ $p_f=2.5\times10^{-3}$ $A_c=7.1m^2$ $A=2.4\times10^{3}m^2$ $\beta_0=0.56$ No avalanche	$\beta=-0.11$ $p_f=.54$ $A_c=1.6m^2$ $A=1-2m^2$ $\beta_0=-4.77$ Avalanche ($600m^2$)
19 Sept. 1982 mean tensile strength $=5000 N/m^2$ (naturally triggered)		$\beta=6.86$ $p_f<10^{-7}$ $A_c=0.72m^2$ $A=>10^{9}m^2$ $\beta_0=1.19$ Avalanche ($10^{4}m^2$)	$\beta=6.23$ $p_f<10^{-7}$ $A_c=1.08m^2$ $A=>10^{9}m^2$ $\beta_0=-3.02$ Avalanche
10 Aug. 1983 mean tensile strength $=5500 N/m^2$ (no avalanche)		$\beta=2.82$ $p_f=2.4\times10^{-3}$ $A_c=1.13m^2$ $A=1080m^2$ $\beta_0=1.13$ No avalanche	$\beta=2.12$ $p_f=1.7\times10^{-2}$ $A_c=1.13m^2$ $A=150m^2$ $\beta_0=-4.62$ Local failures
1 Aug. 1984 mean tensile strength $=2100 N/m^2$ (triggered by a skier)		$\beta=4.85$ $p_f=4.8\times10^{-7}$ $A_c=1.96m^2$ $A=9.4\times10^{5}m^2$ $\beta_0=0.72$ No avalanche	$\beta=-2.43$ $p_f=.99$ $A_c=0.98m^2$ $A=<1m^2$ $\beta_0=-18.5$ Avalanche ($88m^2$)
28 Aug. 1984 mean tensile strength $=5000 N/m^2$ (triggered by a skier)	$120 m^2$	$\beta=2.51$ $p_f=6\times10^{-3}$ $A_c=1.44m^2$ $A=550m^2$ $\beta_0=0.5$ No avalanche	$\beta=1.22$ $p_f=0.11$ $A_c=1.08m^2$ $A=21m^2$ $\beta_0=-10.60$ Avalanche ($120m^2$)

TABLE 2.

PROBABILITY OF PROGRESSION OF FAILURE DOWNSLOPE.

	Number of failed slices								Prob. of one initial failure progressing across 8 slices
	1	2	3	4	5	6	7	8	
13 July 1982	.06 (.95)	.12 (.97)	.20 (.98)	.29 (.98)	.39 (.99)	.48 (.99)	.56 (.99)	.64 (.99)	2.8×10^{-5} (.83)
19 Sept 1982	7×10^{-5} (.023)	2×10^{-4} (.038)	7×10^{-4} (.06)	2×10^{-3} (.09)	.004 (.12)	.008 (.18)	.014 (.24)	.023 (.29)	$<10^{-20}$ (7×10^{-9})
10 Aug 1983	.09 (.26)	.11 (.29)	.13 (.32)	.16 (.35)	.18 (.38)	.20 (.41)	.22 (.44)	.25 (.47)	4×10^{-7} (2.7×10^{-4})
1 Aug 1984	.04 (1.0)	.08 (1.0)	.14 (1.0)	.22 (1.0)	.31 (1.0)	.41 (1.0)	.51 (1.0)	.61 (1.0)	3.9×10^{-6}) (1.0)
28 Aug 1984	.22 (.64)	.26 (.67)	.30 (.70)	.34 (.73)	.39 (.76)	.43 (.78)	.48 (.80)	.52 (.8)	8.2×10^{-4} (.083)

Probability of failure of an unfailed slice immediately downslope from the failed slices. Probabilities in brackets are those when a skier loaded the slope. These values have been calculated by assuming the basal shear strength under the failed slices had dropped to a residual value of one half the normal average strength.

the analysis.

The other two sets of measurements (13 July 1982, and 1 August 1984) did show some correlation between adjacent areas, and for these we have used the shear-derived "scales of fluctuation" for use in eqn.7 (where $\delta_x=\delta_y$). Vanmarcke (1983) noted that when the most likely failure area was smaller than the "correlation area" $\delta_x\delta_y$, the first crossing analysis became more approximate, its accuracy depending on whether the process was Gaussian and whether it was mean square differentiable. We are uncertain whether these conditions apply, but in such cases we used the "correlation area" in eqn.7 to evaluate the probability of failure somewhere on a slope.

Table 1 lists the probability of local failure for each slope (of a particular size, and load - see appendix 3). The table shows for slopes which had avalanched, the probabilities ranged from about 10^{-2} to about 0.99 (disregarding the naturally occurring avalanche of 19 September 1982). Also listed is the approximate size of the avalanches which occurred after a skier had jumped on the slope, and the size of slope over which we expect (with 90% probability) the occurrence of one local failure. We would expect to find at least one such failure on typical sized slopes (of the order $10^4 m^2$), provided the reliability ratio was not too high (<3.5). These results are in fig.4a.

The results show how some slopes may be easily driven into instability by an extra load such as the weight of a skier contributing to the driving force. The extra weight may be particularly significant for low density and/or thin slabs. The most likely failure area is then concentrated under that extra load and the size is strongly influenced by the distribution of weight. For determining failure probabilities with skier loading in table 1, we have assumed falling or turning skiers would load a slope by about four times their body weight (280kg vertically), distributed over a minimum area of $1m^2$. If the extra load caused the safety margin to decrease sufficiently, "local" failures could cluster, causing

an area larger than that predicted by the above equations to fail. Further, the length of path taken by each skier, and the number of skiers would determine the number of "components" affected by the extra loading. The remainder of the slope would not be subjected to the extra loading and the probability of failure somewhere on the slope would be the sum of the probabilities evaluated for the loaded and unloaded sections (using eqn.3 or eqn.7).

The fracture which occurred naturally on 19 September 1982 does not fit the above model, and the probability of a "local" failure on the slope was calculated to be less than 10^{-7}. The low probabilities resulted from high safety margin values caused by large contributions to the resisting forces from the slab peripheries (sideshear and tensile strengths). It is possible that equilibrium metamorphism may have caused an increase of snow strength during the interval after failure and before testing (about 12 hours). However, even if a very low tensile strength ($2000 N/m^2$) was used in the model, the likelihood of a fracture initiating was still calculated to be less than 10^{-7}.

A more likely reason for the anomaly is that the sliding limit model was not a good description of the failure. On several occasions we have observed a substantial reduction of basal shear strength after a small compression had been applied perpendicular to the failure plane. Such a force could presumably collapse existing grains and grain bonds in a weak layer and would incur not only bending stresses in the slab but also a reduction of basal shear strength. Perla and LaChapelle (1970) showed how these perturbations would increase the principal stress in a slab. We have no measurements of the forces required to collapse the layers for the event on the 19 September 1982, but the snow stratigraphy did show a thick (about 40mm depth of 1mm diam. recrystallised grains) weak layer under the slab which would both be weak in compression and allow limited bending of the slab. A safety margin for a bending limit equilibrium could in theory be formulated and treated in a probablistic way in much the same way as the sliding limit safety margin.

Also it is possible that seismic activity or glacial movement may have initiated this avalanche. In fact, a network of instruments used to study effects of a raised lake level had been installed in the Pukaki basin about 60 kms from the Tasman neve. At about 11pm on the evening of 18 September, a shake of magnitude 2.7 (approximately equivalent to Richter's local scale) was recorded. The microearthquake was focused some 20km from the Tasman neve at a depth of about 10km. We suspect the effects of such a sized shake would be minimal, but any ground acceleration could cause an avalanche because relatively small strains are often sufficient to fracture snow (see for example Narita,1980 and McClung,1977).

Progressive failure.

The most likely failure area has been found to be small (of the order of 0.1-4m^2). For an initial failure over an area of similar size to the observed avalanches, the calculated probability is very small, ($<<10^{-7}$). This suggests that many avalanches may be initiated by relatively small local failures which then progress across adjacent areas.

The limit analysis applied to progressive failure (table 2) indicates that if a failure had initiated naturally, the probability of the failure progressing downslope through eight more slices was small ($8x10^{-4}$ on 28 August 1984 to $4x10^{-7}$ on 10 August 1983). With the extra weight of a skier, the probability of progression often increased considerably, and for the slopes which did avalanche with the extra weight of a skier, the progression probability was calculated to be always greater than 0.085. An avalanche did not occur on 10 August 1983, and the estimated probability of failure progression was $2.7x10^{-4}$.

Disregarding the data of 19 September 1982, for slopes which had avalanched, the progression probability was greater than about $8x10^{-2}$, and for non avalanche slopes the progression probability was less than about $3x10^{-4}$. These values are graphed in fig.4b.

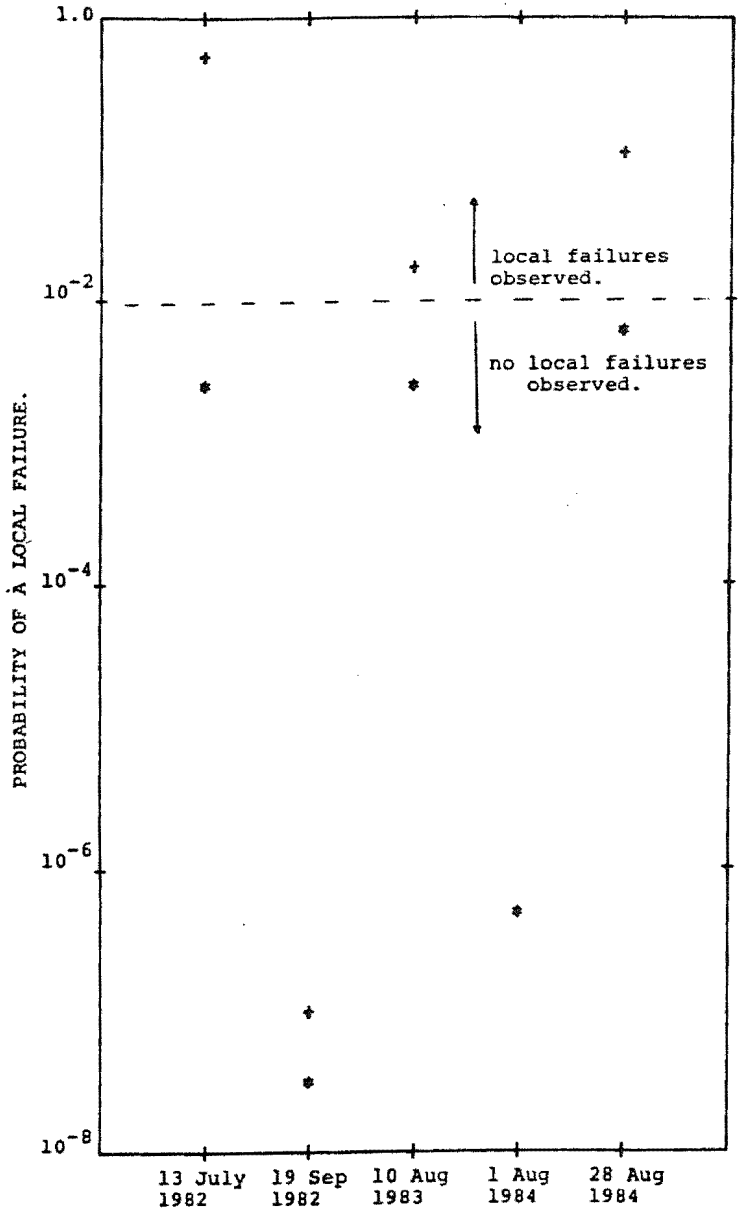

Fig.4a: Probability of a local failure for each of the events studied.

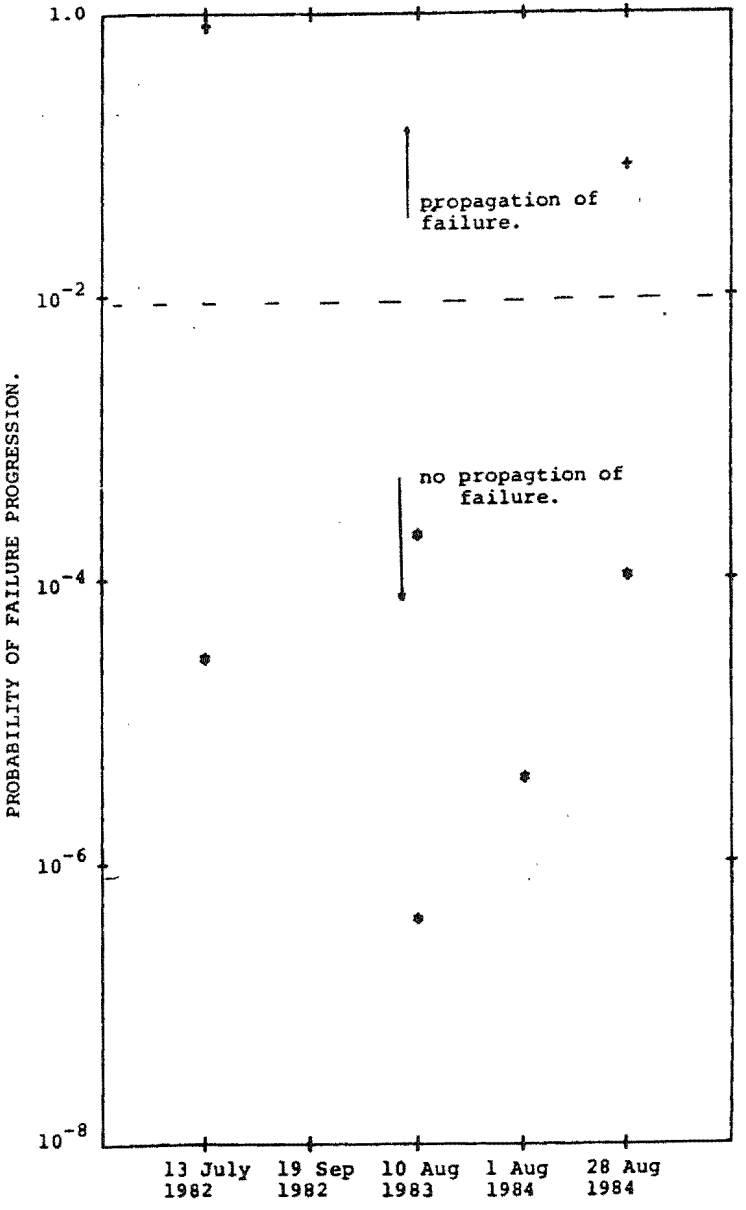

Fig.4b: Probability of progression of a local failure for each of the events studied.

Average strength values have been used in the calculations and we have not accounted for clustering of low (or high) strengths (which might be expected). Also the basal shear strength is assumed to be one half the average value under slices which had failed. If the failed slices strain-soften to fractions less than 0.5, a higher load would be available to drive the failure progression and failure could progress more easily than shown in table 2. If McClung's (1979a) energy criterion can be satisfied (ie.an excess of energy was available to overcome the resistance at the end zone of a softening band), the area under an unfailed slice may also strain soften. Further, it may be more appropriate to use a dynamic, rather than static, strain softened shear strength. The resulting decrease in resistance would allow the failure to progress more easily than shown in table 2.

DISCUSSION OF RESULTS AND IMPLICATIONS FOR SNOW STABILITY ASSESSMENT.

1) Basal shear strength.

Vanmarcke (1977a) showed the "scale of fluctuation" was related to the average length the process was above (or below) its mean value, and in fact the half wavelength, $\lambda/2$, of the process could be approximated by:

$$\lambda/2 = 1.25\delta$$

For the five slopes analysed, the "scale" derived from the shear measurements varied from 0.11 to 1.8m (appendix 3), which indicates the values fluctuated with relatively short wavelengths (0.28m to 2.25m). We are uncertain how typical these patterns of fluctuation are, but note that Sommerfeld (in prep.) also found large spatial variability of basal shear measurements made in Colorado.

In an earlier paper we suggested that variations of strength might originate from local air-flow patterns close to the time of deposition of the snow layer (Conway and Abrahamson,1984a). We have commonly measured the wavelength of surface snow waves to be similar to the wavelength of the strength values and suspect that such patterns during storms would influence basal snow strength. More slowly varying

fluctuations could be caused by large dunes or drifts of snow behind discontinuities in terrain, which not only might change the strength but also the loading on the slope. Avalanches often occur after periods when snow has been transported by wind and during such times, duning and rippling of snow is common (see for example Kobayashi,1979 or Fohn and Meister,1983).

The wavelength of measurements downslope (19 September 1982) did not differ significantly from those measured across slopes. Although we do acknowledge that the pattern may vary for some slopes (depending perhaps on the orientation and spacing of the ripples or dunes), as a first approximation, the assumption that the strength distribution is similar both down and across slopes seems reasonable.

For the five slopes in this study, the standard deviation of the pooled measurements of shear strength was almost 50%, which further indicates that a single shear strength measurement would not adequately describe the mean value. It is also interesting to note that when increasing the distance over which a mean was taken the mean shear strength usually varied by less than 10% of the mean of the "point" values, but it drifted by about 30% on 13 July 1982 . This suggests that this data was not strictly statistically homogeneous, and the mean strength changed slowly across the slope.

To estimate the mean, standard deviation and correlation of a spatially varying process, the optimum sampling intervals need to be one half the length δ. If the observed patterns of small fracture areas and short-scaled fluctuations are typical, we need to sample at close intervals (about 0.5m), to make a reasonable slope stability assessment.

If one could be certain the mean strength was not changing slowly across a slope, the mean and variance of the shear strength could be estimated with just a few closely spaced measurements. However especially over large slopes, a more slowly varying trend in strength may exist, with a pattern of rapid fluctuations superimposed. In such cases, in order to estimate the fast as well as the slowly fluctuating

trends a cluster of measurements at intervals of one half the scale associated with the slowly varying trend would be appropriate. Adequate snow stability assessment would need measurement of slow changes in mean shear strength and the associated scale of fluctuation. This is particularly evident in the measurements made on 13 July 1982 (see also Conway and Abrahamson,1984), where several closely spaced measurements at one location only might have resulted in an unreasonably high (or low) estimate of the mean shear strength value.

2) Tensile strength.

The area of tensile fracture was about $0.025m^2$ compared with areas of about $0.12m^2$ for shear strength measurements. We expect the variance of measurements over small sized samples to be larger than those over large sized samples, but the tensile measurements have been averaged over several layers of the slab, and so the averaged variance would be less than that for a single layer. In fact, the standard deviation calculated from the pooled measurements of tensile strength (27% from 54 measurements) was less than that for the shear strength measurements (48% from 191 measurements).

Estimates of tensile strength were often made from a correlation of previous tests against measurements of slab density. By changing the estimate used to calculate the safety margin, we could plot the variation of the minimum reliability ratio against the estimate. Fig 3 is such a plot for two of the cases studied, and shows that the reliability ratio was not particularly sensitive to increases of tensile strength beyond a certain value (because we have allowed the standard deviation to increase proportionally with tensile strength). The strength estimates were always in the range where the reliability ratio was not very sensitive to changes of tensile strength, so the selection of a value for the strength was not critical.

Fig 3 also shows the minimum reliability ratio when the tensile, compressive and side-shear strengths are zero (ie. considering only the basal shear strength and the driving forces). Values of this parameter β_0 for the other slopes are

listed in table 1. This is the condition most commonly proposed for assessment of slope stability (see for example, Roch,1966 or Perla,1980), but we think that estimate is rather conservative at least when considering initial local failure. The estimate is somewhat more realistic when considering progression of failure.

The effective tensile strength of a snow slab may be influenced by the slab depth. Because a slab can deform in shear, we expect tensile strain in the slab to be greatest close to the end of a basal slip zone. For deep and/or soft slabs (which might shear deform considerably over the depth), the tensile stress would decrease near the slab upper surface, and so part of the slab above a certain height would not contribute significantly to the resistance to fracture. We expect therefore, a deep slab to fail at lower apparent values of tensile strength. Because snow slabs consist of layers of different snow (with varying Young's modulii), the stress would be expected to be concentrated in layers which were: (a) close to a basal weak layer; (b) of high Young's modulus.

Schubert (1975) noted, for most powders, that cracking occurred after small strain disturbances and Narita (1980,1983) observed cracks after small tensile strains in snow samples. On a larger scale, we expect a minor strain disturbance would cause tensile cracking of a snow slab and possible failure.

These factors may have also contributed to the initiation of the avalanche observed on 19 September 1982, which was unexpected from the straight-forward analysis.

3) Reliability ratios.

The relative contributions from the slab boundary resistances and the basal shear resistances to the value of the reliability ratio are clearly shown in fig.3 and table 1 (by comparing β and β_0 values). In all cases inclusion of the slab boundary strengths in the model increased the calculated reliability ratio significantly, and we think these effects need to be considered in a model of slope stability.

The proposal that avalanches initiate from a failure over a small area is supported by field observations of fracture sequences (see for example, notes in appendix 3). The estimated fracture sizes are similar to those suggested by Sommerfeld and Gubler (1983) who analysed accoustic emissions when snow was fracturing. Gubler (1978) also suggested some avalanches might be caused by an initial failure which propagated.

Apart from that for the 19 September 1982, analysis of measurements from the slopes studied show that the minimum reliability ratio was less than 2.2 after loading for all slopes (see table 1 and appendix). It is also interesting to note that before loading, the minimum ratios were greater than 2.5 and the slopes had not avalanched. However the events of 13 July 1982 (β=2.81; Area=600m^2) and 28 August 1984 (β=2.51; Area=120m^2) were close to containing at least one local failure somewhere on the slope prior to extra loading. The small size of the slope on 10 August 1983 would have inhibited failure, and the measurements and analysis suggest the avalanche triggered by skiing on 1 August 1984 would not have occurred naturally.

As outlined in the appendix, except for the event on 19 September 1982, all slopes studied failed locally when triggered by a skier near the crown regions. The "local" failure on the 10 August 1983 did not propagate and become an avalanche. We have already discussed possible reasons for the anomalies surrounding the event of 19 September 1982.

4) Propagation.

We suspect the release of elastic strain energy associated with the fractures would enhance failure propagation and that our estimates of propagation probabilities are lower than those occurring on slopes. However the event of 10 August 1983 stands out with a much lower probability of failure progression than those avalanches which did release, supporting our analysis.

Again the avalanche which occurred naturally (19 September 1982) does not appear to fit the model.

As an extreme simplification of the analysis above, we could propose a conservative criterion for assessing slope stability:

(1) assume a local failure will occur somewhere on the slope, especially when extra loading occurs.

(2) after a local failure, the failed slice is supported at the compressive boundary and basal region (which has shear softened).

(3) provided the compressive strength is sufficient, load will be transferred onto an adjacent unfailed slice when the (gravitational) shear stress at the base of the failed slice exceeds the strain-softened shear stress.

(4) if this force redistribution can cause progression of failure, the criterion for failure depends on the strain softening ratio which describes the reduction of the basal strength from normal to residual values. Data available (McClung,1977 and Conway and Abrahamson,1984b), show this ratio to vary for different snow (and rates of strain), but it may be close to 0.5. In such a case, for failure to progress at all, the shear stress due to gravity would have to exceed one half the mean normal strength. That is, for failure:

$$\rho gh\sin\theta > 0.5\sigma_b \qquad (11)$$

This of course is an extreme estimate because the slab boundary forces (which have been neglected), would also inhibit progression, and the strain softening ratio may deviate from 0.5.

It is interesting to note that this stability criterion is the same as that found by Sommerfeld and King (1979) who recommended, using quite different reasoning, that the basal shear strength measurements should be modified by a factor of 0.5 and compared with the shearing load for an estimate of slope stability.

The above criterion predicts that all of the cases studied (including those of 19 September and 10 August) would avalanche even without extra loading, provided the fracture

could initiate (see appendix 3 for a summary of the strength values) The model does predict that the snow of 10 August 1983 was the least likely to propagate (strength:stress ratio was 0.73 compared with 0.38-0.64 for the other slopes), in agreement with observed events.

5) An acceptable level of reliability.

On the basis of the full analysis for each of the events we studied, Fig.4a and fig.4b show local failure probabilities, and probabilities of such failures progressing. If the event of 19 September is excluded, it can be deduced that a local failure could be expected if the probability was greater than about 10^{-2}, when the probability was less than about $6x10^{-3}$, the slope could be assumed stable. Slopes which showed a progression probability greater than about $8x10^{-2}$ had avalanched, while those with probabilities less than about $8x10^{-4}$ had not (excluding the event of 19 September). At least for this data, the progressive failure criterion more clearly distinguishes between stable and unstable slopes than the criterion of failure initiation.

It would be useful to make measurements over more slopes to confirm whether these levels are typical and consistant, especially as the consequence of an avalanche can often be fatal. It is also interesting to note when assessing the wisdom for people to use a slope or not, Whitman (1984) surmised that the probability of crack occurrence in most engineering structures was often at least 10^{-2}.

6) Dynamic loading.

Dynamic loading and response are discussed by several authors (see for example Lomnitz and Rosenbleuth,1976), and Johnson (1980) modeled the response of snow to dynamic loads. In this paper, we have not attempted to model this type of behaviour, but we suspect that inclusion of the dynamic response of snow would improve the model, especially for failures involving explosives, falling masses, and crack propagation.

CONCLUSIONS

Probability theories applied to limit equilibrium methods have been used successfully for four out of the five snow slopes studied, and it seems likely that the event which did not fit the model was caused by effects beyond the scope of the static sliding equilibrium approach. No doubt the model could be improved by considering stress-strain relationships within the slab, energy balances, different failure modes, or by using improved estimates of yield strengths.

The simple model does fit the other slopes, and the theory incorporates and is consistant with characteristics often observed at avalanche events:

1) Snow properties, in particular those related to strength, vary spatially over a slope. In order to determine a reasonable estimate of the means and variances of these properties and statistical correlations between them, several sets of contiguous measurements may be needed on each slope.

2) Statistical analysis indicates that the combination of large slopes and moderate snow strengths means that an initial failure is likely to occur somewhere on a slope. The area of the initial fracture is small (about $1m^2$), and will become an avalanche only if it can propagate over the rest of the slope. Stability analyses should therefore concentrate on aspects of fracture propagation, and an important related property is the degree of shear strain softening after small displacements. For a given load, this property together with the strength of the slab above the weak layer, may control the rate of failure progression.

3) The location of an initial fracture depends on the spatial distribution of snow properties. The weight of say a skier on the snow can often contribute to the probability of failure and subsequent propagation. This contribution may be particularly significant for shallow, low density slabs overlying a weak basal layer. It is well known that most avalanche casualties are caused by people triggering relatively small avalanches (Perla,1980).

4) A lack of information, errors of measuring as well as spatial variability all contribute to the uncertainty surrounding the values of the safety margins. Analysis of

more slopes would improve our knowledge of threshold probability levels for safe and unsafe slopes.

A mountain traveller generally makes subjective decisions about possible consequences of being avalanched on a particular slope, and the reliability analysis can offer some objectivity to a decision making process.

ACKNOWLEDGEMENTS.

The Department of Lands and Survey (Wellington, New Zealand) and the University of Canterbury (Christchurch, New Zealand) provided financial support for the study. Mt. Cook Airlines provided transport to the field area, and assistance from Mt. Cook National Park staff was invaluable. We are grateful to all these people for their assistance.

LIST OF REFERENCES.

Bader, H.:(1962) "The physics and mechanics of snow as a material". US Army Cold Regions Science and Engineering, Hanover, New Hampshire. 79pp.

Bader, H., Haefeli, R., Bucher, E., Neher, J., Eckel, O., and Thams, Chr.:(1954) In "Snow and its metamorphism", 313pp, illus. Snow, Ice and Permafrost Res. Estab., Transl. 14. Corps Eng., U.S. Army, Wilmette, Ill.

Bishop, A.W.:(1955) "The use of the slip circle in the stability analysis of slopes". Geotechnique, Vol. 5, No. 7, p7-17.

Brown, C.B., Evans, R.J. and LaChapelle, E.R.:(1972) "Slab avalanching and the state of stress in fallen snow". Journal of Geophysical Research, Vol 77, No. 24, P4570-4580.

Chowdhury, R.N.:(1980) "A reassessment of limit equilibrium concepts in geotechnique". In Application of Plasticity and Generalised Stress-Strain in Geotechnical Engineering,(R.N. Yong and E.T. Selig eds.) Am. Soc. of Civil Engineers.

Conway, H. and Abrahamson, J.:(1984a) "Snow stability index". Journal of Glaciology, Vol. 30, No. 106, p321-7.

Conway, H. and Abrahamson, J.:(1984b) "Snow and avalanche research at Tasman saddle - a progress report of the

winter,1984". Unpublished report.

Fohn, P.M.B. and Meister, R.:(1983) "Distribution of snow drifts on ridge slopes: measurements and theoretical approximations". Annals of Glaciology, Vol.4, p52-57.

Gubler, H.:(1978) "An alternate statistical interpretation of the strength of snow". Journal of Glaciology, Vol. 20, No. 83, p343-357.

Harr, M.E.:(1977) "Mechanics of Particulate Media". Chapter 11, p403-54, McGraw-Hill, New York, N.Y.

Johnson, J.:(1980) "A model for snow slab failure under conditions of dynamic loading". Journal of Glaciology, Vol.26, No.94, p245-254.

Kobayashi, S.:(1979) "Studies on interaction between wind and dry snow surface". Contrib. Inst. Low Temp. Sci., Hokkaido Univ., Ser.A, No. 29, p1-64.

Law, K.T. and Lumb, P.:(1978) "A limit equilibrium analysis of progressive failure in the stability of slopes". Canadian Geotechnical Journal, Vol. 15, No. 1, p113-122.

Lomnitz, C. and Rosenbleuth, E.:(1976)" Seismic risk and engineering decisions" Elsevier, The Netherlands.

McClung, D.M.:(1977) "Direct simple shear tests on snow and their relation to slab avalanche formation". Journal of Glaciology, Vol. 19, No. 81, p101-109.

McClung, D.M.:(1979a) "Shear fracture precipitated by strain softening as a mechanism of dry slab release". Journal of Geophysical Research, Vol. 84, No. B7, p3519-3526.

McClung, D.M.:(1979b) "In-situ estimates of the tensile strength of snow utilizing large sample sizes". Journal of Glaciology, Vol. 22, No. 87, p321-29.

Mellor, M.:(1975) "A review of basic snow mechanics" IAHS AISH Publ. 114, (Snow mechanics symposium, 1974), p251-291.

Molerus, O.:(1982) "Invited Review: Flow behaviour of cohesive materials". Chem. Eng. Commun. Vol.15, p257-289.

Morgenstern, N.R. and Price, V.E.:(1965) "The analysis of the stability of general slip surfaces". Geotechnique, Vol. 15, No.1, p79-93.

Narita, H.:(1980) "Mechanical behaviour and structure of snow under uniaxial tensile stress". Journal of Glaciology, Vol 26, No. 94, p275-282.

Narita, H.:(1983) "An experimental study on tensile fracture of snow". Contrib. Inst. Low Temp. Sci., Hokkaido Univ., No. 2625, Series A, No. 32.

Palmer, A.C. and Rice, J.R.:(1973) "The growth of slip surfaces in progressive failure of over-consolidated clay". Proc. Royal Society London, Ser. A, No. 332, p527-548.

Perla, R.I.:(1975) "Stress and fracture of snow slabs". IAHS-AISH No. 114, (Snow mechanics symposium, 1974), p208-211.

Perla, R.I.:(1980) "Avalanche release, motion and impact". In Dynamics of Snow and Ice Masses, (S. Colbeck, ed.), Chapter 7, p397-462, Academic Press, New York.

Perla, R.I. and LaChapelle, E.R.:(1970) "A theory of snow slab failure". Journal of Geophysical Research, Vol. 75, No. 36, p7619-7627.

Rice, S.O.:(1944) "Mathematical analysis of random noise". Bell System Technical Journal, Vol.23, p282-323; and Vol.24, p46-156.

Roch, A.:(1966) "Les decenchements d'avalanches". International Symposium of Scientific Aspects of Snow and Ice Avalanches. International Association of Hydrological Sciences Publication, No. 69, p182-195.

Salm, B.:(1975) "Principles of structural control in avalanches". In Avalanche Protection in Switzerland. USDA Forest Service General Technical Report RM-9, Translation of: Lawinenschutz in der Schweis. Rocky Mountain Forest and Range Experment Station, Ft. Collins, Co.

Sarhan, A.E. and Greenberg, B.G.:(1956) "Estimation of location and scale parameters by order statistics from singly and doubly censored samples,Part 1, The normal distribution up to samples of size 10". Ann. Math. Statist., Vol. 29, p79-105.

Sarhan, A.E. and Greenberg, B.G.:(1962) In "Contributions to Order Statistics" (Sarhan, A.E. and Greenberg, B.G., eds.), Chapter10c, p206-269, Wiley and Sons, Inc.

Schubert, H.:(1975) "Tensile strength of agglomerates", Powder technology, Vol.11, p.107-119.

Schwedes, J.:(1975) "Shearing behaviour of slightly

compressed cohesive granular materials". Powder technology, Vol.11, p59-67.

Sommerfeld, R.A.:(1973) "Statistical problems in snow mechanics". U.S. Dept. of Agriculture, Forest Service General Report, RM-3, p29-36.

Sommerfeld, R.A.:(1974) "A Weibull prediction of the tensile strength-volume relationship in snow". Journal of Geophysical Research, Vol. 79, No. 23, p3353-3356.

Sommerfeld, R.A.:(1980) "Statistical models of snow strength". Journal of Glaciology, Vol. 26, No. 94, p217-223.

Sommerfeld, R.A.:(in prep.) "Spatial variation of shear strengths of avalanche sliding surfaces".

Sommerfeld, R.A. and King, R.M.:(1979) "A recommendation for the application of the Roch index for slab avalanche release". Journal of Glaciology, Vol. 22, No. 88, p547-549.

Sommerfeld, R.A. and Gubler, H.:(1983) "Snow avalanches and acoustic emissions". Annals of Glaciology, Vol. 4, p271-276.

Spencer, E.:(1967) "A method of analysis of the stability of embankments assuming parallel interslice forces". Geotechnique, Vol. 17, No. 1, p11-26.

Teichroew, D.:(1956) "Tables of expected values of order statistics and products of order statistics for samples of size 20 and less from the normal distribution". Ann. Math. Statist., Vol.27, p427-451.

Teichroew, D.;(1962) In "Contributions to Order Statistics". (Sarhan, A.E. and Greenberg, B.G., eds.), Chapter 10b, p190-205, Wiley and Sons, Inc..

Vanmarcke, E.H.:(1975) "On the distribution of the first-passage time for normal stationary random processes". Journal of Applied Mechanics, trans. ASME, Vol.42,p215-220.

Vanmarcke, E.H.:(1977a) "Probablistic modeling of soil profiles". Journal of Geotech.Eng. Div., ASCE, Vol. 103, No. GT11, p1227-1246.

Vanmarcke, E.H.:(1977b) "Reliability of earth slopes". Journal of Geotech. Eng. Div., ASCE, Vol. 103, No. GT11, p1247-1265.

Vanmarcke, E.H.:(1980) "Probablistic stability analysis

of earth slopes". Engineering Geology. Vol.16, No. 1, p29-50.

Vanmarcke, E.H.:(1983) "Random Fields, analysis and synthesis". MIT Press, Cambridge, Massachusetts.

Whitman, R.V.:(1984) "Calculated risk in Geotechnical engineering". Journal of Geotech. Eng. Div., ASCE, Vol. 110, No. 2, p145-188.

Appendix 1: Sequence of slab failure.

In order to formulate a model of fracture, we require the sequence of fracture in a slab. There are several criteria one could use for fracture; we use the comparison of the resolved maximum and yield stress.

Perla (1980), made some numerical calculations for an inclined, rectangular slab which was clamped at the side and upslope boundaries, but free on the downslope boundary. This clamping caused the maximum principal stresses to be highest near the upper corners of the slab. From elasticity theory, the maximum principal stress is likely to be larger than the principal shear stress (which acts on a plane 45° to the principal tensile stress). If the tensile and sideshear yield strengths are similar (Bader,1962 and Salm,1975), we expect the slab to fail first in tension and then in side-shear.

Further, if the Youngs' modulii for compression and tension are similar (Mellor,1975), the compression-stressed downslope section of the slab will yield similar maximum stresses to those found in the upslope tensile section. Thus if the compressive yield strength is twice the tensile strength (Bader,1962, Salm,1975), an increase of stress would be more likely to induce a failure in the tensile rather than compressive region.

The following order of failure would therefore be expected: tensile, sideshear, and then compressive failure. This order of failure was also suggested by Brown et al.(1972).

Perla (1975) considered a two-dimensional slab which was linearly elastic, isotropic and homogeneous. He showed for a slab which was clamped along its base, the maximum principal stress near the top of the slab increased as the Poisson ratio increased (ie.clamping would influence hard slabs more than soft slabs). Also as the Poisson ratio increased, the stress became more uniform across the slab profile. Even for soft slabs, the stresses varied by only about 10% over the depth of the slab, which suggests that use of average stress values is suitable for a first approximation.

Appendix 2a: Estimation of the mean safety margins.

For evaluating the safety margin defined by eqn.2, asumptions are required in assigning values to each component, and these are outlined below. It is well known that snow strength is time and rate dependent (Haefeli [Bader et al.,1954], Narita,1980,1983), and any estimate of snow strength in a slab can only be approximate, particularly when a slab consists of layers of different snow types.

Vanmarcke (1977b) suggested that for soils, the shear strength would have a Gaussian probability distribution, but for snow, Gubler (1978) favoured a log-normal distribution for the links or "fundamental units" defined as force conducting elements. Part of his argument was that the strength cannot be negative, and the log-normal distribution characterises bond and grain diameters in many sintered materials. Sommerfeld and King (1979) found that no single distribution accurately fitted all of their shear strength measurements, and used a distribution which best fitted the particular data. To simplify calculations and because of Gubler's reasoning, we used a log-normal distribution to describe both shear and tensile strength data.

Our method of measuring basal shear strength had definite upper and lower limits (see Conway and Abrahamson,1984). For samples where the down-slope gravitational weight of snow exceeded the basal shear strength, the column failed before loading and the strength could only be taken to be less than the gravitational weight. For samples which were stronger than the range of our test equipment, the true strength was greater than the applied stress.

To use all measurements and arrive at an unbiased estimate of population mean and variance, we converted the values of shear strength to logarithms and made use of order statistics and "best linear estimate" techniques outlined by Sarhan and Greenberg(1956,1962). Estimates of the mean and standard deviation of a distribution can be made by multiplying each observation within the range measured by an appropriate coefficient. The coefficients for normal

distributions of sample size 20 or less, have been calculated and tabulated by Sarhan and Greenberg.

Teichroew (1956,1962), tabled expected values of ordered values of normal distributions. Once an estimate of the mean and standard deviation of the distribution had been made, these tables could be used to estimate the "censored values" (values lying in the upper and lower extremes), and we then used a random number table to assign these values to a position on the slope. For these calculations, 35 shear measurements (out of a total of 87) were censored values. The tensile tests were not limited in this manner, and so none of the measurements were censored. The numbers for specific cases are shown in appendix 3.

When averaging shear and tensile strength measurements over increasingly larger lengths (up to 5m), there was no significant decrease in the mean strength. Sommerfeld (1980), used a combination of series-element and parallel-element theories to estimate strength of large volumes of snow from measurements on small volumes (predictions of strength over areas of $0.1m^2$ from measurements over $0.01m^2$). He predicted a decrease in strength as the test volume became large, and thought an "infinite" sample size might be about $1m^3$. If Sommerfeld's approach is correct, then it may apply (in the shear strength case) only to shear areas less than our sample size ($0.1m^2$).

McClung(1979b) measured tensile strength using large sample areas ($0.12m^2$), and graphed strength against snow density. From his plot and our data (fig.2) it can be seen the range as well as the mean of measured strengths increased with density, which supports the argument that tensile strength is distributed log-normally. We made no measurements of the sideshear and compressive strengths of a slab. However we have assumed that these strengths can be expressed as ratios of the slab tensile strength. Mellor (1975) reviewed experimental snow data and suggested for dry snow, the ratio of tensile:compressive strength was one at low densities ($100-250kg/m^3$), and decreased with increasing density. Mellor

also summarised shear strength measurements from various sources and comparison of these measurements showed that the tensile strength (centrifugal method) could be 10 times higher than the shear strength measured by vanes or shear boxes (for a given density). However Bader (1962) and Salm (1975) suggested the tensile strength was approximately equal to the shear strength, and about one half the compressive strength. We have used these ratios for calculations of a safety margin.

Appendix 2b: Estimation of the variance of safety margins.

An estimate of the variance of a safety margin is required for the probability analysis, and for the estimate, we include uncertainties derived from density, depth, slab boundary strengths as well as those from basal shear strength. If the contributions are statistically independent, the variance of a safety margin (for a particular area) may be written:

$$\mathrm{Var}(SM) = (\tilde{\sigma}_b B_x B_y)^2 + (\tilde{T}hB_x)^2 + 2(\tilde{S}hB_y)^2 + (\tilde{\rho}gh\sin\theta B_x B_y)^2 + \tilde{h}^2[(TB_x)^2 + 2(SB_y)^2 + (\rho g\sin\theta B_x B_y)^2] \quad (1A)$$

These contributions decrease with increasing averaging area, each characterised by a "scale of fluctuation", and so for a particular area an estimate of the variance of basal shear strength and slab depth can be made from the set of data.

Our one set of contiguous measurements of tensile strength indicate that these values, as were the shear strength measurements, were essentially uncorrelated or exhibited slight correlation (reflected by the small scales of fluctuations"). Because of this, for a first approximation we have used the variance function from the basal shear strength measurements to also describe the decay of the variance tensile and sideshear strength.

By considering a slab to consist of i layers, each of thickness h_i, and density ρ_i, the average slab density over the total slab depth h, may be written:

$$\bar{\rho} = \Sigma_i \rho_i h_i / h$$

and the variance: $\mathrm{var}(\rho) = \Sigma[(h_i/h)^2(\tilde{\rho}_i)^2]$

where $\tilde{\rho}_i$ is the standard deviation of the layer density.

We have measured density variations within a wind-deposited snow layer of up to 10%. If we take $\tilde{\rho}_i = 0.1\bar{\rho}_i$, and consider that a typical slab consists of five layers of equal thickness, then the variance:

$$\text{var}(\rho) = 5(1/5)^2(0.1\bar{\rho})^2$$
$$= \rho^2/500$$

Using these approximations, an estimate of the variance of a safety margin can be obtained by solving eqn.1A.

Appendix 3 - Summary of measurements taken from five slopes.

1) 13 July 1982 - Cornicewall: 18 shear strength measurements (9 were less than the downslope gravitational load) were made across the crownwall of an avalanche that we had ski-released. Jumping near the crown had caused local failure of a section about $4m^2$ in area, which slid about .7m before the rest of the slab fractured. The avalanche was about 30m wide and 20m long.

spacing between shear measurements:	0.89m
bed surface angle:	47°
slab density:	$140kg/m^3$.
downslope weight of slab:	$431N/m^2$
basal shear strength at "points":	$549\pm345N/m^2$
"scale" between shear measurements:	1.84m
slab depth:	.43±.09m
"scale" between depth measurements:	1.03m
tensile strength (3 measurements):	$1073\pm388N/m^2$

2) 19 September 1982 - Cornicewall: 19 shear strength measurements (5 were less than the downslope gravitational load) were made down the flankwall of an avalanche that had released naturally about 15-24 hrs previously. The avalanche was caused by high snowfall and wind transport of snow (depths of 1-2m were measured), overlying some 1mm faceted crystals which formed a layer up to 40mm thick. The avalanche was about 150m wide and 80m long.

spacing between shear measurements:	0.7m
bed surface angle:	34°
slab density:	$290kg/m^3$
downslope weight of the slab:	$1478N/m^2$

basal shear strength at "points":	1840±572N/m^2
"scale" between shear measurements:	.21m
slab depth:	0.93±.10m
"scale" between depth measurements:	2.26m
estimate of tensile strength:	3000-8000N/m^2

3) 10 August 1983 - Cornicewall: 11 shear strength measurements (5 were less than the downslope gravitational load) were made across the slope. Extensive jumping on the slope resulted in local failures where slabs about two metres square slid a short distance. The fractures did not propagate. The shear layer consisted of 0.5-1.5mm diam graupel at temp.= -5.0°C.

spacing between shear measurements:	0.75m
bed surface angle:	35-50°
slab density:	280kg/m^3
downslope weight of the slab:	758 N/m^2
basal shear strength at "points":	1111±397N/m^3
"scale" between shear measurements:	.19m
slab depth:	.43±.16m
"scale" between depth measurements:	.5m
estimate of tensile strength:	3000-8000N/m^3

4) 1 August 1984 - Cornicewall: 19 shear strength measurements (9 were less than the downslope gravitational load) were made across the slope. This small avalanche (12.5m wide and 7m long) was ski released from near the middle of the crownwall. The slab consisted of rounded, wind affected, partly metamorphosed snow, and sheared on some very, very soft new snow (1mm diam. partly rimed capped columns, columns, dendrites and needles).

spacing between shear measurements:	0.7m
bed surface angle:	35-56°
slab density:	180kg/m^3
downslope weight of the slab:	204N/m^2
basal shear strength at "points":	271±158N/m^2
"scale" between shear measurements:	0.97m
slab depth:	.18±.03m
"scale" between depth measurements:	0.87m

estimate of tensile strength: 1200-3000N/m^2

5) 28 August 1984 - Cornicewall: 20 shear strength measurements (7 were less than the downslope gravitational load) were made across the slope. This small avalanche (12m x 10m) required jumping on skis for release. The slope had been wind loaded with heavily rimed and rounded snow crystals, and this slab was overlying some low density snow which also contained surface hoar which had developed during previous fine weather. After the initial fracture, we released a further section of the slope (about 5m further north).

spacing between shear measurements:	.6m
bed surface angle:	45-49°
slab density:	260kg/m^3
downslope weight of the slab:	465 N/m^2
basal shear strength at "points":	559±273N/m^2
"scale" between shear measurements:	.11m
slab depth:	.25±.08m
"scale" between depth measurements:	1.72m
estimate of tensile strength:	2000-8000N/m^2

Appendix 4: tensile strength measurements.

A total of 15 tensile strength measurements were made spatially across the Cornicewall on the 14 September 1985. The slab consisted of partly metamorphosed new snow at -6°C.

slab density:	180kg/m^3
slope angle:	20°
approx. area of tensile tests:	0.025m^2
spacing between measurements:	0.8m
"point" tensile strength:	2780±30%N/m^2
"scale" between tensile measurements:	0.45m
slab depth:	.22±.02m
"scale" between depth measurements:	.44m

Appendix: Basic program to determine optimum size of local failure, and the probability of further progression of the failure.

```
10 OPEN "CORN.DAT" FOR OUTPUT AS FILE#1
15 PRINT #1,"OPTIMUM FAILURE SIZE FOR LOCAL FAILURE AND SUBSEQUENT PROPOGATION -FROM PROP.BAS"
20 DIM AF(25),AL(25),H(25),HF(25),S(8),F(8),D(8),MS(8)
30 INPUT "DATE OF AVALANCHE=";D;M$;Y
40 PRINT #1, "DATE";D; ;M$;     ;Y
50 INPUT "LOCATION OF AVALANCHE=";L$
51 PRINT #1, "LOCATION OF AVALANCHE=";L$
55 INPUT "TOTAL NUMBER OF MEASUREMENTS=";NI
60 INPUT "SLAB DENSITY=";SD;  "SLOPE ANGLE=";SA
70 INPUT "HORIZONTAL DISTANCE BETWEEN SAMPLES=";BX
80 PRINT #1, "TOTAL NUMBER OF MEASUREMENTS=";NI
85 PRINT #1, "HORIZONTAL DISTANCE BETWEEN SAMPLES =";BX
90 PRINT #1, "SLAB DENSITY=";SD;  "SLOPE ANGLE=";SA
91 SA=(SA*3.1414)/180
95 J=0
96 J=J+1
100 INPUT "SHEAR STRENGTH=";AF(J);    "DEPTH OF FRACTURE=";H(J)
105 PRINT #1, "NO.=";J;"SHEAR STRENGTH=";AF(J);   "DEPTH=";H(J)
106 IF J<>NI GOTO 96
107 EW=0
110 NM=26
111 INPUT "ESTIMATE OF TENSILE STRENGTH";TS
119 PRINT #1,"ESTIMATE OF TENSILE STRENGTH=";TS
120 I=0
121 I=I+1
122 DY=I*BX
1950 REM SUBROUTINE FOR ALPHA ST DEV
1995 T1=0
1996 T2=0
1997 T3=0
1998 T4=0
1999 T5=0
2000 T6=0
2001 T7=0
2002 T8=0
2005 S1=0
2006 S2=0
2007 S3=0
2008 S4=0
2009 S5=0
2010 S6=0
2011 S7=0
2012 S8=0
2015 Z1=0
2016 Z2=0
2017 Z3=0
2018 Z4=0
2019 Z5=0
2020 Z6=0
2021 Z7=0
2022 Z8=0
2025 H1=0
2026 H2=0
2027 H3=0
2028 H4=0
2029 H5=0
2030 H6=0
2031 H7=0
2032 H8=0
2036 W1=0
2037 W2=0
2038 W3=0
2039 W4=0
2040 W5=0
2041 W6=0
2042 W7=0
2043 W8=0
2046 FOR K=1 TO NI
2047 AL(K)=AF(K)
2048 A1=LOG(AL(K))
2050 T1=T1+A1
2060 S1=S1+A1^2
2061 H1=H(K)
2062 W1=W1+H1
2063 Z1=Z1+H1^2
2070 NEXT K
2075 H1=W1/NI
2076 Z1=SQR((Z1-(W1^2)/NI)/(NI-1))
2079 ZF=Z1
2080 Y1=Z1/ZF
2081 A1=T1/NI
2090 S1=SQR((S1-(T1^2)/NI)/(NI-1))
2096 RF=S1*EXP(A1)
2097 V1=(S1*EXP(A1))/RF
2130 FOR K=1 TO NI-1
2131 H2=(H(K)+H(K+1))/2
2132 Z2=Z2+H2^2
2133 W2=H2+W2
2140 A2=(AL(K)+AL(K+1))/2
2150 T2=T2+LOG(A2)
2160 S2=S2+(LOG(A2))^2
2170 NEXT K
2171 H2=W2/(NI-1)
2173 Z2=SQR((Z2-(W2^2)/(NI-1))/(NI-2))
2175 Y2=Z2/ZF
2180 A2=T2/(NI-1)
2190 S2=SQR((S2-(T2^2)/(NI-1))/(NI-2))
2191 V2=(S2*EXP(A2))/RF
2230 FOR K=1 TO (NI-2)
2231 H3=(H(K)+H(K+1)+H(K+2))/3
2232 Z3=Z3+H3^2
2234 W3=W3+H3
2240 A3=(AL(K)+AL(K+1)+AL(K+2))/3
2250 T3=T3+LOG(A3)
2260 S3=S3+(LOG(A3))^2
2270 NEXT K
2271 H3=W3/(NI-2)
```

```
2272 Z3=SQR((Z3-(W3^2)/(NI-2))/(NI-3))
2274 Y3=Z3/ZF
2280 A3=T3/(NI-2)
2290 S3=SQR((S3-(T3^2)/(NI-2))/(NI-3))
2291 V3=(S3*EXP(A3))/RF
2330 FOR K=1 TO (NI-3)
2331 H4=(H(K)+H(K+1)+H(K+2)+H(K+3))/4
2332 Z4=Z4+H4^2
2334 W4=W4+H4
2340 A4=(AL(K)+AL(K+1)+AL(K+2)+AL(K+3))/4
2350 T4=LOG(A4)+T4
2360 S4=S4+(LOG(A4))^2
2370 NEXT K
2371 H4=W4/(NI-3)
2372 Z4=SQR((Z4-(W4^2)/(NI-3))/(NI-4))
2373 Y4=Z4/ZF
2380 A4=T4/(NI-3)
2390 S4=SQR((S4-(T4^2)/(NI-3))/(NI-4))
2391 V4=(S4*EXP(A4))/RF
2430 FOR K=1 TO (NI-4)
2431 H5=(H(K)+H(K+1)+H(K+2)+H(K+3)+H(K+4))/5
2432 Z5=Z5+H5^2
2433 W5=W5+H5
2440 A5=(AL(K)+AL(K+1)+AL(K+2)+AL(K+3)+AL(K+4))/5
2450 T5=T5+LOG(A5)
2460 S5=S5+(LOG(A5))^2
2470 NEXT K
2471 H5=W5/(NI-4)
2472 Z5=SQR((Z5-(W5^2)/(NI-4))/(NI-5))
2473 Y5=Z5/ZF
2480 A5=T5/(NI-4)
2490 S5=SQR((S5-(T5^2)/(NI-4))/(NI-5))
2491 V5=(S5*EXP(A5))/RF
2530 FOR K=1 TO (NI-5)
2531 H6=(H(K)+H(K+1)+H(K+2)+H(K+3)+H(K+4)+H(K+5))/6
2532 Z6=Z6+H6^2
2533 W6=W6+H6
2540 A6=(AL(K)+AL(K+1)+AL(K+2)+AL(K+3)+AL(K+4)+AL(K+5))/6
2550 T6=T6+LOG(A6)
2560 S6=S6+(LOG(A6))^2
2570 NEXT K
2571 H6=W6/(NI-5)
2572 Z6=SQR((Z6-(W6^2)/(NI-5))/(NI-6))
2573 Y6=Z6/ZF
2580 A6=T6/(NI-5)
2590 S6=SQR((S6-(T6^2)/(NI-5))/(NI-6))
2591 V6=(S6*EXP(A6))/RF
2630 FOR K=1 TO (NI-6)
2631 H7=(H(K)+H(K+1)+H(K+2)+H(K+3)+H(K+4)+H(K+5)+H(K+6))/7
2632 Z7=Z7+H7^2
2633 W7=W7+H7
2640 A7=(AL(K)+AL(K+1)+AL(K+2)+AL(K+3)+AL(K+4)+AL(K+5)+AL(K+6))/7
2650 T7=T7+LOG(A7)
2660 S7=S7+(LOG(A7))^2
2670 NEXT K
2671 H7=W7/(NI-6)
2672 Z7=SQR((Z7-(W7^2)/(NI-6))/(NI-7))
2673 Y7=Z7/ZF
2680 A7=T7/(NI-6)
2690 S7=SQR((S7-(T7^2)/(NI-6))/(NI-7))
2691 V7=(S7*EXP(A7))/RF
2700 R7=(NI-7)
2730 FOR K=1 TO (NI-7)
2731 H8=(H(K)+H(K+1)+H(K+2)+H(K+3)+H(K+4)+H(K+5)+H(K+6)+H(K+7))/8
2732 Z8=Z8+H8^2
2734 W8=W8+H8
2740 A8=(AL(K)+AL(K+1)+AL(K+2)+AL(K+3)+AL(K+4)+AL(K+5)+AL(K+6)+AL(K+7))/8
2750 T8=T8+LOG(A8)
2760 S8=S8+(LOG(A8))^2
2770 NEXT K
2771 H8=W8/(NI-7)
2772 Z8=SQR((Z8-(W8^2)/(NI-7))/(NI-8))
2773 Y8=Z8/ZF
2780 A8= T8/(NI-7)
2790 S8=SQR((S8-(T8^2)/(NI-7))/(NI-8))
2791 V8=(S8*EXP(A8))/RF
2800 IF I=1 THEN 2801 ELSE 2804
2801 HR=H2
2802 VR=V2
2803 YR=Y2
2804 IF I=2 THEN 2805 ELSE 2808
2805 HR=H3
2806 VR=V3
2807 YR=Y3
2808 IF I=3 THEN 2809 ELSE 2812
2809 HR=H4
2810 VR=V4
2811 YR=Y4
2812 IF I=4 THEN 2813 ELSE 2816
2813 HR=H5
2814 VR=V5
2815 YR=Y5
2816 IF I=5 THEN 2817 ELSE 2820
2817 HR=H6
2818 VR=V6
2819 YR=Y6
2820 IF I=6 THEN 2821 ELSE 2824
2821 HR=H7
2822 VR=V7
2823 YR=Y7
2824 IF I=7 THEN 2825 ELSE 3520
2825 HR=H8
2826 VR=V8
2827 YR=Y8
3400 REM TO CALCULATE VARIANCES OF BASAL SHEAR FORCE
3520 S2=RF*VR*V2
3530 S3=RF*VR*V3
3540 S4=RF*VR*V4
3550 S5=RF*VR*V5
3560 S6=RF*VR*V6
```

```
3570 S7=RF*VR*V7
3580 S8=RF*VR*V8
3620 REM TO CALCULATE THE TOTAL RESISTING FORCES (Q)
3636 P2=TS*H2/DY
3637 Q2=TS*HR/BX
3638 G2=EXP(A2)+P2+2*Q2
3640 P3=TS*H3/DY
3642 Q3=TS*HR/(2*BX)
3644 G3=EXP(A3)+P3+2*Q3
3650 P4=TS*H4/DY
3652 Q4=TS*HR/(3*BX)
3654 G4=EXP(A4)+P4+2*Q4
3660 P5=TS*H5/DY
3662 Q5=TS*HR/(4*BX)
3664 G5=EXP(A5)+P5+2*Q5
3670 P6=TS*H6/DY
3672 Q6=TS*HR/(5*BX)
3674 G6=EXP(A6)+P6+2*Q6
3680 P7=TS*H7/DY
3682 Q7=TS*HR/(6*BX)
3684 G7=EXP(A7)+P7+2*Q7
3690 P8=TS*H8/DY
3692 Q8=TS*HR/(7*BX)
3694 G8=EXP(A8)+P8+2*Q8
3800 REM TO CALCULATE THE DRIVING FORCES (B)
3801 LW=EW-9.8*SIN(SA)
3810 Q=SD*9.8*SIN(SA)
3829 M2=Q*H2
3830 AX=BX*DY
3831 IF AX>1 THEN 3835
3832 B2=M2+LW*BX*DY
3833 GOTO 3840
3835 B2=M2+LW/(BX*DY)
3840 M3=Q*H3
3841 IF AX>.5 THEN 3845
3842 B3=M3+LW*BX*2*DY
3843 GOTO 3850
3845 B3=M3+LW/(BX*2*DY)
3850 M4=Q*H4
3855 B4=M4+LW/(BX*3*DY)
3860 M5=Q*H5
3865 B5=M5+LW/(BX*4*DY)
3870 M6=Q*H6
3875 B6=M6+LW/(BX*5*DY)
3880 M7=Q*H7
3885 B7=M7+LW/(BX*6*DY)
3890 M8=Q*H8
3895 B8=M8+LW/(BX*7*DY)
3900 REM TO CALCULATE THE MARGINS OF SAFETY (D)
3902 D2=(G2-B2)
3903 D3=(G3-B3)
3904 D4=(G4-B4)
3905 D5=(G5-B5)
3906 D6=(G6-B6)
3907 D7=(G7-B7)
3908 D8=(G8-B8)
3910 REM TO CALCULATE CONTRIBUTIONS TO THE VARIANCE OF THE SAFETY MARGIN
3925 FT=VR*ZF/HR
3930 E2=S2^2+(M2^2)/500+((.27*P2*V2)^2)+2*(.27*Q2*VR)^2+2*(Q2*FT)^2+((P2*Y2*ZF/H2)^2)*5+(M2*Y2*FT)^2
3940 E3=S3^2+(M3^2)/500+((.27*P3*V3)^2)+2*(.27*Q3*VR)^2+2*(Q3*FT)^2+((P3*Y3*ZF/H3)^2)*5+(M3*Y2*FT)^2
3950 E4=S4^2+(M4^2)/500+((.27*P4*V4)^2)+2*(.27*Q4*VR)^2+2*(Q4*FT)^2+((P4*Y4*ZF/H4)^2)*5+(M4*Y4*FT)^2
3960 E5=S5^2+(M5^2)/500+((.27*P5*V5)^2)+2*(.27*Q5*VR)^2+2*(Q5*FT)^2+((P5*Y5*ZF/H5)^2)*5+(M5*Y5*FT)^2
3970 E6=S6^2+(M6^2)/500+((.27*P6*V6)^2)+2*(.27*Q6*VR)^2+2*(Q6*FT)^2+((P6*Y6*ZF/H6)^2)*5+(M6*Y6*FT)^2
3980 E7=S7^2+(M7^2)/500+((.27*P7*V7)^2)+2*(.27*Q7*VR)^2+2*(Q7*FT)^2+((P7*Y7*ZF/H7)^2)*5+(M7*Y7*FT)^2
3990 E8=S8^2+(M8^2)/500+((.27*P8*V8)^2)+2*(.27*Q8*VR)^2+2*(Q8*FT)^2+((P8*Y8*ZF/H8)^2)*5+(M8*Y8*FT)^2
4000 REM TO CALCULATE  THE NORMALISED VARIATES(RELIABILITY RATIOS)
4280 E2=SQR(E2)
4290 N2=D2/E2
4310 E3=SQR(E3)
4320 N3=D3/E3
4340 E4=SQR(E4)
4350 N4=D4/E4
4370 E5=SQR(E5)
4385 N5=D5/E5
4400 E6=SQR(E6)
4410 N6=D6/E6
4430 E7=SQR(E7)
4440 N7=D7/E7
4460 E8=SQR(E8)
4470 N8=D8/E8
4475 IF N2>NM THEN 4500
4480 NM=N2
4482 EC=E2
4485 AC=EXP(A2)
4486 KC=HR
4487 UC=YR
4488 YC=Y2
4490 DC=DY
4494 BC=BX
4495 HC=H2
4497 SC=S2
4500 IF N3>NM THEN 4530
4510 NM=N3
4511 AC=EXP(A3)
4512 DC=DY
4513 BC=2*BX
4514 HC=H3
4516 SC=S3
4519 EC=E3
4521 KC=HR
4522 UC=YR
4523 YC=Y3
4530 IF N4>NM THEN 4560
4531 NM=N4
4532 AC=EXP(A4)
4533 DC=DY
4534 BC=3*BX
4536 HC=H4
4537 SC=S4
4540 EC=E4
```

```
4541 KC=HR
4542 UC=YR
4543 YC=Y4
4560 IF N5>NM THEN 4590
4561 NM=N5
4562 AC=EXP(A5)
4563 DC=DY
4564 BC=4*BX
4566 HC=H5
4567 SC=S5
4570 EC=E5
4571 KC=HR
4572 UC=YR
4573 YC=Y5
4590 IF N6>NM THEN 4630
4611 NM=N6
4612 AC=EXP(A6)
4613 DC=DY
4614 BC=5*BX
4616 HC=H6
4617 SC=S6
4620 EC=E6
4621 KC=HR
4622 UC=YR
4623 YC=Y6
4630 IF N7>NM THEN 4660
4631 NM=N7
4632 AC=EXP(A7)
4633 DC=DY
4634 BC=6*BX
4636 HC=H7
4637 SC=S7
4640 EC=E7
4641 KC=HR
4642 UC=YR
4643 YC=Y7
4660 IF N8>NM THEN 4671
4661 NM=N7
4662 AC=EXP(A7)
4663 DC=DY
4664 BC=7*BX
4666 HC=H8
4667 SC=S8
4670 EC=E8
4671 KC=HR
4672 UC=YR
4673 YC=Y8
4674 IF I<>7 GOTO 121
4675 IF BC*DC>1 THEN 4678
4676 BC=1
4677 DC=1
4678 IF EW<>0 THEN 4690
4680 PRINT #1, "NO EXTRA LOAD ON THE SLOPE"
4685 GoTo 4700
4690 PRINT #1, "LOAD ON SLOPE=";EW;"KILOGRAMS"
4700 PRINT #1, "MIN.RELIABILITY, MOST PROBABLE FAILURE AREA.DEPTH ETC."
4709 PRINT #1 USING "LENGTH OF SLICE=##.## WIDTH OF SLICE=##.##";DC;BC
4710 PRINT #1 USING "MIN. RELIABILITY=####.##";NM
4711 PRINT #1 USING "BASAL SHEAR OF MIN=#####  SD OF BASAL SHEAR=####";AC;SC
4713 PRINT #1 USING "SLAB DEPTH=#.###";HC
4720 REM FOR PROPOGATION - RESISTING FORCES OVER CRITICAL SLICE
4730 INPUT "STRAIN SOFTENING RATIO FOR FAILED SLICE=";SR
4731 PRINT #1, "STRAIN SOFTENING RATIO FOR FAILED SLICE=";SR
4732 INPUT "STRAIN SOFTENING RATIO FOR UNFAILED SLICE=";SRU
4733 PRINT #1, "STRAIN SOFTENING RATIO FOR UNFAILED SLICE=";SRU
4736 PRINT #1, "FOR PROPOGATION DOWN-SLOPE - NO TENSILE OR COMPRESSIVE HOLDUP"
4750 QC=TS*KC/BC
4760 GC=SRU*AC+2*QC
4770 REM FOR DRIVING FORCES ON SLICE
4780 FOR L=1 TO 8
4790 LW=EW*9.8*SIN(SA)/(BC*DC)
4800 D(L)=(L+1)*SD*HC*9.8*SIN(SA)-(L*SR*AC)+LW
4810 REM FOR MARGIN OF SAFETY, VARIANCE AND RELIABILITY RATIO.
4820 MS(L)=GC-D(L)
4830 S(L)=(EC-.27*TS*HC*VC/DC-(1-SRU)*SC)^2+L*(SC*SR)^2+(L*(SD*9.8*SIN(SA)*HC)^2)/500
4831 S(L)=S(L)+2*L*(QC*UC*ZF/KC)^2+L*(SD*9.8*SIN(SA)*UC*YC*ZF)^2+5*L*(TS*YC*ZF/BC)^2
4840 N(L)=MS(L)/(SQR(S(L)))
4850 PRINT #1, "NO. OF FAILED SLICES=";L
4860 PRINT #1 USING "RELIABILITY RATIO OF UNFAILED SLICE=###.####";N(L)
4870 NEXT L
4880 INPUT "TRY ANOTHER LOAD/ETC?-TYPE 'RET' TO QUIT OR THE LOAD=";EW
4890 IF EW<>0 THEN 110
5055 CLOSE#1
5060 STOP
```

A FIELD TEST TO ASSESS SNOW SLOPE STABILITY.

By H. Conway, J. Abrahamson and R. Young.
(Department of Chemical and Process Engineering, University of Canterbury, Private Bag, Christchurch, New Zealand.)

ABSTRACT.

A simple field test of snow slope stability is proposed, which allows decisions about a number of factors recently described by Conway and Abrahamson (1984). These include spatial variation of snow strength along a slope, and progression of failure from a localised initial failure. Strength within the snow slab is considered as well as that at its base.

A snow saw is required for the test, and because a number of tests can be made in a few minutes, much information on the state of the slope can be obtained in a practical time.

INTRODUCTION.

Most techniques used for snow stability assessment rely on some interpretive skills of the observer as well as special equipment (for example snow stratigraphy tests, a ram penetrometer, explosives, shear tests as outlined by Sommerfeld,1984, or Conway and Abrahamson,1984, the wedge test of LaChapelle and Ferguson,1980). The "shovel test" (described by Sommerfeld,1984), enables an estimate of the extra downslope force required to overcome basal resisting forces, and requires only simple equipment to perform (a snow shovel and saw). Some interpretive skills are required to assign a rating to the extra force needed for failure and then to relate it to the stability of the slope.

Recent studies (Conway and Abrahamson,1984, and Sommerfeld,in prep.) have found significant spatial variability of snow strength. More recently Conway and Abrahamson,(companion paper - referred to as CA below), have allowed for this spatial variability in assessing the stability of a snow slope. They have combined a simple force excess criterion (imposed forces minus a combination of

resisting forces acting together on a certain section of the slope), with a probabilistic description of the variables. A "local" failure was considered to occur when the forces driving a localised section of the snow slab (the downslope component of gravitational weight plus any extra forces such as a skier), exceeded the forces resisting the loads (the resistance around the peripheries, including the base of the section of slab). Their conclusion was that the most likely failure area was about 1m x 1m in size. Furthermore, on large slopes with moderate snow strengths, such a "local" failure was likely to occur at least once on many slopes.

Because the most likely failure area was found to be small compared with observed sizes of avalanches, an initial failure needs to propagate in order to cause an avalanche. From CA, a local failure would be expected on all but small slopes of relatively high strength, so occurrence of such a failure appears not to be a sufficient criterion for slope instability. Instead it was proposed in CA that the probability of a local failure propagating to adjacent snows should be the primary consideration for slope failure assessment.

Scales of spatial variability.

We think wind may strongly influence the patterns of distribution of both snow strength and snow depth - and hence driving force. We have noted surface ripples left after winds, and measured wavelengths (peak to adjacent peak distance) in the wide range 10mm to about 15m. Commonly however the spacing was less than 5m. Because we believe that the basal shear strength depends on the conditions of local deposition of the snow forming that layer, we expect the basal shear strength may vary with wavelengths of similar range to those of snow ripples. In fact, for the six completed sets of spatial measurements of snow strength across slopes, the average wavelength of the shear strength ranged from about 0.3m to 4.6m (the "wavelength" here was taken to be 2.5 times the correlation length - see CA).

Slope risk assessment depends on adequate estimates of both the mean and the variation of strength. It is clear that with a semi-periodic variation, measurements should be made over at least one entire wavelength. In the absence of knowledge of the wavelength, the tests should ideally be made over 15m, but often a series over a smaller distance will give an adequate description. If snow loading or snow strength change gradually but considerably over a slope as might be expected in drifts behind obstacles, the slope should be subdivided into sections which can be regarded as closely similar, and sets of tests on each section would be necessary.

An unequivocal test which can satisfy the above requirements, uses simple equipment, and can be done with minimum expenditure of energy and time, is described below.

THE PROPOSED "SAW TEST".

This test requires the use of a saw with appreciable thickness and longer than most snow saws. The thickness is required to leave a gap in the snow to enable observation of block movement and to prevent an isolated block from fouling surrounding snow when moving parallel to the cut. We found that a saw made from a 10mm thick plywood, 1m in length to the handle, with teeth made by cutting 50mm diam semi-circular notches, was a satisfactory tool.

The steps of the test are:

(1) Choose a position close to a potential crown zone and make a single sawcut about 1.5m long, across the slope to a depth greater than the suspected shear plane.

(2) 1m above the centre of the single sawcut, simulate a failed critical area by sawcutting the four boundaries of a square column 1m x 1m to a depth greater than the suspected failure plane (see fig.1). The sawcuts are best made vertically (to avoid bending of the column). Continue the cross-slope cuts out to the side by about 100mm to allow observation of the plane of slip.

(3) (a) Note whether the column has failed in basal shear.

(b) If the column has failed, note whether the extra

weight of the failed column has caused the snow immediately below it to fail in sideshear (ie. whether the lower sawcut has closed).

(4) Ski on to the top of the column, note any failure, and then jump (to simulate a turn or a fall), and note whether fracture has occurred and whether it has propagated and caused the lower sawcut to close.

(5) If the failure has still not progressed to the lower snow, an assessment of the level of stability is possible by making sawcuts from the extremities of the lower sawcut (e and e'), towards the column until failure occurs (see fig.1).

(6) To allow for any spatial variability of strength, a number of such tests should be made contiguously (see fig.2). In most cases 5 such tests should be sufficient to determine a reasonable stability estimate, but more may be needed in some situations. To avoid disrupting adjacent tests when isolating blocks while still making contiguous measurements, it is best to work down a slope with succeeding tests, as shown in fig.2. The horizontal cuts can be made first as the experimenter moves down one side, and the vertical cuts made after each jump test.

If the first three tests show failure progression, the slope should be considered unstable. In fact, if one half or more of the total number of tests (with extra load applied) show failure progression, the slope should be considered unstable. If snow strengths or loadings are likely to differ considerably at another location on the slope, a further series of tests at that location would be desirable.

DISCUSSION OF THE TESTS.

The test allows for several factors which are expected to influence slope stability:

(1) especially for hard slabs, the strength within the slab may be sufficient to prevent progressive failure, and we think this strength in addition to basal shear strength should be included in a stability assessment. On the other hand, for soft slabs the upper snow layers may compress rather than transmit forces to adjacent snow, and cause "point release"

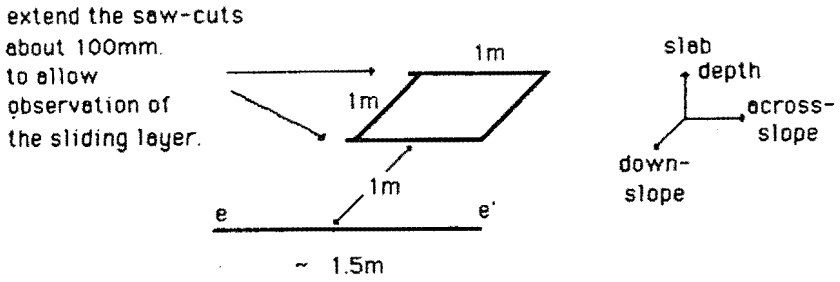

Isolate a snow block as shown above, 1m above the centre of a single saw-cut, ee'. The saw-cuts should be made vertically and to at least the depth of the suspected weak layer in the snowpack.

Figure 1.

Preparation of snow columns for the proposed saw test.

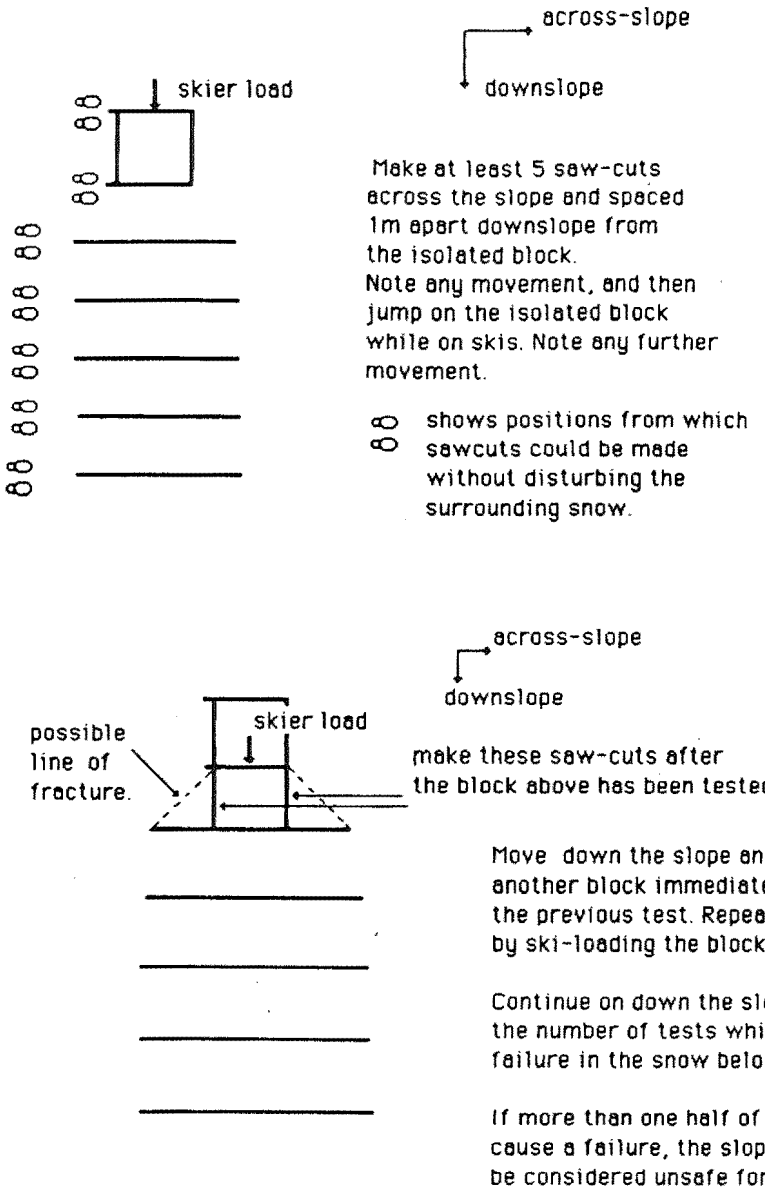

Fig.2: Method of testing for propagation of failure with skier loading. By repeating the test the spatial variability can be ascertained.

rather than "slab" type avalanches. The behaviour of both hard and soft slabs will be shown up in the progression part of the above test.

After a small movement, the shear strength of snow may drop from its original value (McClung,1977). When we cut the four boundaries of a column (step 2 above), a local failure has not been strictly simulated unless the column moves and the basal strength takes its residual value. We have found however that when a skier loads an isolated column, the column generally slips and thus simulates a local failure. The shear strength of the basal surface of this $1m^2$ column will in many instances, have assumed a lower "residual" value before the column transmits load to its downslope neighbour.

(2) the forces driving the slab downslope are influenced by: (a) slope angle, (b) slab depth and density, and (c) an external load such as a skier.

All of these factors are implicit in the test. We are particularly interested if a skier will cause an avalanche by standing or jumping on a slope. A skier may make a significant contribution to the forces driving the avalanche in situations when the slab consists of low density snow and is shallow. Several skiers on a slope not only increase the total load but also, by traversing a larger area, increase the probability of causing an initial "local" failure and progression.

Provided the sawcuts are sufficiently deep to penetrate the sliding layer, it is not important to know the location of the layer prior to the tests. However after the test, the depth to the layer most likely to slide under the weight of a skier can be easily measured. If fracture depths for a region are typically greater than 1m, a saw longer than 1m would be required.

A cutting edge could be made by clipping some plastic teeth on to a ski edge or to ski poles. This would save carrying a saw, and would also increase the depth to which one could isolate columns.

At the present time we have not made sufficient tests using the described technique to confidently set limits which might differentiate potential avalanche slopes from stable slopes. Our suggested "half failure" rule is largely derived from previous experimental work (CA) and will be improved by experience with this test. Also we cannot locate the weakest "statistically homogeneous" zone on a slope, but because the series of tests can be made rapidly (5 snow columns took about 5 minutes to isolate using the saw mentioned above), it is possible to make several series of tests with a minimum expenditure of energy and time. The tests also do not disrupt a slope for skiing, should it be judged stable.

In the tests described above, we have considered propagation of the failure downslope, but a similar set of experiments could be made to study failures progressing across slopes.

CONCLUSIONS.

A simple field test based on findings from a companion paper (CA) is proposed. The test follows work with a static force balance model, together with a statistical model of failure probability, and is a test for failure progression rather than one for initial failure. The test is easily and quickly made, and with experience should yield unequivocal information about slope stability.

ACKNOWLEDGEMENTS.

The Department of Lands and Survey (Wellington, New Zealand) and the University of Canterbury (Christchurch, New Zealand) provided financial support for the study. Mt. Cook Airlines provided transport to the field area, and assistance from Mt. Cook National Park staff was invaluable. We are grateful to all these people for their assistance.

LIST OF REFERENCES.

Conway, H. and Abrahamson, J.: (1984) "Snow stability index". Journal of Glaciology, Vol.30, No.106, p321-327.

Conway, H. and Abrahamson, J.: (accompaning paper) "Snow slope stability - a probablistic approach".

LaChapelle, E.R. and Ferguson, S.A.: (1980) "Snowpack

structure: stability analysed by pattern-recognition techniques". Journal of Glaciology, Vol.29, No.94, p506-511.

McClung, D.M.: (1977) "Direct simple shear tests on snow and their relation to slab avalanche formation". Journal of Glaciology, Vol.19, No.81, p101-109.

Sommerfeld, R.A.: (1984) "Instructions for using the 250cm2 shear frame to evaluate the strength of a buried snow surface". USDA Rocky Mountain Forest and Range Experiment Station Research Note, RM-446, 6pps.

Sommerfeld, R.A.: (in prep.) "Spatial variation of shear strengths of avalanche sliding surfaces".

Cold Regions Science and Technology, 11 (1985) 199–202
Elsevier Science Publishers B.V., Amsterdam – Printed in The Netherlands

Short communication

REMOTE SENSING OF SNOW ACCUMULATION

W.M. Earl, G.R. Grey, H. Conway and J. Abrahamson
Department of Chemical and Process Engineering, University of Canterbury, Private Bag, Christchurch (New Zealand)

(Received October 10, 1984; accepted in revised form March 14, 1985)

ABSTRACT

New snow depth provides a valuable tool for forecasting avalanches. We have modified an ultrasonic rangefinder available from Polaroid, and have mounted the unit at the top of a tripod. By taking hourly measurements, the changes in distance between the transducer and the snowpack can be evaluated. Blowing snow during storms shows up as scattered data, and at the end of a storm the readings become stable. The data indicate the length of the storm as well as the new snow increment.

THE ULTRASONIC UNIT

Ultrasonic wave reflection devices have been used in several cases to measure new snow depth (e.g., Caillet et al., 1979; Gubler, 1981; Ludwig and Dick, 1983; Marbouty and Pougatch, 1983). We have adapted and packaged a commercially available ultrasonic ranging unit to measure the accumulation or ablation of snow beneath a tripod as an input to a remote weather station.

The kitset (supplied by Polaroid Corporation, MA, U.S.A.) consists of an instrument-grade transducer and two printed circuits. On one of these boards is a three-digit display which shows the distance from the transducer to a target in the range of 0.28–10 m with a resolution of 0.03 m. This display is updated every second when a six volt power supply is connected to the electronics.

INTERFACING FOR DATA LOGGING

We have added a third printed board to the package. One part of the board processes the output signal into a form suitable for a data logger or for radio telemetry. The display supplied with the unit is multiplexed, and we have chosen to take three signals from the Polaroid board and decode them to give a simple eight-bit binary output (see Fig. 1). This output can easily be read by data logging equipment.

The other part consists of a simple R–C clock oscillator divided down to give a pulse every hour. This pulse, which lasts for about five seconds, closes a relay to give power to the ultrasonic system. The ultrasonic system takes five readings, to allow the readings to stabilize. The last reading appears on the output bus as an eight-bit binary word. The electronic clock uses very little power (6 mA), and its use enables the average battery current drain to be reduced from 120 mA (continuous ultrasonic system operation) to 6 mA.

PACKAGING OF THE UNIT

The rangefinder transducer was sealed into the bottom of a sturdy fibreglass box with silicone rubber and used a plastic cone to provide some protection for the transducer from blowing snow (see Fig. 2). It was important to ensure that the cone did not interfere with the transducer signals. The three printed circuit boards were mounted inside the box, with the board containing the display uppermost so the display could easily be checked manually. The clear perspex lid has a rubber gasket, and also a tube running through it with a rubber balloon attached inside. This was designed to keep the box dry and to allow for pressure changes due to altitude, or temperature changes which we thought could rupture the diaphragm in the transducer. We also used a small bag of silica gel in the box. One multiway connector was

0165-232X/85/$03.30

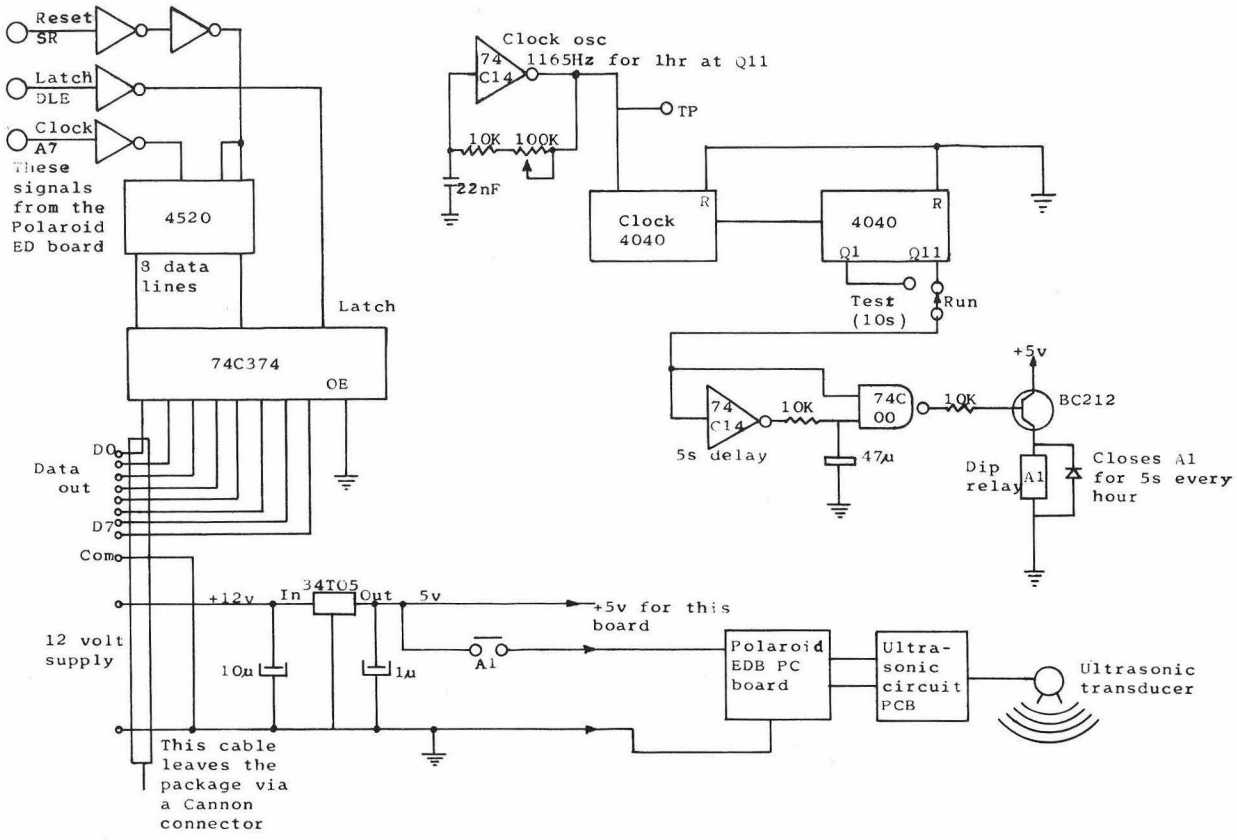

Fig. 1. Supply interface and control P.C.B. for the ultrasonic snow depth measurements.

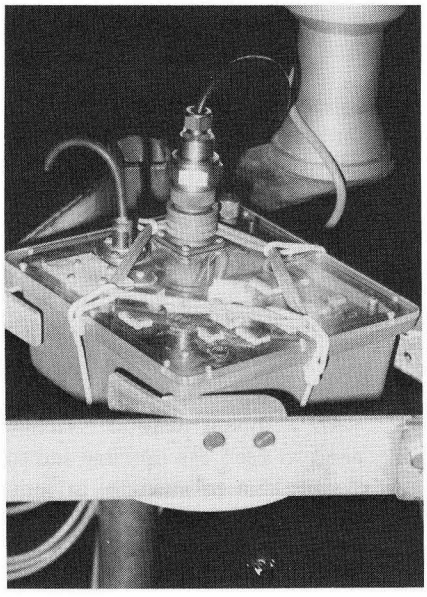

used to carry power and data lines to and from the unit.

Outside dimensions of the unit (excluding the removable protective cone) are 200 mm X 200 mm X 80 mm and the total weight is 1.6 kg.

RESULTS FROM THE RANGEFINDER

The unit has withstood two winter seasons at 2130 m on the Tasman Glacier (New Zealand). It has been mounted at the top of a tripod with some other instruments, and the data recorded on a small data logger. At present, we are commissioning a radio telemetry system to Mount Cook Village which is about 35 km from the site.

Figure 3 shows a plot of some of the data col-

Fig. 2. Photograph of the packaged unit at the top of the tripod.

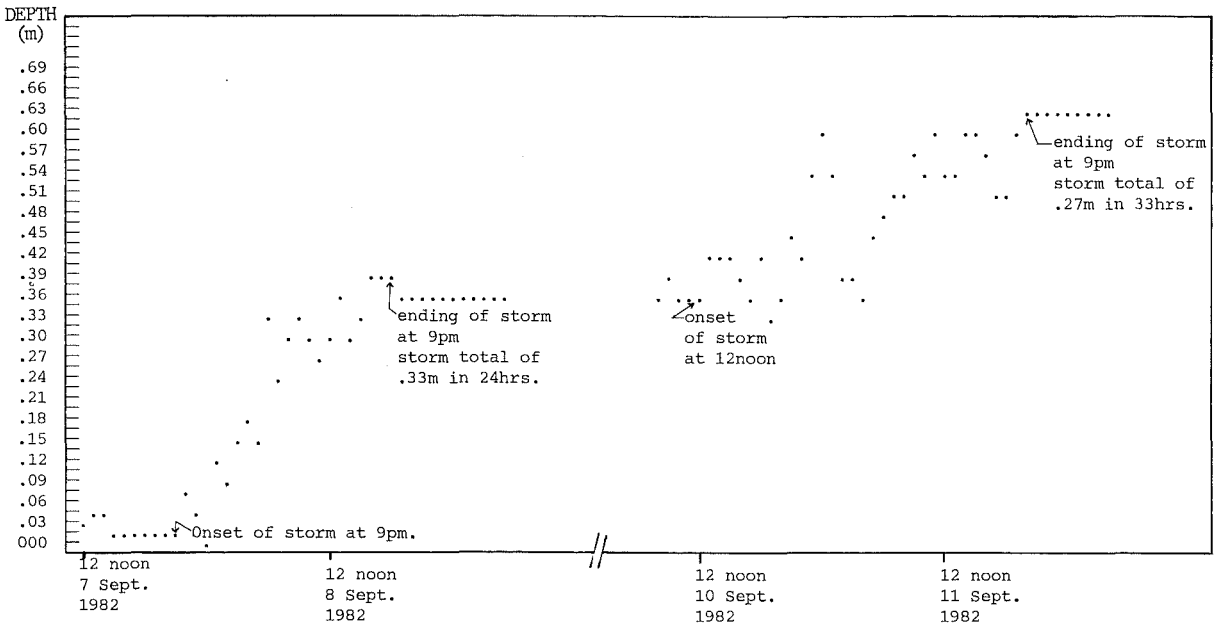

Fig. 3. A typical plot of new snow accumulation from two storm events on the Tasman Glacier (Mount Cook, New Zealand).

lected over several days in September 1982. Resolution of the device, as previously mentioned, is about 0.03 m. The speed of sound in a gas is inversely proportional to the square root of the gas density. For a temperature range of 10°C, assuming perfect gas behaviour, the change in air density is likely to cause errors in distance measurements of about 2%. The maximum distance from the top of our tripod to the snow surface was about 2 m, so this error represents a distance drift of about 0.04 m due to temperature changes. Air temperature measurements were logged together with the depths shown in Fig. 3, and during the relevant days in September, air temperatures ranged from −1.2 to −6.5°C. Thus, the depth data shown did not require temperature compensation. Provision for a temperature correction, necessary for temperature variations above 10°C, is easily made by digital means in our recording system, as the air temperature is always measured. The accuracy and stability of the device, when checked with a rule, at intervals during the winter season, was within 0.03 m.

We suspect that most of the scatter in data during the storm periods was caused by reflection of signals from blowing snow. This gave us an indication of the onset and ending of periods of blowing snow, and the resultant accumulation or ablation. We could best estimate the average rate of snowfall or ablation at the ends of storm periods.

CONCLUSIONS

We have adapted an ultrasonic ranging unit available from the Polaroid Corporation to remotely measure the snow accumulation or ablation. The data from the unit provides a valuable input to avalanche forecasting, indicating the time of onset and ending of the storm and also the depth of accumulation.

ACKNOWLEDGEMENTS

The University of Canterbury sponsored the project and financial assistance came from the Department of Lands and Survey (Wellington, New Zealand).

REFERENCES

Caillet, A., D'Aillon, F.G. and Zawadski, I. (1979). An ultrasound low power sonar for snow thickness measurements.

Proc. 36th Annual Eastern Snow Conf., 7–8 June 1979, Alexandria Bay, NY, pp. 108–116.

Gubler, H. (1981). An inexpensive remote snow-depth gauge based on ultrasonic wave reflection from the snow surface. J. Glaciol., 27 (No. 95): 157–163.

Lugwig, R. and Dick, P. (1983). Erfahrungen mit einem automatischen Schneehohenmesser auf Ultraschallbasis. Tagungsber., Electronik und Lawinen, Graz, 24–28 April, 1979, Inst. f. Electronik, Tech. Univ. Graz, pp. 264–266.

Marbouty, D. and Pougatch, B. (1983). Scheepegel mit Ultraschall. Tagungsber., Electronik und Lawinen, Graz, 24–28 April, 1979, Inst. f. Electrotechnik, Tech. Univ. Graz, pp. 257–263.

Journal of Glaciology, Vol. 30, No. 106, 1984

SNOW STABILITY INDEX

By H. CONWAY *and* J. ABRAHAMSON

(Department of Chemical and Process Engineering, University of Canterbury, Private Bag, Christchurch, New Zealand)

ABSTRACT. Field tests have been developed to measure the shear and tensile strengths of large volumes of snow. Basal shear strengths were measured across and down some slabs of snow, giving highly variable strengths. These measurements support the idea that the basal region of an avalanche may contain zones where the basal shear strength exceeded the gravitational shear stress (i.e. pinning areas) with weak zones between (deficit areas) where the shear strength was less than the gravitational shear stress. The slab tensile stresses induced by these deficit areas would become high if either the deficit length (down-slope) was large, or the deficit itself was large. Measurements of tensile strengths of slabs above weak layers, together with the down-slope gravitational stress of a snow slab, suggest that deficit lengths of only several metres are often sufficient to cause a local tensile failure. In some cases, this local failure may propagate across the remainder of the slope (depending on the pinning distribution) and cause an avalanche. We propose that the *maximum* local deficit, rather than the mean slope deficit of basal shear stress, and the *maximum* length of the local deficit, are the first important parameters to consider when evaluating slope stability in the field, since the magnitude of these factors determine the probability of a local tensile failure.

RÉSUMÉ. *Indicateur de stabilité de la neige.* Des tests de terrain ont été développés pour la mesure des limites de cisaillement et de tension pour de grands volumes de neige. Des limites de cisaillement à la base ont été mesurés transversalement et longitudinalement pour des couvertures de neige, conduisant à des efforts hautement variables. Ces mesures confortent l'idée que la région basale d'une avalanche peut contenir des zones où l'effort limite de cisaillement à la base dépasse la contrainte de cisaillement de gravité (c'est-à-dire les zones en butée) intercalées avec des zones de faiblesse (zones de déficit) où l'effort de cisaillement limite est inférieur à la contrainte de cisaillement due au poids. Les contraintes de traction dans la couche, créées par ces zones dé déficit, peuvent prendre des valeurs élevées soit parce que les longueurs (selon la pente) où s'exerce ce déficit sont étendues, soit parce que le déficit lui-même est important. Des mesures de limite de rupture en traction pour des plaques au-dessus de couches faibles, en même temps que des mesures de contraintes de pesanteur pour une plaque de neige, suggèrent que les longueurs de déficit de quelques mètres seulement sont suffisantes pour créer une rupture locale en traction. Dans certains cas, cette rupture locale peut se propager à travers le reste de la pente (suivant la concentration des contraintes) et être la cause d'une avalanche. Nous proposons que le *maximum* du déficit local, plutôt que la moyenne du déficit de la contrainte de cisaillement pour toute la pente, et que le *maximum* de longueur du déficit local, soient les premiers des paramètres importants à prendre en considération pour évaluer la stabilité de la pente puisque l'amplitude de ces facteurs détermine la probabilité d'une rupture locale en traction.

ZUSAMMENFASSUNG. *Index für die Schnee-Stabilität.* Zur Messung der Scher- und Zugfestigkeit grosser Schneepakete wurden Feldprüfverfahren entwickelt. Die Scherfestigkeit am Untergrund wurde an einigen Schneeplatten quer und längs gemessen, wobei sich sehr unterschiedliche Werte ergaben. Diese Messungen stützen die Annahme, dass der untere Teil einer Lawine Zonen enthalten dürfte, wo die Scherfestigkeit die Scherspannung infolge der Schwerkraft übertrifft (sog. Haftgebiete), mit Schwächezonen (Defizitgebieten) dazwischen, wo die Scherfestigkeit geringer ist als die Scherspannung infolge der Schwerkraft. Die Zugspannungen in der Platte, verursacht durch diese Defizitgebiete, würden hoch werden, wenn entweder die Defizitlänge (hangabwärts) oder das Defizit selbst gross ist. Messungen der Zugfestigkeit von Platten über schwachen Schichten, kombiniert mit der hangabwärts gerichteten Schwerkraftspannung einer Schneeplatte, lassen vermuten, dass Defizitlängen von nur einigen Metern oft genügen, um lokal einen Bruch infolge des Zuges zu verursachen. In einigen Fällen kann sich dieser lokale Bruch über den ganzen Hang fortpflanzen (in Abhängigkeit von der Verteilung der Haftkräfte) und eine Lawine auslösen. Wir schlagen vor, dass anstelle des mittleren Defizits der basalen Scherspannung am Hang das *maximale* lokale Defizit und die *maximale* Länge desselben als Hauptparameter bei der Abschätzung der Hangstabilität im Feld herangezogen werden, da die Grösse dieser Faktoren die Wahrscheinlichkeit eine lokalen Zugbruches bestimmen.

INTRODUCTION

Most slab failure models assume a weak basal layer (Perla, 1980), and a shear frame first used by Roch (1966) has been used by many to study this layer. Variations of a "shear index" (i.e. the ratio of the shear strength of a snow layer, measured with a shear frame, to the gravitational shear stress) in the basal zones of avalanches have been previously documented and mainly attributed to either the small size of the shear frame used (Sommerfeld, 1973, 1980; Perla, 1977; Sommerfeld and King, 1979) or test-rate effects (McClung, 1977, 1979; Perla and others, 1982; Montmollin, 1982). In this paper, we report on basal shear measurements made with larger basal test areas, and series of measurements made across slopes and down slopes.

Perla and LaChapelle (1970) derive equations to estimate the tensile stress t_{xx} induced by a shear perturbation (superimposed on the infinite slab situation) in the basal zone:

$$t_{xx} = (X/Z)\pi_{xz} \qquad (1)$$

where t_{xx} is the order of magnitude of the induced tensile stress in the x direction (down-slope), π_{xz} is the basal perturbation of shear stress, 2X is the length of the perturbation, and Z is the depth of the slab.

Equation (1) shows that an index relating basal weakness to tensile failure should include not only the magnitude of the weakness, but also the length over which the perturbation exists (2X), the slab thickness (Z) and the tensile strength of the slab. When a weak zone is large, or the shear strength is small, high stresses are induced in the slab which could promote local failure.

Once a slope has failed locally, propagation of the failure would depend upon the distribution of stresses and strengths at the boundaries of the local failure. Zones of high strength (pinning areas) may inhibit propagation, but conditions may effectively cause the removal of the pinning areas and result in widespread failure.

In a similar model, Stuiver and others (1981) propose that the West Antarctic ice sheet is pinned at various boundary zones, and they use a computer model to consider the effects of removal of various pinning areas. Chowdhury and A-Grivas (1982) deal with this problem using a probabilistic model. For a soil slope, they consider the probable distribution of the shear-strength/shear-stress ratio, and the interaction between adjacent elements, to determine the probability of crack progression.

FIELD STUDIES

To study local shear strengths at basal zones, we embedded a large shear frame (which had dimensions 300 mm x 300 mm x 50 mm and weighed 1 kg) on the snow surface. With a saw, we cut out a column around the frame to isolate the block from effects of side shear and compressive and tensile hold-up, to a depth greater than the suspected fracture plane. It was found

that embedding the frame before isolating the column reduced disturbance of the sample. A slope-parallel pull was applied to the frame with a calibrated spring until failure occurred somewhere down the column. We noted the surface area of the fracture, the depth of the fracture, slab density, and the bed surface angle. These measurements made it possible for us to calculate the gravity component of stress parallel to the slope. The sum of this and the measured force to failure, divided by the shear area, gave the shear strength (see Figure 1).

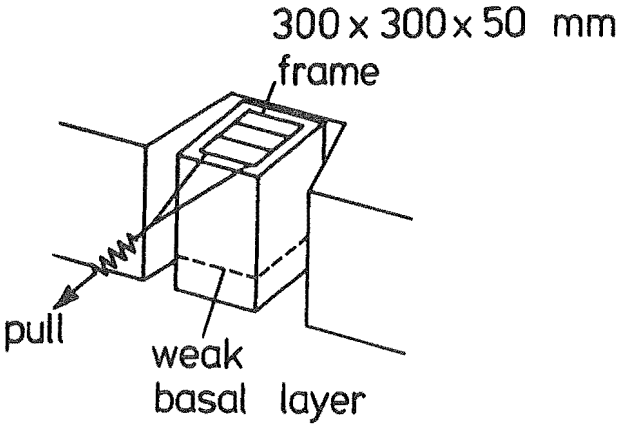

Fig. 1. Shear-test measurements at the weakest basal layer. The weak layer was at a depth z from the surface and the average density ρ of the snow above the weak layer was measured. The bed surface angle Θ and the force F_s in the down-slope x direction required to fracture the column were measured. Typical shear areas A_s over which the force was applied were about 0.15 m².

In cases where the shear strength of the basal layer was small compared with the "ploughing strength" of the surface snow from which the frame was being pulled, the column sheared before the frame ploughed through the surface snow. In situations where the surface snow was weak, we re-embedded the frame in a lower layer and repeated the test.

This test has several advantages over the traditional shear-frame test:
(1) The weakest sliding layer did not need to be precisely located before the test and detailed analysis of the snow stratigraphy above the shear layer was not necessary.
(2) The normal loading over the shear layer was retained during the test.
(3) Disturbance of the weak layer when placing the frame was minimized.

The disadvantage of this test was the possibility of a bending mode of failure, and we noticed this especially with deep columns (depth greater than about 1.5 m) with no well-defined, low-strength sliding layer. In these cases, applied stresses were high (about 4000 N/m²) and the yield surface was often stepped. To eliminate some of the bending moment, we built a frame which could be inserted just above the suspected shear layer. This shear frame was similar to our other frame, but had one side which could be detached, which enabled it to be inserted from one side of the column just above the suspect layer. The other (detachable) side could then be attached to the frame and a force applied to the column. This frame was not as easy nor as fast to use as the frame placed on the snow surface.

Testing times for the application of load were of the order of 0 to 5 s to failure, but our control of the instantaneous rate of loading was poor. However, a simple local basal shear stability index α could be computed from the ratio of the local shear strength to the gravitational shear stress

$$\alpha = (F_s/A_s + \bar{\rho}'gz' \sin\Theta)/(\bar{\rho}gz \sin\Theta) \qquad (2)$$

where F_s is the applied force required to shear the column, A_s the shear area over which the force is applied, $\bar{\rho}$ the mean slab density, g the gravitational acceleration, z' the depth of snow above the fracture plane when the test was made (with a corresponding $\bar{\rho}'$ as the mean snow density of the snow to depth z'), z the depth to the fracture plane from the snow surface, and Θ the bed surface angle. By weighing a small column and dividing by the shear area, we could often measure the product of the mean slab density ($\bar{\rho}$) and depth (z) directly. Columns that slid before they could be completely isolated were assigned an index (α) of less than 1.

Once the weak layer had been identified, we made tensile tests of the slab above this layer. We isolated a column from effects of side shear and compressive hold-up with a saw, and inserted one of the frames described above on each side of the sample (as shown in Figure 2). The frames were linked to a rod which also had a calibrated spring attached. We then slid a stiff and essentially frictionless stainless-steel plate up the weak layer to remove basal shear

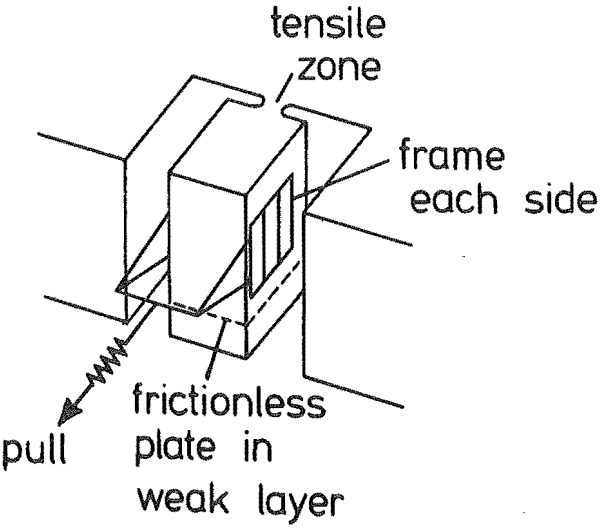

Fig. 2. Tensile tests of a slab above a weak layer. The scooped shape in the tensile zone helped relieve stress concentration in that area (A_T) which was typically about 0.1 m² in these tests. The frictionless plate had been inserted at a depth z from the surface at an angle of Θ to the horizontal in the up-slope direction. The pull F_T required in the down-slope (x) direction was measured.

support, and used a scoop at the tensile zone to reduce the cross-sectional area and hence the force required to fracture the sample. Also, rounding off the cut by the scoop relieved stress concentrations. Again rate control was poor but tests were generally over a time of 0 to 15 s to fracture. The area of fracture was usually about 0.1 m². The force applied to fracture the column, together with measurements of slab density, bed surface angle, and area of fracture, enabled us to calculate a tensile strength σ_T of the slab:

$$\sigma_T = (F_T + \bar{\rho}gzab \sin\Theta)/A_T \qquad (3)$$

where F_T is the applied force required to fracture the column in tension, A_T the area of tensile failure, and abz is the snow column volume.

If the shear stress on the weakest basal layer in a snow pack exceeds its shear strength (locally) we have a deficit, or lack of support π_{xz}. Ignoring side-shear support, π_{xz} is taken here to be the difference between the gravitational shear stress and

the local shear strength. By combining Equation (1) and Equation (2) and substituting for π_{xz} (assuming $\rho = \rho'$ and $z = z'$), the induced tensile stress is given by

$$t_{xx} = X(1 - \alpha)\bar{\rho} g \sin\Theta . \qquad (4)$$

This stress approaches or exceeds the tensile strength as α approaches zero and/or X becomes larger. In fact, for zero shear strength over a slab length of 2X, (in which case $\alpha = 0$), and where X is sufficiently large (X_c) so that the induced tensile stress equals or exceeds the tensile strength ($t_{xx} \geq \sigma_T$), then

$$X_c = \sigma_T / \bar{\rho} g \sin\Theta \qquad (5)$$

Brown and others (1972) also use this simple model (considering the influence of Poisson effects to be small) to give a measure of the critical deficit length $2X_c$ in the direction of the slope. We have used Equation (5) to calculate appropriate values of X_c from our σ_T measurements.

FIELD AREA

We made the field measurements reported below on slopes around the upper Tasman Glacier (2100 m) in the Mount Cook National Park over the New Zealand 1981 and 1982 winters. This is a region of high snowfall, where storm cycles may typically deposit 0.3 - 1.5 m of dry snow with a density range of 40 to 250 kg/m³. Winter snow-pack temperatures may vary from -2°C to -25°C, and most slopes have a glacial base. The area is noted for considerable wind strength and most snow-falls are associated with wind.

SUMMARY OF FIELD MEASUREMENTS

Shear indices measured on the crown walls of eight avalanched slopes yielded a total of 93 values of α, which had a mean and standard deviation of 1.57 and 1.29 respectively, with a range of $6.82 \geq \alpha \geq 0$. For comparison, 18 slopes which had not fractured (63 measurements) gave values for α mean and standard deviation of 4.25 and 2.78 respectively with a range of $13.3 \geq \alpha \geq 0$.

Figure 3 shows, for all the above slopes, a plot of the smallest measured α against the longest length over which this smallest α was found. Where multiple tests (about 0.5 to 1 m apart) were made across, rather than down slopes, we included these in our plot also. Figure 3 shows a distinction between fractured and unfractured slopes, in that for all the fractured slopes, at least one value of the index α was less than 1. Most slabs that had not avalanched had a minimum shear index greater than 1. One unfractured slope did have an index less than 1. Slopes adjacent to this particular slope, and of similar aspect, had avalanched.

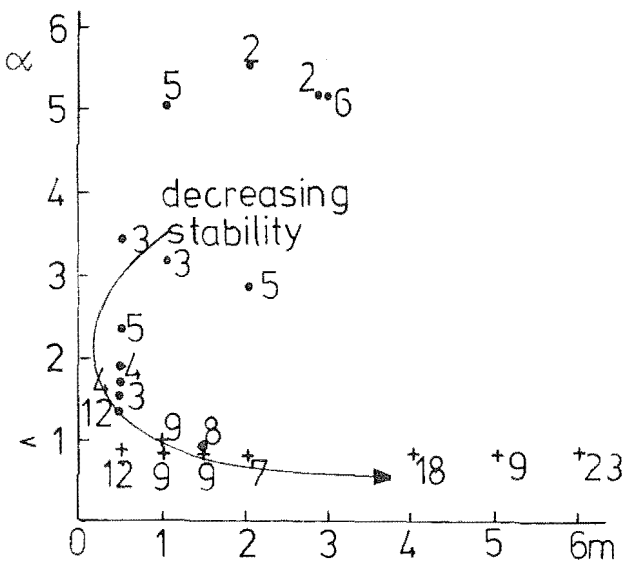

Fig. 3. Plot of the minimum shear index measured on each slope against the maximum length of this weakest zone measured on each slope. The total number of tests on each slope is listed beside each point, (+ denotes measurements made on slopes that had avalanched, • denotes measurements made on slopes that had not avalanched).

Table I lists tensile-type measurements made on various slopes, including the minimum and mean X_c evaluated from Equation (5) (using tensile strengths

TABLE I. TENSILE-TYPE MEASUREMENTS FOR SNOW SLOPES

State of slope	*Bed surface angle* deg	*Mean slab density* kg/m³	*No. of tensile measurements*	*Mean tensile strength* N/m²	*Minimum* X_c m	*Mean* X_c m	*Minimum* α *measured*	*Minimum shear strength* N/m²	*Maximum when* $\alpha < 1$
nf	28	185	4	1342	1.13	1.58	2.70	780	
nf	35	236	1	3450	2.60	2.60	3.46	1100	
nf	43	160	2	1965	1.46	1.80	1.77	635	
nf	33	200	2	8770	5.94	8.22	< 1	<1110	0.75
nf	33	244	2	2670	1.95	2.05	2.85	1675	
nf	43	224	2	2937	1.93	1.96	2.33	1400	
nf	38	227	4	5386	2.34	3.93	7.8	3220	
ls	30	90	2	84	0.17	0.21	-	114	
ls	29	160	2	370	0.36	0.49	-	380	
ls	35	60	3	318	0.63	0.94	-	213	
ls	40	60	2	113	0.25	0.30	-	10	
ss	47	140	3	1073	0.68	1.07	< 1	<320	1.0
ss	30	212	1	2320	2.23	2.23	< 1	<620	1.0
hs	35	250	2	15050	10.25	10.71	< 1	<1320	0.75

where: nf = not fractured
ls = loose slide
ss = soft slab
hs = hard slab

calculated from Equation (3). On slopes where $\alpha < 1$, half the maximum length (maximum X) containing this weakness is also listed in Table I.

BASAL PINNING MEASUREMENTS

Two examples of basal strength variations found on fractured slopes are shown in Figure 4 (across a crown wall) and Figure 5 (down a flank wall).

The fracture of 13 July 1982 (Figure 4) shows a variable crown-wall depth, ranging from 0.32 to 0.54 m. In some places, we observed a second shear layer above the bed surface, and this also is plotted in Figure 4. The avalanche had been ski-released near the northern flank wall, and Figure 4 shows that the fracture propagated across the slope through a pinned zone (7.5 m to 13 m), into another weak zone. Our shear tests across this crown wall were made at 1 m spacings and covered the entire width of the avalanche. The avalanche was classified as a soft slab (slab density of 140 kg/m^3) and had sheared within a very soft layer of new snow.

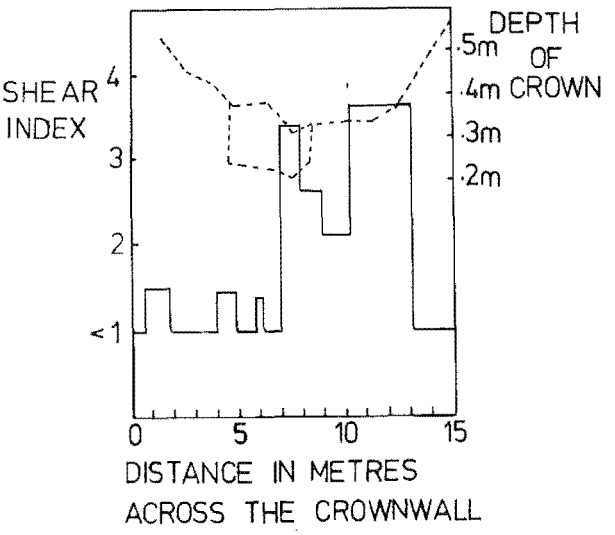

Fig. 4. Fracture depth and basal shear index across the crown wall of a fracture on the cornice wall, 13 July 1982. Average slab density: 140 kg/m^3. Bed surface angle: 47°. Sliding layer: very soft, 0.5-1 mm new snow, including columns, capped columns, stellars, needles, and plates at -8.4°C. The avalanche was ski-released near the northern flank wall, and the total number of tests made was 18.

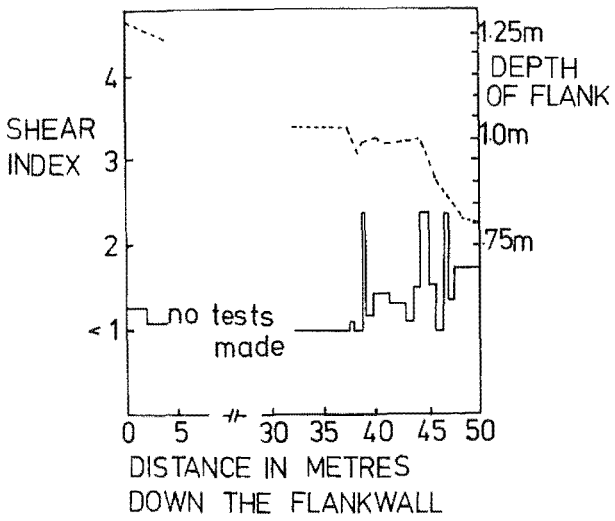

Fig. 5. Fracture depth and basal shear index down a flank wall of a fracture on the cornice wall, 19 September 1982. Average slab density: 290 kg/m^3. Bed surface angle: 30-35°. Sliding layer: 30 mm of soft 1 mm faceted crystals (radiation recrystallized) at -7.0°C. The avalanche released naturally from new-snow loading and the total number of tests made was 23.

The fracture of 19 September 1982 released naturally, sliding on a layer of buried faceted crystals (radiation recrystallized snow that had been buried by a new snow-fall). Shear measurements were made down parts of the northern flank wall of this avalanche (lack of time prevented us from covering the whole fracture flank). Distances between measurements could be as small as 0.5 m, but often they were spaced further apart.

DISCUSSION

The average number of shear-strength measurements made on each fracture in this study was about twelve, and distances between measurements varied from 0.5 m to 10 m. On non-fractured slopes which had higher values of α, fewer measurements and a lower frequency of tests were made, unless we found a low value of α ($\alpha < 2.0$). In these instances, the tests were clustered around that area to determine the extent of the weakness.

On avalanched slopes, we tried to make the measurements soon after the event to minimize effects of metamorphism of the snow. Although this was not possible at all times, most tests were made within 24 h of the event. The cold snow temperatures typical of the area (generally less than -5°C at the shear layer), also would inhibit sintering.

We suspect that our measurements of the shear index α could be in error by up to 20%. Most of this error originated in the measurements of the gravitational force down the slope, but other errors arose from measurements of the shear area, and the extra force required to fracture the sample.

By measuring shear strengths at closely similar stress rates (test times of 0 to 5 s to failure), we hoped to avoid major variations within our measurements due to rate effects. McClung (1977) and de Montmollin (1982) showed that shear strengths depend strongly on test rates and their results suggest that our shear tests would be within the "brittle" range.

Not all the variability in the shear index can be attributed to experimental accuracy. Some of the columns failed before they could be completely isolated from tensile, compressive, and side-shear support, while columns just 0.5 m away required up to 1500 N/m^2 extra shear stress in the down-slope direction (an increase of α by about 300%). In view of this, we have accepted that much of the measured strength variability was due to actual variability of snow properties at the shear layer.

Sommerfeld and King (1979) and Sommerfeld (1980) have proposed that much of the variability and high values of the shear indices may be due to the sample size. They used Daniels (1945) parallel-element theory to provide an explanation of the size and stress relationships of snow in limited areas to those over unlimited areas, and suggested a strength ratio of 0.81 for an area ratio of ∞:0.1 m^2. The measurements of the shear index described in this paper have not been modified by this ratio.

If we regard the local shear index α as a random variable, we can plot a probability-density function of the index, and the risk of local shear failure (ignoring other means of support) is, by definition, the probability that the actual factor of safety will be less than one. For slopes in our study that had avalanched, the average probability of shear failure determined in this manner was about 33%, and for non-failed slopes about 12%. These results compare with

the data from Perla (1977) where he summarized, for 80 avalanches, the mean and standard deviations of α to be 1.66 and 0.98 respectively, which indicates a failure probability of about 25%. Vanmarcke (1977) dealt with earth slope-stability problems using a three-dimensional probability model. He considered the spatial variability of shear strengths and a characteristic correlation distance for the shear strengths. Adjustments to his model could also be made to consider slow variations of average shear strength, which may be useful for considering sintering or weakening processes in a basal layer.

The two examples in Figures 4 and 5 showing basal shear-index variation along extended distances suggest that the shear index α may not be distributed about a single maximum (especially in Figure 4 where data were collected across a crown wall), and so a straight-forward statistical approach may be deceptive.

The examples also show that even though the slope had failed, pinning areas (with local basal shear strength greater than the gravitational shear stress) occurred over about 45% of the total area tested. This suggests that the mean index may not be as critical as the *smallest* index, and the *size* of the zone over which it is small (the shear deficit area), when assessing a slope stability. Figure 3 suggests that if any zones of weakness ($\alpha < 1$) are detected with a minimum number of tests, then the slope should be considered unstable.

We investigated the critical size of the shear deficit ($2X_c$) by considering the tensile strengths of the slabs and making a calculation using Equation (5). Tensile-strength measurements of slabs above weak layers were not made on all the slopes studied, but the tests made are listed in Table I. We suspect errors in the calculated tensile strengths of up to 20% due to errors in measuring the down-slope gravity force, the extra force required to fracture the sample, and the tensile fracture area. The variation in times to failure in our test (2 s to 15 s) are in the brittle range of tests suggested by Narita (1980) and again we infer that the error due to different rates between our tests would not have a large effect on the yield strength σ_T that we have estimated.

The calculation of $2X_c$ listed in Table I shows values small compared with the full slab length ($2X_c$ = 0.34 m to 21 m). In most cases where we had made shear tests over extended distances, the lengths of the shear deficit zones were smaller than $2X_c$. This suggests that in most cases, we did not locate the primary fracture area during our limited number of field tests.

We are as yet unclear about the relationship between our measured local indices (and $2X_c$) and the prediction of total slab failure. Boundary conditions and geometric effects have been suggested as important by Perla and others (1982). Little is known about the rate of strain during avalanche fractures, and this rate may differ significantly from that during the field tests. Narita (1980) demonstrated a strong dependence of the tensile yield strength on the test rate (yield strengths for ductile failures were up to 40% higher than yield strengths for brittle failures). McClung (1979), showed that some snow strain-softened during shear, depending on the snow type and rate of shear. Some snows also exhibited a residual shear strength of only half that of the peak shear strength. Furthermore, our calculations do not consider support from side shear (and also partial basal pinning when calculating $2X_c$).

Despite these uncertainties in interpretation of the tests, from a purely empirical point of view, there is one basis for a practical assessment of slope stability. As shown in Figure 3, we found a basal deficit with at least one test on each slope that had avalanched. We also note that, in most cases, we had located this deficit with less than ten tests, although on large slopes more than ten tests may be required to locate a pocket of weakness (see Fig. 3).

It is interesting to note that (from Table I) in four surface snows where low tensile strengths (80 to 370 N/m) combined with low shear strengths (10 to 380 N/m) were measured, loose avalanches occurred on nearby slopes. Perla (1980) mentions that this sort of avalanche starts in loose cohesionless surface layers and these measurements support this concept.

We think that the variations of strength of the shear layer often originate from local air-flow patterns during deposition of snow. The deposited snow itself often shows significant local variation in its bulk properties, especially that property sensitive to texture (permeability). We recorded air permeability variations of up to 300% in otherwise closely similar new snow which had been deposited by wind down a slope (Conway and Abrahamson, 1984).

Bagnold (1941) observed drifts of sand caused by wind channelling through irregularities in a cliff top. Depending on the wind direction and the shape of the cliff top, drifting was more concentrated in some places than others. He described the formation of longitudinal (down the slope) dunes from the lee eddies. Tabler (1980) summarized such drift observations behind snow fences, and found that the lee drift geometry was characterized by a length proportional to the fence height H, and a cross-sectional area proportional to H . He also noted an increase in snow density behind the fence (due to increased densification with snow depth). These observations may be applicable to variations in geometry at ridge tops, and a complex series of drift distributions could be expected behind an irregular-shaped ridge crest (see Fig. 6).

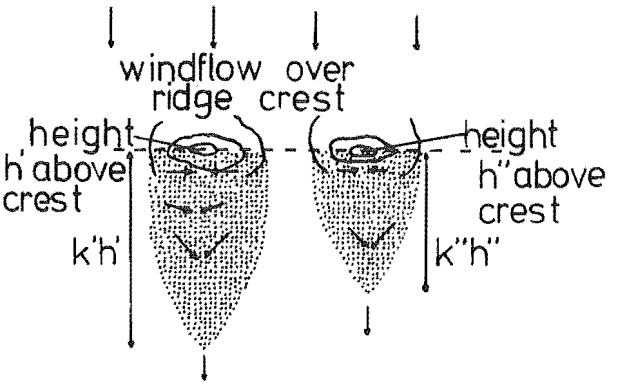

Fig. 6. Longitudinal drift patterns behind an idealized crest showing formation of drift bands across a slope (similar to Tabler's (1980) drift behind snow fences). The arrows indicate local air velocities.

Bagnold (1941) also observed transverse ripples or dunes normal to the local wind direction, and suggested that these may have a periodic distribution or may be short and irregular (depending on the particle density of the transported medium). Dyunin (1967) and Kobayashi (1979) recorded periodic fluctuations of snow transport rates (thought to be due to turbulence) and suggested that these may be associated with rippling or duning of depositing snow.

We argue below that these two types of deposition - large longitudinal drifting and small-scale duning - may be superimposed on some slopes, and may account for observed snow property patterns. In particular, our measurements *across* the crown wall of an avalanche (Fig. 4) show an uneven distribution of snow depth above the bed surface which appears to have been caused by large-scale drifting past the irregularities in the ridge crest. The uneven distribution of the drifting snow would not only change the gravitational loading at the shear layer, but also may have affected the properties of the shear layer as it was being deposited. For example, in Figure 4, if the drifting

proportions across the ridge were similar for the deposition of the weak layer and the deposition of the slab, we would expect the weak-layer thickness to vary across a slope in similar proportions to the slab thickness. The thickness of the weak layer may have a strong influence on the shear strength (this is dealt with later in this discussion). Whatever the mechanism, the step change in shear index shown in Figure 4 (located between 7 and 13 m) being a change over a larger scale, is likely to be a step change across one of these longitudinal lee drifts.

The characteristics of the α distribution on the southern side of the crown wall (Fig. 4) and down the flank wall of an avalanche (Fig. 5) show fluctuations of much smaller period. These fluctions of strength can be related to the irregular transverse-type ripple described by Bagnold (1941) and in Figure 4, these appear to be superimposed on the weak zone created behind the ridge crest. On the slopes described in Figure 5, we did not find large areas of high α, which suggests we were sampling in a relatively weak band up the slope with irregular duning causing irregular shear variations.

Bridgewater (1980) determined the minimum width of a failure zone in hard particulate powders, by describing the shearing surface roughness in terms of particle size. In this way, he estimated a minimum shearing zone about ten particle diameters in thickness within a much thicker particle layer. In many of the shear layers we observed, the thickness of the weak layer was less than ten particle diameters. Although Bridgewater's approach may not be strictly applicable to crystals that can deform, we expect for these thin shear layers that the surface roughness of the stronger adjacent layers will intrude into the shearing zone. The shear strength can then be expected to be sensitively dependent on the local thickness of the weak layer. Both the streaming drifting and the irregular or regular duning above could cause variations in this thickness, and hence variations in shear strength.

McClung (1977, 1979) has suggested strain-softening as a possibility for basal weakening and progressive failure of some slabs. If a deficit zone is such that it can cause local straining in the surrounding snow, then the shear softening in these neighbouring areas may cause progressive failure through a pinning area. This would be an effective means of removing pinning areas and linking weak zones under a slab.

Our arguments above support Gubler's (1978) suggestion (for some avalanche releases) of an initial primary shear fracture which could then propagate over a slope. This general mechanism is also supported by field observations of artificially controlled slopes where trigger zones for an avalanche may occur at positions other than the crown wall. How pinning areas and their distribution affect crack propagation needs further study, but our tests suggest that if any basal shear deficit is found, then propagation is likely. Chowdhury and A-Grivas (1982) present a probabilistic model for the progression of shear failure in a soil slope. Although we do not think that the shear layer can be treated as statistically homogeneous (at least in the horizontal direction), this approach may prove useful in different sub-areas of a slope.

CONCLUSIONS

We measured high variability of the basal shear strength of snow under slabs over small distances (0.5 m) and so we considered the potential sliding plane for an avalanche to consist of weak basal zones (deficit areas) between zones of higher strength (pinning areas). A local failure would become more likely as the basal shear strength became small, or the area of the deficit became large.

Our measurements so far suggest that the critical length of reduced basal shear strength required to cause a tensile failure in the slab may be small (1 m or less) in many cases. This size is similar to fracture sizes estimated by Sommerfeld and Gubler (1983) who estimated fracture areas of 0.1 m to 1 m radius using the frequency spectra of low-frequency acoustic emissions. Because this critical length may be small, we found that the primary concern when assessing slope stability should be to determine whether a basal shear deficit occurs at any position over the slope.

During our field tests over extended areas on unstable slopes, we generally found a deficit shear area within ten tests, but these tests were time-consuming when covering large areas. A shear test which would enable a user to make a large number of measurements in a short time would be useful for assessing slope stability — especially for large slopes.

Our stability index α does not consider the pining-area distribution in relation to crack propagation after the initial primary fracture, but our measurements to date suggest that a failure may propagate through areas of high strength that are of similar size to the weak areas.

We found, as a general rule, that if (with a limited number of tests) we found an area where the shear index was less than one, then there were other larger areas of deficit and the slope was unstable. Future work may establish the probability of failure given the number of tests and the distribution of the shear indices found.

ACKNOWLEDGEMENTS

Financial support for the study came from the Department of Lands and Survey (Wellington, New Zealand), University of Canterbury (Christchurch, New Zealand), Mountain Safety Council of New Zealand, and Mt Hutt Ski Company. Mt Cook Airlines Company provided aircraft access to the field area, and the assistance of Mt Cook National Park Staff with the field experiments was invaluable. The New Zealand Meteorological Office provided the weather instruments. The Department of Chemical and Process Engineering (University of Canterbury) sponsored the project and helped develop the concepts and test equipment for the project.

REFERENCES

Bagnold, R.A. 1941. *The physics of blown sand and desert dunes*. London, Methuen and Co. Ltd.

Bridgewater, J. 1980. On the width of failure zones. *Géotechnique* (London), Vol. 30, No. 4, p. 533-36.

Brown, C.B., *and others*. 1972. Slab avalanching and the state of stress in fallen snow, [by] C.B. Brown, R.J. Evans, and E.R. LaChapelle. *Journal of Geophysical Research*, Vol. 77, No. 24, p. 570-80.

Chowdhury, R.N., *and* A-Grivas, D. 1982. Probablistic model of progressive failure of slopes. *Journal of the Geotechnical Engineering Division, American Society of Civil Engineers*, Vol. 108, No. GT6, p. 803-19.

Conway, H., *and* Abrahamson, J. 1984. Air permeability as a textural indicator of snow. *Journal of Glaciolog*, Vol. 30, No. 106, p. 328-33.

Daniels, H.E. 1945. The statistical theory of the strength of bundles of threads. I. *Proceedings of the Royal Society of London*, Ser. A, Vol. 183, No. 995, p. 405-35.

Dyunin, A.K. 1967. Fundamentals of the mechanics of snow storms. (*In* Ōura, H., *ed. Physics of snow and ice: international conference on low temperature science. . . . 1966 . . . . Proceedings*, Vol. 1, Pt. 2. [Sapporo], Institute of Low Temperature Science, Hokkaido University, p. 1065-73.)

Gubler, H. 1978. An alternate statistical interpretation of the strength of snow. *Journal of Glaciology*, Vol. 20, No. 83, p. 343-57.

Kobayashi, S. 1979. Studies on interaction between wind and dry snow surface. *Contributions from the Institute of Low Temperature Science*, Ser. A, No. 29.

McClung, D.M. 1977. Direct simple shear tests on snow and their relation to slab avalanche formation. *Journal of Glaciology*, Vol. 19, No. 81, p. 101-09.

McClung, D.M. 1979. Shear fracture precipitated by strain softening as a mechanism of dry slab avalanche release. *Journal of Geophysical Research*, Vol. 84, No. B7, p. 3519-26.

Montmollin, V. de. 1982. Shear tests on snow explained by fast metamorphism. *Journal of Glaciology*, Vol. 28, No. 98, p. 187-98.

Narita, H. 1980. Mechanical behaviour and structure of snow under uniaxial tensile stress. *Journal of Glaciology*, Vol. 26, No. 94, p. 275-82.

Perla, R.I. 1977. Slab avalanche measurements. *Canadian Geotechnical Journal*, Vol. 14, No. 2, p. 206-13.

Perla, R.I. 1980. Avalanche release, motion, and impact. (*In* Colbeck, S.C., *ed. Dynamics of snow and ice masses*. New York, etc., Academic Press, p. 397-462.)

Perla, R.I., *and* LaChapelle, E.R. 1970. A theory of snow slab failure. *Journal of Geophysical Research*, Vol. 75, No.36, p. 7619-27.

Perla, R.I., *and others*. 1982. The shear strength index of alpine snow, by R.[I.] Perla, T.M.H. Beck, and T.T. Cheng. *Cold Regions Science and Technology*, Vol. 6, No. 1, p. 11-20.

Roch, A. 1966. Les variations de la résistance de la neige. *Union de Géodésie et Géophysique Internationale. Association Internationale d'Hydrologie Scientifique. Commission pour la Neige et la Glace. Division Neige Saisonnière et Avalanches. Symposium international sur les aspects scientifiques des avalanches de neige, 5-10 avril 1965, Davos, Suisse*, p. 86-99. (Publication No. 69 de l'Association Internationale d'Hydrologie Scientifique.)

Sommerfeld, R.A. 1973. Statistical problems in snow mechanics. *U.S. Dept. of Agriculture. Forest Service. General Technical Report* RM-3, p. 29-36.

Sommerfeld, R.A. 1980. Statistical models of snow strength. *Journal of Glaciology*, Vol. 26, No. 94, p. 217-23.

Sommerfeld, R.A., *and* Gubler, H. 1983. Snow avalanches and acoustic emissions. *Annals of Glaciology*, Vol. 4, p. 271-76.

Sommerfeld, R.A., *and* King, R.M. 1979. A recommendation for the application of the Roch index for slab avalanche release. *Journal of Glaciology*, Vol. 22, No. 88, p. 547-49.

Stuiver, M., *and others*. 1981. History of the marine ice sheet in West Antarctica during the last glaciation: a working hypothesis, by M. Stuiver, G.H. Denton, T.[J.] Hughes, and J.L. Fastook. (*In* Denton, G.H., *and* Hughes, T.J., *ed. The last great ice sheets*. New York, Wiley-Interscience, p. 319-436.)

Tabler, R.D. 1980. Geometry and density of drifts formed by snow fences. *Journal of Glaciology*, Vol. 26, No. 94, p. 405-19.

Vanmarcke, E.H. 1977. Earth slope reliability. *Journal of the Geotechnical Engineering Division, American Society of Civil Engineers*, Vol. 103, No. GT11, Proc. Paper 13365, p. 1247-65.

MS. received 1 September 1983 and in revised form 3 January 1984

Journal of Glaciology, Vol. 30, No. 106, 1984

AIR PERMEABILITY AS A TEXTURAL INDICATOR OF SNOW

By H. CONWAY *and* J. ABRAHAMSON

(Department of Chemical and Process Engineering, University of Canterbury, Private Bag, Christchurch, New Zealand)

ABSTRACT. Two air-permeability devices were developed and measurements were made to study the relationship between air permeability and structure of different snow types. Permeabilities varied both with position and direction in the snow-pack, and changed with time as metamorphic changes occurred. A marked increase of air permeability was noted as faceted crystals grew due to radiation recrystallization. In other observations, as a snow-pack densified and crystals became more rounded (destructive metamorphism) the air permeability decreased. Measurements were made of air permeability of snows that had been subjected to a creeping tensile strain, and initial tests indicated that the changes in air permeability due to strain, even to rupture, were significant, but small compared with the intrinsic variability of snow.

RÉSUMÉ. *Perméabilité à l'air et texture de la neige.* Deux perméamètres ont été conçus et réalisés pour étudier la texture de la neige. Dans un manteau neigeux la perméabilité varie d'un point à l'autre mais elle est également anisotrope et peut évoluer au cours du temps. Une augmentation sensible de la perméabilité à l'air est observée lors du développement de cristaux automorphes (métamorphose constructive); par contre lorsque la couche de neige se compacte et les cristaux s'arrondissent (métamorphose destructive) la perméabilité décroît. Sur des échantillons soumis à une traction, le fluage (jusqu'à la rupture) entraîne une modification significative de la perméabilité à l'air. Mais cette modification est faible comparée aux variations intrinsèques de perméabilité de la neige.

ZUSAMMENFASSUNG. *Luftdurchlässigkeit als ein Textur-Indikator von Schnee.* Es wurden zwei Vorrichtungen zur Feststellung der Luftdurchlässigkeiten entwickelt und zum Stadium der Schneetextur benutzt. Die Durchlässigkeiten variierten sowohl mit der Lage wie mit der Ausrichtung in der Schneedecke und änderten sich zeitlich mit metamorphischen Vorgängen. Eine beträchtliche Zunahme der Durchlässigkeit trat ein, als facettierte Kristalle infolge von Rekristallisation durch Strahlung wuchsen. Bei anderen Beobachtungen nahm die Durchlässigkeit ab, wenn sich die Schneedecke verdichtete und die Kristalle gerundet wurden (destruktive Metamorphose). Die Luftdurchlässigkeit von Schnee, der einer kriechenden Zugspannung unterworfen wurde, wurde gemessen; Anfangsversuche zeigten, dass die Änderungen der Luftdurchlässigkeit infolge von Belastung, sogar bis zum Bruch, bedeutend sind, jedoch klein im Vergleich zur inneren Veränderlichkeit des Schnees.

INTRODUCTION

Gubler (1978) suggests that the tensile strength of snow is a function of snow *texture* rather than simply a function of density. Most descriptions of snow texture have been based on the analysis of thin sections (Good, [1975]; Kry, 1975; Narita, 1980) where parameters such as the type of grain, the area of bonds, the number of bonds per grain, and how these bonds link several grains together, were studied.

Both Shimizu (1970) and Martinelli (1971) suggest that air permeability may also give an indication of snow texture. Field evidence by Martinelli (1971) shows that correlation with air permeability explains some of the scatter in the tensile strength/density relationship for snow. His data suggest that at any given density there is a certain texture or permeability of snow for which the tensile strength is a maximum.

Observations by Narita (1980) on samples that had been subjected to uniaxial tension show the formation of small cracks across the sample, perpendicular to the direction of deformation, when the strain-rate was not too small (greater than about 10^{-5} s^{-1}, depending on the snow temperature and density). Narita also observed that bonds were preferentially cut rather than elongated, although at the lowest strain-rates (10^{-6} s^{-1}), the tensile deformation was thought to be associated with rearrangement of grains rather than crack formation.

Our measurements in this study were made to evaluate the usefulness of air permeability in characterizing snow texture. More specifically, our measurements of air permeability were:

1. on snow of various densities, grain type, and size;
2. on snow of similar age, density, and type so we could evaluate the intrinsic variability and independence of permeability from these measures, in a given snow-pack;
3. on snow where metamorphic change was apparent;
4. on snow that had been subjected to a creeping tensile strain, to determine whether cracks or bond elongation as observed by Narita (1980) could be detected with the technique.

The first portable air-permeability device used in these experiments relied on an air supply from a tank that was pressurized just before the test. Later we developed another smaller device with a hand-operated fan to provide an air flow.

THE AIR PERMEOMETERS

1. *The tank permeometer*

A schematic drawing of this device is shown in Figure 1. The four litre tank, which was pressurized to about 350 kPa with a hand pump, was connected to a pressure gauge and a rapidly activated on/off valve. We could remove the sampling head from the device to sample a 0.312 l sample of snow. The head has a 1.1 mm diameter orifice at the base through which flowed air from the pressurized tank. The flow-rate was a function of gas temperature, tank pressure, and atmospheric pressure (i.e. corrected for altitude), (Conway and Abrahamson, unpublished [a]). A Dwyer inclined manometer (0-80 mm water gauge with a resolution of 1 mm water) was connected to a tapping on the side of the head to enable us to measure the pressure drop over the sample. We made the sampling head from methylmethacrylate tubing to minimize heating from radiation (melting was observed when we used a metal sampler), and a rubber O-ring at the base of the sample guarded against edge leakage effects. Some glass fibre pads at the base of the head, dispersed

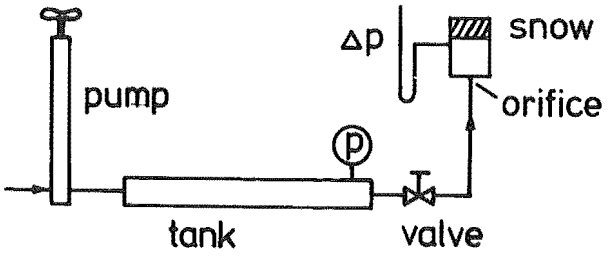

Fig. 1. Schematic drawing of the tank permeometer.

the air flow through the sample and stopped venturi effects at the manometer tapping. The overall dimensions of the permeometer (excluding the pump) were 500 mm x 350 mm x 300 mm and the weight was 6.2 kg.

2. *The blower permeometer*

A sketch of this device and a photograph are shown in Figure 2. This more portable device (weighing 1 kg), was 280 mm long and 90 mm in diameter with a removable handle to drive the fan. We used two Dwyer (0-80 mm water gauge) inclined manometers, one to give us an estimate of air flow-rate (via pressure drop across an 8 mm diameter orifice below the fan), and the other to measure the pressure drop over the sample. The fan had a gearing of 1:40, and superficial air velocities of up to 90 mm s^{-1} were possible. The vortex induced by the fan required an 8-bladed radial baffle system above the impellor to avoid vortex penetration to the pressure tapping just below the sample, and to disperse the air evenly through the sample. Again the sampler was made from methylmethacrylate tubing and the sample volume was 0.363 l.

EXPERIMENTAL PROCEDURE

We made most of the experiments described, on the upper Tasman Glacier (altitude 2100 m) in the Mt Cook National Park over the New Zealand 1981 and 1982 winters. This is a region of high snow-fall where storm cycles may typically deposit 0.3-1.5 m of generally dry snow with new-snow density in the range 40-250 kg/m^3. Winter snow-pack temperatures may vary from -2°C to -25°C and most slopes are glacially based. The area is noted for considerable wind strength and most snow-falls are associated with wind.

Our samples were cylindrical in shape and were generally taken with the axis perpendicular to the snow surface (Z direction) although some were taken with the axis parallel to the slope both up-slope (X direction), and across-slope (Y direction), to study the anisotropic nature of the snow. We measured crystal size and type with a 14x hand lens and grid, and used the classification system outlined by Sommerfeld and LaChapelle (1970) to describe the crystals. We also recorded density, snow temperature, slope profile, and angle at each site.

Darcy's law states for low velocities (in the laminar flow region), the rate of flow of a fluid through a bed of particles is directly proportional to the pressure gradient causing the flow. Thus, if a volumetric flow-rate Q flows through a sample of cross-sectional area A and length L under a pressure difference ΔP between the ends, then:

$$Q/A = \frac{B\Delta P}{L}$$

where B is a constant (fluid permeability which is dependent on the properties of the fluid as well as the pore structure of the medium).

Some of the major experimental problems and effects of changing flow-rates and sample size are discussed in a report by Conway and Abrahamson (unpublished [a]). That report showed that the permeability B did not change significantly with increasing flow-rates within the range of flow-rates used (velocities of 50-100 mm/s), although the permeabilities measured were probably influenced by some turbulence within the snow pores, and could be up to 16% high compared with those for flow-rates expected in the strictly laminar regime (using the Ergun correlation - see Bird and others, 1960, p. 196-200). Conway and Abrahamson recorded about 27% reduction in permeability when using a smaller sample area (sample diameter reduced from 90 mm to 53.3 mm), and they attributed most of the change to the higher range of velocities used with subsequent increased turbulent flow. They also included a calculation comparing the 53.3 mm diameter sample with the 90 mm diameter sample to determine the effect of wall leakage of air and concluded that this effect was small.

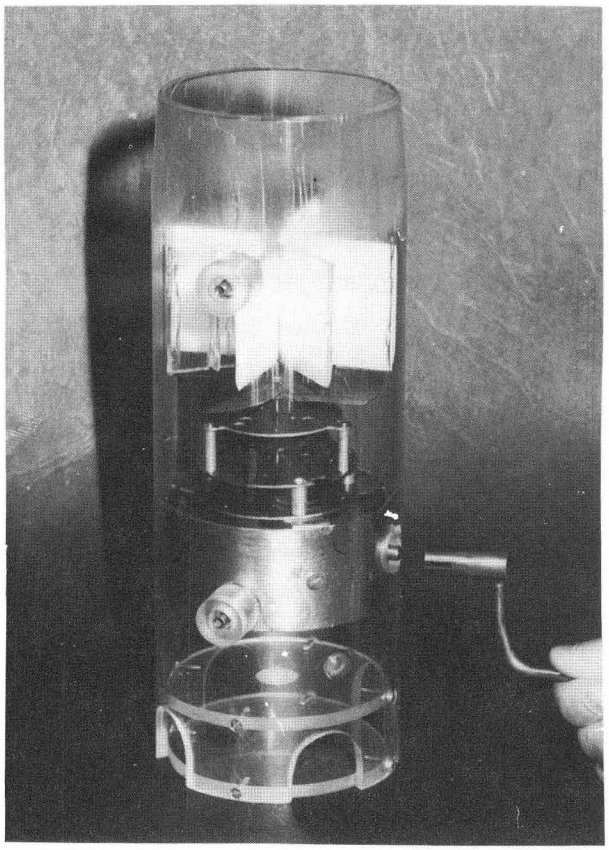

Fig. 2. A sketch and photograph of the blower air permeometer.

RESULTS OF TESTS

1. *Air permeability-density relationship of snow*

The distribution of air permeability of snow of various types is given as a function of density in Figure 3, together with data from Shimizu (1970). We note a general agreement with Shimizu's measurements. As observed by Shimizu (1970) and Martinelli (1971), no unique relationship between air permeability and density could be found.

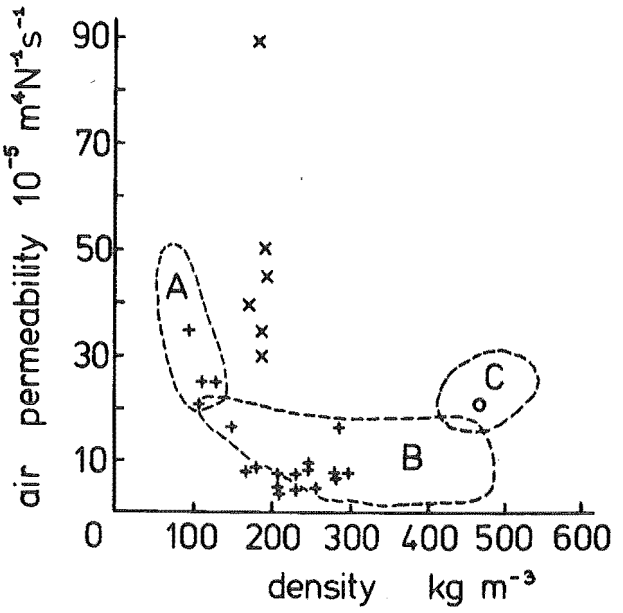

Fig. 3. Air permeability of snow of various types, compared with density. This study: x = temperature-gradient (TG) snow, + = fine-grained snow (less than 1 mm), o = coarse-grained snow (2-5 mm). Broken lines from Shimizu (1970): A = new snow, B = fine-grained compacted snow, C = coarse-grained snow.

2. *Air permeability variability of snow of similar age and type*

Perla (1978) suggested density variations of at least 10% in wind-deposited snow, and we recorded considerable variation of snow strengths (at the same site and time) on the slopes of the upper Tasman Glacier during the 1981 and 1982 winters.

At several sites, we took samples in the X, Y, and Z directions and recorded direction-to-direction variations of up to 20% of the mean permeability. We analysed the data statistically by comparing the difference of the means in each direction with the pooled error standard deviation. The difference of permeability in the X and Y directions was not always significant, but the mean air permeability of snow measured in the Z direction was always significantly lower (0.01 level) than those measured in the X or Y directions. Care was taken to sample always within a layer of more than 90 mm depth, to avoid stratification.

Repeated tests at the same site, sampling in the Z direction, gave standard deviations of up to 15% of the mean air permeability of the snow. Although some of this variability may be from our experimental error (e.g. flow-rate readings, manometer readings, sample disturbance), we think that much of the scatter is due to the intrinsic variability of the snow.

3. *Air permeability changes with metamorphic changes in the snow*

We revisited several sites during times of no-precipitation and recorded the change of air permeability of the same layer. Some of these cases are summarized below. At each site at any time, we have listed the number of readings taken (n) and the standard deviation (SD) together with the mean permeability measurement. Snow types are classified after Sommerfeld and LaChapelle (1970).

1. Over a period of eight fine cold days (maximum screen air temperature = -1.4°C, minimum screen air temperature = -9.4°C), radiation recrystallization of snow just under a surface crust occurred.

At one site (slope = 10°, west aspect), crystal structure and size changed from 0.5-1 mm early temperature-gradient (TG) crystals to 1-2 mm TG crystals. Although the snow density did not alter (190 kg/m^3) and snow temperature remained at -7.2°C, the air permeability increased from 28.1 x 10^{-5} m^4 N^{-1} s^{-1} (SD = 3.5 x 10^{-5}, n = 18) to 45.7 x 10^{-5} m^4 N^{-1} s^{-1} (SD = 4.0 x 10^{-5}, n = 16).

At another site (slope 32°, south aspect) similar structure and size changes occurred on snow with a density of 174 kg/m^3 and temperature -10°C, and the air permeability increased from 33.2 x 10^{-5} m^4 N^{-1} s^{-1} (SD = 4.0 x 10^{-5}, n = 12) to 95.4 x 10^{-5} m^4 N^{-1} s^{-1} (SD = 9.3 x 10^{-5}, n = 8). On this same surface snow, we measured a decrease of the mean shear strength (measured with a 0.09 m^2 shear frame) from 380 N/m^2 to 218 N/m^2 over the same time period.

2. Similar weather conditions during another period of three fine days caused some faceted crystals to develop under a surface crust. The air permeability of the snow just below the surface crust increased from: 8.9 x 10^{-5} m^4 N^{-1} s^{-1} (SD = 0.6 x 10^{-5}, n = 12) to 12.5 x 10^{-5} m^4 N^{-1} s^{-1} (SD = 1.0 x 10^{-5}, n = 9) for an initial snow density of 240 kg/m^3 and snow temperature of -20°C.

3. Over another period of five days, a new snow layer near the surface changed from new snow, to equitemperature type snow, and finally to radiation-recrystallized snow. These trends are plotted in Figure 4 and show decreasing permeability with destructive metamorphism, and increasing permeability with constructive metamorphism.

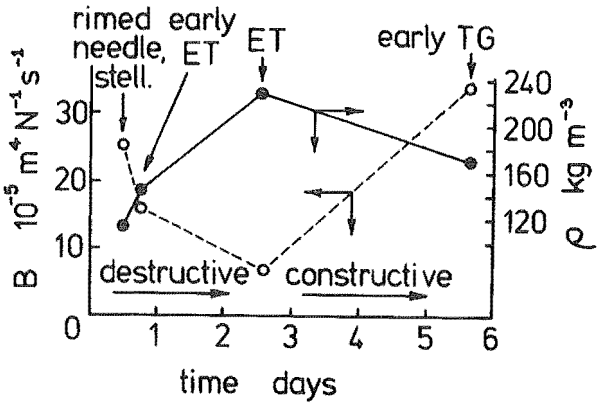

Fig. 4. Change of air permeability of snow with metamorphic changes. For about 2.5 d after the initial snow-fall of heavily rimed needle and stellar crystals, the snow temperatures were between -0.5°C and -3.8°C. Equitemperature (ET) metamorphism and densification of the snow was rapid. Some fine cold weather over the next five days caused recrystallization of the surface snows (TG type snow) and the snow temperature lowered to -6.5°C. Broken line is the permeability change; solid line is the density change.

4. *Air permeability changes with tensile strain*

We investigated the possibility that the variability of air permeability of snow is due to tensile strain causing localized cracks or crystal elongation, by comparing air permeability of snow that we had artificially strained, with similar snow that had not been strained. A device described by Conway and Abrahamson (unpublished [b]), strained a sample by pulling apart two aluminium plates which had been frozen onto the ends of the sample. The other technique we used for straining a sample was to isolate a snow column on a slope from effects of side-shear and compressive hold-up with saw cuts, also isolating it from effects of basal shear with a frictionless plate that we could slide under the column (see

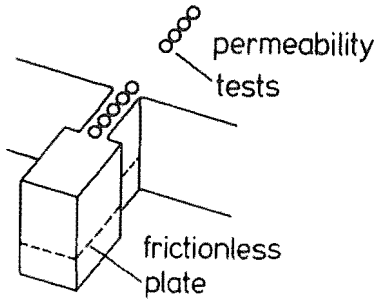

Fig. 5. One method used to strain a sample of snow on the slope to enable a comparison of air permeability of strained snow with that of undisturbed snow.

Fig. 5). The column could be left to creep from the gravity pull on the snow above the plate, or one could apply an additional force on the column by inserting some clamps on the sides of the column and pulling these with a calibrated spring; details of this are included in Conway and Abrahamson, 1984.

Average strain-rates between the end plates in the tensile tester were from 5.9×10^{-5} s^{-1} to 1.3×10^{-6} s^{-1}. We were not always certain of the actual strain over the sample since we did observe some development and widening of cracks between the snow and the plates which would suggest that the strain within the sample would be smaller than the strain measured across the end plates. In other cases, the strain was measured between markers in the snow itself. Narita (1980) found that the strain at which visible cracks occurred in a sample under tension depended on the strain-rate as well as the snow properties, and in our tests, the strains were not sufficient to cause visible cracks. However, measurements of the air permeability of samples that had been strained in the tensile tester were significantly higher (0.05 confidence level) than air permeabilities of closely similar snow that had not been strained. Figure 6 shows the changes in permeability after strain as a function of the (tensile) strain. Our initial measurements appear to indicate an increase of permeability with increased strain, in line with the cracks observed by Narita (1980) at higher strains. More measurements are required to confirm this trend.

We did not measure strain over the columns of snow which were strained *in situ* (as in Figure 5), but we did find an increase of air permeability when we compared strained samples with undisturbed samples. One set of typical data is shown in Figure 7.

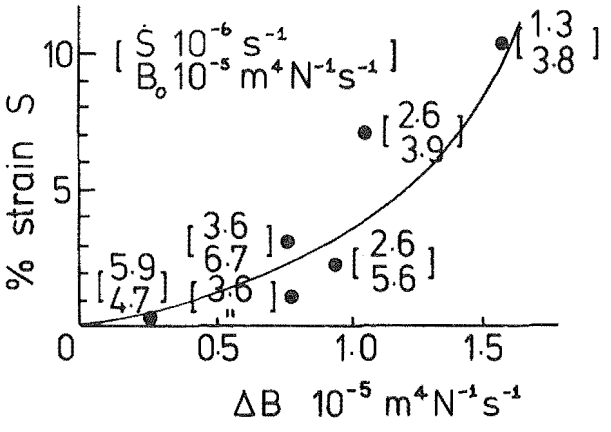

Fig. 6. A plot showing ΔB, the increase of air permeability after strain, with strain. The average strain-rate and air permeability of snow that had not been strained are shown in brackets after each point.

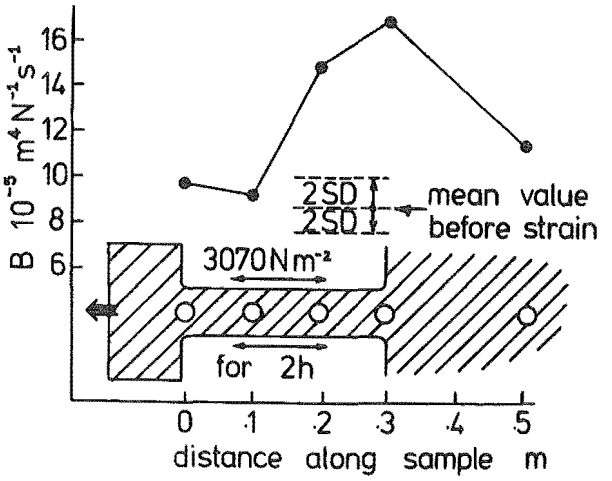

Fig. 7. A plot of the air permeability of snow up a column that had been strained for 2 h as shown in Figure 5.

5. *Permeability changes with position on slopes*

We measured large differences of permeability (up to 300%) down slopes in samples of similar age, density, temperature, crystal size, and type. Two examples of permeability measurements down slopes are shown in Figure 8. We made a number of observations

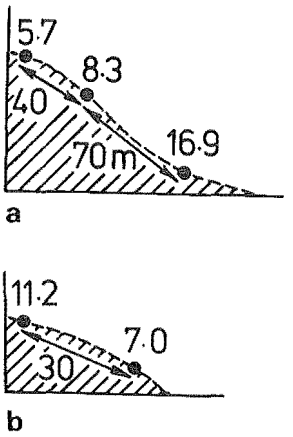

Fig. 8. (a) The change of air permeability of snow with position down the cornice wall, 13 October 1981.
Top position: wind blown, 0.5 mm equitemperature (ET) type crystals, density = 270 kg/m^3; T = -5.2°C; slope angle = 20°; B = 5.7 x 10^{-5} m^4 N^{-1} s^{-1} (SD = 0.5 x 10^{-5}, n = 18).
Middle position: wind blown 0.5 mm equitemperature (ET) type crystals, density = 240 kg/m^3; T = -7.0°C; slope angle = 43°; B = 8.3 x 10^{-5} m^4 N^{-1} s^{-1} (SD = 0.7 x 10^{-5}, n = 12).
Lower position: wind-blown 0.5 mm equitemperature (ET) type crystals, density = 270 kg/m^3; T = -5.5°C; slope angle = 30°; B = 16.9 x 10^{-5} m^4 N^{-1} s^{-1} (SD = 1.9 x 10^{-5}, n = 12).
(b) The change of air permeability of snow with position down the Nosedive, 23 June 1982.
Top position: 0.5 - 1 mm needles and broken stellar crystals, density = 150 kg/m^3; T = -8.0°C; slope angle = 15°; B = 11.2 x 10^{-5} m^4 N^{-1} s^{-1} (SD = 1.8 x 10^{-5}, n = 12).
Lower position: 0.5 - 1 mm needles and broken stellar crystals, density = 165 kg/m^3; T = -8.0°C; slope angle = 30°; B = 7.0 x 10^{-5} m^4 N^{-1} s^{-1} (SD = 0.5 x 10^{-5}, n = 11).

at each site, and an analysis of the variation due to the change of site down the slopes showed the permeability between sites to be significantly different. Although the measurements were made on slopes that often avalanche, we did not observe instability of any of the slopes either before or after the measurements.

DISCUSSION

Often we found it difficult to sample a uniform layer due to the wind stratification of the snow, but once a layer had been isolated with a spatula, a homogeneous sample could be obtained. Care needed to be taken to keep the sampler aligned during sampling especially in the denser snows, which were more difficult to penetrate.

The first (tank) air permeometer was bulky and required considerable effort to pressurize the cylinder with the handpump. Sometimes the orifice partly blocked with snow or water and gave an erroneous airflow reading. A permeability measurement could be achieved with this device within about five minutes.

The blower air permeometer was less bulky and easier to operate, but the gear train (ratio 1:40) required for a reasonable air flow-rate was delicate and care had to be taken in keeping snow and grit out of the gears. The average time for a permeability measurement was less than one minute.

Scatter in our permeability-density plot was similar to that found by Shimizu (1970) (see Fig. 3). We also observed high variability of air permeability over small areas (less than 1 m^2) and this suggests significant variation also of other snow properties over similar small areas (in particular snow strength). More measurements on closely similar samples are required before one could show whether or not any quantitative relationships between air permeability and strength exist.

One cause of the variations of snow-pack properties could be the depositional characteristics of wind-blown snow. The differences between measurements of air permeability in samples taken in different directions support this concept, as does the high variability of permeability measured within small areas. Several studies have measured periodic fluctuations in snow transport (e.g. Dyunin, 1967; Kobayashi, 1979), and have suggested that these could cause dunes in the snow. Again, more measurements are required to determine whether the variation of permeability is also periodic and related to this type of deposition.

Measurements on columns of snow that had been strained (Fig. 7), showed not only a significant increase of permeability after strain, but also a much higher scatter. If the increase of permeability is closely related to crystal elongation or cracks formed due to strain, then the high variations of permeability that we measured within the strained sample would support the evidence of Singh and Smith (1980), who found non-uniform strain along samples that had been subjected to a tensile stress.

The large variations of air permeability measured down slopes (Fig. 8), were probably caused by several factors. If the changes were related solely to strain, one might expect to observe high permeability in the tensile zone of a snow slab that is creeping, and relatively lower permeabilities in the neutral and compressive zones. Since the trends we observed on most slopes (four out of the five investigated), were different from this, we suspect that the depositional characteristics (or subsequent metamorphic changes) caused much of the variation. These influences made it difficult to gauge the importance of differential creep on the air permeability at different positions down slopes, especially as the slopes investigated were relatively stable (no avalanches occurred before or soon after testing).

CONCLUSIONS

Air permeability appears to be a useful parameter to give an indication of snow texture, and we developed a small hand-operated permeometer to make rapid field measurements of the air permeability of snow.

We found air permeability to be strongly dependent on metamorphism of the snow, and an increase of permeability appeared to be associated with constructive metamorphism, and a decrease of permeability with destructive metamorphism. We also found a small, but significant increase of permeability after samples had been subjected to tensile strain. We have insufficient data to know whether we could use this technique to identify early stages of run-away creep in a snow-pack, which may lead to instability.

We suggest that a decrease of permeability over a period of time on similar snows is a stabilizing trend in the snow-pack (either due to bond formation and/or destructive metamorphism of the snow), and an increase of permeability over a period of time is a sign of increasing instability (either due to bond elongation or bond breaking due to strain and/or constructive metamorphism of the snow).

ACKNOWLEDGEMENTS

Financial support for the study came from the Department of Lands and Survey (Wellington, New Zealand), University of Canterbury (Christchurch, New Zealand), Mountain Safety Council of New Zealand, and Mt Hutt Ski Company. Mt Cook Airlines Company provided aircraft access to the field area, and the Mt Cook National Park Staff were invaluable in their assistance with the field experiments. The Department of Chemical and Process Engineering (University of Canterbury), sponsored the project and helped develop the concepts and test equipment for the project.

REFERENCES

Bird, R.B., *and others*. 1960. *Transport phenomena. By R.B. Bird, W.E. Stewart, and E.N. Lightfoot.* New York, John Wiley and Sons, Inc.

Conway, H., *and* Abrahamson, J. 1984. Snow stability index. *Journal of Glaciology*, Vol. 30, No. 106, p. 321-7.

Conway, H., *and* Abrahamson, J. Unpublished [a]. Air permeability as a measure of snow structure. Final report, part 3, for the New Zealand Mountain Safety Council. [Produced 1982.]

Conway, H., *and* Abrahamson, J. Unpublished [b]. In situ tests of large volumes of snow. Final report, part 1, for the New Zealand Mountain Safety Council. [Produced 1982.]

Dyunin, A.K. 1967. Fundamentals of the mechanics of snow storms. (*In* Ōura, H., *ed. Physics of snow and ice: international conference on low temperature science. . . . 1966 . . . .Proceedings*, Vol. 1, Pt. 2. [Sapporo], Institute of Low Temperature Science, Hokkaido University, p. 1065-73.)

Good, W. [1975.] Numerical parameters to identify snow structure. [*Union Géodésique et Géophysique Internationale. Association Internationale des Sciences Hydrologiques. Commission des Neiges et Glaces.*] *Symposium. Mécanique de la neige. Actes du colloque de Grindelwald, avril 1974*, p. 91-102. (IAHS-AISH Publication No. 114.)

Gubler, H. 1978. An alternate statistical interpretation of the strength of snow. *Journal of Glaciology*, Vol. 20, No. 83, p. 343-57.

Kobayashi, S. 1979. Studies on interaction between wind and dry snow surface. *Contributions from the Institute of Low Temperature Science, Hokkaido University* (Sapporo), Ser. A, No. 29.

Kry, P.R. 1975. The relationship between the viscoelastic and structural properties of fine-grained snow. *Journal of Glaciology*, Vol. 14, No. 72, p. 479-500.

Martinelli, M., *jr*. 1971. Physical properties of alpine snow as related to weather and avalanche conditions. *U.S. Dept. of Agriculture. Forest Service. Research Paper* RM-64.

Narita, H. 1980. Mechanical behaviour and structure of snow under uniaxial tensile stress. *Journal of Glaciology*, Vol. 26, No. 94, p. 275-82.

Perla, R.I. 1978. Failure of snow slopes. (*In* Voight, B., *ed*. *Rockslides and avalanches. 1. Natural phenomena*. Amsterdam, etc., Elsevier Scientific Publishing Co., p. 731-52. (Developments in Geotechnical Engineering, 14A.)

Salm, B. 1982. Mechanical properties of snow. *Reviews of Geophysics and Space Physics*, Vol. 20, No. 1, p. 1-19.

Shimizu, H. 1970. Air permeability of deposited snow. *Contributions from the Institute of Low Temperature Science, Hokkaido University* (Sapporo), Ser. A, No. 22.

Singh, H., *and* Smith, R.W. 1980. Constant strain-rate tensile testing of natural snow. *Journal of Glaciology*, Vol. 26, No. 94, p. 519. [Abstract.]

Sommerfeld, R.A., *and* LaChapelle, E.R. 1970. The classification of snow metamorphism. *Journal of Glaciology*, Vol. 9, No. 55, p. 3-17.

MS. received 1 August 1983 and in revised form 17 October 1983

SNOW AND AVALANCHE RESEARCH AT TASMAN SADDLE

A PROGRESS REPORT OF THE WINTER, 1984

H.B. Conway
Department of Chemical and Process Engineering
UNIVERSITY OF CANTERBURY

INTRODUCTION

We think the basal shear strength and the distribution of this strength are of primary importance when considering snow slab failures. We have continued to investigate basal shear strength properties under snow slabs using techniques developed by Conway and Abrahamson (1984).

Much of the variability of strength may be caused by wind turbulence which can erode or redistribute snow. We have been using snow poles to study snow accumulation patterns down a slope, and have noted ripples, dunes, and erosional patterns on slopes after windy periods.

In the laboratory, Narita (1980) has made some stress-strain experiments on samples undergoing uniaxial tension, while McClung (1979a) has also measured strain under simple shear conditions. We have designed a strain gauge for the field, and have made strain measurements as we loaded a snow sample in shear. Little is known about rates of failure under avalanche conditions, and some fundamental knowledge of rates of failure in snow may help clarify some avalanche release mechanisms.

We have also compared shear strength measurements after a sample has failed, with the stress required for the initial failure. Most models of shearing in powders suggest that the shear strength of a material is comprised of a cohesive component and a frictional component. We think the stress required for the first failure would be that required to overcome both the cohesive and the frictional components of shear strength, while the residual stress may consist largely of the frictional component of the shear strength. If the cohesive component is removed (by partial failure), and the frictional component is relatively small, then crack propagation and subsequent widespread failure may result.

During one fine weather period, we measured some diurnal variations of temperature profiles in the upper snow layers. These are preliminary studies in investigation of heat fluxes which influence recrystallisation of the snow.

BASAL SHEAR STRENGTH DISTRIBUTION

We used test techniques developed by Conway and Abrahamson (1984), on slopes around the Tasman neve. Some of these tests are summarised below, and the snow stratigraphy in each case is listed in Appendix 1.

(1) Cornicewall, July 4, 1984

A medium-hard slab of snow overlay some soft snow on a short

slope (see Figure 1). We dug a series of pits (22 total) and found a significant weak zone over at least 6 m of the slope (see Figure 2). The depth of the slab varied from 350 to 480 mm (480 mm at the tensile zone), and the bed slope angle varied from 32 to 47 degrees.

Although we found an extensive weak zone on this slope, we could not release the slab as an avalanche. We suspect that the slab was probably pinned at the sides and in the compressive and tensile zones. The small length of the slope would have also contributed to the stability with compressive hold up.

We did not measure the tensile strength of the slab but by using a simple formula derived by Perla and La Chapelle (1970), and assuming the basal shear and sideshear pinning to be zero, we can find a minimum value of tensile strength:

$$\sigma_T \cdot h \cdot w = \rho g h \sin\theta \, w \, \ell/2$$

where σ_T = slab tensile strength

h = slab depth

w = slab width

ρ = slab density

ℓ = total length of the zone where basal strength is zero

Using our figures for this slope:

$$\sigma_T > \frac{300 \times 9.8 + 0.4 \times 6/2}{0.4} = 6420 \text{ N/m}^2$$

since the slope did not fail.

This strength is not unreasonable for the medium-hard slab (see Conway and Abrahamson [1984], and McClung [1979b]).

(2) Fracture on Hochstetter Dom, July 4, 1984

This was a medium sized (3) avalanche which had released naturally after the previous snowfall (see Appendix 1). The fracture depth was very variable, and there were a large number of tensile cracks just above the crownwall. Narita (1983) also observed this sort of crack both in the field, and during some of his laboratory tests at medium strain rates ($10^{-7} < \dot{\varepsilon} < 10^{-4} s^{-1}$).

He suggests that these would be ductile type tensile failures.

Much of the variability measured in the shear strength/stress ratio could be attributed to the variability both in the depth of the slab, and more importantly, to the discontinuities we observed in the thickness and extent of the shear layer.

At one zone, we measured a strength/stress ratio of less than one over a distance of 4 m and at others, the strength/stress ratio was high (we could not make the column shear). At places where the column would not shear, we often could not find the weak layer in the stratigraphic section. This

supports the concept that wind may transport weak-layer snow into pockets just prior to the deposition of the slab.

(3) A Ski-Released Fracture on the Cornicewall, 28 July 1984

This avalanche which was ski released, consisted of varying amounts of wind deposited snow over some new snow which had been recrystallised and faceted (see Appendix 1). A sketch of the fracture and positioning of pits is shown in Figure 3. Parts of the slope above position B had some large tensile cracks where the slab had moved about 0.1 m. We did not do shear tests on areas that had already partly slipped.

Point C would be close to a position where three skiiers passed by prior to the wind deposition and formation of the slab. It is probable that these skiiers would have disturbed the potential shear layer (while it was still at the snow surface), and hence stopped the subsequent avalanche from propagating beyond this point.

Shear tests that we made between points A to C shows the zone to be weak (all columns except one released before they were completely isolated from tensile, sideshear and compressive hold up). The weak layer under this slab was not only thick (0.19 m at pit B), but also continuous and we think this reflected in the continuity of the weakness measured.

(4) A Ski-Released Fracture on the Cornicewall, 1 August 1984

This was a small avalanche (about 12.5 m wide with 7 m length) which was ski-released near the centre (see Figure 4). The soft slab varied in depth from 0.12 m to 0.25 m and overlay some very soft new snow (see Appendix 1). We dug 20 pits across the crown regions, measuring shear strengths and these are sketched in Figure 5.

As I approached the release points, cracks appeared under my skis, indicating the instability. This avalanche required more energy for its release compared with the avalanche of 28 July 1984.

(5) A Ski-Released Avalanche on the Cornicewall, 28 August 1984

The wind-deposited slab probably overlay some recrystallised snow (we ski-released the slab during a storm and detailed crystal analysis was difficult). The slab varied in depth from 0.14 m to 0.39 m. Figures 6 and 7 show sketches of the pit positions across the crownwall, and the variation of shear strength across the crown respectively.

Figure 7 shows that the fracture propagated through some relatively strong zones from the trigger point, and also shows the small size of weakness required to initiate the fracture. The initial fracture did not propagate to the area to the

north (pits 17 - 20), but we did ski-release this area after we had completed the shear tests.

Further north along the Cornicewall, we could not cause the slope to slide, although some cracks and small movements of blocks did occur.

(6) Hochstetter Dom Fracture, 17 September 1984.

This was a large fracture stretching about 600 m across the shoulder of the Dom. It occurred some time during the storm, 10-14 September. The slab was hard, consisting of a thick raincrust and stratified graupel layers, and the weak layer appears to consist of a loose layer of 3 mm graupel (see Appendix 1).

The metamorphic changes in the snowpack had probably changed the strengths of the snow between the time of the event and our observations. At our first pit on the western flankwall, the fracture depth was about 1.6 m and the snow temperature at this depth was -3.8 degrees celsius, and at 1.0 m, the temperature was -3.6 degrees celsius, and at 0.5 m, -3.2 degrees celsius.

This lack of gradient, and warm temperatures is conducive to equitemperature type metamorphism, and we found it difficult to find the shear layer.

We dug a profile pit on the crown, about 50 m above the pit on

the flankwall, and this is described in Appendix 1. The slab was 0.64 m thick at this point and the shear occurred at the graupel layer (crystals 3 mm size).

We could complete only four shear tests, which covered only a very small section of the crownwall. One column slid before it had been completely isolated, but we were uncertain whether the shear layer had been disturbed when we were isolating the column. The other columns (all of which were at a spacing of 3 m to 5 m apart) showed shear strength/stress ratios of at least 1.5. Although our pits may not have been in the weakest zones, we also felt that some of this apparent stability was due to metamorphic processes that would have occurred in the 3 to 7 days after the avalanche.

SNOW DISTRIBUTION PATTERNS

We think that wind transportation and redistribution of snow caused much of the strength variations we have measured. During storms, we have observed depositional features such as dunes and ripples, and have measured migration of these, and also erosional scouring. These features cause small scale irregularities and roughness in a snowpack which could result in strength variations. So far, we have not found the patterns to be reproducable (except in very general terms). This makes it difficult to assess the distribution of strength patterns within the snowpack by observing surface features.

Fohn and Meister (1983) developed a model to fit their

measurements of snow drifts on ridge slopes. They also note that complex patterns of snow drift develop behind discontinuities, especially when the flow is not fully developed.

The effects upon snow stability are:

(1) there is an increase of snow loading behind an obstacle.
(2) Discontinuities in the snow depth distribution could cause stress concentrations.
(3) Schmidt and Randolph (1981) pointed out that most drifting snow particles are more rounded than the precipitation crystals from which they derive, and as a result, could form a poorly bonded layer.

We made some measurements in 1983 and continued these on the Cornicewall in 1984. As well as investigating the snow distribution down a slope, we also wanted to investigate the possibility that the tensile zone for avalanches (the crown wall), may be related to the "zone of separation" of the wind which had transported the snow. The zone of separation for a particular shape of mountain, moves depending on windspeed and direction (Scorer, 1972), and so is difficult to characterise. Fohn and Meister (1983), found the ridge shape and sharpness had a strong influence on the patterns of erosion and accumulation.

Our results from 1983 and 1984 are shown in Figures 8 and 9 respectively. The slope used during 1983 is about 400 m south

of that used in 1984. The Cornicewall has a gentle slope (about 8 degrees) exposed to the prevailing NW wind direction, and the profile steepens as the aspect changes to SE. The slope adjacent often avalanched during or after storms. The high snowfalls (up to 3 m per storm) in the area meant that we often lost our bamboo snowpoles which we had placed down the slope.

Apart from the NE storm which fell with little wind on 30 August 1984, all the plots show a peak in snow depth distribution down the slope. This is also noticeable in the two cases where erosion had occurred over most of the slope, but deposition had occurred at a position (see Figures 8 and 9). The position of the peak in snow depth for a particular shape depends on the drift flux which depends on wind speed and direction, and we do not have accurate measurements of these factors.

It is also interesting to note that during the 1983 storms, all the peaks of depth recorded were <u>above</u> the expected tensile zone for a slab avalanche when considering slope geometry (see Figure 8).

SHEAR-STRAIN MEASUREMENTS

McClung (1979) pointed out the possible significance of the shear strain softening that he measured in a laboratory (McClung 1977). We wanted to do some similar experiments in the field, using large snow samples.

We fitted a linear potentiometer (0-75 mm) made of conducting plastic into a P.V.C. tube (50 mm diam., 300 mm long). The tube had two vertical fins, each 50 mm deep and 300 mm wide, mounted on it perpendicular to its axis, so that it could be anchored onto the snow surface. We connected one end of a string to the potentiometer, and the other to a 300 x 300 x 50 mm shear frame (see Figure 10). By loading the frame, and measuring the electrical resistance of the potentiometer on a digital volt meter we could measure the strain for varying loads.

This system has several disadvantages compared with a constant strain rate device, one of the main ones being that once the peak shear strength (as found by McClung, 1977) was reached, the sample failed and the strain gauge reached its maximum. This meant we could not measure the residual shear strength unless we disconnected the strain gauge. We also found it difficult to apply the stress at a constant rate. The advantage of this device is that it is relatively easy to operate. We made several tests, and two series of tests are plotted in Figures 11 and 12. As previously mentioned, rate control was poor, but these tests to failure took from 0.5 to 16 minutes which are relatively rapid (McClung, 1977).

Figure 11 shows some shear strain measurements made on some heavily rimed crystals which appeared to have undergone equitemperature metamorphism. We were unsure if the jerky type curve is a function of our loading rate or measuring device or of the snow properties.

In two cases, we reset the strain gauge and measured a residual strength after the peak failure. All the the tests were in closely similar snow, and the mean peak shear strength was 993 + 267 N/m2 (5 readings) and the mean residual strength was 227 + 48 N/m2 (6 readings).

Figure 12 shows some shear strain measurements on new snow (average density 52 kg/m3). This snow did not show any strain softening effects, and the mean shear strength was 163 + 24 N/m2 (4 readings).

These measurements support the concept that the shear strength of a material consists of both a cohesive component and a frictional component. The older snow described in Figure 11 would have had time to sinter and form cohesive bonds. Since our rates of loading were relatively rapid (thus preventing further rebonding during the test), we infer that the peak strength is an indication of the breaking of the cohesive part of the snow, and the residual strength is associated with the frictional component. Furthermore, it appears the new snow described in Figure 12, may not have sintered very much and so no peak strength was observed, and the strength measured would have been largely associated with the frictional component. These properties have also been observed in clays (e.g. Soydemir 1977, Bjerrum 1973) and in powders (e.g. Schwedes 1975).

To further investigate some of these properties, we decided to simplify the experiments and do a shear test (without the

strain gauge), and then do a further test with the same snow to determine the residual (frictional component) strength. In some of these tests we allowed some time between tests to determine effects of rebonding. The mean strengths and standard deviations are listed in Table 1 for various snow types. The figures in brackets are the number of tests made.

Table 1 shows that snow that had been partly metamorphosed did exhibit residual shear strengths that were lower than the peak strengths, at these strain rates. This trend was especially noticed in the graupel layers where the residual strength measured in one case was as little as 12% of the peak strength. Since graupel is generally deposited at warm temperatures, we would expect some rapid bonding between crystals. These measurements support field observations where although graupel layers may appear to be loose in a snowpack when mobilised, the cohesive component is often high, and it is relatively rare to find avalanches which have failed at these layers.

The experiments where the sample was allowed to stand for either one or five minutes after the initial shear show that rebonding may be significant over this time, especially when the snow temperature is warm.

We are uncertain about rates of failure in a slab avalanche situation, but McClung (1979) pointed out that strain softening of snow may be of importance in crack propagation. Several studies (for example Sommerfeld and Gubler (1983), Conway and Abrahamson (1984)) have found that fractures may

initiate in small zones (less than 1 m3) before propagating over wider areas. Furthermore, Conway and Abrahamson (1984) have observed fractures to propagate through apparently strong basal zones, and the strain softening mechanism may help to explain how this crack propagation occurs.

CONCLUSIONS

Our measurements this winter support the model of a snow slab being pinned unevenly over the basal zone, as well as around the periphery of the slab. Although the basal strength on the slope observed on July 4, Cornicewall, appeared to be low, the slab did not release as an avalanche, probably because of the pinning around the edges. We made extensive shear measurements on four unstable slopes, and less extensive measurements on two other avalanched slopes. These measurements support our interpretation of earlier observations (see Conway and Abrahamson, 1984) which indicated that avalanches may be initiated in a relatively small area (trigger zone), and a crack may propagate through stronger zones. This causes a major uncertainty in predicting avalanches since the trigger zone may be small and difficult to find when compared with the whole slope.

Our measurements of the large decreases of shear strength after some slip has occurred in some snows are preliminary measurements aimed at gaining an insight into the mechanism of crack propagation.

The snow accumulation measurements down the Cornicewall, the variable depths of crown walls, and the variable thickness of shear layers, all emphasise the difficulties of interpreting the position of the trigger area from meteorological measurements. Although a thick weak layer may cause a more consistent weakness than a thin layer, and a deep slab may produce a greater downslope load than a thin slab, predicting where the weakest area exists is of primary importance for making an assessment of a slope. We plan on making some creep measurements by placing markers across a slope to determine whether these might show that one section of a slope is creeping faster than another, thus indicating a weak basal layer. We also have an untested device for making rapid spot shear strength tests across a slope.

ACKNOWLEDGEMENTS

The project has been sponsored by the Department of Chemical and Process Engineering (University of Canterbury), with a financial grant from the Department of Lands and Survey (Wellington). Mount Cook Airlines Company provided aircraft access to the area and Mount Cook National Park staff helped considerably with the field work. I would like to thank all of these groups for their support.

REFERENCES

Bjerrum, L., 1973, Problems of soil mechanics and

construction on soft clays, Proceedings of the eighth International Conference of Soil Mechanics and Foundation Engineering, Moscow, Volume 1.3, p111-159.

Conway, H. and Abrahamson, J., 1984, Snow Stability Index, In Press, Journal of Glaciology.

Fohn, P.M.B. and Meister, R., 1983, Distribution of Snow Drifts on Ridge Slopes: Measurements and Theoretical Approximations, Annals of Glaciology, 4, p52-57.

McClung, D.M., 1977, Direct Simple Shear Tests on Snow and their Relation to Slab Avalanche Formation, Journal of Glaciology, 19(81), p101-109.

McClung, D.M., 1979a, Shear Fracture Precipitated by Strain Softening as a Mechanism of Dry Slab Avalanche Release, Journal of Geophysical Research, 84, B7, p3519-3526.

McClung, D.M., 1979b, Insitu Estimates of the Tensile Strength of Snow Utilising large Sample Sizes, Journal of Glaciology, 22, p321-329.

Narita, H., 1980, Mechanical Behaviour and structure of snow under uniaxial tensile stress, Journal of Glaciology, 26, p275-282.

Narita, H., 1983, An experimental study on tensile fracture of snow, Contribution Inst. Low Temp. Science, No. 2625, Series A, No. 32.

Schmidt, R.A. and Randolph, K.L, 1981, Predicting deposition of blowing snow in trenches from particles trajectories, Presented at Western Snow Conference in Utah, 1981.

Schwedes, J., 1975, Shearing behaviour of slightly compressed cohesive granular materials, Powder Technology, 11, p59-67.

Scorer, R., 1972, In "Clouds of the World", Lothian Publishing Co. (Pty) Limited, Melbourne.

Sommerfeld, R.A. and Gubler, H., 1983, Snow avalanches and acoustic emissions, Annals of Glaciology, 4, p271-276.

Soydemir, C., 1977, Potential models for shear strength generation in soft marine clay, In Geotechnical aspects of soft clays, (Editors, R.P. Brenner and E.W. Brand), The International Symposium on Soft Clay, Bangkok, 1977.

SNOW TYPE	PEAK STRENGTH N/m^2	RESIDUAL STRENGTH N/m^2	RESIDUAL AFTER 1 MINUTE N/m^2	RESIDUAL AFTER 5 MINUTES N/m^2	RESIDUAL STRENGTH N/m^2
New Snow Density = 50 T = -9.6°C	272±54 (3)	272±54 (3)	-	-	-
0.1-0.2 mm Partly Radiation-Recrystallised Snow Density = 200 T = -6.6°C	363±63 (3)	179±14 (7)	-	-	-
0.1-0.2 mm Partly Radiation-Recrystallised Snow Density = 150 T = -4.4°C	272 (3)	218 (9)	-	-	-
2 mm Needles Density = 140 T = -1.8°C	402±80 (5) 345±16 (3)	222±41 (13) -	- -	- 299±28 (3)	- 245±38 (2)
2 mm Needles Becoming Rounded Density = 160 T = -1.4°C	345±66 (6) 317±42 (3)	241±47 (14)	- 308±42 (3)	- -	- 190±40 (2)
2 mm Graupel	1307±154 (2)	163 (2)	-	422±19 (2)	-
Up to 4 mm Graupel Density = 260 T = -6.2°C	>1200 (8)	498 (8)	-	-	-

TABLE 1: A summary of mean peak shear strengths measured and residual strengths either immediately after the first test or 1 or 5 minutes after. The figures in brackets are the number of tests made on each snow type, using separate samples.

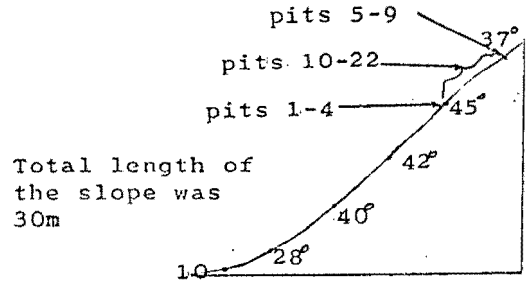

Shape of slope and position of pits on the Cornicewall July 4 1984.

Figure 1

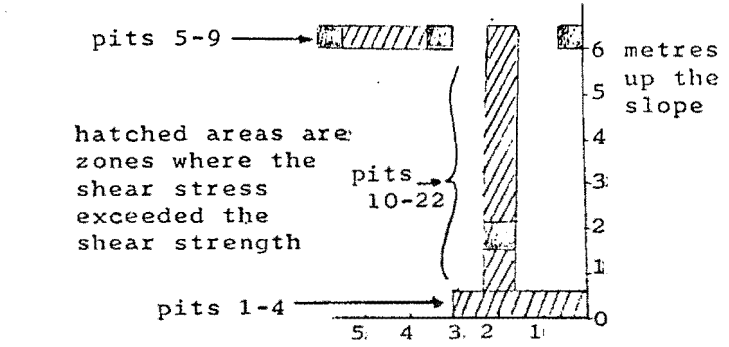

Zones of weakness and pinned areas measured on the Cornicewall, 4 July 1984.

Figure 2

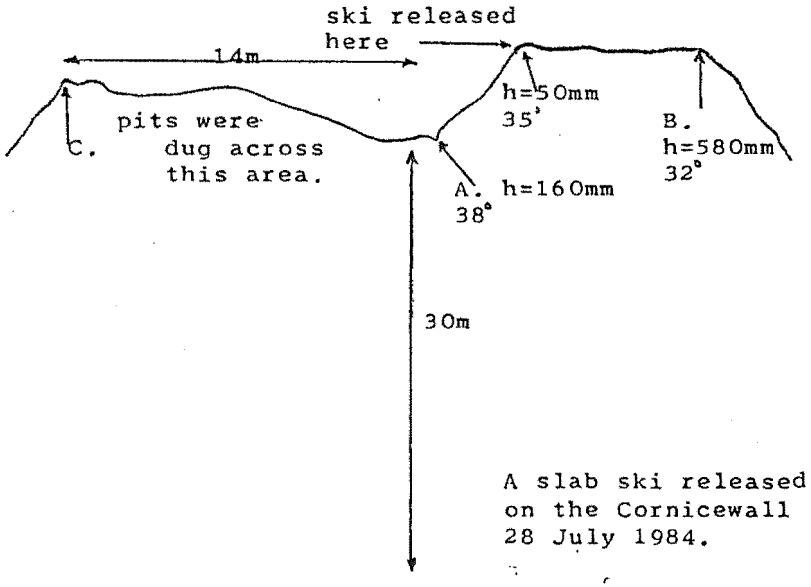

A slab ski released on the Cornicewall 28 July 1984.

Figure 3

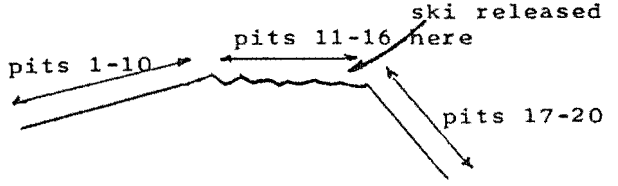

bed surface angle:40
A small slab; 12.5m wide, 6.9m long.

A slab ski released on the Cornicewall 1 August 1984.

Figure 4

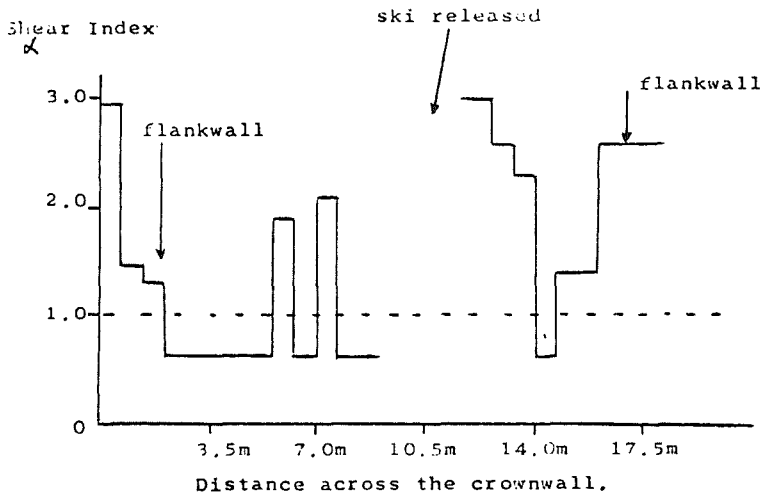

Figure 5.
Basal shear index measured across the crownwall of a fracture on 1 August 1984. The avalanche was ski released near the middle. Slab density: 180kg/m^3. Bed surface angle: 32 to 52 degrees. Depth of the fracture varied from 160mm to 250mm.

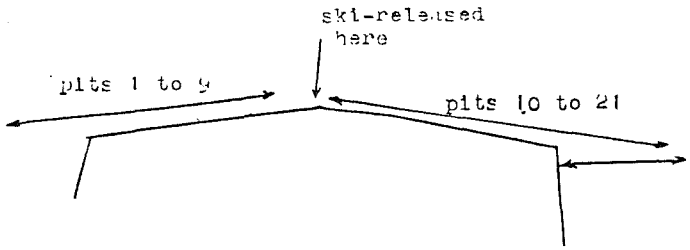

bed surface angle 45 to 49
depth of fracture varied from 0.14m to 0.39m

Figure 6
A slab ski-released on the Cornicewall 28 August

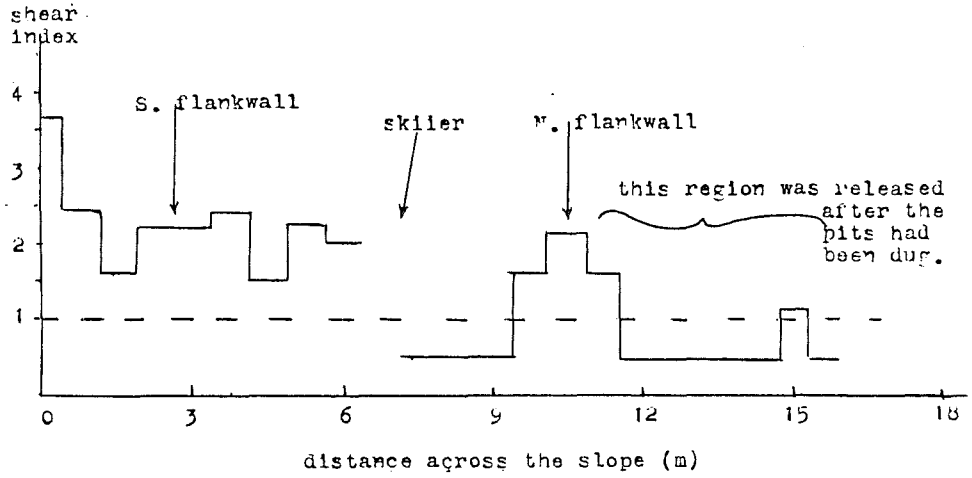

Figure 7
Basal shear index measured across the crownwall of a fracture on 28 August 1984. Slab density 260. Columns with an index of less than 1, had slid before they could be completely isolated. Pit spacing was 0.75m.

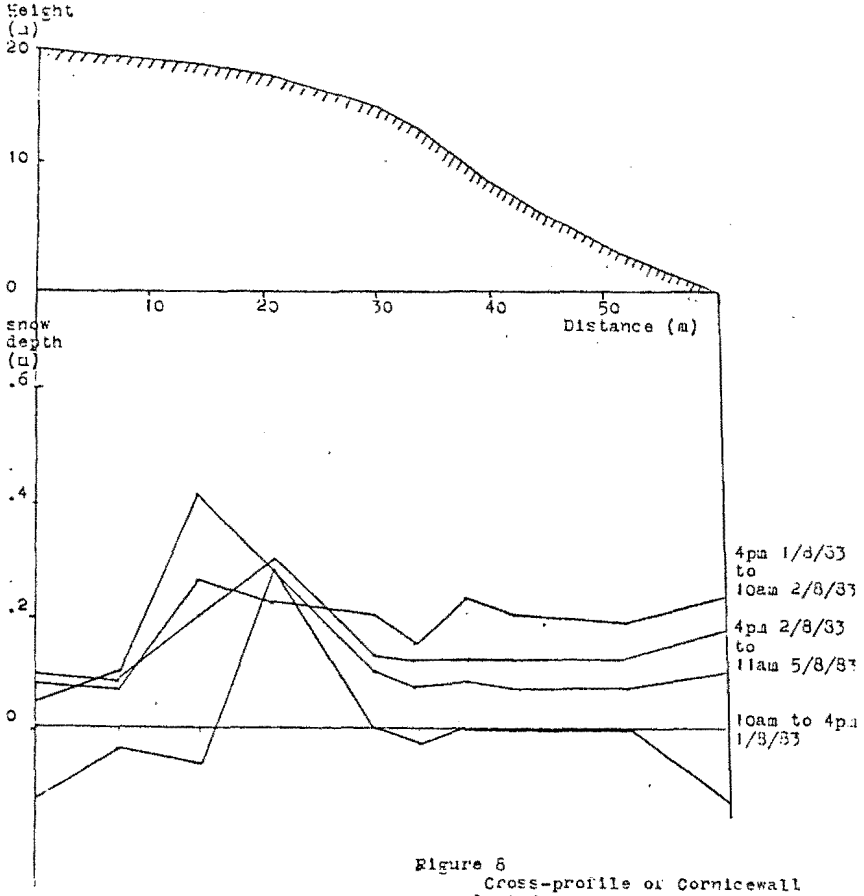

Figure 8
Cross-profile of Cornicewall on selected storms during 1983.

Figure 9
Cross-profile of Cornicewall during selected storms of 1984.

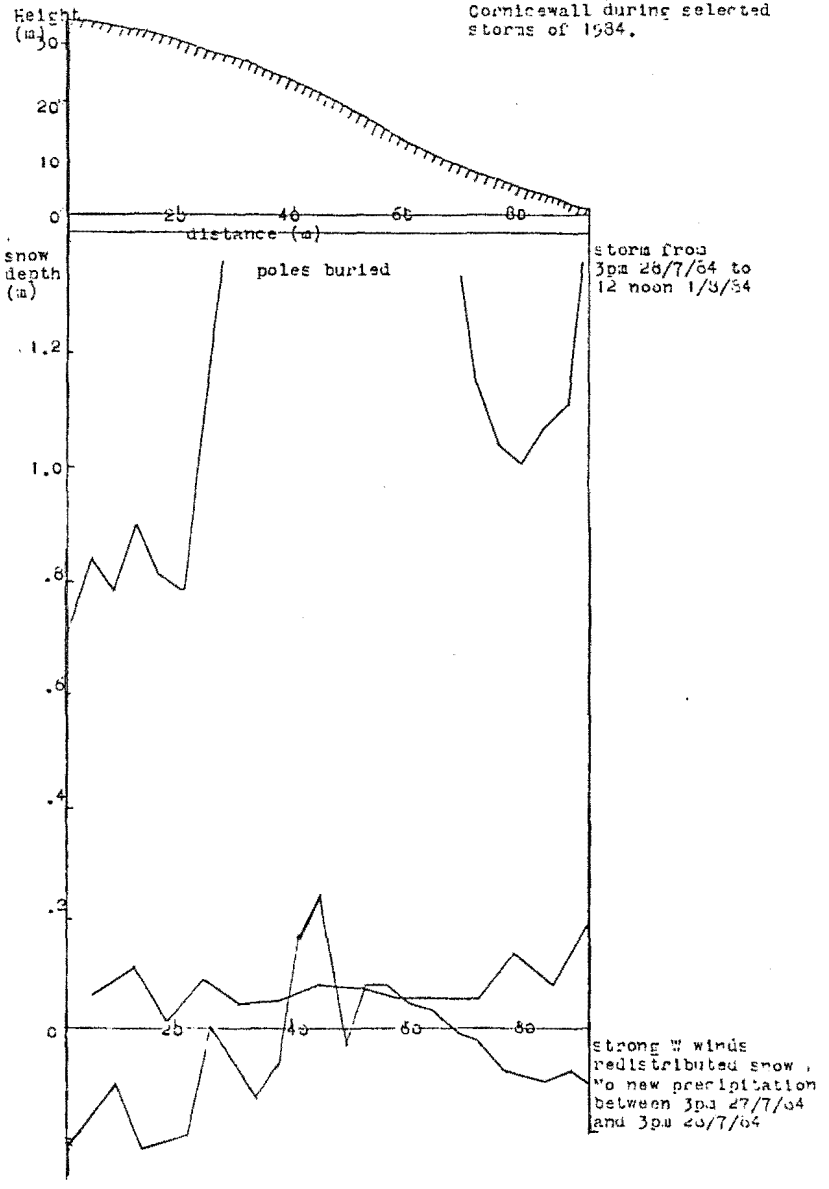

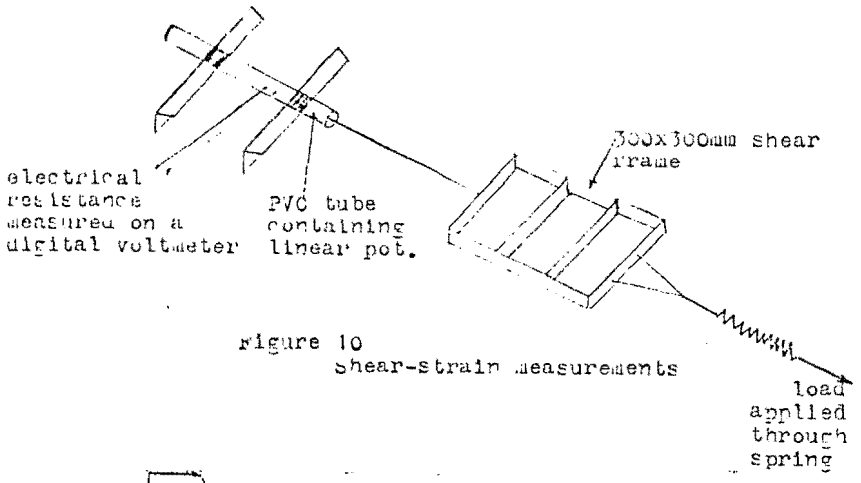

figure 10
Shear-strain measurements

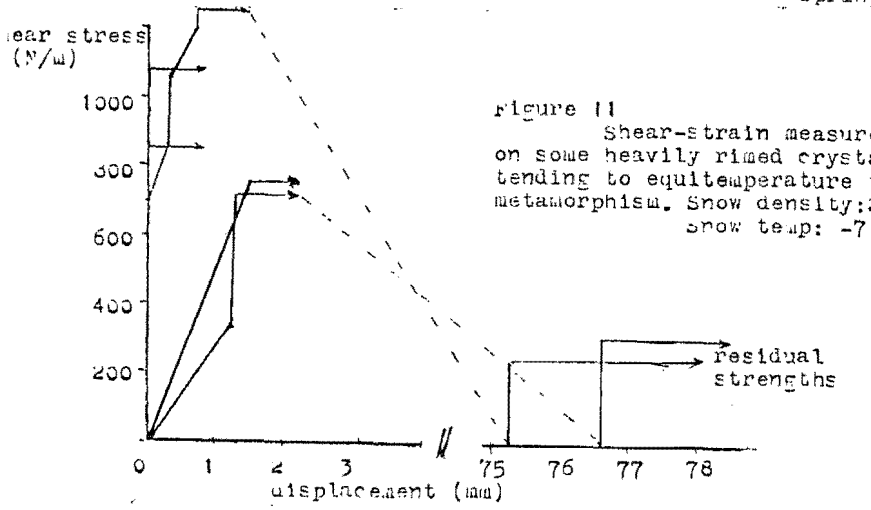

figure 11
Shear-strain measurements on some heavily rimed crystals tending to equitemperature type metamorphism. Snow density:200
Snow temp: -7.2

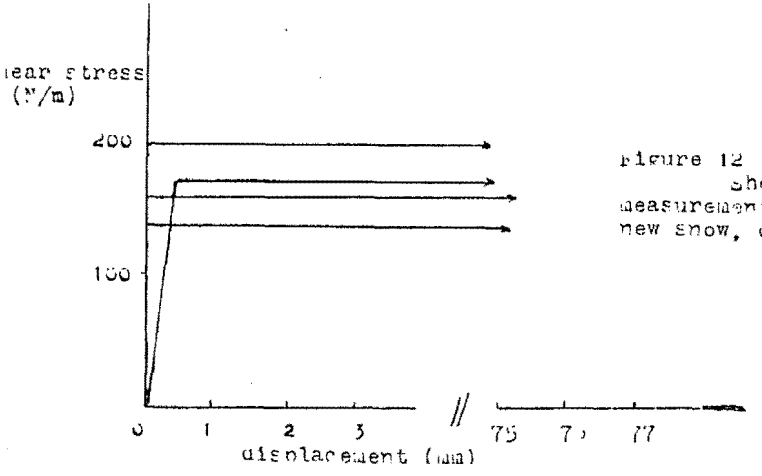

figure 12
Shear-strain measurements on some new snow, density:52
temp: -2.8

Cornicewall 4/7/34

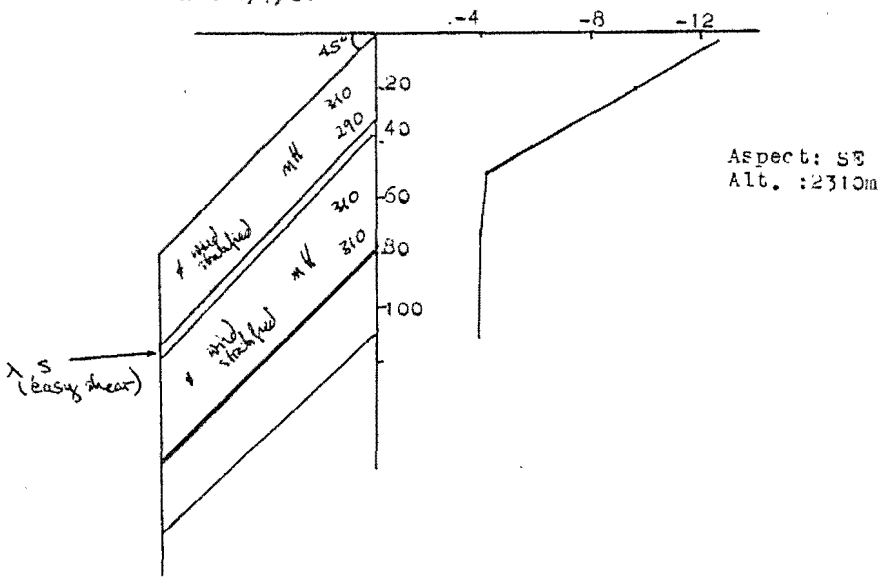

Aspect: SE
Alt. :2310m

Hochstetter Dom fracture 4/7/34

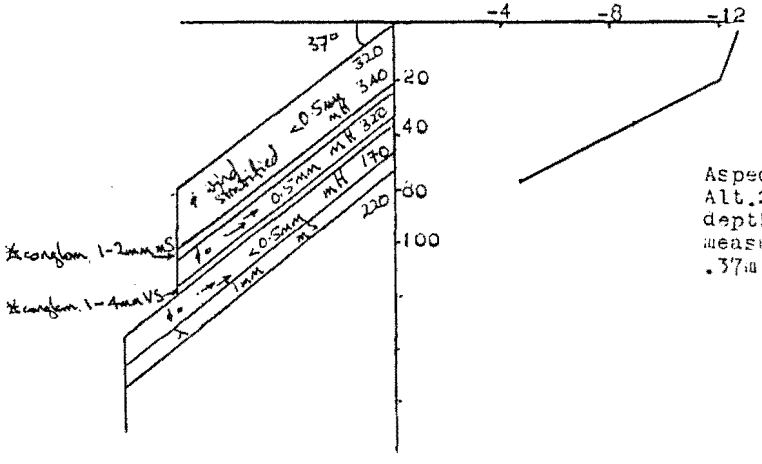

Aspect: SE
Alt.2500m
depth of fracture measured varied from .37m to .73m

Cornicewall ski-released fracture 26/7/84

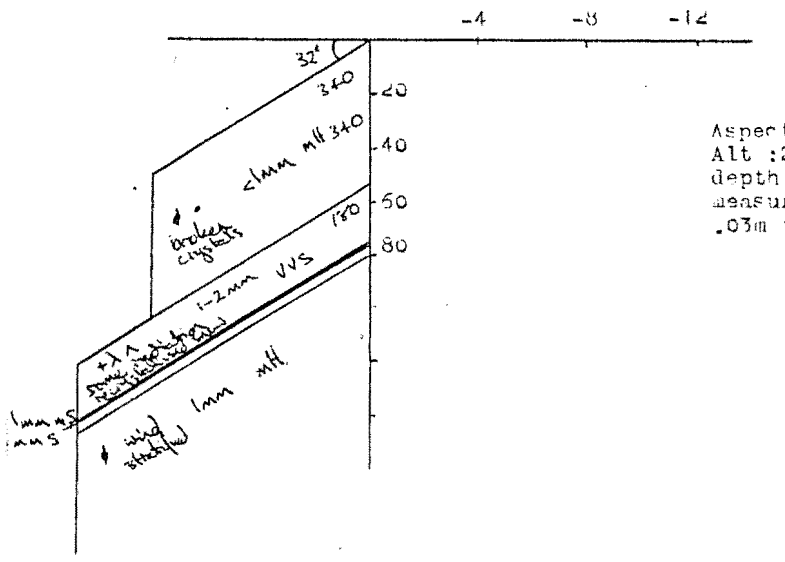

Aspect:SE
Alt :2310m
depth of fracture measured varied from .03m to .58m

Cornicewall ski-released fracture 28/8/84

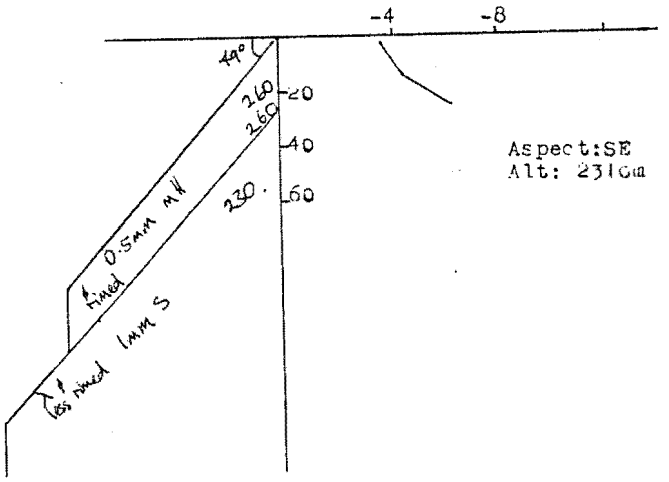

Aspect:SE
Alt: 2310m

Cornicewall ski-released fracture 1/8/84

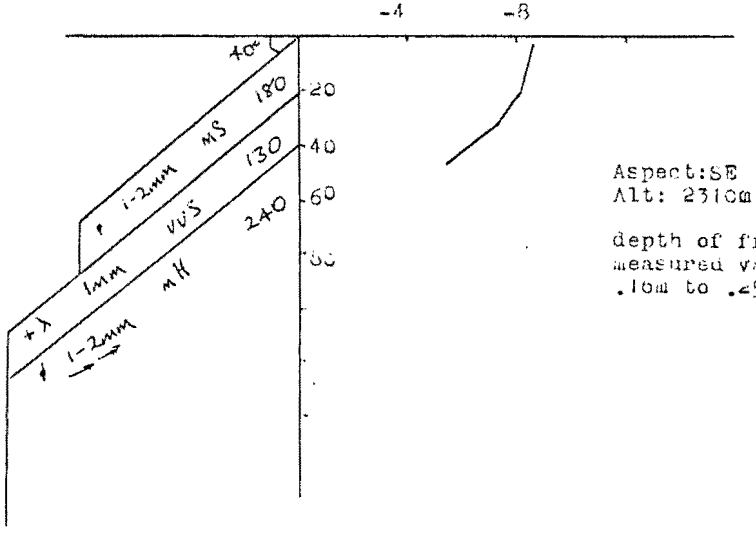

Aspect:SE
Alt: 2310m

depth of fracture measured varied from .10m to .<5m.

HochstetterDom fracture 17/9/84

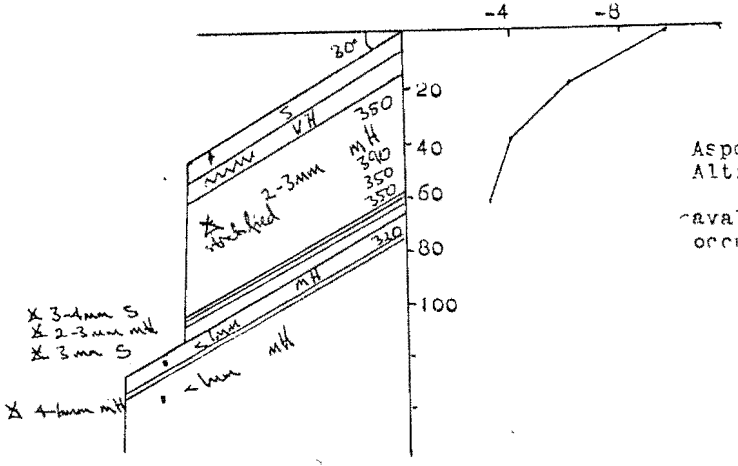

Aspect: SE
Alt: 2550m

avalanche probably occurred on 13/9/84

MOUNTAIN AVALANCHE FORECASTING USING METEOROLOGICAL DATA FROM MT COOK VILLAGE

H. CONWAY October 1983

INTRODUCTION

Most models for slab avalanche failure demand a weak basal shear layer overlain by a relatively stiff snow slab (Perla, 1980). McClung (1979) suggested that for a tensile failure in a slab the rate of tensile creep must exceed the rate of sintering of the slab.

Conditions and crystal types which are likely to form weak layers are:

(i) free water at a layer

(ii) a surface hoar layer or radiation recrystallised layers, subsequently buried by further snowfall.

(iii) depth hoar layers.

(iv) a poorly bonded layer deposited some time during the storm (for example large (1 - 2mm) dendrite crystals) that has been subsequently buried.

If the surface snows are loose and cohesionless, conditions are more conducive to point release avalanches rather than slab releases. If the surface snows have some cohesion, they may fail as a slab, provided McClung's (1979) criterion is satisfied. Watanabe (1980) found that tensile failure would occur only if either the temperature or the load increased at a fast enough rate. The rate was found to vary depending on snow types.

The load on a snow slope can increase in many ways, some of these being,

(i) increase of precipitation.

(ii) wind transport of snow can scour some slopes and deposit large snow loads on other slopes.

(iii) shear strain softening (McClung 1979) may increase the length of a weak layer which, by decreasing the basal support of a slab, effectively increases the tensile stress on the slab.

(iv) Removal of pinning areas (as suggested by Conway and Abrahamson 1983) may similarly effectively increase the downslope load.

(v) external loads such as glacial movement causing icecliff collapses, or people may be sufficient to cause failure.

Narita (1980) showed that tensile failure occurred at relatively low stresses when the rate of loading was fast (brittle type failure) when comparedwith slower rates of loading (ductile failures). This also suggests that if the loads on a slope increased at a rapid rate, a failure is more likely than if the load is increased gradually.

Sintering of the snowpack occurs much more rapidly as temperatures approach $0^{o}C$, but as mentioned previously, free water at these high temperatures, can lubricate the shear layer and cause failure.

MT COOK DATA

Most avalanche activity occurs during or directly after a storm (Perla and Martinelli, 1976), so we tried to identify storm types that might show unstable trends. In theory, a reverse type storm (a storm which starts from the south and is followed by a change in direction to the North or Northwest) will produce an inverted density profile in the snowpack. This stratigraphy should be more conducive to avalanche formation when compared with a Normal type storm (storms which start from the North or Northwest, and then clear from the South or Southwest). Normal storms and Southerly storms (which deposit low density snow at the surface of the snowpack) could be more likely to produce point release avalanches.

To be of use for the Mt Cook avalanche forecast, we looked at the meteorological data collected in the village, and compared it with avalanche activity that had been recorded.

Ho (1982) identified Normal, Reverse, NW, S and E storms for the 1977 and 1978 Mt Cook winters, and we combined his summary with data collected during the 1981 and 1982 seasons.

Of a total of 90 storm cycles during the winter months (June to October), 38% were Normal storms, 23% S storms, 11% Reverse storms and 2% E storms.

Avalanching (either slab release or point release or both) was recorded after about 90% of the total storm periods. Major events (greater than five avalanches observed) were recorded after 68% of the total storm periods.

If we considered major events (greater than five avalanches observed) of slab releases, then we found we could expect a major event after 47% of all storms. However, if the storm, was either Reverse, NW, or Normal, we could expect major slab activity after about 60% of these storms. If the storm was from the S, major slab release occurred after about 24% of the storms.

During the 1981 and 1982 winters, we analysed the precipitation and minimum temperature data from the village. Perla and Everts (1983) found that the precipation (in mm of water) summed for the three day period before the events was an important variable. With our data, although major events often occurred after periods of high precipation rates, this trend was not always observed and this index did not significantly improve the prediction of an avalanche event. (see appendix). We also considered the minimum temperature measured during the storm to determine whether this might improve the correlation (a low temperature might be conducive to forming a low density, weak layer). Analysis of this parameter did not show any useful relationship to avalanche occurrence.

DISCUSSION OF THE DATA

Conway and Abrahamson (1983a) suggested that small, local variations in strength may control a slope stability. They also suggested that these variations may be due to the variable properties of wind deposited snow. Prediction of meteorological factors such as precipation rate, precipation type etc, at such local sites is very difficult - especially from a position as distant from the starting zones as the Mt Cook Village.

The weather data was based on observations recorded at 9 am each morning in the village. Young and Conway (1983) described the large errors likely when comparing Mt Cook Village weather data with Tasman Saddle data, and this would add uncertainty to the avalanche - weather correlation

Conway and Abrahamson (1983b) also found that weak layers in the Tasman Saddle area could often consist of buried radiation recrystallised snow. (formed prior to the storm), or very thin weak layers (less than 1mm thick) deposited probably during a brief change in weather conditions during the storm. At least three major avalanche cycles during the 1982 season occurred after fine cold periods had caused recrystallisation of surface snow, and these conditions have not been considered in this paper. The once daily weather readings (at 9am) from the village are not only likely to have a poor correlation with on site data, but are likely to miss subtle and rapid changes in conditions which may produce thin weak layers. More continuous on site records such as those produced hourly by a remote weather station would improve the input for the avalanche forecast considerably.

Storms in the mountains often precipatated up to 2 metres of new snow, and this combined with considerable relocation of snow due to wind transport often covered avalanches by the time the storm cycle had finished. Avalanche observation during storms was often not possible due to poor visibility and so the observations of avalanche occurrence were generally limited to those near the end of storms. Added to this recording anomolie, the number of recordings was, often related to the number and location of observers in various areas (observing different aspects as well as altitude differences).

These factors add to the difficulties in correlating avalanche occurrence with storm conditions. An indication of the change in recording patterns and awareness of avalanche events may be that during the 1977 and 1978 seasons (40 storm periods) major slab release events were recorded after only 33% of the storms, while during the 1981 and 1982 seasons (50 storm periods) major events were recorded after 56% of the storms. Although some of this difference may be a result of seasonal changes, I suspect that much of the increase in records of later years is a result of a change in the recording awareness of observers.

CONCLUSIONS

Avalanche activity can be expected after 90% of all winter storms and major slab avalanche activity after 47% of all storms. Southerly type storms did not provide as much slab activity as other storm types (Reverse, Normal or NW) which all produced similar amounts of avalanching.

Only very general trends can be predicted with once daily weather observation from the village and further refinement of the correlation using meterologica parameters was found to be complex.

In order to make specific assessments of a slope stability using past and present meterological observations, more continuous data recorded near the avalanche starting zones would be required. The remote weather station described by Conway and Abrahamson (1983b) fulfills this requirement.

REFERENCES

Conway, H. and Abrahamson, J. 1983a : "Snow Stability Index" Submitted to Journal of Glacialogy.

Conway, H. and Abrahamson, J. 1983b : "A Summary of Weather and Snow Conditions at the Tasman Saddle area during the winters of 1980 - 82." Unpublished report.

Ho, C.W. 1982 : MSc thesis. University of Otago.

McClung, D.M. 1979 : "Shear fracture precipated by strain softening as a mechanism of dry slab release." Journal of Geophysical Research. Vol 84, No B7, p 3519-3526.

Narita, H. 1980: "Mechanical behaviour and structure of snow under uniaxial tensile stress." Journal of Glacialogy, Vol 26, No 94, p. 275-282.

Perla, R.I. 1980 : "Avalanche release, motion and impact." In dynamics of snow and ice masses. (S. Colbeck ed.) Chapter 7, p. 397-462, Academic, New York.

Perla, R.I. and Martinelli, M.Jr. 1976: Avalanche Handbook. U.S. Department of Agriculture, Forest Service, Agriculture Handbook 489.

Perla, R.I. and Everts, K. 1983 : "On the placement and mass of avalanche explosives : experience with helicopter bombing and preplanted charges." Annals of Glaciology, No 4, p 222-227.

Watanabe, Z, 1980 : "Tensile strain and fracture of snow." Journal of Glaciology, Vol 26, No 94, p. 255-265.

Young, R.S.B. and Conway, H. 1983 : "Comparisons of weather between the Tasman Saddle area and Mt Cook Village, winter 1982." unpublished report.

COMPARISONS OF WEATHER BETWEEN THE TASMAN SADDLE AREA AND MT COOK VILLAGE WINTER 1982

BY: R YOUNG
H CONWAY

INTRODUCTION

Data collection which began on a regular basis at Tasman Saddle Hut (2318m asl) during the winter of 1981 was continued during the 1982 season. Data was collected from the beginning of June until early October and up to 105 days readings are available for comparison and analysis with the Mt Cook Village data. If a significant relationship can be established between these two sites, this would be a valuable aid for the avalanche forecasting programme.

Avalanche forecasting is partly based on meterological data from national, regional and local sources. Weather forecasts issued by the Christchurch weather office for the Mount Cook area provide a general overview of future weather patterns for the forecaster. However more refined local data is essential for accurately predicting the local avalanche hazard.

The most important parameters for the avalanche forecaster are precipitation, windrun and direction, and temperature. The complex geography of the mountains strongly influences the local mountain weather patterns, making it difficult to extrapolate, except in general terms, data collected from one site to another site.

Following the 1981 season, Conway and Abrahamson (1982) used some limited data to establish relationships between village weather and Tasman Saddle weather data, and this report attempts to further refine this relationship based on data collected during the 1982 season.

CORRELATIONS BETWEEN TASMAN SADDLE AND MT COOK VILLAGE

(i) WINDRUN
The Mount Cook Village site is sheltered somewhat by trees close to the anerometer, and the site at Tasman Saddle Hut (on the roof of the hut) is subject to local turbulance both around the hut and from the large cliff in front of the hut.

In 1982, a Munroe cup counter at the hut was read daily at 6.15am and compared with readings at Mount Cook Village at the same time on 76 occassions between June and October 1982.

The regression line comparing these sets of data was :
Wind (Tasman Saddle) = 243 + 1.2 x Wind (Village).
where the wind measurements are the total km run over the past 24 hours.
The residual standard deviationabove and below the regression line was 256 km.

These results compare with the data from 1981 where a Lambrecht anerometer was used on the hut and compared with the village data. This regression line was : Wind (Tasman Saddle) = 263 + 1.42 Wind (Village) with a residual standard deviation of $\pm$ 159 km (see Conway and Abrahamson, 1982)

Further refinement of the correlation was attempted by grouping the data from different wind directions, and comparing these with the Tasman Saddle data. Grouping of the data in this way did not help to improve the correlation coefficient.

(ii) PRECIPITATION
A. Village - Tasman Saddle
Conway and Abrahamson (1983) mention the difficulties of measuring a representative precipitation accumulation at Tasman Saddle due to local transport and redeposition of snow.

However, a linear regression between the daily snowfall measured at Tasman Saddle (cm of snow) and the precipitation in the village (mm of water equivalent) using 34 daily measurements, resulted in a regression line:
Snowfall (Tasman Saddle) = 9.5 + 0.69 x precipitation (Village).
The residual standard deviation was $\pm$ 13.3 cm of snow.

We found a slightly better correlation coeficient when we considered storm totals rather than daily measurements, although separation of data into storms of different directions did not show any improvement in the correlation coefficient.

Wind runs recorded during times of precipitation were greater than 2.5 ms^{-1} on about 83% of the periods measured and at these times, redeposition of snow was occurring. The correlation could not be improved by considering the windrun and the snowfall, although more data may prove this to be more useful.

B. Tasman Saddle Hut - Surrounding slopes
Conway and Abrahamson (1983) listed comparisons of snow accumulation at the hut with the Cornice Wall, the Nosedive pole and the Nosedive slope for storms which were generally from the Westerly quarter and of high windspeed (a daily mean speed of 6.6 ms^{-1}). The regression lines show that the accumulation on the Cornice Wall under these conditions (Cornice Wall is an East aspected slope) is about 2.5 times greater than that at the hut, and accumulation on the Nosedive is closely similar to that at the hut snowpole (the Nosedive is a South aspected slope).

We have often observed considerable variation of snow accumulation depths, and further study of accumulation at different sites is important for estimating conditions which may cause a slope to be 'sheltered' or 'lee'.

(iii) TEMPERATURES
All temperatures were read at 6.15am daily at both the village and Tasman Saddle Hut during the recording period

All the temperature relationships between the two sites exhibit a large amount of scatter. We estimated that some of the error (about 2% of the period) may have been due to measurement errors such as the screen filling with snow, or the wind vibrating maximum and/or minimum thermometers, thus causing erroneous readings.

A. Dry Bulb Temperatures
The Dry Bulb regression equation was:
Dry Bulb Temperature (Tasman Saddle) = -5.9 + 0.21 x Dry Bulb Temperature (Village), where the temperatures were measured in ^{o}C. This equation has a poor correlation coefficient (r = 0.29), and the residual standard deviation was $\pm$ 6.6^{o}C.

Breakdowns of Dry Bulb temperatures based over specific periods such as calm days, NW/N wind days, SW/S wind days and raining in the village days, produced varying results with the best correlations occuring when NW/W wind periods (r = 0.59) and raining in the village (r = 0.49) were used.

Only 16 data points were available from the 1982 season for considering the rain in the village period, and so the data base was expanded to include the 1981 and 1983 data (n = 31). This resulted in a regression equation:
Dry Bulb (Tasman Saddle) = -7.3 + 0.49 x Dry Bulb (Village),
here the temperatures were measured in ^{o}C when it was raining in the village. This has a residual standard deviation of $\pm$ 4.5^{o}C.

B. Maximum Temperatures
The maximum temperature regression equation was:
Maximum temperature (Tasman Saddle) = -4.4 + 0.3 x Maximum Temperature (Village where the Temperatures are in ^{o}C. This has a residual standard deviation of $\pm$ 10.4^{o}C.

C. Minimum Temperatures
The minimum temperature regression equation was:
Minimum Temperature (Tasman Saddle) = -9.6 + 0.2 x Temperature (Village) where the temeratures are in the ^{o}C. This had a residual standard deviation of $\pm$ 8.8^{o}C.

DISCUSSION OF DATA

(i) WINDRUN
The windrun data shows a large amount of scatter, and this limits the usefulness of the established regression equation.

Factors contributing to this scatter include not only the local wind effects at each site (for example, during fine cold periods, a katabatic wind from the North East was often recorded at the Tasman Saddle) but also riming and icing of the anerometers (riming was recorded about 13% of the period June to October at Tasman Saddle).

Windrun figures are useful to establish likely amounts of wind transport of snow, and the extent of wind scouring on exposed snow surfaces. Observations at Tasman Saddle indicate that transport of snow was common when the wind velocity was greater than 3ms^{-1} (260 km run per day) and during the 1982 season, this occurred about 60% of the period measured. Based on the regression line the conditions for transport would be likely to occur when the village windrun is greater than 14 km per day.

(ii) PRECIPITATION
The regression equation established for precipitation also shows a considerable amount of scatter but again offers a guide to amounts of snowfall at higher elevations. We observed considerable variability in measurements over distances of 200m (Cornice Wall compared with Tasman Saddle hut) and so over 35 km (distance between Mount Cook Village and Tasman Saddle hut), a high residual standard deviation ($\pm$ 13.3 cm of snow) is not unexpected.

An alternative method of estimating precipitation along the main divide has also been used. If the village precipitation is multiplied by a factor of 1.6, then this has to be used as an estimate of the water equivalent of precipitation on the main divide. If the new snow density is considered to be 160 kgm^{-3}, similar results to the regression line are obtained when the village precipitation ranges from about 10 to 25 mm water equivalent. At lower village rainfalls, Tasman Saddle precipitation tends to be higher than predicted by this equation, and at higher village rainfalls, Tasman Saddle precipitation tends to be lower than those predicted.

(iii) TEMPERATURES
Although the measuring errors previously mentioned may account for some of the scatter in the temperature correlations, we suspect that much of the scatter is a result of kinetic lapse rate changes, as conditions change from dry adiabatic to moist adiabatic. This concept is supported by the improvement in the correlation when comparing temperatures when it was raining in the village.

Reradiation of heat caused by the continual presence of snow at the Tasman Saddle site is also likely to affect temperatures at this site. We are also uncertain of the factors affecting the lag time between temperatures at each site, and this could also contribute somewhat to the scatter.

The high scatter of the data limits the use of the correlations in predicting freezing levels from data recorded in the village.

Assuming a linear relationship between freezing levels and temperature, we can use the regression equation to determine the expected freezing level:
$Z = 105 \times$ (Village Temperature) + 760
where Z is the estimated freezing level during periods of rain in the village in metres.

Village temperature is measured in ^{o}C. The residual standard deviation is $\pm$ 470 m which is rather high.

CONCLUSIONS

We are uncertain how typical the 1982 winter was when compared with other winters, but our results show that correlations comparing weather data between two distant sites (Tasman Saddle and Mount Cook Village) in mountaineous terrain are difficult. However, when an observer, or a remote weather station is not available, we did find some general trends which may be useful, even though the standard deviations are high.

These correlations are summarised below, together with the standard deviation expected on each measurement:

1. WIND
Wind (Tasman Saddle) = 243 + 1.2 x Wind (Village)
measured in km run in 24 hours; standard deviation = ± 256 km
Wind transport of snow can be expected when the village wind run exceeds 14 km/day.

2 PRECIPITATION
Snowfall (Tasman Saddle) = 9.5 + 0.69 x Precipitation (Village)
Snowfall measured in cm at hut, precipitation in mm water.
The standard deviation = ± 13.3 cm snow.
Accumulation on the Nosedive can be expected to be closely similar to the figure for the hut pole, and accumulation on the Cornice Wall, about 2.5 times this figure.

3. TEMPERATURES
Dry Bulb temperature (Tasman Saddle) = -5.9 x 0.21 x Dry Bulb temperature (Village)
where the temperatures are in ^{o}C and the standard deviation is ± 6.6^{o}C.
For moist conditions (raining in the Village) a regression equation to determine freezing levels is: Z = 105 x Temperature (Village) + 760
where Z = freezing level in metres.
Temperature is measured in ^{o}C and the residual standard deviation is ± 470 m.

REFERENCES

Conway, H and Abrahamson, J : (1982) " Weather Data Report, Winter 1981." Final report, Part 2, for the Mountain Safety Council.

Conway, H and Abrahamson, J : (1983) Unpublished. " A Survey of Weather and Snow conditions at the Tasman Saddle area during the winters of 1980 - 1982 "

A SUMMARY OF WEATHER AND SNOW CONDITIONS AT THE TASMAN SADDLE AREA

DURING THE WINTERS' OF 1980 - 1982

BY: *H. Conway and J. Abrahamson*
Department of Chemical and Process Engineering
University of Canterbury
Private Bag
Christchurch
NEW ZEALAND

ABSTRACT

As part of a study of snow mechanics, some weather and general snowpack analysis was carried out on the Upper Tasman Glacier in the Mt Cook National Park. Considerable variation of the snowpack properties was found, and attributed mainly to fluctuations of meteorological conditions during storms.

To aid forecasting of avalanches in one area from information taken from another location (for example the Tasman Saddle Region from Mt Cook Village) a remote weather station was built. This station measured windspeed, wind direction, air temperature and new snow depth, at the end of each hour, and recorded this information in a battery-powered data logger.

THE TASMAN SADDLE AREA

We used the Tasman Saddle Hut as a base for making weather and snowpack observations around the Upper Tasman Glacier (see figure 1). The hut is situated on a rock outcrop 2320 m asl. near the head of the Tasman Glacier in the Mt Cook National Park of New Zealand (S latitude 43° 30.5'; E longitude 170° 20.5'). The area is bounded to the North and West by the main divide of the Southern Alps which rise to 3060 m (Mt Elie de Beaumont) about 3 km from the hut, and this divide causes a major orographic barrier to the prevailing westerly winds. The Tasman Glacier drops away to the south west, and about 1.75 km to the south of the hut the Malte Brun range rises to 2190 m. 1.75 m to the east, Tasman Saddle (2392 m) divides the Tasman and Murchison Glaciers. Immediately to the south of the hut the rock outcrop drops steeply about 150 m to the glacier.

Most of the area has a glacial base and like most glaciers in the region has been downwasting since about 1916 (Burrows, 1973). This downwasting has changed slope profiles on some avalanche paths.

The glacial base and high snowfalls (up to 3 m during a storm cycle) tend to inhibit formation of depth hoar. However, cold temperatures (we recorded screened air temperatures of -16°C during July 1982), and periods of clear skies did cause recrystallisation of snow near the surface of the snowpack due to temperature gradients from radiation losses during June and July 1982. Subsequent snowfalls on top of these layers resulted in many avalanches. The glacial terrain can cause some additional problems for mountain travellers. We often observed deep slabs that had been initiated by a collapsing serac or icecliff and had then propagated over large areas far from the trigger zone.

Crevasses across avalanche paths can also prove hazardous to a traveller since even a small avalanche could bury a person in a crevasse under a large quantity of snow.

During the months from June to September 1982, we recorded mean daily windspeeds greater than 2.5 m/s for about 60% of the time and a daily mean maximum of 14 m/s in September. These high windspeeds combined with the turbulence associated with the mountains often resulted in considerable redistribution of the snow, and duning and scouring of snow over the slopes were a common occurrence.

WEATHER INSTRUMENTS

(1) Temperatures

A Stevenson screen located near the hut contained drybulb, maximum and minimum thermometers. A mechanical thermograph was also in the screen, but often was not useable.

(2) Snow Depth

We used a snowpole about 200 m north of the hut to measure snow accumulation. The strong and turbulent winds in the area cause considerable redistribution of snow and so we used several other poles in different locations to compare snow accumulation depths.

(3) Windspeed and Direction

During the 1981 season we used a Lambrecht anemometer mounted near the hut to record windspeed and direction. During the 1982 season we mounted a Munroe cup counter on the hut which we read daily and at the same time we recorded the wind direction.

(4) Other Observations

We also recorded other observations such as cloud-cover, weather conditions, visibility, snow conditions and avalanche occurrence daily at 6:15 a.m. Together with temperatures, windspeed and direction and the new snow depth, we passed this information to Mt Cook village by radio for the avalanche hazard forecast (Irwin, 1983) and for the Christchurch Meteorology Office.

REMOTE WEATHER STATION

Avalanche occurrence is directly related to meteorological conditions, and although the relationship is not fully understood, weather observations do help avalanche forecasting. Weather conditions can vary widely over small areas in the mountains, which makes it difficult for an observer in one location to predict conditions at another area.

In an attempt to solve this problem - in particular, the problem of forecasting conditions at Tasman Saddle from observations made at Mt Cook Village - we designed a weather station capable of recording air temperature, new snow depth, wind direction and windspeed.

The data collected was recorded hourly on a Tasman Data Logger which could be left for periods of 30 days.

The instruments were mounted on a tripod made from 50 mm diameter aluminium tubing. Each leg could be unscrewed into two sections, each 1.5 m long, and a 400 mm diameter plate was attached at the base of each leg to anchor the tripod in the snow (see figure 16).

Air temperature was recorded by a downward pointed thermocouple, shielded inside a white P.V.C. tube which oriented itself into the wind and was angled at 45° to allow snow to fall out of the tube. The new snow depth measurements were

made using a Polaroid ultrasonic range finder mounted at the top of the tripod. This measured the distance to the snow surface, and during times of storms, or times of blowing snow, a scatter of data was recorded. This not only enabled us to record the new increment of snow, but also gave an indication of the duration of the storm. Windspeed was measured with an electrical counter, on the shaft of a robust cup anemometer, and the wind direction measured by mounting a vane on a viscous damped oil bearing within 16 reed switches, arranged to give a stepwise resistance read-out.

SNOWPACK OBSERVATIONS

We collected basic snowpit data on a variety of avalanche paths according to procedures laid down in UNESCO/IAHS/WMO (1970). We defined the stratigraphy of the snowpack and for each layer we recorded the depth from the snow surface, snow hardness, crystal type and size, stage of metamorphism of the snow, snow density, and temperature. By developing a portable air permeability device we could measure the air permeability of snow and get an indication of snow texture and hence strength (Conway and Abrahamson, 1983a). We also made an estimation of the snowpack stability by developing a shear strength test to test for weak layers in the snowpack. By determining the gravitational loading and measuring the slope angle we could compute a local shear index for the snowpack (Conway and Abrahamson, 1983b).

WEATHER AND SNOWPACK DATA

(1) 1980 Winter

Some snowpit data that we collected around the same area during the 1980 winter are also included in this report and are listed in appendix 1A.

In early July, a four day stormy westerly period resulted in 1.61 m of new snow being deposited at a snowpole near the hut. This resulted in many large slab avalanches and one almost 2 m deep occurred on the Nosedive slope (S aspect) (see figure 3). The wind-stratified slab consisted of wind crusts and graupel and was sliding on a layer of buried recrystallised snow (see appendix 1A). We observed similar stratigraphy on the Murchison headwall the following day

(4 July 1980) and although that slope had not avalanched, other slopes in the vicinity had fractured.

Another storm cycle in early August from the SW deposited about 0.58 m of snow over two days and was associated with strong winds. Although we did observe some loose avalanches on steep slopes, no slab avalanches occurred in the area. Two pits dug on different slopes (Hochstetter Dom shoulder (9/8/80), and the Nosedive (10/8/80)) were again typified by wind crusts and graupel clusters with no good shear layers (appendix 1A).

Many new slab avalanches occurred on steep slopes after a storm during 10 - 14 August 1980. The storm started with very strong W - SW winds which eroded 0.15 m of snow away from the snowpole. Strong W winds continued through the storm depositing 0.91 m of snow at the pole near the hut and 1.30 m on the Alymer traverse (S aspect). A snowpit on the Alymer traverse (14/4/80) indicated a layer of 2 - 4 mm graupel conglomerates that fell out of the pit wall at a depth of about 0.5 m (appendix 1A).

More snow from the NW fell between 15 - 16 August and was followed by a strong cold S storm on 17 August. A total of 0.70 m of snow was deposited near the hut and we observed numerous avalanches and signs of avalanches that had been subsequently covered with further snow. A pit on the Murchison headwall (17/8/80) again was typified by stratified graupel layers with few sliding layers. However, a fracture triggered artificially (by a skiier on the Cornicewall (18/8/80)) was about 0.31 m deep and consisted of the S deposited snow sliding on top of the NW deposited snows (appendix 1A).

The data we collected during 1980 was not continuous but the periods that we did record were typified by snowfalls associated with strong winds resulting in stratified snowpits often containing layers of large graupel conglomerates. Measured snow temperatures varied from -3.5°C to -19.5°C, and new snow densities varied from 110 to 295 kg/m^3.

(2) 1981 Winter

Weather and snowpit data are not continuous for the 1981 season either, but where records are available they are summarised if figure 4 and appendix 1B respectively.

Although we did not record weather data prior to the profile described from the Cornicewall (11/9/81) it did show a weak layer at about 1.30 m consisting of 1 - 2 mm recrystallised snow (appendix 1B).

Strong SW winds and a total of 0.53 m of new snow at the hut snowpole deposited varying depths of snow at different locations between 12 - 15 September 1981. Many avalanches had been subsequently covered by further snowfall, but many were still visible on steep slopes in the area and cornice breaks triggered another slide on the Cornicewall (15/9/81) (figure 5). A pit dug on the Nosedive (13/9/81) just above a fracture that had been triggered by an iceblock revealed that a weak layer of conglomerates and needles at 0.43 m deposited during the storm, provided the sliding layer (appendix 1B). A similar crystal structure was also evident on the Cornicewall (14/9/81) at 0.44 m and this fractured the following day when part of the cornice broke and triggered the avalanche (appendix 1B). A pit on the Murchison headwall (15/9/81) also showed a series of windcrusts with weaker layers in between; the weakest being at 0.66 m. Some slab avalanches had occurred on the steep slopes to each side of the headwall, but we found the actual headwall to be relatively stable.

Strong W to NW winds continued and considerable redistribution of snow occurred through at least until early October when our records finished. The winds caused dunes and scouring on slopes and a total of 1.16 m of snow accumulated at the hut pole between 23 September and 3 October 1981. We observed avalanches during brief clearances during the storm on steep slopes and considerable avalanche activity at lower altitudes was observed by the Mt Cook Park staff on 29 September. These were probably the start of the spring avalanche cycle with rain lubricating the snows. Although the Murchison headwall (East aspect) did not appear to have avalanched by 28 September, a pit in the area (appendix 1B) indicated considerable instability due to a weak shear layer at about 1.14 m. The sliding layer consisted of a thin layer of very soft partially metamorphosed snow mixed with graupel up to 3 mm in diameter. On the Nosedive the following day (S aspect) the upper snows were also wind stratified graupel and partially metamorphosed snow with a weak layer at 0.43 m of only slightly metamorphosed snow which was very soft.

As with snow observed during the 1980 season, the snowpits dug in 1981 were typified by considerable wind stratification and relatively stiff layers of

graupel conglomerates with weak snows in between providing the shear layers. The weak layers we generally associated with periods during the storm cycle when temperatures may have been lower, causing a change in precipitated crystal type.

We think these periods were also associated with times of lower windspeeds. Measured snow temperatures varied from -1.4°C to -11°C, and new snow densities varied from 90 to 250 kg/m^3.

(3) 1982 Winter

Weather and snowpit data for the 1982 winter are summarised in figure 6 and appendix 1C respectively. During this season we placed snowpoles on the upper Tasman neve and near the top of the Nosedive in an effort to compare accumulation in those areas with that at the hut snowpole. A summary of this data is shown in table 1 and figure 7. The windrun which we read daily from the cup counter is also included in the summary, together with the general direction of the storm.

A W storm on June 2 (probably with some rain as well as snow), caused a very hard ice layer at least 100 mm thick over the upper Tasman region. A S snow with light winds followed on 3 June, depositing 0.1 - 0.2 m of low density snow (about 150 kg/m^3) on many slopes, although some slopes did not accumulate this snow and the ice was still exposed. For the following 16 days an intense anticyclone remained slow moving over the country and resulted in fine weather. During this time the S deposited snow developed a slight crust and below this crust the crystals developed facets and grew up to 3 mm in diameter. We measured temperature gradients of up to 12°C/m in the snowpack and measured air permeability increases from 33 x 10^{-5} m^4 N^{-1} s^{-1} to 95 x 10^{-5} m^4 N^{-1} s^{-1} (Conway and Abrahamson 1983a). A W airstream between 21 - 22 June deposited 0.88 m of new snow at the Tasman Saddle hut snowpole, and was associated with strong winds (30 - 40 knots) and considerable wind transport of snow. We recorded approximately 30 avalanches on 23 June in the area, mainly on the S aspect slopes where the temperature gradient crystals were most prevalent. Many of the avalanches were covered by subsequent snow indicating they had released early in the storm cycle. Appendix 1C lists snowpit analyses done sometime after the initial S snow had deposited (Nosedive 10/6/82) and then after the slope had fractured and had then been covered with more snow (Nosedive 23/6/82). This pit and excavations around the crownwall, showed that the slope had avalanched after about 0.30 m of snow had accumulated above the [illegible] subsequent snowfall amounted to about 0.47 m.

The W cycle was followed by a S storm on the 25 June and this was characterised by a high humidity (up to 150 mm of rime grew on metal objects near the hut). Considerable wind transport also occurred during this storm which deposited 0.35 m of new snow at the hut snowpole. We recorded about 15 avalanches again mainly on slopes with a S aspect. One such fracture was on the Hochstetter Dom shoulder and this was about 600 m wide and 400 m long, again sliding on the recrystallised snow at a depth of about 0.95 m (see appendix 1C and figure 8).

A further period of fine cold weather with no precipitation occurred between June 26 until July 12. Although this caused strong temperature gradients in the snowpack (see Nosedive 3/7/82 in appendix 1C), the upper snow density was high (about 270 kg/m^3) and the crystal structure and air permeability of the snow did not change as dramatically as the period in June, (Conway and Abrahamson 1983a). A snow pit during this period on a N facing slope of Able (4/7/82) showed that the area had been subject to considerable wind erosion and very little accumulation. Some large faceted crystals (up to 2 mm in diameter) had developed early in the season and had been buried only to 0.25 m by subsequent snowfalls. The lack of loading on this slope would have been the reason for it not failing during the June storm cycles.

W to SW winds, often very strong (we recorded a mean daily windspeed of 11 m s^{-1} on July 18 1982) caused considerable wind transport of snow between July 12 and July 22. A total of 0.93 m of new snow accumulated at the hut measuring pole but larger depths accumulated on lee slopes. We observed a total of 39 avalanches in the area at various times during the storm, and these were generally on E or NE aspect slopes. We worked on one fracture (figure 9) which had been ski released on the Cornicewall (13/7/82) and found considerable variation in the depth of fracture across the crownwall (0.32 - 0.54 m) and also variations in the basal shear strength of the slab (see Conway and Abrahamson 1983b). We did not observe an obvious stratigraphic change at the shear plane and the shearing appeared to have occurred within a very soft layer of new deposited snow (Crystal types included columns, capped columns, stellars, plates and needles - see appendix 1C).

Appendix 1C includes further snowpack analyses that we made on the Cornicewall during the storm period (Cornicewall 15/7/82; Cornicewall 19/7/82; Cornicewall 20/7/82). We found large flaws and cracks which were up to 500 mm long by

50 mm wide in the snowpack near the profile of 15/7/82. We attributed these flaws to a partial failure of the snowpack (figure 10). The profile that we analysed on the 19/7/82 was near a small sluff which we caused by kicking a cornice onto the slope. The fracture was small and the bed surface consisted of medium-hard and well bonded snow, and the shear plane consisted of some very soft wind deposited snow (appendix 1C). Again we measured considerable variation in the depth of the crownwall. The pit dug on the 20/7/82 contained about 0.18 m of very soft snow which was tending to sluff as a loose slide rather than forming a slab. We measured very low shear strengths (80 N/m^2) and low tensile strengths of this snow (320 N/m^2), in accord with the loose slide behaviour (Conway and Abrahamson 1983b).

More fine cold weather followed the storm until 30 July when another NW air-stream crossed the region depositing a total of 1.20 m of new snow at the hut snowpole by August 2. This snowfall was again associated with strong winds (mean daily average of 9.7 m/s on August 1) and was often heavily rimed conglomerates of graupel. Wind redistribution of snow continued until August 6 and many avalanches occurred, but only on very steep E and N slopes in the area. A snowpit dug on the Nosedive (6/8/82) showed the typical well bonded nature of the snowpack. A clearance of four days was followed by 0.31 m of new snow from the W on August 10, but with no new visible avalanches. A snowpit dug on the Cornicewall (11/8/82) did not have any good shear planes.

Weather and snowpit observations were intermittent during the rest of August and early September but the period was typified by strong W winds and further snowfalls. One pit that we dug on the Cornicewall (6/9/82) indicated that the shear strength of the surface snow was low (about 300 N/m^2) but generally the snowpack was well bonded below this layer (see appendix 1C). On 7 September an icefall triggered a large slab on Hochstetter Dom, and analysis of this fracture showed that the slab was sliding on a melt-freeze crust that varied from 0.57 m to 0.84 m in depth.

Futher strong W or SW winds and 0.60 m of new snow on 7 - 8 September produced only a few sluffs on some slopes. One pit that we dug on Hochstetter Dom (9/9/82) again showed some low density snow at the surface and well bonded layers deeper in the snowpack and no good shear planes.

Some radiation recrystallised snow developed near the surface during a fine period between 14 - 16 September and this was followed by a period of strong W winds (we recorded a mean daily windspeed of 14.0 $m\ s^{-1}$ on 19.9.82) and 0.45 m of new snow was deposited near the hut. On the Cornicewall (19/9/82) up to 1.25 m of new snow was deposited and a large hard slab avalanche occurred at this depth (figures 11a, 11b, 11c). Similar fractures also occurred on Alymer col (figure 12) and we observed avalanches that had been subsequently covered by drifting snow on many other slopes. We dug a series of pits up the flankwall of the fracture on the Cornicewall (19/9/82) and measured variable fracture depths (in some places a double fracture had occurred) and considerable variation of shear strength at the weak layer (see appendix 1C and Conway and Abrahamson, 1983).

During the 1982 season we measured snow temperatures varying from -1.0°C to -19.9°C and new snow densities that varied from 60 - 280 kg/m^3. Figure 7 shows the effects of wind in redistributing snow during 1982, and often this redistribution not only occurred at times of precipitation, but also at times of strong winds and no precipitation. As well as causing variation in snow depth this also often caused scouring on some slopes and duning of snow on other slopes (see figure 13, 14).

RESULTS FROM THE AUTOMATIC WEATHER STATION

The data logger (or alternatively the tape recorder used to interrogate the data logger) required an interface so that the data could be transferred to the Chemical and Process Engineering Department's computer. A suitable programme incorporating the instrument calibrations was used to calculate and print the weather information. The programme used, and a typical set of data are shown in appendix II.

DISCUSSION

(1) Weather Instruments

The Stevenson screen, and especially the thermograph were prone to filling with drifting snow. Snow that had blown into the screen and around the thermometers caused erroneous readings about 2% of the times measured, and often made the

thermograph inoperable. We have not yet found a suitable screen to protect this instrument and to enable it to function successfully. We suspected that vibrations of the screen during windy periods may have altered the maximum and/or minimum temperature readings on several occasions.

On two occasions, strong winds blew the snowpoles away. We found it difficult to find a sheltered and representative snow accumulation site close to the hut, but never the less the measurements and comparisons made at various sites (table 1 and figure 7) are useful for predicting snow depths on often avalanched slopes, given measurements near the hut.

The cup anemometers were prone to icing (this occurred in about 13% of the period June to September 1982 - see figure 2). Icing on the Lambrecht anemometer affected not only the cups and vane, but also the mechanical recording mechanism. This made it difficult to interpret daily weather data since icing of the mechanism changed the time basis of the chart.

(2) Weather Station

The design and building of the weather station was not completed until August 1982, so we have only one months data from the instrument. Periods of icing were easily recognised in the data - these were typified by periods of no wind and no wind direction change. When ice around the temperature probe melted, it caused a short circuit which caused an erroneous temperature reading. More care has since been taken to protect the temperature probe.

In an effort to protect the ultrasonic transducer we mounted it inside a plastic cone. Some care was required to have the cone of such a shape and material to prevent signals reflecting from the cone.

Some of the data from the data logger was obviously incorrect. We were uncertain whether this problem originated within the data logger memory or during the extraction of the data onto magnetic tapes. We suspected that a problem arose from the low temperatures of the tapes and we always made at least three recordings of the data in an attempt to record a correct set of data.

The cold conditions also reduced battery life considerably, and precautions were taken to ensure that we had batteries with sufficient energy to drive the instruments.

(3) Snow Measurements

A primary requirement for a slab type failure of snow is a weak basal layer (Perla, 1980), and McClung (1979) suggests that failure will occur when the rate of shearing creep in the weak layer exceeds the rate of settlement normal to the slope.

In all of our snowpits we located the weakest layer, calculated the downslope loading at this layer (by measuring the slab density and slope angle), and measured a local shear strength. These measurements enabled us to calculate a local "factor of safety" by evaluating the ratio of strength available along the potential failure surface to that required for failure to occur (Conway and Abrahamson, 1983b).

1. Weak Layers

Of nine profiles that we observed on fracture-lines, four had fractured at recrystallised snow layers and five showed that the avalanche had slid at weak layers of soft or very soft new snow. Potential sliding layers at other pits were generally layers of soft new snow which had been deposited sometime during the most recent storm. Often the weak layers were thin (about 1 mm) and we think that these may be deposited during lulls in the storm or during brief periods when the crystals being deposited are less rimed (a cooler period).

Although the snowpits often contained layers of graupel and rounded conglomerates up to 4 mm diameter, these layers were generally well bonded and did not provide layers of easy shearing.

Some of the new snow layers within some snow profiles were found to collapse when we applied only small normal forces (say 200 N/m^2), and several times we measured a decrease of shear strength at that layer after the collapse. We attributed this weakening to be associated with the change of structure of the layer after the collapse, and this sort of failure could be an important mechanism for some avalanche releases. This mechanism was only noticed on soft layers that consisted of low-density needles and/or broken stellar crystals.

We found large variations in our calculated "factor of safety" values, (we measured changes of up to 300% over 0.5 m intervals. We think these

variations were caused mainly by the depositional characteristics of blowing snow (Conway and Abrahamson 1983b). Figure 15 shows a weak layer which fluctuated in its depth below the surface snow.

2. The slabs

Slab densities of slopes that had fractured varied in the range 100 - 290 kg/m^3. The slabs often consisted of wind stratified partially metamorphosed snow and/or graupel layers.

In several cases where the surface snow had been deposited with little wind, we found the surface snow to be weak in tensile as well as shear strength and this snow released as point releases rather than slabs. This would support the concept that loose snow avalanches start in cohesionless surface layers of snow (Perla, 1980).

WIND DEPOSITION OF SNOW

Rates of loading on a snow slope may be important to assess slope stability since rapid loading can cause the rate of creep to exceed the rate of settlement in the shear layer (McClung, 1979), or cause a more brittle-like fracture at a low load compared with a ductile failure in the slab (Narita, 1980). We also think that turbulence associated with winds can cause duning as suggested by Dyunin (1967) and Kobayashi (1979), which could cause discontinuities in a shear layer.

Table 1 and figure 7 show the effects of wind on snow accumulation at various sites in the Tasman Saddle area. 87% of the precipitation recorded was during periods of SW-W-NW storms, and the Cornicewall (E aspect) can generally be considered a "lee slope". The hut stake is subject to some scouring from strong winds, and the Nosedive has a S aspect and W winds are often funnelled across the slope. Figure 7 shows that the Nosedive accumulates a similar quantity of snow to that shown at the hut stake; but the Cornicewall accumulates considerably more and the difference generally increases as the snowfall depth increases.

In his review, Schmidt (1982) mentions that threshold windspeeds determine transport rates and that cohesive forces at the snow surface determine the

threshold windspeeds. Although we have not collected any detailed data from the Tasman Saddle region, redistribution of snow was common on days when the mean daily windspeed exceeded 3 m s^{-1}.

AVALANCHE OCCURRENCE

Because snow accumulation from precipitation and/or drifting may be high (up to 3 m during a storm), we often found it difficult to determine the number of avalanches that occurred during the storm, since often the high amounts of deposition would obscure the avalanches. The number of avalanches recorded was therefore a conservative estimate.

Although most instability in the snowpack was related to periods of snowfall or periods of wind redistribution of snow, some periods of precipitation did not produce avalanches in the area (see figures 3 and 6). One such period in early September 1982 was typified by strong W or NW winds (mean windspeed between 1 - 11/9/82 was 6.2 m/s) and high precipitation (a total of 2.20 m of snow was deposited at the hut snowstake). Although avalanching was recorded at lower altitudes by Mt Cook Park staff, only one slab avalanche (triggered by an iceblock collapse) occurred in the Tasman Saddle area. As previously discussed conditions that are necessary for slab avalanching include a weak shear layer and sufficient loading above this weak layer. Analysis of the snowpack profile showed that although the storm had deposited a dense and wind stratified load on the slope, no weak layers had been deposited at any time during the storm and none existed in the snowpack prior to the storm. These factors would inhibit avalanche formation.

More frequent weather measurements would be required to determine conditions within the storm that might cause a weak layer to develop, but the present data shows that we could expect to observe avalanches in the area after a period of precipitation about 60% of the time.

CONCLUSIONS

Weather data and snowpack information collected at Tasman Saddle (the highest weather station in New Zealand) has provided a useful basis for the Mt Cook

avalanche forecast scheme, and also in understanding mountain weather and snowpack conditions. More frequent and regular localised measurements are required to facilitate understanding of which meteorological conditions can result in unstable snowpacks, and the remote weather station can fulfill this need.

In the future, we plan to convert the system to enable interrogation of the data by VHF radio. This would enable Mt Cook Park staff to access the data at selected times through the day.

ACKNOWLEDGEMENTS

Financial support for the study came from the Department of Lands and Survey (Wellington, New Zealand), University of Canterbury (Christchurch, New Zealand), Mountain Safety Council of New Zealand, and Mt Hutt Ski Company. Mt Cook Airlines Company provided aircraft access to the field area, and the assistance of Mt Cook National Park Staff with the field experiments was invaluable. The New Zealand Meteorological Office provided the weather instruments. The Department of Chemical and Process Engineering (University of Canterbury) sponsored the project and helped develop the concepts and test equipment for the project.

REFERENCES

Burrows, C.J.: (1973) "Studies on some glacial moraines in New Zealand", N.Z. Journal of Geology and Geophysics, 16, p 831-855.

Conway, H. and Abrahamson, J.: (1983a) (in preparation) "Air permeability as a textural indicator of snow", (to be submitted to Journal of Glaciology).

Conway, H. and Abrahamson, J.: (1983b) (in preparation) "Snow stability index", (to be submitted to Journal of Glaciology).

Dyunin, A.K.: (1967) "Fundamentals of the mechanics of snow storms", Physics of Snow and Ice, Vol. 1, Part 2, (H Oura, ed.), p 1065-1073, Inst. of Low Temp. Sci., Hokkaido Univ., Sapporo, Japan.

Irwin, C.S.: (1983) "A report on the Mt Cook avalanche hazard forecasting scheme 1982", unpublished report to Lands and Survey Department, New Zealand.

Kobayashi, S.: (1979) "Studies on interaction between wind and dry snow surface", Contrib. Inst. of Low Temp. Sci., Hokkaido Univ., Ser. A, No. 29, p 1-64.

McClung, D.M.: (1979) "Shear fracture precipitated by strain softening as a mechanism of dry slab release", Journal of Geophysical Research, Vol. 84, No. B7, P 3519-3526.

Narita, H.: (1980) "Mechanical behaviour and structure of snow under uniaxial tensile stress", Journal of Glaciology, Vol. 26, No. 94, P 275-282.

Perla, R.I.: (1980) "Avalanche release, motion and impact", Dynamics of Snow and Ice Masses, (S. Colbeck, ed.), Chapter 7, p 397-462, Academic, New York.

Schmidt, R.A.: (1982) "Properties of blowing snow", Reviews of Geophysics and Space Physics, Vol. 20, No. 1, p 39-44.

UNESCO/IAHS/WMO: (1970) "Seasonal snow cover", United Nations Educational, Scientific and Cultural Organisation, Paris, Technical Papers in Hydrology, No. 2, 38 p.

LIST OF FIGURE CAPTIONS

FIGURE 1: A sketch map of the Upper Tasman Glacier.

FIGURE 2: (a) Riming on the anemometer.
(b) Riming on the Stevenson screen.

FIGURE 3: Stratigraphy analysis of a 2 m crownwall on the Nosedive slope, July 3, 1980.

FIGURE 4: Meteorological data and avalanche occurrence data collected at the Tasman Saddle area, 1981.

FIGURE 5: Cornice triggered slab on September 15, 1981.

FIGURE 6: Meteorological data and avalanche occurrence data collected at the Tasman Saddle area, 1982.

FIGURE 7: Comparison of snow accumulation data at the hut with data on the Nosedive pole, Nosedive slope, and Cornicewall slope.

FIGURE 8a: Hochstetter Dom crownwall, June 26, 1982.

FIGURE 8b: Aerial photograph of Hochstetter Dom fracture of 26 June, 1982.

FIGURE 9: Statigraphy analysis of a ski released avalanche on the Cornicewall July 13, 1982.

FIGURE 10a/b: Cracks in the snowpack observed on the Cornicewall July 15, 1982 due to partial slope failure.

FIGURE 11a: Partially drifted-over crownwall on the Cornicewall slope, 19 September, 1982.

FIGURE 11b: Northern flankwall of Cornicewall fracture, 19 September 1982.

FIGURE 11c: Shear strength analysis using a strain gauge on the Cornicewall fracture of 19 September 1982.

FIGURE 12: Fracture on Alymer Col, September 19, 1982.

FIGURE 13: Strong winds often caused redistribution of snow.

FIGURE 14: Periods of strong winds often caused scouring and duning of snows in the area.

FIGURE 15: A weak layer (marked with matches) which fluctuated in its depth below the surface snow.

FIGURE 16: The remote weather station. The Tasman data logger is mounted on a tripod leg; temperature, windspeed and direction, and snow depth instruments are mounted at the top of the tripod.

FIGURE 17: A typical computer print-out from the remote weather station.

TABLE I

DATE	SNOW ACCUMULATION (meters)				WIND		COMMENTS
	HUT POLE	CORNICE PITS	NOSEDIVE POLE	NOSEDIVE PITS	MEAN DAILY SPEED m/s	DIRECTION AT 6.15 am	
8/6/82	.14	-	.19	.23	-	S	scouring evident on some slopes
21-23/6/82	.88	2.16	.79	.78	6.7	W	many avalanches occurred after this storm
25-26/6/82	.35	-	.09	-	-	S	anemometer rimed but strong S winds scoured S aspects
13/7/82	.32	.58	-	-	6.0	SW	irregular snow surface and lots of drifting snow
13-15/7/82	.28	.54	-	-	6.0	SW	considerable wind transport of snow
12-15/7/82	.60	1.12	.43	.45	6.0	SW	-
3/8/82	1.20	-	1.00	-	-	SW	-
5/8/82	.15	-	.15	.18	7.2	SW	many point releases had occurred
11/8/82	.31	.25	-	-	5.7	W	a well bonded snow pack
7/9/82	.25	-	.18	-	4.8	W	considerable drift of snow
7-11/9/82	.83	-	.90	-	7.7	W	a well bonded and wind deposited snow pack
19/9/82	.43	1.25	.30	-	9.4	W	wind deposited hard slabs occurred on many slopes

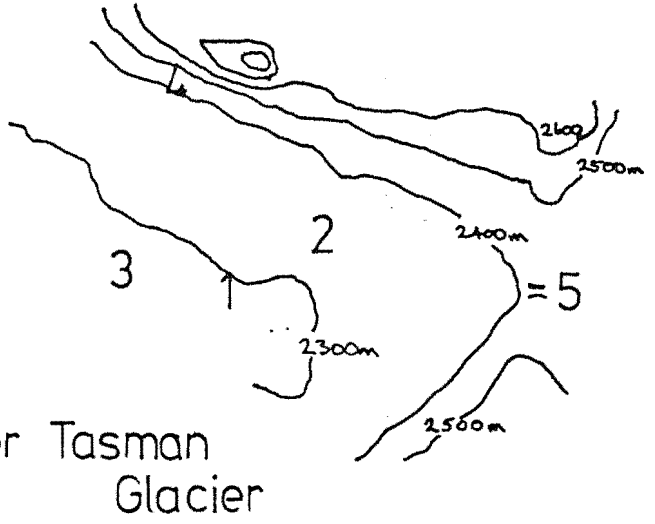

1 Hut, snowpole and screen.
2 Cornicewall slope
3 Nosedive pole and nosedive slope
4 Hochstetter Dom slope
5 Murchison Headwall slope

fig.1

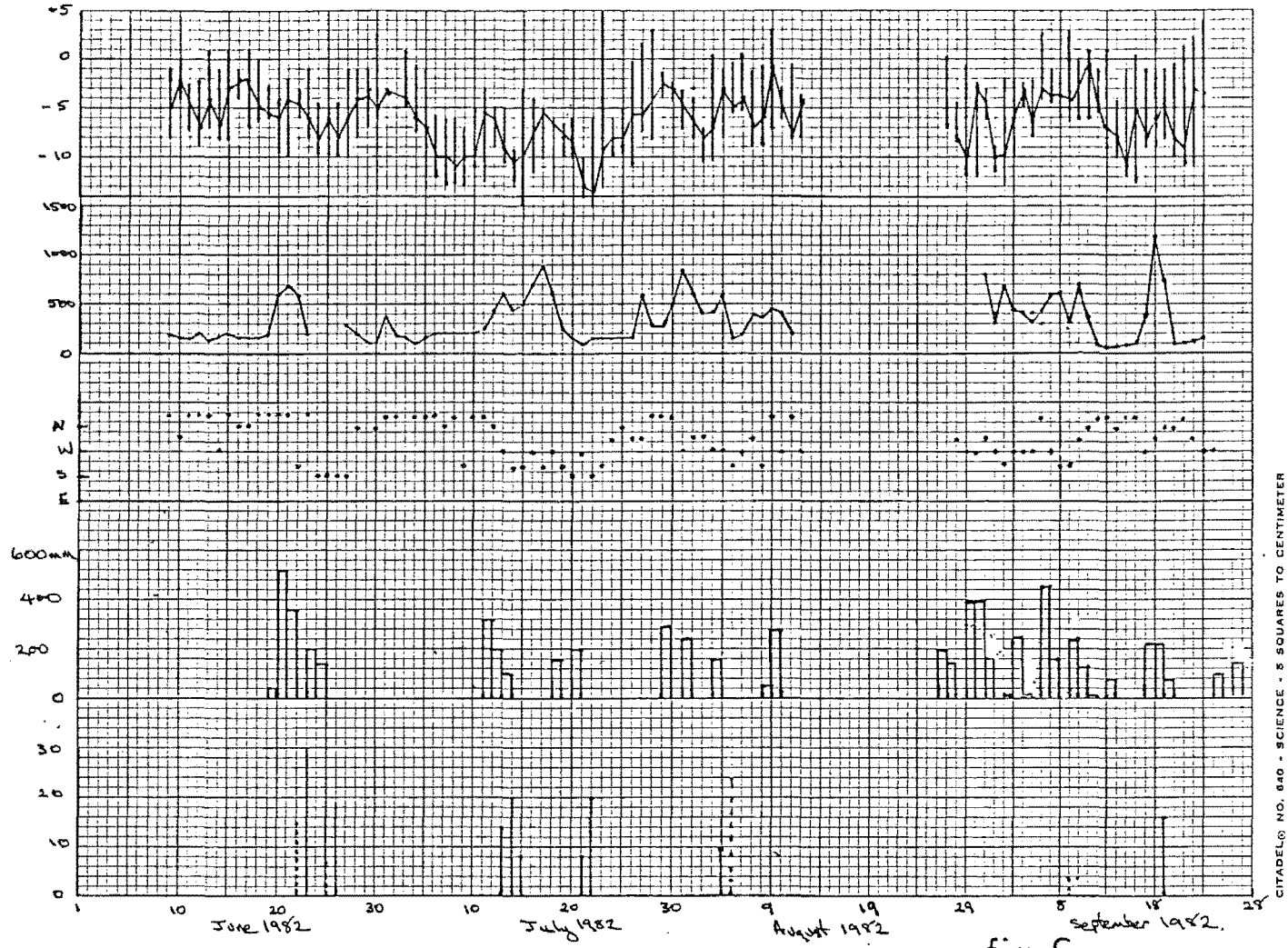
+5
0
-5
-10
1500
1000
500
0
N
W
S
E
600mm
400
200
0
30
20
10
0
1
10
20
30
10
20
30
9
19
29
8
18
28
June 1982
July 1982
August 1982
September 1982.
CITADEL® NO. 640 - SCIENCE - 5 SQUARES TO CENTIMETER

fig. 6

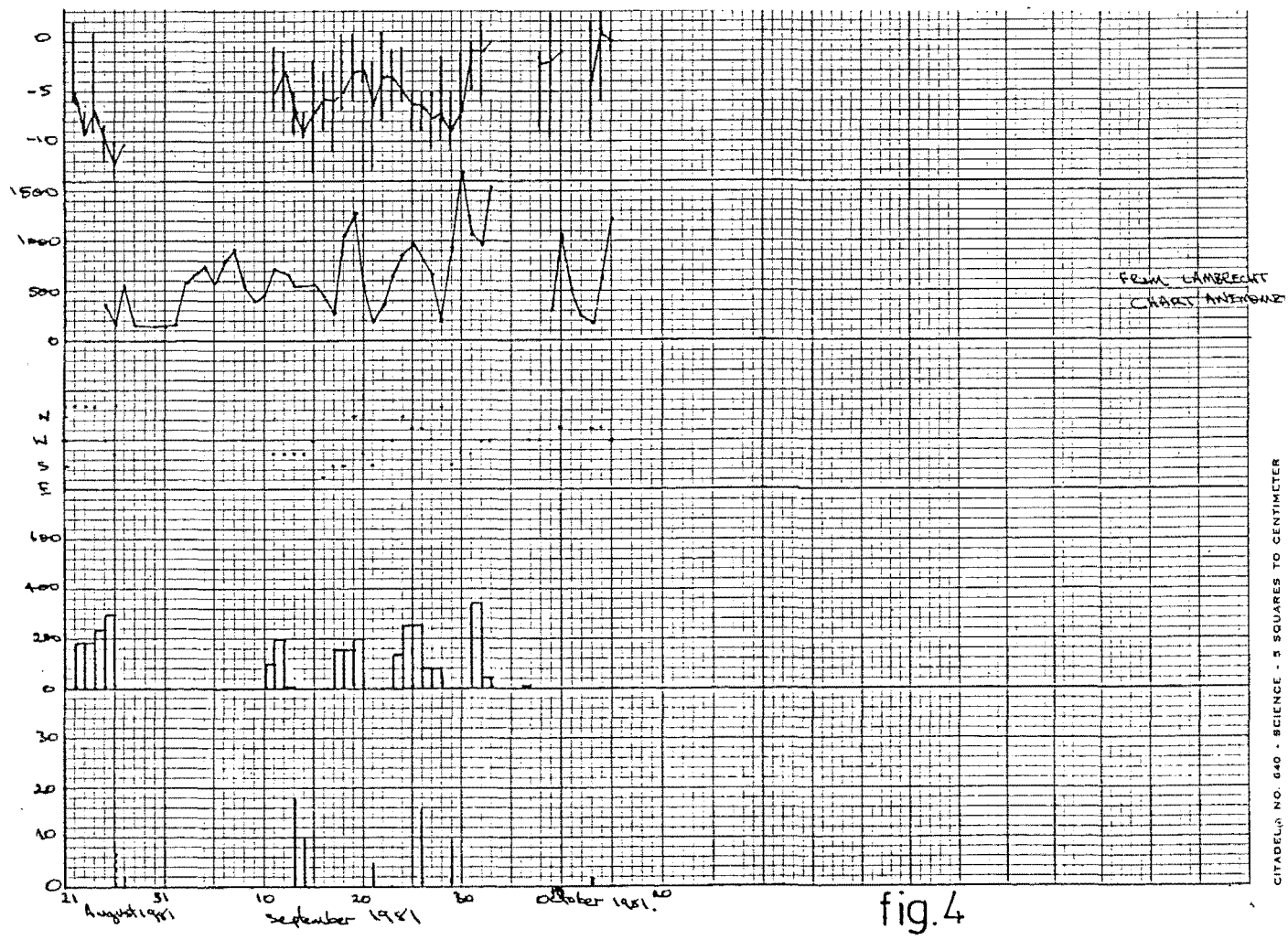
0
-5
-10
1500
1000
500
0
FROM CAMBRECHT
CHART ANTENNE
N
W
S
E
600
400
200
0
30
20
10
0
21
31
10
20
30
40
August 1981
September 1981
October 1981.
CITADEL® NO. 640 - SCIENCE - 5 SQUARES TO CENTIMETER

fig. 4

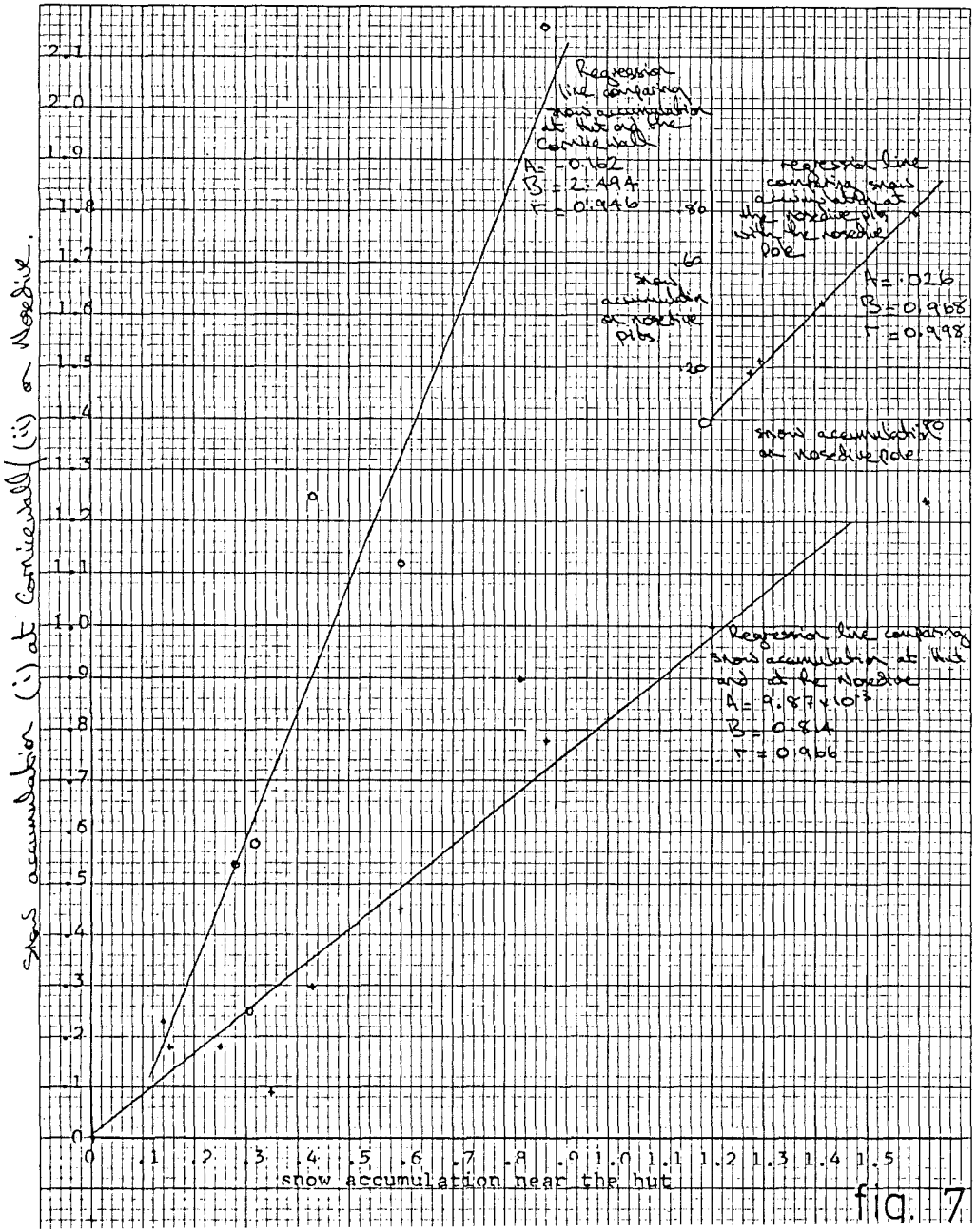

fig. 7

NOSEDIVE FRACTURE (3/7/80)

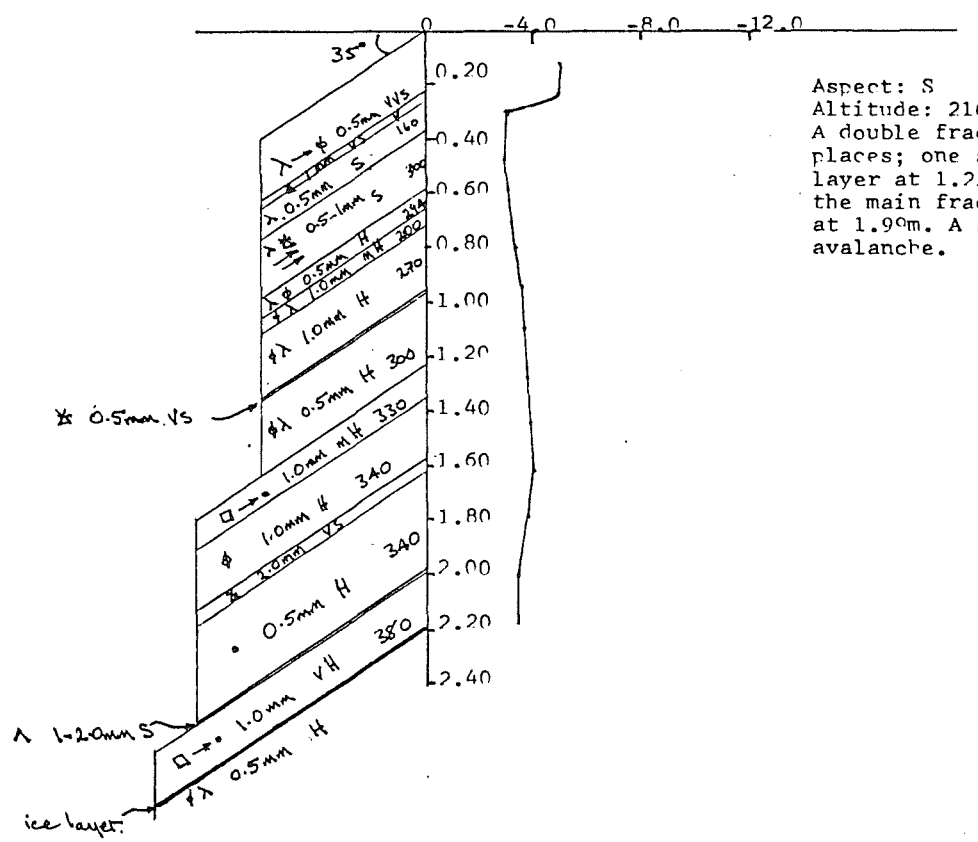

Aspect: S
Altitude: 2160m
A double fracture in places; one sliding layer at 1.23m, and the main fracture wa at 1.90m. A size 3-4 avalanche.

MURCHISON HEADWALL (4 /7/80)

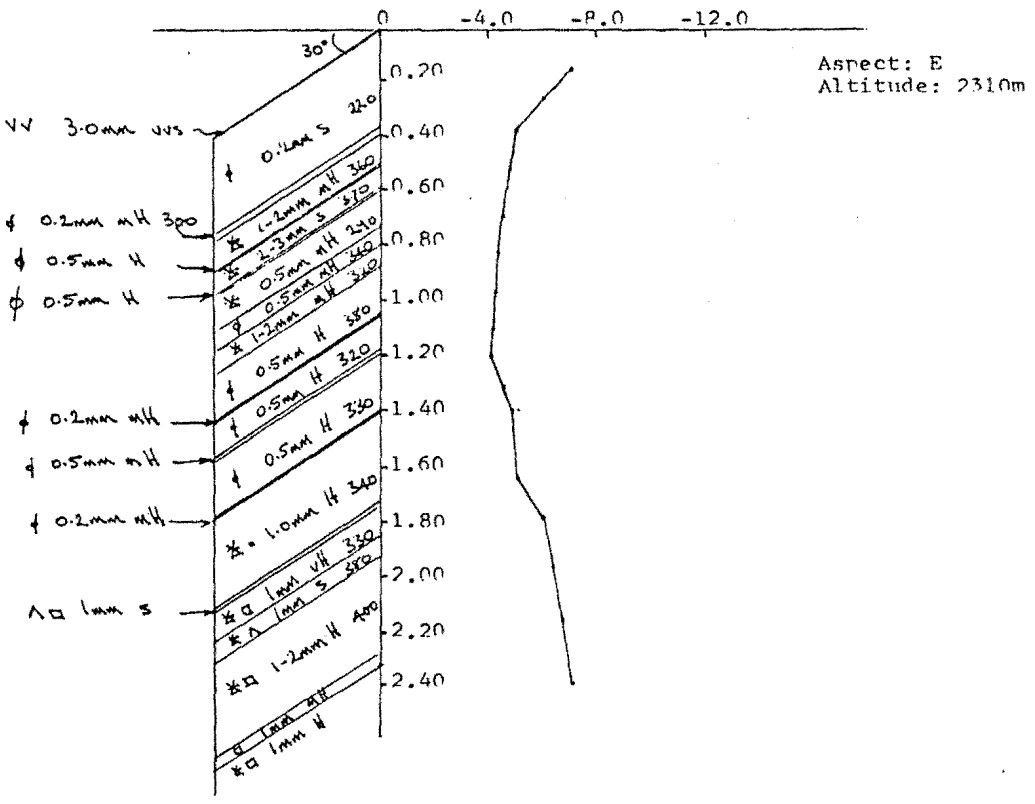

HOCHSTETTER DOM SHOULDER (9/8/80).

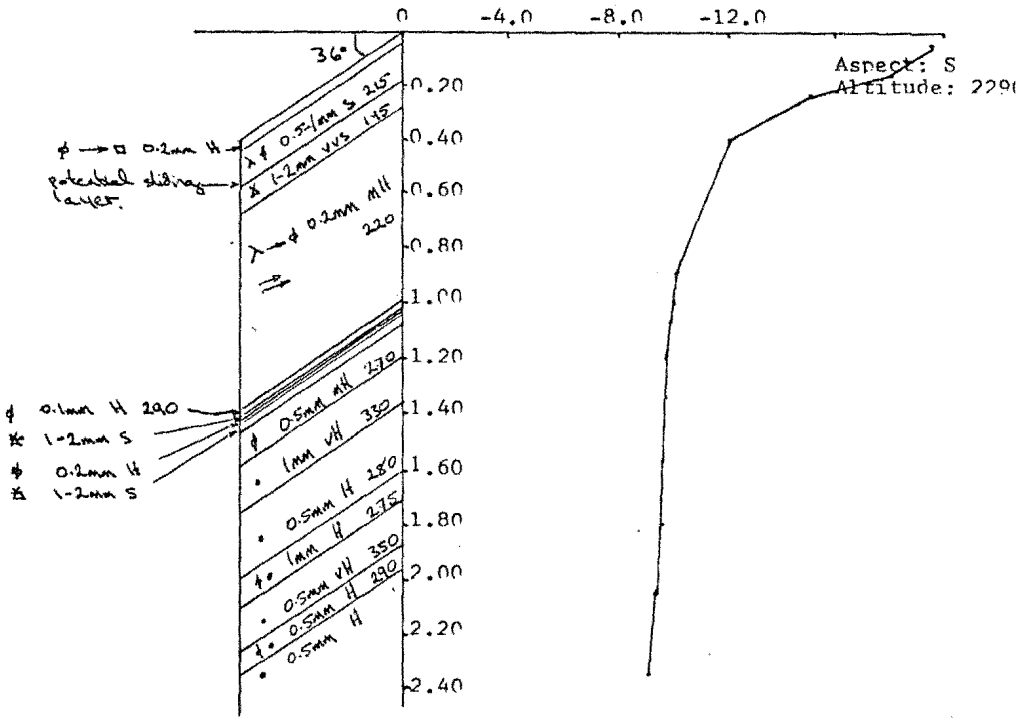

NOSEDIVE (10/8/80)

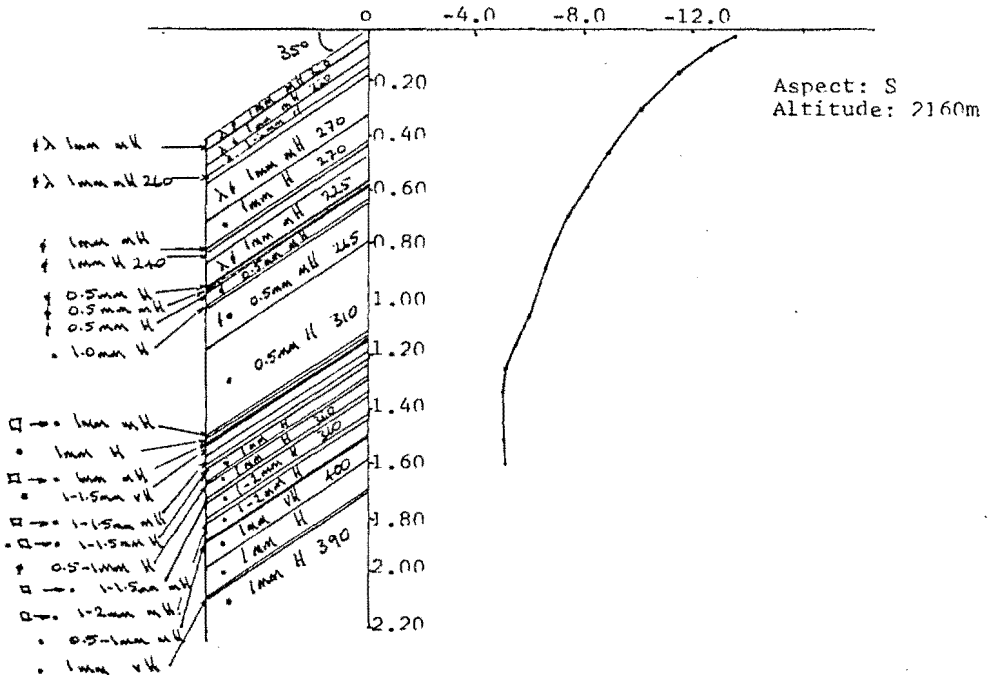

ALYMER TRAVERSE (14/8/80)

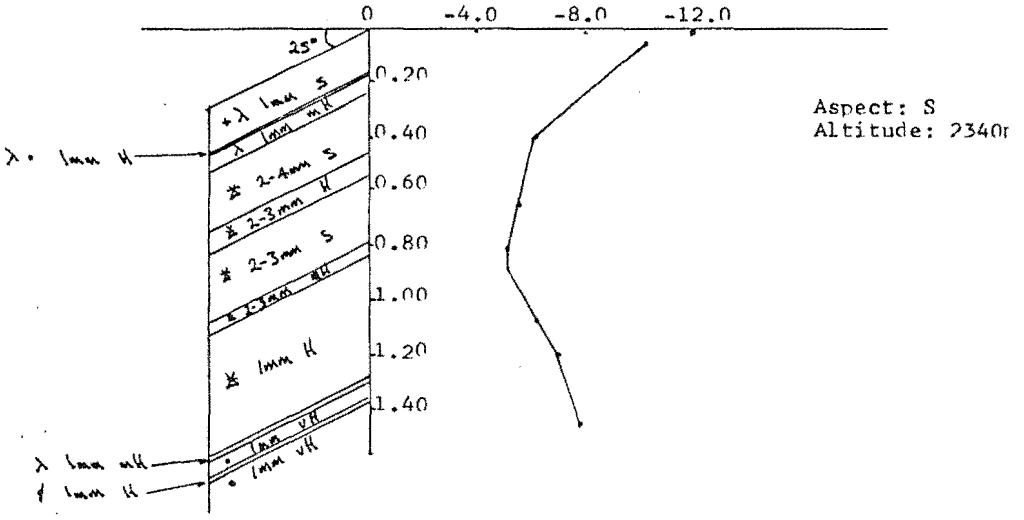

CORNICEWALL FRACTURE (18/8/80)

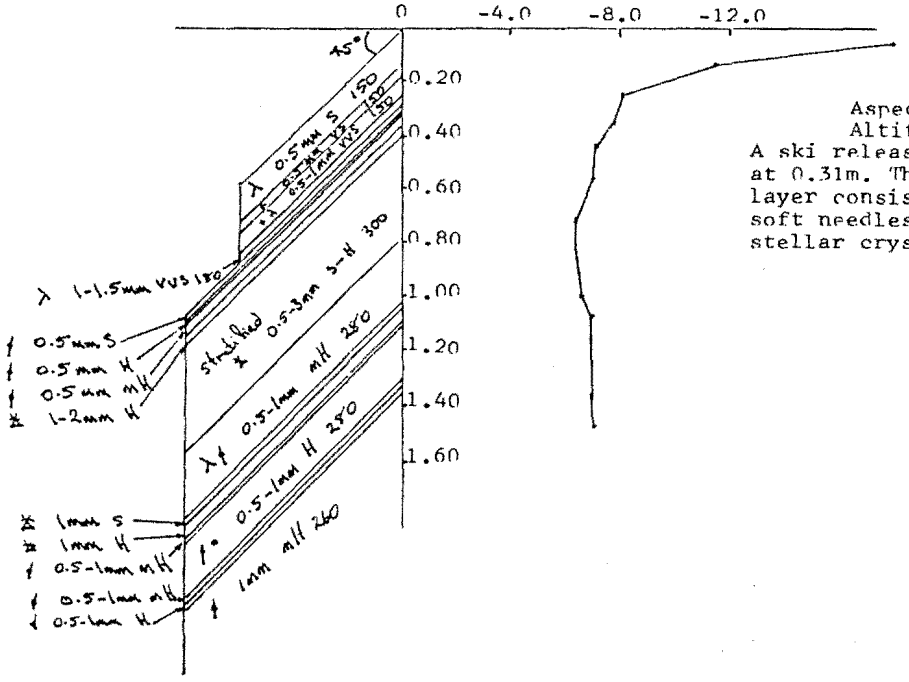

Aspect: SE
Altitude: 2310m
A ski released fracture at 0.31m. The sliding layer consisted of very soft needles and broken stellar crystals.

MURCHISON HEADWALL (17/8/80)

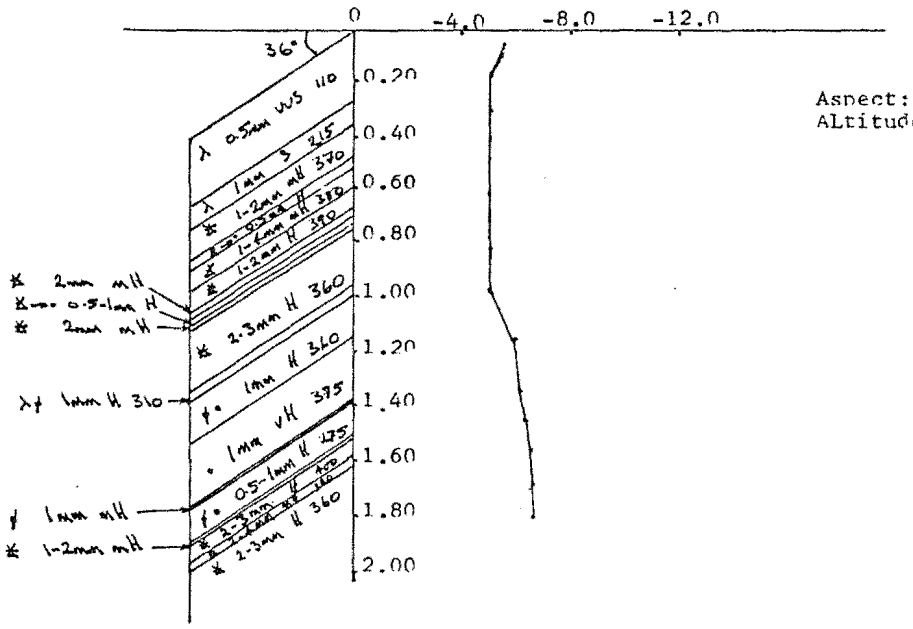

Aspect: E
ALtitude: 2310m

CORNICEWALL (11/9/81)

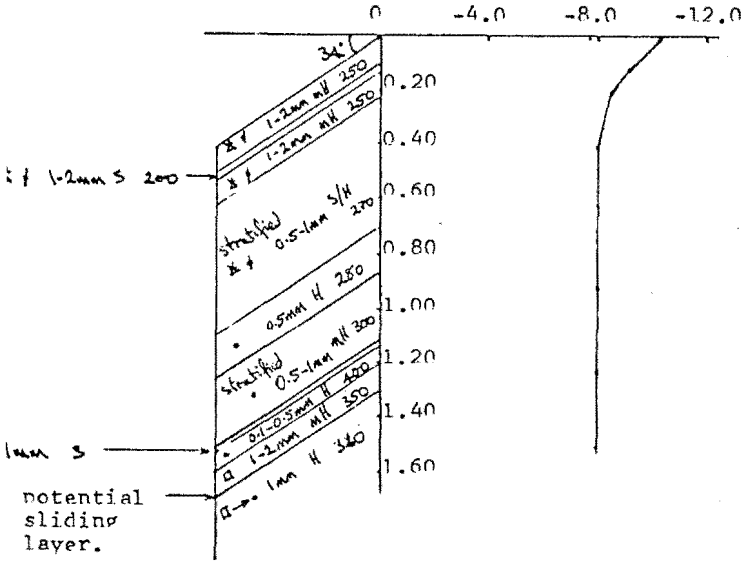

Aspect: SE
Altitude: 2310m

CORNICEWALL (14/9/81)

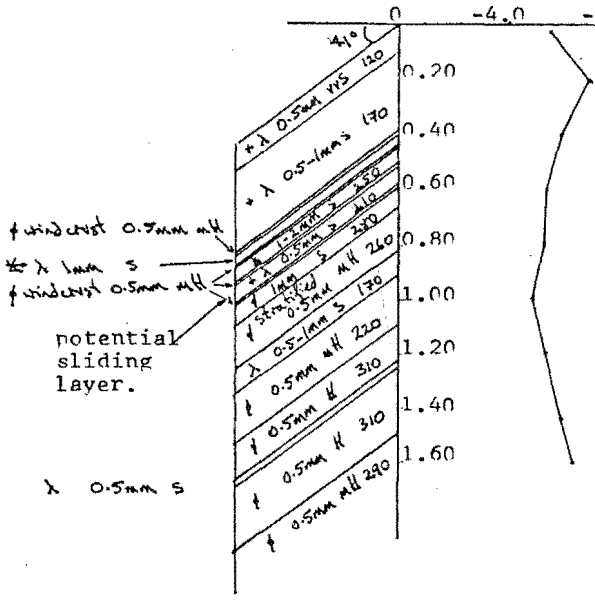

Aspect: SE
Altitude: 2310m
On 15 September part of a cornice fell about 50m from this pit and triggered an avalanche that slid to a depth of 0.60m.

NOSELIVE FRACTURE (13/9/81)

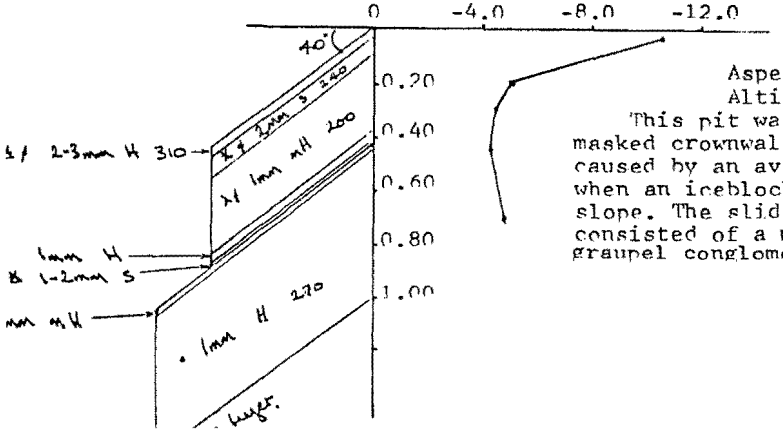

Aspect: S
Altitude: 2160m
This pit was dug 1m above a masked crownwall which had been caused by an avalanche occurring when an iceblock fell onto the slope. The sliding layer at 0.43m consisted of a mixture of graupel conglomerates and needles.

MURCHISON HEADWALL(15/9/81)

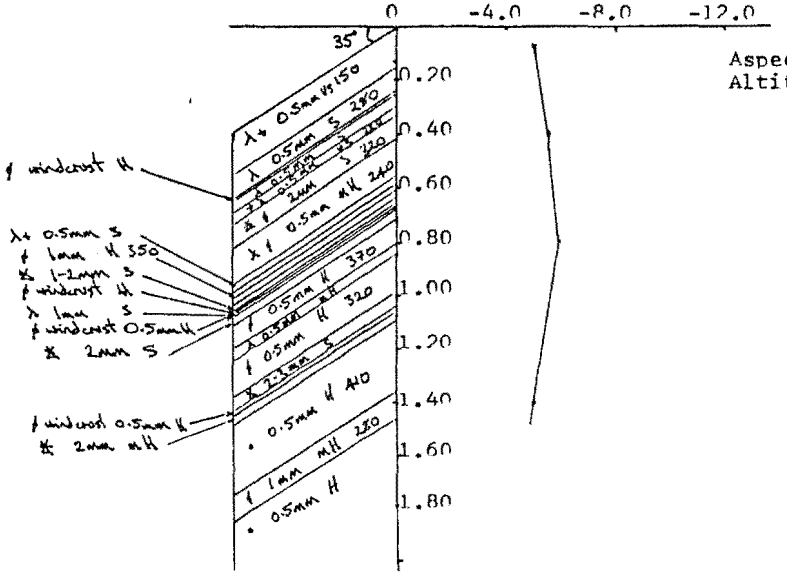

Aspect: E
Altitude:2310m

CORNICEWALL (14/9/81)

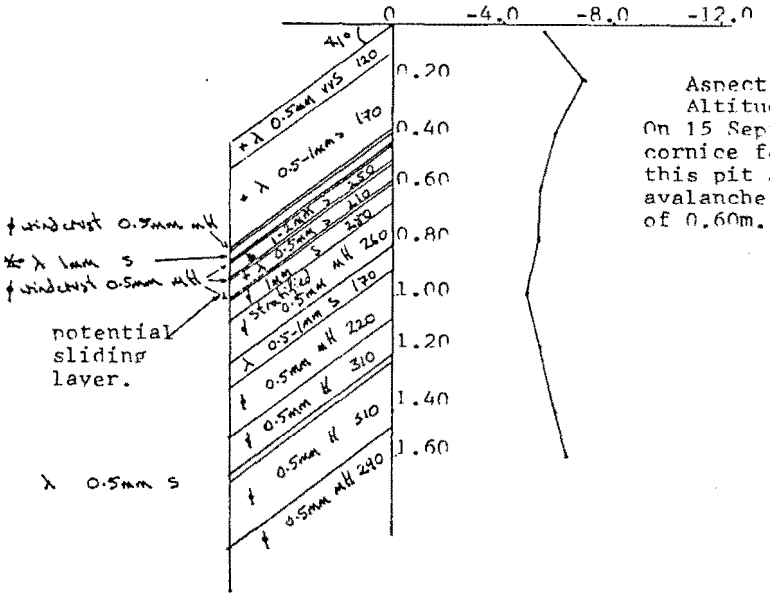

Aspect: SE
Altitude: 2310m
On 15 September part of a cornice fell about 50m from this pit and triggered an avalanche that slid to a depth of 0.60m.

CORNICEWALL (11/9/81)

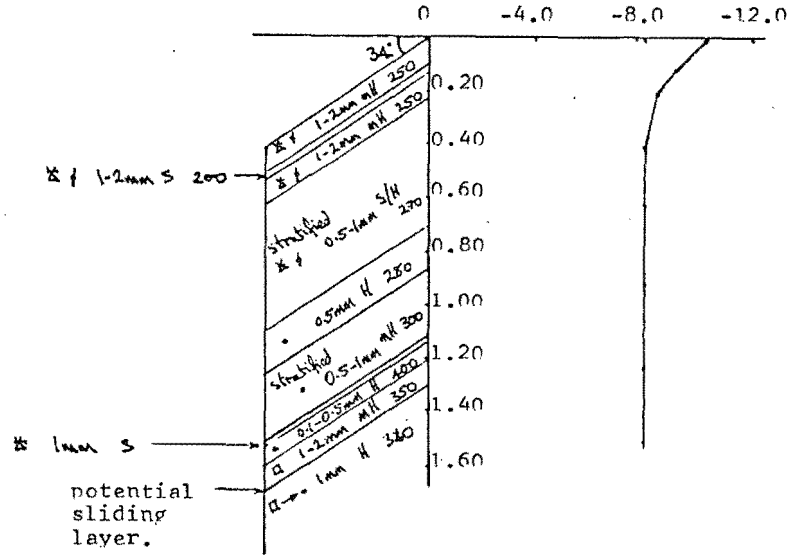

Aspect: SE
Altitude: 2310m

MURCHISON HEADWALL(15/9/81)

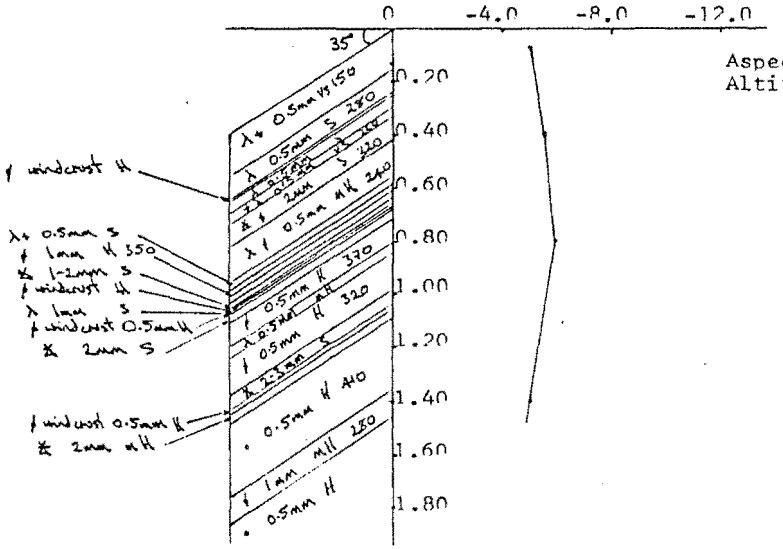

Aspect: E
Altitude:2310m

NOSEDIVE FRACTURE (13/9/81)

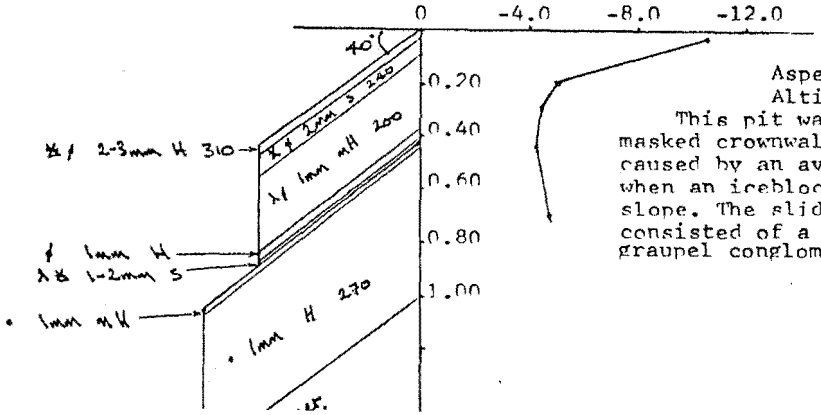

Aspect: S
Altitude: 2160m
This pit was dug 1m above a masked crownwall which had been caused by an avalanche occurring when an iceblock fell onto the slope. The sliding layer at 0.43m consisted of a mixture of graupel conglomerates and needles

MURCHISON HEADWALL (28/9/81)

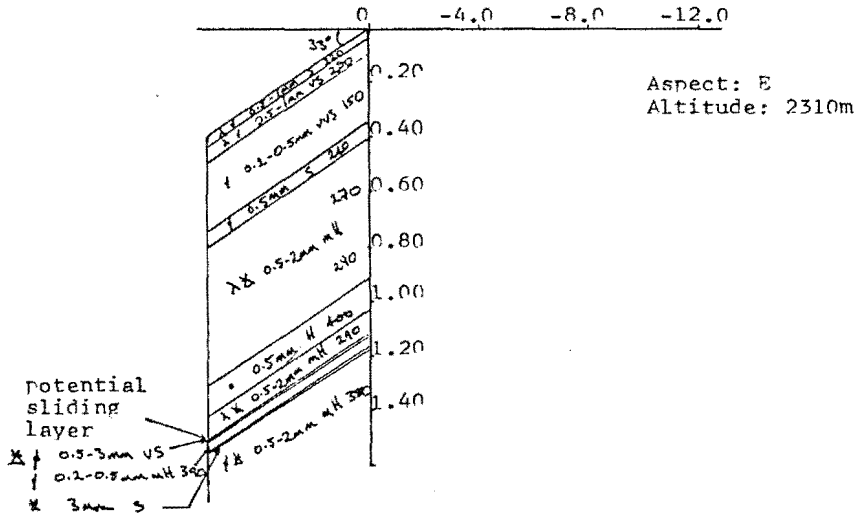

Aspect: E
Altitude: 2310m

NOSEDIVE (10/6/82)

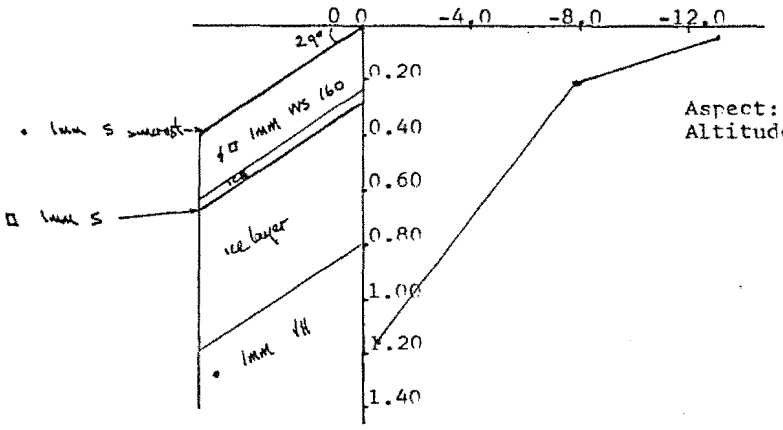

Aspect: S
Altitude: 2160m

CORNICEWALL (29/9/81)

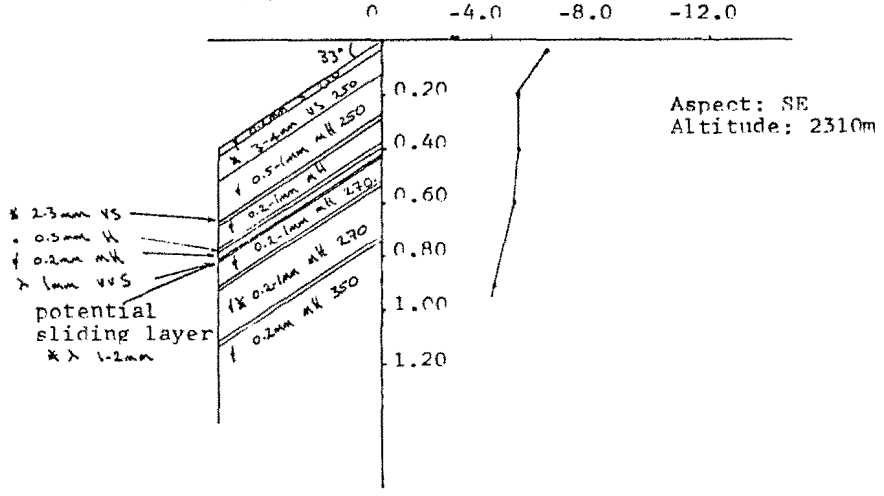

Aspect: SE
Altitude: 2310m

NOSEDIVE FRACTURE (23/6/82)

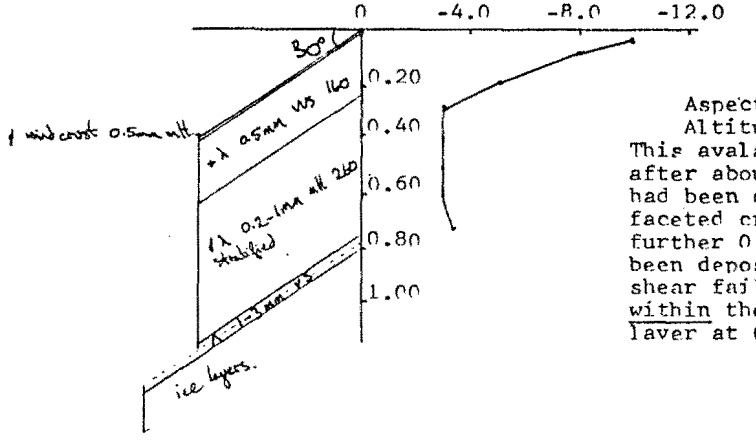

Aspect: S
Altitude: 2160m
This avalanche had occurred after about 0.30m of snow had been deposited above the faceted crystals, and then a further 0.47m of snow had been deposited. The basal shear failure had occurred within the recrystallised layer at 0.77m.

These correlations are summarised below, together with the standard deviation expected on each measurement:

1. WIND
Wind (Tasman Saddle) = 243 + 1.2 x Wind (Village)
measured in km run in 24 hours; standard deviation = ± 256 km
Wind transport of snow can be expected when the village wind run exceeds 14 km/day.

2 PRECIPITATION
Snowfall (Tasman Saddle) = 9.5 + 0.69 x Precipitation (Village)
Snowfall measured in cm at hut, precipitation in mm water.
The standard deviation = ± 13.3 cm snow.
Accumulation on the Nosedive can be expected to be closely similar to the figure for the hut pole, and accumulation on the Cornice Wall, about 2.5 times this figure.

3. TEMPERATURES
Dry Bulb temperature (Tasman Saddle) = -5.9 x 0.21 x Dry Bulb temperature (Village)
where the temperatures are in ^{o}C and the standard deviation is ± 6.6^{o}C.
For moist conditions (raining in the Village) a regression equation to determine freezing levels is: Z = 105 x Temperature (Village) + 760
where Z = freezing level in metres.
Temperature is measured in ^{o}C and the residual standard deviation is ± 470 m.

REFERENCES

Conway, H and Abrahamson, J : (1982) " Weather Data Report, Winter 1981." Final report, Part 2, for the Mountain Safety Council.

Conway, H and Abrahamson, J : (1983) Unpublished. " A Survey of Weather and Snow conditions at the Tasman Saddle area during the winters of 1980 - 1982 "

A SUMMARY OF WEATHER AND SNOW CONDITIONS AT THE TASMAN SADDLE AREA

DURING THE WINTERS' OF 1980 - 1982

BY: *H. Conway and J. Abrahamson*
Department of Chemical and Process Engineering
University of Canterbury
Private Bag
Christchurch
NEW ZEALAND

ABSTRACT

As part of a study of snow mechanics, some weather and general snowpack analysis was carried out on the Upper Tasman Glacier in the Mt Cook National Park. Considerable variation of the snowpack properties was found, and attributed mainly to fluctuations of meteorological conditions during storms.

To aid forecasting of avalanches in one area from information taken from another location (for example the Tasman Saddle Region from Mt Cook Village) a remote weather station was built. This station measured windspeed, wind direction, air temperature and new snow depth, at the end of each hour, and recorded this information in a battery-powered data logger.

THE TASMAN SADDLE AREA

We used the Tasman Saddle Hut as a base for making weather and snowpack observations around the Upper Tasman Glacier (see figure 1). The hut is situated on a rock outcrop 2320 m asl. near the head of the Tasman Glacier in the Mt Cook National Park of New Zealand (S latitude 43° 30.5'; E longitude 170° 20.5'). The area is bounded to the North and West by the main divide of the Southern Alps which rise to 3060 m (Mt Elie de Beaumont) about 3 km from the hut, and this divide causes a major orographic barrier to the prevailing westerly winds. The Tasman Glacier drops away to the south west, and about 1.75 km to the south of the hut the Malte Brun range rises to 2190 m. 1.75 m to the east, Tasman Saddle (2392 m) divides the Tasman and Murchison Glaciers. Immediately to the south of the hut the rock outcrop drops steeply about 150 m to the glacier.

Most of the area has a glacial base and like most glaciers in the region has been downwasting since about 1916 (Burrows, 1973). This downwasting has changed slope profiles on some avalanche paths.

The glacial base and high snowfalls (up to 3 m during a storm cycle) tend to inhibit formation of depth hoar. However, cold temperatures (we recorded screened air temperatures of -16°C during July 1982), and periods of clear skies did cause recrystallisation of snow near the surface of the snowpack due to temperature gradients from radiation losses during June and July 1982. Subsequent snowfalls on top of these layers resulted in many avalanches. The glacial terrain can cause some additional problems for mountain travellers. We often observed deep slabs that had been initiated by a collapsing serac or icecliff and had then propagated over large areas far from the trigger zone.

Crevasses across avalanche paths can also prove hazardous to a traveller since even a small avalanche could bury a person in a crevasse under a large quantity of snow.

During the months from June to September 1982, we recorded mean daily windspeeds greater than 2.5 m/s for about 60% of the time and a daily mean maximum of 14 m/s in September. These high windspeeds combined with the turbulence associated with the mountains often resulted in considerable redistribution of the snow, and duning and scouring of snow over the slopes were a common occurrence.

WEATHER INSTRUMENTS

(1) Temperatures

A Stevenson screen located near the hut contained drybulb, maximum and minimum thermometers. A mechanical thermograph was also in the screen, but often was not useable.

(2) Snow Depth

We used a snowpole about 200 m north of the hut to measure snow accumulation. The strong and turbulent winds in the area cause considerable redistribution of snow and so we used several other poles in different locations to compare snow accumulation depths.

(3) Windspeed and Direction

During the 1981 season we used a Lambrecht anemometer mounted near the hut to record windspeed and direction. During the 1982 season we mounted a Munroe cup counter on the hut which we read daily and at the same time we recorded the wind direction.

(4) Other Observations

We also recorded other observations such as cloud-cover, weather conditions, visibility, snow conditions and avalanche occurrence daily at 6:15 a.m. Together with temperatures, windspeed and direction and the new snow depth, we passed this information to Mt Cook village by radio for the avalanche hazard forecast (Irwin, 1983) and for the Christchurch Meteorology Office.

REMOTE WEATHER STATION

Avalanche occurrence is directly related to meteorological conditions, and although the relationship is not fully understood, weather observations do help avalanche forecasting. Weather conditions can vary widely over small areas in the mountains, which makes it difficult for an observer in one location to predict conditions at another area.

In an attempt to solve this problem - in particular, the problem of forecasting conditions at Tasman Saddle from observations made at Mt Cook Village - we designed a weather station capable of recording air temperature, new snow depth, wind direction and windspeed.

The data collected was recorded hourly on a Tasman Data Logger which could be left for periods of 30 days.

The instruments were mounted on a tripod made from 50 mm diameter aluminium tubing. Each leg could be unscrewed into two sections, each 1.5 m long, and a 400 mm diameter plate was attached at the base of each leg to anchor the tripod in the snow (see figure 16).

Air temperature was recorded by a downward pointed thermocouple, shielded inside a white P.V.C. tube which oriented itself into the wind and was angled at 45° to allow snow to fall out of the tube. The new snow depth measurements were

made using a Polaroid ultrasonic range finder mounted at the top of the tripod. This measured the distance to the snow surface, and during times of storms, or times of blowing snow, a scatter of data was recorded. This not only enabled us to record the new increment of snow, but also gave an indication of the duration of the storm. Windspeed was measured with an electrical counter, on the shaft of a robust cup anemometer, and the wind direction measured by mounting a vane on a viscous damped oil bearing within 16 reed switches, arranged to give a stepwise resistance read-out.

SNOWPACK OBSERVATIONS

We collected basic snowpit data on a variety of avalanche paths according to procedures laid down in UNESCO/IAHS/WMO (1970). We defined the stratigraphy of the snowpack and for each layer we recorded the depth from the snow surface, snow hardness, crystal type and size, stage of metamorphism of the snow, snow density, and temperature. By developing a portable air permeability device we could measure the air permeability of snow and get an indication of snow texture and hence strength (Conway and Abrahamson, 1983a). We also made an estimation of the snowpack stability by developing a shear strength test to test for weak layers in the snowpack. By determining the gravitational loading and measuring the slope angle we could compute a local shear index for the snowpack (Conway and Abrahamson, 1983b).

WEATHER AND SNOWPACK DATA

(1) 1980 Winter

Some snowpit data that we collected around the same area during the 1980 winter are also included in this report and are listed in appendix 1A.

In early July, a four day stormy westerly period resulted in 1.61 m of new snow being deposited at a snowpole near the hut. This resulted in many large slab avalanches and one almost 2 m deep occurred on the Nosedive slope (S aspect) (see figure 3). The wind-stratified slab consisted of wind crusts and graupel and was sliding on a layer of buried recrystallised snow (see appendix 1A). We observed similar stratigraphy on the Murchison headwall the following day

(4 July 1980) and although that slope had not avalanched, other slopes in the vicinity had fractured.

Another storm cycle in early August from the SW deposited about 0.58 m of snow over two days and was associated with strong winds. Although we did observe some loose avalanches on steep slopes, no slab avalanches occurred in the area. Two pits dug on different slopes (Hochstetter Dom shoulder (9/8/80), and the Nosedive (10/8/80)) were again typified by wind crusts and graupel clusters with no good shear layers (appendix 1A).

Many new slab avalanches occurred on steep slopes after a storm during 10 - 14 August 1980. The storm started with very strong W - SW winds which eroded 0.15 m of snow away from the snowpole. Strong W winds continued through the storm depositing 0.91 m of snow at the pole near the hut and 1.30 m on the Alymer traverse (S aspect). A snowpit on the Alymer traverse (14/4/80) indicated a layer of 2 - 4 mm graupel conglomerates that fell out of the pit wall at a depth of about 0.5 m (appendix 1A).

More snow from the NW fell between 15 - 16 August and was followed by a strong cold S storm on 17 August. A total of 0.70 m of snow was deposited near the hut and we observed numerous avalanches and signs of avalanches that had been subsequently covered with further snow. A pit on the Murchison headwall (17/8/80) again was typified by stratified graupel layers with few sliding layers. However, a fracture triggered artificially (by a skiier on the Cornicewall (18/8/80)) was about 0.31 m deep and consisted of the S deposited snow sliding on top of the NW deposited snows (appendix 1A).

The data we collected during 1980 was not continuous but the periods that we did record were typified by snowfalls associated with strong winds resulting in stratified snowpits often containing layers of large graupel conglomerates. Measured snow temperatures varied from -3.5°C to -19.5°C, and new snow densities varied from 110 to 295 kg/m^3.

(2) 1981 Winter

Weather and snowpit data are not continuous for the 1981 season either, but where records are available they are summarised if figure 4 and appendix 1B respectively.

Although we did not record weather data prior to the profile described from the Cornicewall (11/9/81) it did show a weak layer at about 1.30 m consisting of 1 - 2 mm recrystallised snow (appendix 1B).

Strong SW winds and a total of 0.53 m of new snow at the hut snowpole deposited varying depths of snow at different locations between 12 - 15 September 1981. Many avalanches had been subsequently covered by further snowfall, but many were still visible on steep slopes in the area and cornice breaks triggered another slide on the Cornicewall (15/9/81) (figure 5). A pit dug on the Nosedive (13/9/81) just above a fracture that had been triggered by an iceblock revealed that a weak layer of conglomerates and needles at 0.43 m deposited during the storm, provided the sliding layer (appendix 1B). A similar crystal structure was also evident on the Cornicewall (14/9/81) at 0.44 m and this fractured the following day when part of the cornice broke and triggered the avalanche (appendix 1B). A pit on the Murchison headwall (15/9/81) also showed a series of windcrusts with weaker layers in between; the weakest being at 0.66 m. Some slab avalanches had occurred on the steep slopes to each side of the headwall, but we found the actual headwall to be relatively stable.

Strong W to NW winds continued and considerable redistribution of snow occurred through at least until early October when our records finished. The winds caused dunes and scouring on slopes and a total of 1.16 m of snow accumulated at the hut pole between 23 September and 3 October 1981. We observed avalanches during brief clearances during the storm on steep slopes and considerable avalanche activity at lower altitudes was observed by the Mt Cook Park staff on 29 September. These were probably the start of the spring avalanche cycle with rain lubricating the snows. Although the Murchison headwall (East aspect) did not appear to have avalanched by 28 September, a pit in the area (appendix 1B) indicated considerable instability due to a weak shear layer at about 1.14 m. The sliding layer consisted of a thin layer of very soft partially metamorphosed snow mixed with graupel up to 3 mm in diameter. On the Nosedive the following day (S aspect) the upper snows were also wind stratified graupel and partially metamorphosed snow with a weak layer at 0.43 m of only slightly metamorphosed snow which was very soft.

As with snow observed during the 1980 season, the snowpits dug in 1981 were typified by considerable wind stratification and relatively stiff layers of

graupel conglomerates with weak snows in between providing the shear layers. The weak layers we generally associated with periods during the storm cycle when temperatures may have been lower, causing a change in precipitated crystal type.

We think these periods were also associated with times of lower windspeeds. Measured snow temperatures varied from -1.4°C to -11°C, and new snow densities varied from 90 to 250 kg/m^3.

(3) 1982 Winter

Weather and snowpit data for the 1982 winter are summarised in figure 6 and appendix 1C respectively. During this season we placed snowpoles on the upper Tasman neve and near the top of the Nosedive in an effort to compare accumulation in those areas with that at the hut snowpole. A summary of this data is shown in table 1 and figure 7. The windrun which we read daily from the cup counter is also included in the summary, together with the general direction of the storm.

A W storm on June 2 (probably with some rain as well as snow), caused a very hard ice layer at least 100 mm thick over the upper Tasman region. A S snow with light winds followed on 3 June, depositing 0.1 - 0.2 m of low density snow (about 150 kg/m^3) on many slopes, although some slopes did not accumulate this snow and the ice was still exposed. For the following 16 days an intense anticyclone remained slow moving over the country and resulted in fine weather. During this time the S deposited snow developed a slight crust and below this crust the crystals developed facets and grew up to 3 mm in diameter. We measured temperature gradients of up to 12°C/m in the snowpack and measured air permeability increases from 33 x 10^{-5} m^4 N^{-1} s^{-1} to 95 x 10^{-5} m^4 N^{-1} s^{-1} (Conway and Abrahamson 1983a). A W airstream between 21 - 22 June deposited 0.88 m of new snow at the Tasman Saddle hut snowpole, and was associated with strong winds (30 - 40 knots) and considerable wind transport of snow. We recorded approximately 30 avalanches on 23 June in the area, mainly on the S aspect slopes where the temperature gradient crystals were most prevalent. Many of the avalanches were covered by subsequent snow indicating they had released early in the storm cycle. Appendix 1C lists snowpit analyses done sometime after the initial S snow had deposited (Nosedive 10/6/82) and then after the slope had fractured and had then been covered with more snow (Nosedive 23/6/82). This pit and excavations around the crownwall, showed that the slope had avalanched after about 0.30 m of snow had accumulated above the faceted crystals, and subsequent snowfall amounted to about 0.47 m.

The W cycle was followed by a S storm on the 25 June and this was characterised by a high humidity (up to 150 mm of rime grew on metal objects near the hut). Considerable wind transport also occurred during this storm which deposited 0.35 m of new snow at the hut snowpole. We recorded about 15 avalanches again mainly on slopes with a S aspect. One such fracture was on the Hochstetter Dom shoulder and this was about 600 m wide and 400 m long, again sliding on the recrystallised snow at a depth of about 0.95 m (see appendix 1C and figure 8).

A further period of fine cold weather with no precipitation occurred between June 26 until July 12. Although this caused strong temperature gradients in the snowpack (see Nosedive 3/7/82 in appendix 1C), the upper snow density was high (about 270 kg/m^3) and the crystal structure and air permeability of the snow did not change as dramatically as the period in June, (Conway and Abrahamson 1983a). A snow pit during this period on a N facing slope of Able (4/7/82) showed that the area had been subject to considerable wind erosion and very little accumulation. Some large faceted crystals (up to 2 mm in diameter) had developed early in the season and had been buried only to 0.25 m by subsequent snowfalls. The lack of loading on this slope would have been the reason for it not failing during the June storm cycles.

W to SW winds, often very strong (we recorded a mean daily windspeed of 11 m s^{-1} on July 18 1982) caused considerable wind transport of snow between July 12 and July 22. A total of 0.93 m of new snow accumulated at the hut measuring pole but larger depths accumulated on lee slopes. We observed a total of 39 avalanches in the area at various times during the storm, and these were generally on E or NE aspect slopes. We worked on one fracture (figure 9) which had been ski released on the Cornicewall (13/7/82) and found considerable variation in the depth of fracture across the crownwall (0.32 - 0.54 m) and also variations in the basal shear strength of the slab (see Conway and Abrahamson 1983b). We did not observe an obvious stratigraphic change at the shear plane and the shearing appeared to have occurred within a very soft layer of new deposited snow (Crystal types included columns, capped columns, stellars, plates and needles - see appendix 1C).

Appendix 1C includes further snowpack analyses that we made on the Cornicewall during the storm period (Cornicewall 15/7/82; Cornicewall 19/7/82; Cornicewall 20/7/82). We found large flaws and cracks which were up to 500 mm long by

50 mm wide in the snowpack near the profile of 15/7/82. We attributed these flaws to a partial failure of the snowpack (figure 10). The profile that we analysed on the 19/7/82 was near a small sluff which we caused by kicking a cornice onto the slope. The fracture was small and the bed surface consisted of medium-hard and well bonded snow, and the shear plane consisted of some very soft wind deposited snow (appendix 1C). Again we measured considerable variation in the depth of the crownwall. The pit dug on the 20/7/82 contained about 0.18 m of very soft snow which was tending to sluff as a loose slide rather than forming a slab. We measured very low shear strengths (80 N/m^2) and low tensile strengths of this snow (320 N/m^2), in accord with the loose slide behaviour (Conway and Abrahamson 1983b).

More fine cold weather followed the storm until 30 July when another NW air-stream crossed the region depositing a total of 1.20 m of new snow at the hut snowpole by August 2. This snowfall was again associated with strong winds (mean daily average of 9.7 m/s on August 1) and was often heavily rimed conglomerates of graupel. Wind redistribution of snow continued until August 6 and many avalanches occurred, but only on very steep E and N slopes in the area. A snowpit dug on the Nosedive (6/8/82) showed the typical well bonded nature of the snowpack. A clearance of four days was followed by 0.31 m of new snow from the W on August 10, but with no new visible avalanches. A snowpit dug on the Cornicewall (11/8/82) did not have any good shear planes.

Weather and snowpit observations were intermittent during the rest of August and early September but the period was typified by strong W winds and further snowfalls. One pit that we dug on the Cornicewall (6/9/82) indicated that the shear strength of the surface snow was low (about 300 N/m^2) but generally the snowpack was well bonded below this layer (see appendix 1C). On 7 September an icefall triggered a large slab on Hochstetter Dom, and analysis of this fracture showed that the slab was sliding on a melt-freeze crust that varied from 0.57 m to 0.84 m in depth.

Futher strong W or SW winds and 0.60 m of new snow on 7 - 8 September produced only a few sluffs on some slopes. One pit that we dug on Hochstetter Dom (9/9/82) again showed some low density snow at the surface and well bonded layers deeper in the snowpack and no good shear planes.

Some radiation recrystallised snow developed near the surface during a fine period between 14 - 16 September and this was followed by a period of strong W winds (we recorded a mean daily windspeed of 14.0 m s^{-1} on 19.9.82) and 0.45 m of new snow was deposited near the hut. On the Cornicewall (19/9/82) up to 1.25 m of new snow was deposited and a large hard slab avalanche occurred at this depth (figures 11a, 11b, 11c). Similar fractures also occurred on Alymer col (figure 12) and we observed avalanches that had been subsequently covered by drifting snow on many other slopes. We dug a series of pits up the flankwall of the fracture on the Cornicewall (19/9/82) and measured variable fracture depths (in some places a double fracture had occurred) and considerable variation of shear strength at the weak layer (see appendix 1C and Conway and Abrahamson, 1983).

During the 1982 season we measured snow temperatures varying from -1.0°C to -19.9°C and new snow densities that varied from 60 - 280 kg/m^3. Figure 7 shows the effects of wind in redistributing snow during 1982, and often this redistribution not only occurred at times of precipitation, but also at times of strong winds and no precipitation. As well as causing variation in snow depth this also often caused scouring on some slopes and duning of snow on other slopes (see figure 13, 14).

RESULTS FROM THE AUTOMATIC WEATHER STATION

The data logger (or alternatively the tape recorder used to interrogate the data logger) required an interface so that the data could be transferred to the Chemical and Process Engineering Department's computer. A suitable programme incorporating the instrument calibrations was used to calculate and print the weather information. The programme used, and a typical set of data are shown in appendix II.

DISCUSSION

(1) Weather Instruments

The Stevenson screen, and especially the thermograph were prone to filling with drifting snow. Snow that had blown into the screen and around the thermometers caused erroneous readings about 2% of the times measured, and often made the

thermograph inoperable. We have not yet found a suitable screen to protect this instrument and to enable it to function successfully. We suspected that vibrations of the screen during windy periods may have altered the maximum and/or minimum temperature readings on several occasions.

On two occasions, strong winds blew the snowpoles away. We found it difficult to find a sheltered and representative snow accumulation site close to the hut, but never the less the measurements and comparisons made at various sites (table 1 and figure 7) are useful for predicting snow depths on often avalanched slopes, given measurements near the hut.

The cup anemometers were prone to icing (this occurred in about 13% of the period June to September 1982 - see figure 2). Icing on the Lambrecht anemometer affected not only the cups and vane, but also the mechanical recording mechanism. This made it difficult to interpret daily weather data since icing of the mechanism changed the time basis of the chart.

(2) Weather Station

The design and building of the weather station was not completed until August 1982, so we have only one months data from the instrument. Periods of icing were easily recognised in the data - these were typified by periods of no wind and no wind direction change. When ice around the temperature probe melted, it caused a short circuit which caused an erroneous temperature reading. More care has since been taken to protect the temperature probe.

In an effort to protect the ultrasonic transducer we mounted it inside a plastic cone. Some care was required to have the cone of such a shape and material to prevent signals reflecting from the cone.

Some of the data from the data logger was obviously incorrect. We were uncertain whether this problem originated within the data logger memory or during the extraction of the data onto magnetic tapes. We suspected that a problem arose from the low temperatures of the tapes and we always made at least three recordings of the data in an attempt to record a correct set of data.

The cold conditions also reduced battery life considerably, and precautions were taken to ensure that we had batteries with sufficient energy to drive the instruments.

(3) Snow Measurements

A primary requirement for a slab type failure of snow is a weak basal layer (Perla, 1980), and McClung (1979) suggests that failure will occur when the rate of shearing creep in the weak layer exceeds the rate of settlement normal to the slope.

In all of our snowpits we located the weakest layer, calculated the downslope loading at this layer (by measuring the slab density and slope angle), and measured a local shear strength. These measurements enabled us to calculate a local "factor of safety" by evaluating the ratio of strength available along the potential failure surface to that required for failure to occur (Conway and Abrahamson, 1983b).

1. Weak Layers

Of nine profiles that we observed on fracture-lines, four had fractured at recrystallised snow layers and five showed that the avalanche had slid at weak layers of soft or very soft new snow. Potential sliding layers at other pits were generally layers of soft new snow which had been deposited sometime during the most recent storm. Often the weak layers were thin (about 1 mm) and we think that these may be deposited during lulls in the storm or during brief periods when the crystals being deposited are less rimed (a cooler period).

Although the snowpits often contained layers of graupel and rounded conglomerates up to 4 mm diameter, these layers were generally well bonded and did not provide layers of easy shearing.

Some of the new snow layers within some snow profiles were found to collapse when we applied only small normal forces (say 200 N/m^2), and several times we measured a decrease of shear strength at that layer after the collapse. We attributed this weakening to be associated with the change of structure of the layer after the collapse, and this sort of failure could be an important mechanism for some avalanche releases. This mechanism was only noticed on soft layers that consisted of low-density needles and/or broken stellar crystals.

We found large variations in our calculated "factor of safety" values, (we measured changes of up to 300% over 0.5 m intervals. We think these

variations were caused mainly by the depositional characteristics of blowing snow (Conway and Abrahamson 1983b). Figure 15 shows a weak layer which fluctuated in its depth below the surface snow.

2. The slabs

Slab densities of slopes that had fractured varied in the range 100 - 290 kg/m^3. The slabs often consisted of wind stratified partially metamorphosed snow and/or graupel layers.

In several cases where the surface snow had been deposited with little wind, we found the surface snow to be weak in tensile as well as shear strength and this snow released as point releases rather than slabs. This would support the concept that loose snow avalanches start in cohesionless surface layers of snow (Perla, 1980).

WIND DEPOSITION OF SNOW

Rates of loading on a snow slope may be important to assess slope stability since rapid loading can cause the rate of creep to exceed the rate of settlement in the shear layer (McClung, 1979), or cause a more brittle-like fracture at a low load compared with a ductile failure in the slab (Narita, 1980). We also think that turbulence associated with winds can cause duning as suggested by Dyunin (1967) and Kobayashi (1979), which could cause discontinuities in a shear layer.

Table 1 and figure 7 show the effects of wind on snow accumulation at various sites in the Tasman Saddle area. 87% of the precipitation recorded was during periods of SW-W-NW storms, and the Cornicewall (E aspect) can generally be considered a "lee slope". The hut stake is subject to some scouring from strong winds, and the Nosedive has a S aspect and W winds are often funnelled across the slope. Figure 7 shows that the Nosedive accumulates a similar quantity of snow to that shown at the hut stake; but the Cornicewall accumulates considerably more and the difference generally increases as the snowfall depth increases.

In his review, Schmidt (1982) mentions that threshold windspeeds determine transport rates and that cohesive forces at the snow surface determine the

threshold windspeeds. Although we have not collected any detailed data from the Tasman Saddle region, redistribution of snow was common on days when the mean daily windspeed exceeded 3 m s^{-1}.

AVALANCHE OCCURRENCE

Because snow accumulation from precipitation and/or drifting may be high (up to 3 m during a storm), we often found it difficult to determine the number of avalanches that occurred during the storm, since often the high amounts of deposition would obscure the avalanches. The number of avalanches recorded was therefore a conservative estimate.

Although most instability in the snowpack was related to periods of snowfall or periods of wind redistribution of snow, some periods of precipitation did not produce avalanches in the area (see figures 3 and 6). One such period in early September 1982 was typified by strong W or NW winds (mean windspeed between 1 - 11/9/82 was 6.2 m/s) and high precipitation (a total of 2.20 m of snow was deposited at the hut snowstake). Although avalanching was recorded at lower altitudes by Mt Cook Park staff, only one slab avalanche (triggered by an iceblock collapse) occurred in the Tasman Saddle area. As previously discussed conditions that are necessary for slab avalanching include a weak shear layer and sufficient loading above this weak layer. Analysis of the snowpack profile showed that although the storm had deposited a dense and wind stratified load on the slope, no weak layers had been deposited at any time during the storm and none existed in the snowpack prior to the storm. These factors would inhibit avalanche formation.

More frequent weather measurements would be required to determine conditions within the storm that might cause a weak layer to develop, but the present data shows that we could expect to observe avalanches in the area after a period of precipitation about 60% of the time.

CONCLUSIONS

Weather data and snowpack information collected at Tasman Saddle (the highest weather station in New Zealand) has provided a useful basis for the Mt Cook

avalanche forecast scheme, and also in understanding mountain weather and snowpack conditions. More frequent and regular localised measurements are required to facilitate understanding of which meteorological conditions can result in unstable snowpacks, and the remote weather station can fulfill this need.

In the future, we plan to convert the system to enable interrogation of the data by VHF radio. This would enable Mt Cook Park staff to access the data at selected times through the day.

ACKNOWLEDGEMENTS

Financial support for the study came from the Department of Lands and Survey (Wellington, New Zealand), University of Canterbury (Christchurch, New Zealand), Mountain Safety Council of New Zealand, and Mt Hutt Ski Company. Mt Cook Airlines Company provided aircraft access to the field area, and the assistance of Mt Cook National Park Staff with the field experiments was invaluable. The New Zealand Meteorological Office provided the weather instruments. The Department of Chemical and Process Engineering (University of Canterbury) sponsored the project and helped develop the concepts and test equipment for the project.

REFERENCES

Burrows, C.J.: (1973) "Studies on some glacial moraines in New Zealand", N.Z. Journal of Geology and Geophysics, 16, p 831-855.

Conway, H. and Abrahamson, J.: (1983a) (in preparation) "Air permeability as a textural indicator of snow", (to be submitted to Journal of Glaciology).

Conway, H. and Abrahamson, J.: (1983b) (in preparation) "Snow stability index", (to be submitted to Journal of Glaciology).

Dyunin, A.K.: (1967) "Fundamentals of the mechanics of snow storms", Physics of Snow and Ice, Vol. 1, Part 2, (H Oura, ed.), p 1065-1073, Inst. of Low Temp. Sci., Hokkaido Univ., Sapporo, Japan.

Irwin, C.S.: (1983) "A report on the Mt Cook avalanche hazard forecasting scheme 1982", unpublished report to Lands and Survey Department, New Zealand.

Kobayashi, S.: (1979) "Studies on interaction between wind and dry snow surface", Contrib. Inst. of Low Temp. Sci., Hokkaido Univ., Ser. A, No. 29, p 1-64.

McClung, D.M.: (1979) "Shear fracture precipitated by strain softening as a mechanism of dry slab release", Journal of Geophysical Research, Vol. 84, No. B7, P 3519-3526.

Narita, H.: (1980) "Mechanical behaviour and structure of snow under uniaxial tensile stress", Journal of Glaciology, Vol. 26, No. 94, P 275-282.

Perla, R.I.: (1980) "Avalanche release, motion and impact", Dynamics of Snow and Ice Masses, (S. Colbeck, ed.), Chapter 7, p 397-462, Academic, New York.

Schmidt, R.A.: (1982) "Properties of blowing snow", Reviews of Geophysics and Space Physics, Vol. 20, No. 1, p 39-44.

UNESCO/IAHS/WMO: (1970) "Seasonal snow cover", United Nations Educational, Scientific and Cultural Organisation, Paris, Technical Papers in Hydrology, No. 2, 38 p.

LIST OF FIGURE CAPTIONS

FIGURE 1: A sketch map of the Upper Tasman Glacier.

FIGURE 2: (a) Riming on the anemometer.
(b) Riming on the Stevenson screen.

FIGURE 3: Stratigraphy analysis of a 2 m crownwall on the Nosedive slope, July 3, 1980.

FIGURE 4: Meteorological data and avalanche occurrence data collected at the Tasman Saddle area, 1981.

FIGURE 5: Cornice triggered slab on September 15, 1981.

FIGURE 6: Meteorological data and avalanche occurrence data collected at the Tasman Saddle area, 1982.

FIGURE 7: Comparison of snow accumulation data at the hut with data on the Nosedive pole, Nosedive slope, and Cornicewall slope.

FIGURE 8a: Hochstetter Dom crownwall, June 26, 1982.

FIGURE 8b: Aerial photograph of Hochstetter Dom fracture of 26 June, 1982.

FIGURE 9: Statigraphy analysis of a ski released avalanche on the Cornicewall July 13, 1982.

FIGURE 10a/b: Cracks in the snowpack observed on the Cornicewall July 15, 1982 due to partial slope failure.

FIGURE 11a: Partially drifted-over crownwall on the Cornicewall slope, 19 September, 1982.

FIGURE 11b: Northern flankwall of Cornicewall fracture, 19 September 1982.

FIGURE 11c: Shear strength analysis using a strain gauge on the Cornicewall fracture of 19 September 1982.

FIGURE 12: Fracture on Alymer Col, September 19, 1982.

FIGURE 13: Strong winds often caused redistribution of snow.

FIGURE 14: Periods of strong winds often caused scouring and duning of snows in the area.

FIGURE 15: A weak layer (marked with matches) which fluctuated in its depth below the surface snow.

FIGURE 16: The remote weather station. The Tasman data logger is mounted on a tripod leg; temperature, windspeed and direction, and snow depth instruments are mounted at the top of the tripod.

FIGURE 17: A typical computer print-out from the remote weather station.

TABLE I

DATE	SNOW ACCUMULATION (meters) HUT POLE	CORNICE PITS	NOSEDIVE POLE	NOSEDIVE PITS	WIND MEAN DAILY SPEED m/s	DIRECTION AT 6.15 am	COMMENTS
8/6/82	.14	-	.19	.23	-	S	scouring evident on some slopes
21-23/6/82	.88	2.16	.79	.78	6.7	W	many avalanches occurred after this storm
25-26/6/82	.35	-	.09	-	-	S	anemometer rimed but strong S winds scoured S aspects
13/7/82	.32	.58	-	-	6.0	SW	irregular snow surface and lots of drifting snow
13-15/7/82	.28	.54	-	-	6.0	SW	considerable wind transport of snow
12-15/7/82	.60	1.12	.43	.45	6.0	SW	-
3/8/82	1.20	-	1.00	-	-	SW	-
5/8/82	.15	-	.15	.18	7.2	SW	many point releases had occurred
11/8/82	.31	.25	-	-	5.7	W	a well bonded snow pack
7/9/82	.25	-	.18	-	4.8	W	considerable drift of snow
7-11/9/82	.83	-	.90	-	7.7	W	a well bonded and wind deposited snow pack
19/9/82	.43	1.25	.30	-	9.4	W	wind deposited hard slabs occurred on many slopes

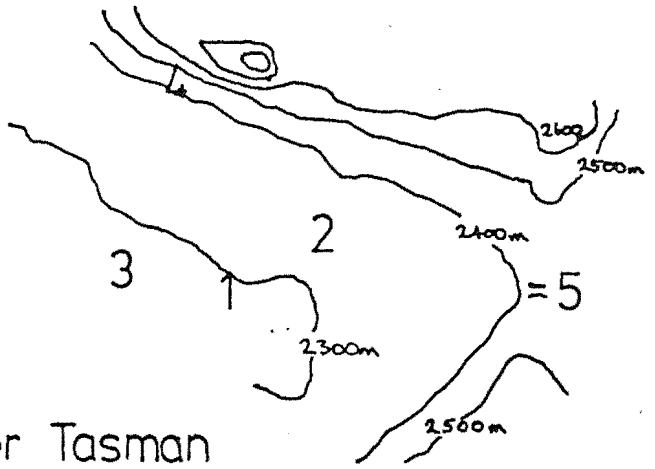

1 Hut, snowpole and screen.
2 Cornicewall slope
3 Nosedive pole and nosedive slope
4 Hochstetter Dom slope
5 Murchison Headwall slope

fig.1

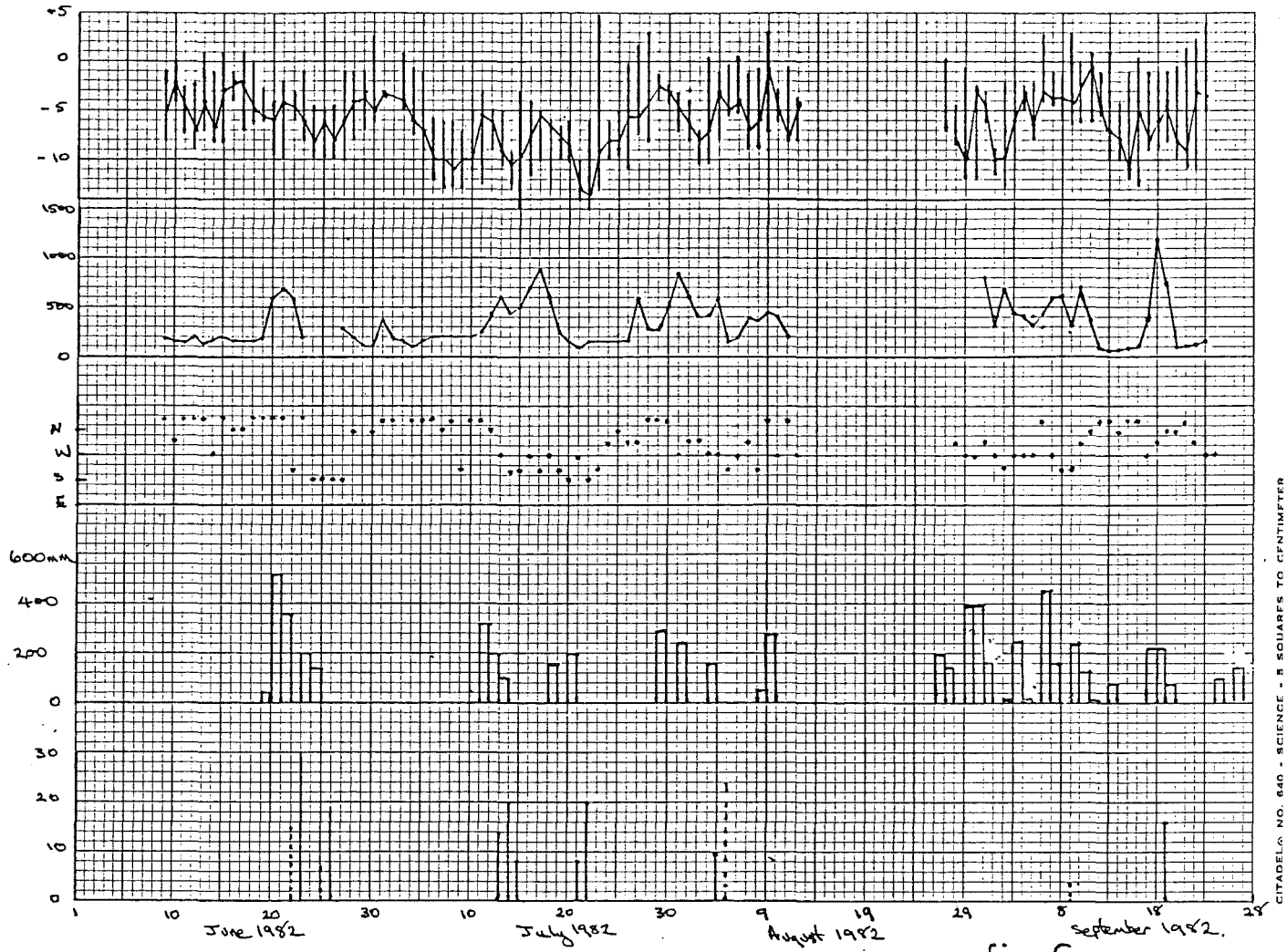
+5
0
-5
-10
1500
1000
500
0
N
W
S
E
600mm
400
200
0
30
20
10
0
1
10
20
30
10
20
30
9
19
29
8
18
28
June 1982
July 1982
August 1982
September 1982.
CITADEL® NO. 640 - SCIENCE - 5 SQUARES TO CENTIMETER

fig. 6

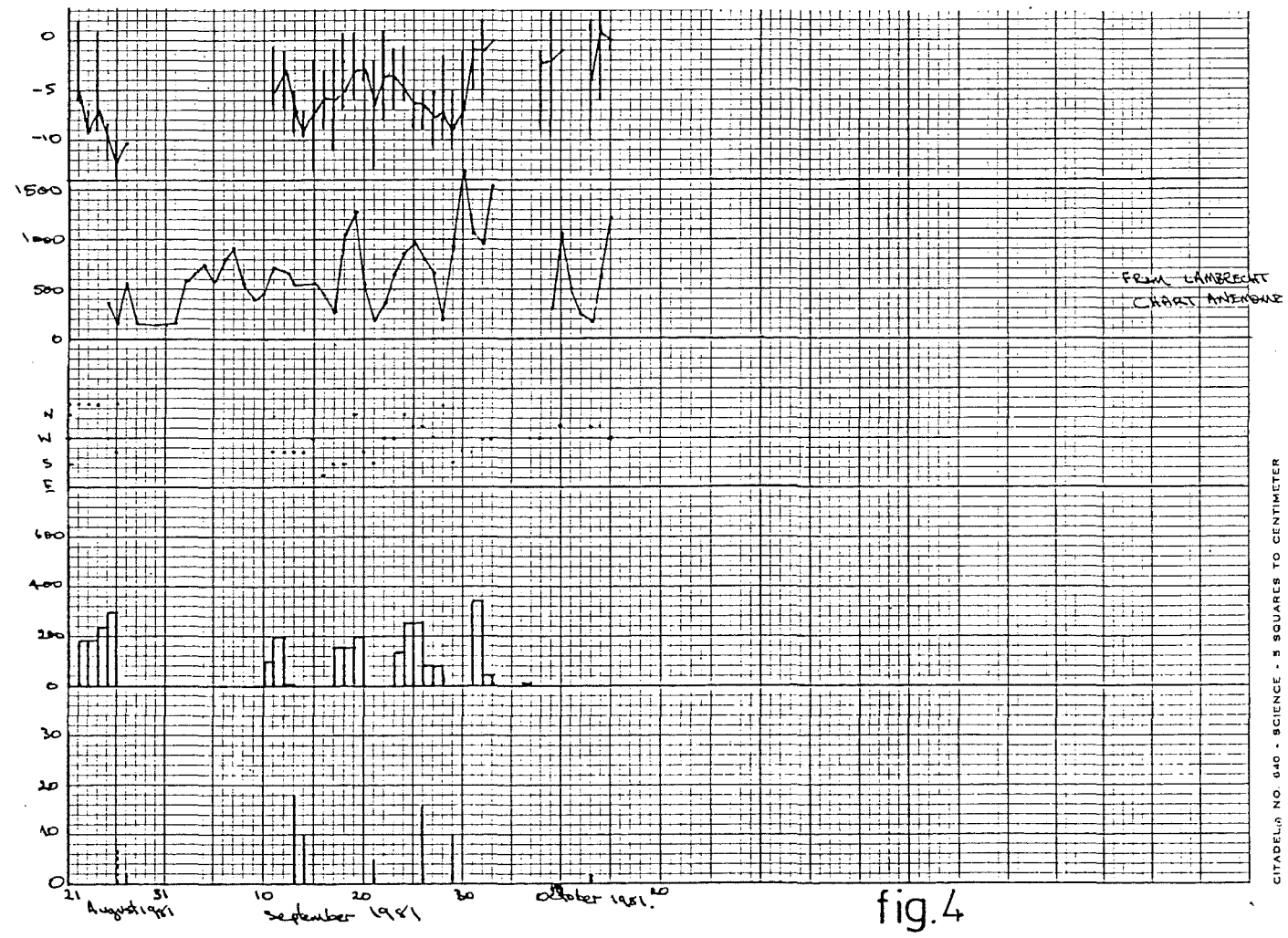
0
-5
-10
1500
1000
500
0
FROM LAMBRECHT
CHART ANEMOMETER
N
W
S
E
600
400
200
0
30
20
10
0
21
31
10
20
30
10
August 1981
September 1981
October 1981.
CITADEL® NO. 640 - SCIENCE - 5 SQUARES TO CENTIMETER

fig. 4

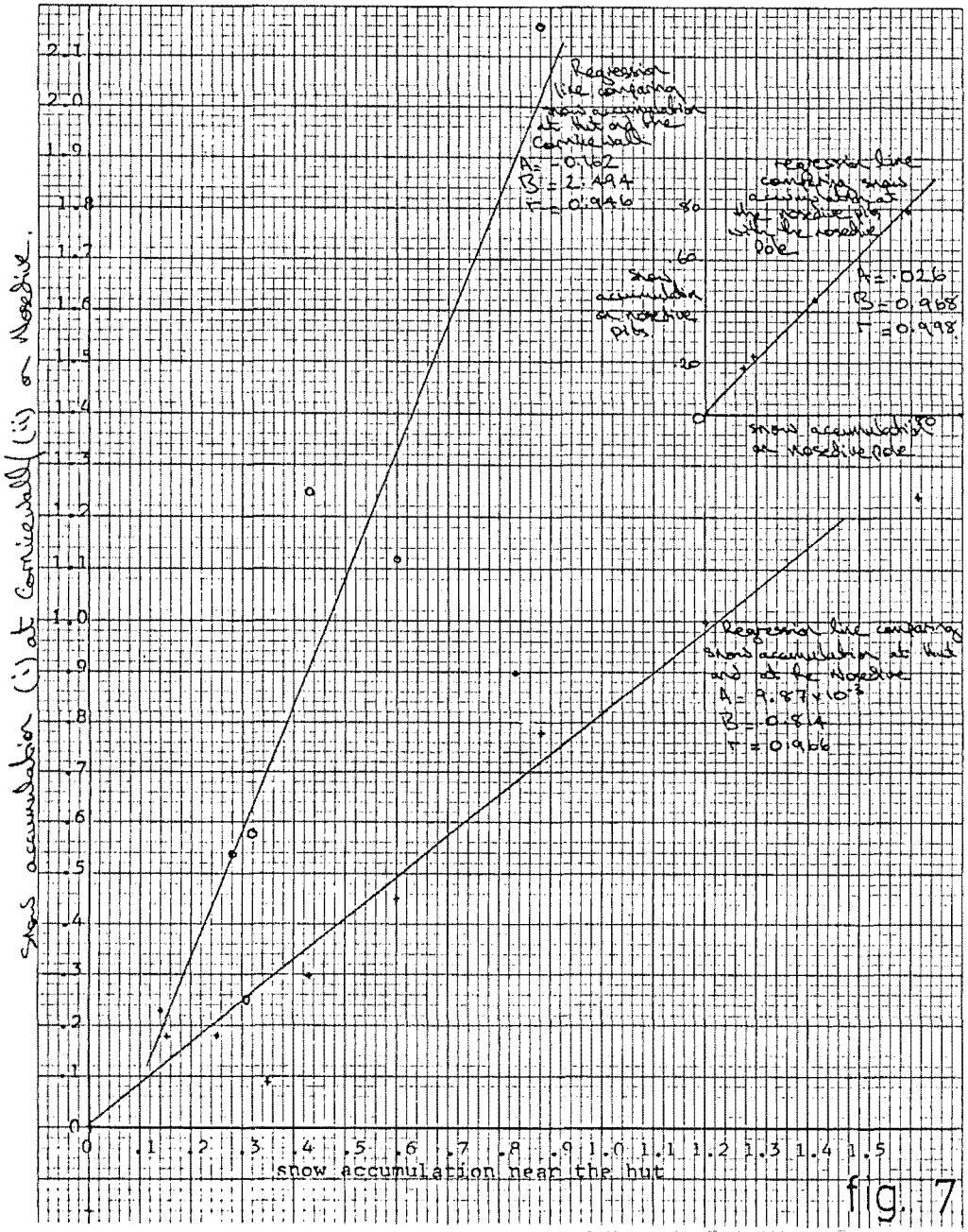

fig. 7

NOSEDIVE FRACTURE (3/7/80)

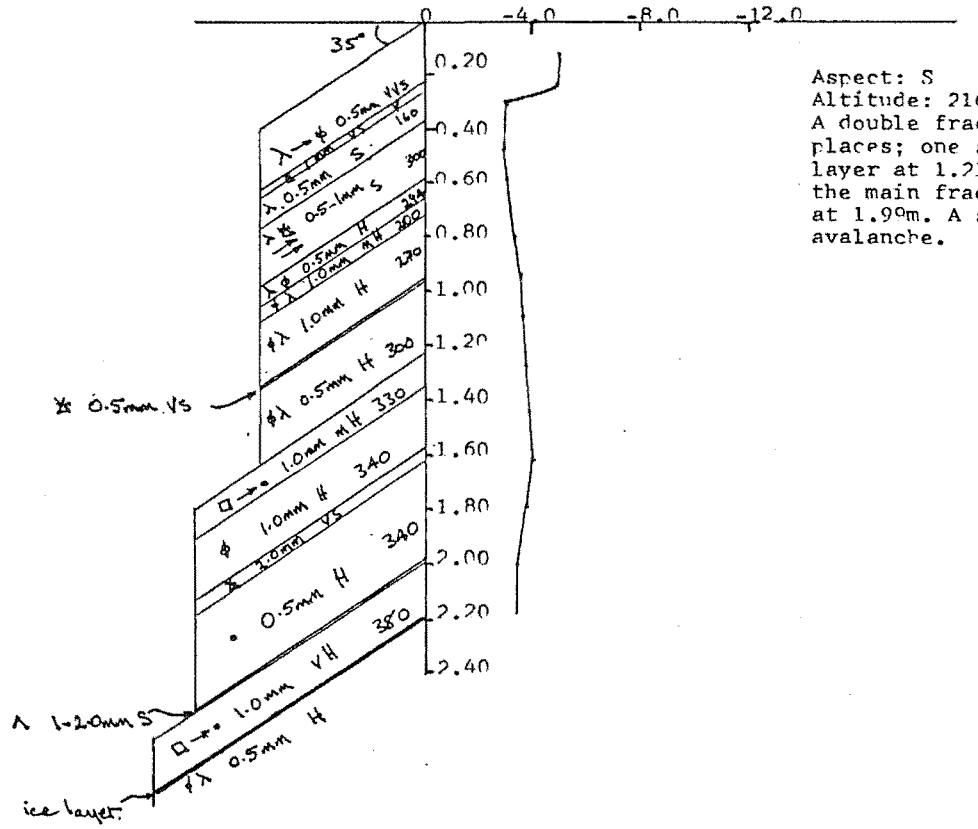

Aspect: S
Altitude: 2160m
A double fracture i
places; one sliding
layer at 1.23m, and
the main fracture w
at 1.90m. A size 3-
avalanche.

MURCHISON HEADWALL (4 /7/80)

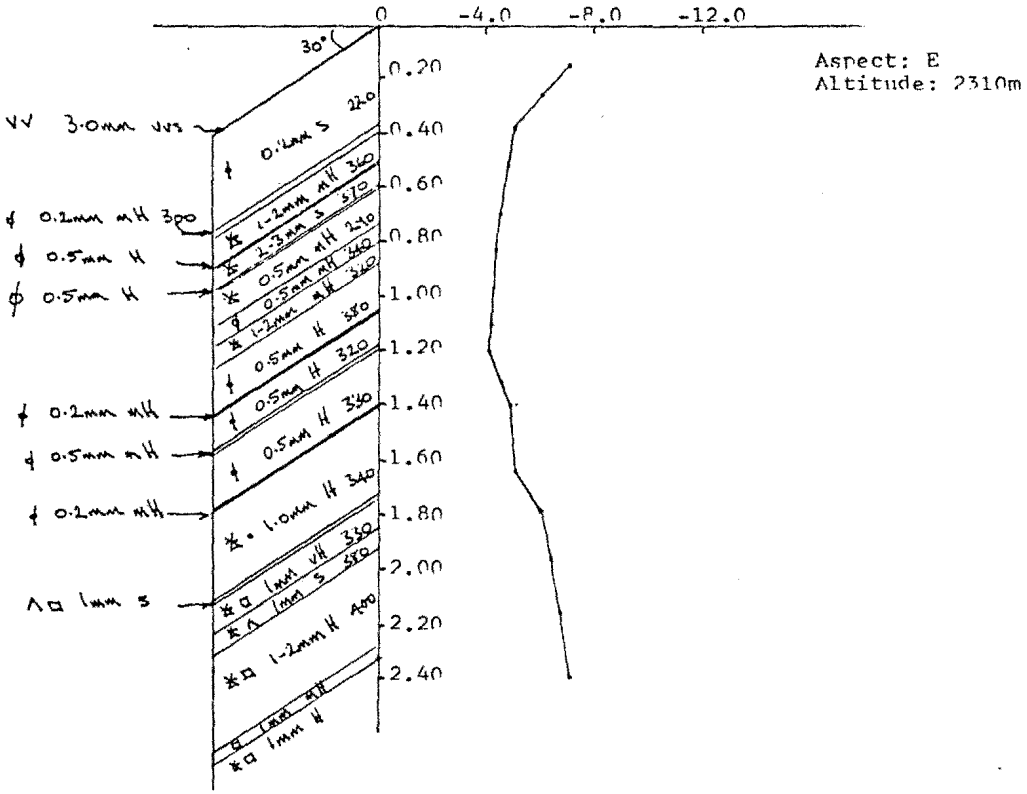

HOCHSTETTER DOM SHOULDER (9/8/80).

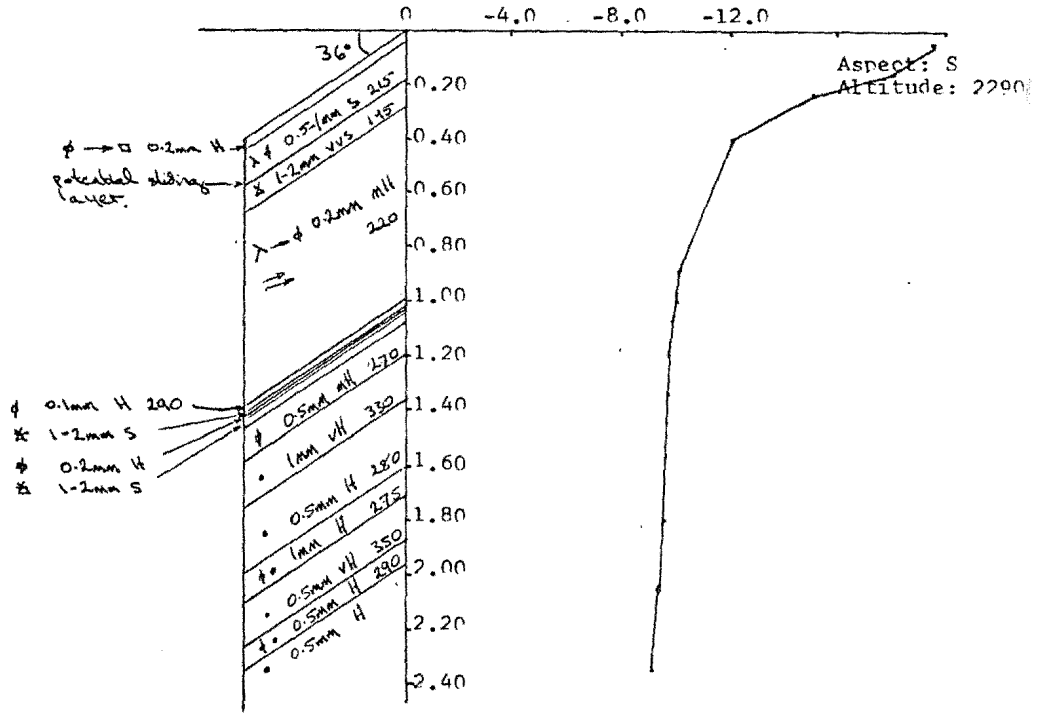

NOSEDIVE (10/8/80)

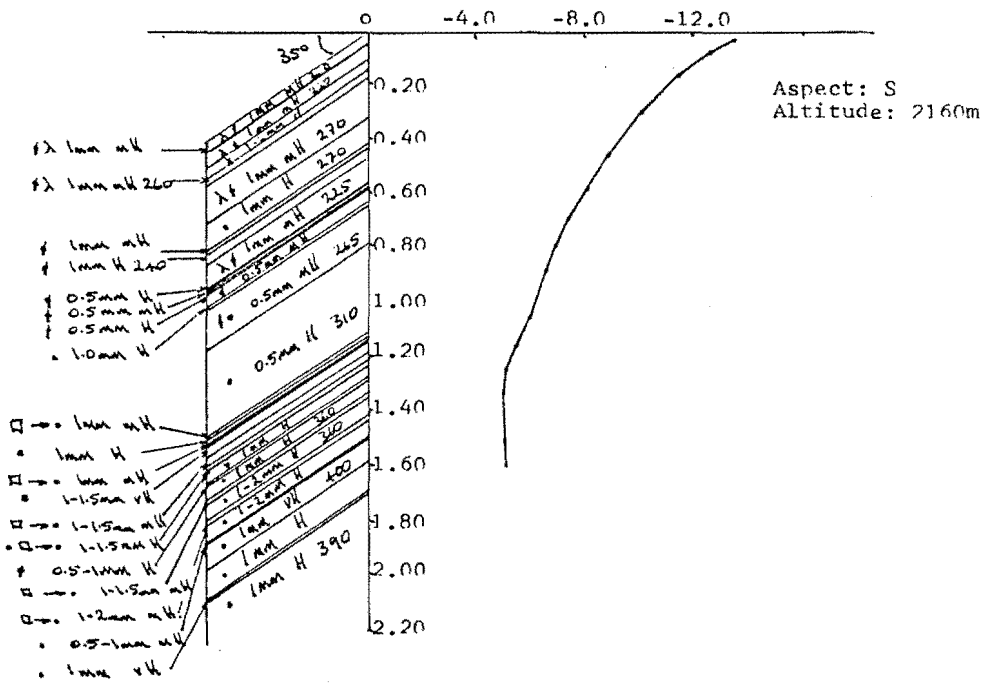

ALYMER TRAVERSE (14/8/80)

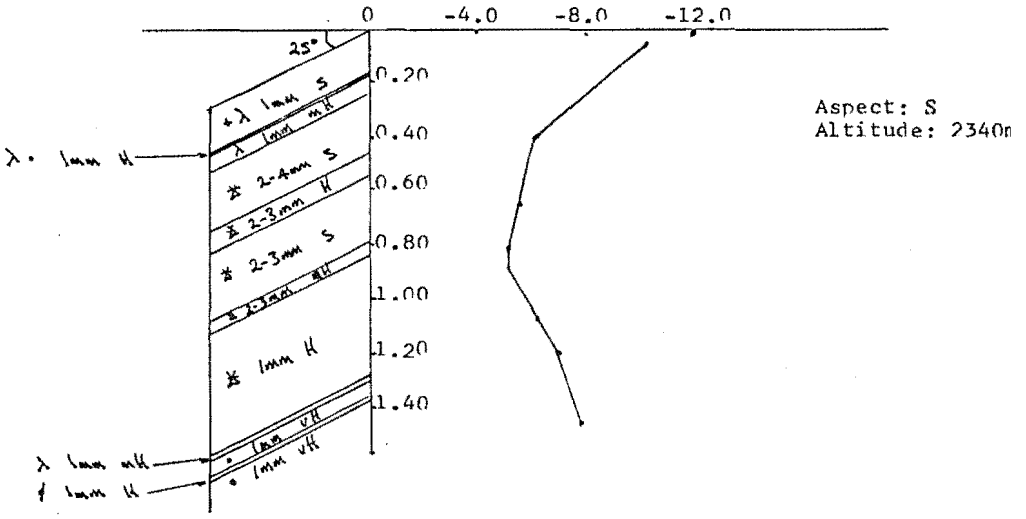

CORNICEWALL FRACTURE (18/8/80)

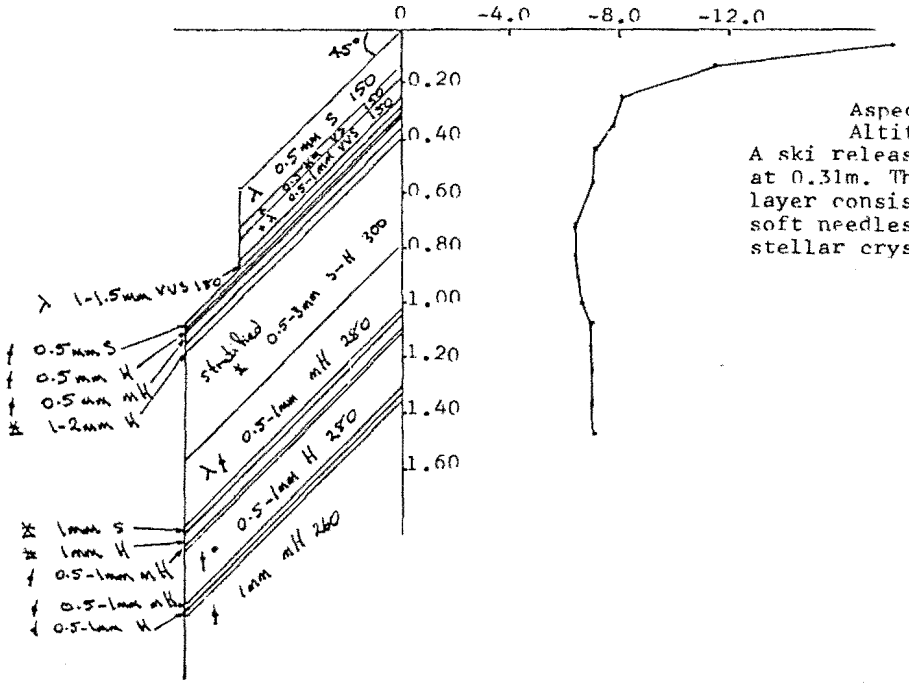

Aspect: SE
Altitude: 2310m
A ski released fracture at 0.31m. The sliding layer consisted of very soft needles and broken stellar crystals.

MURCHISON HEADWALL (17/8/80)

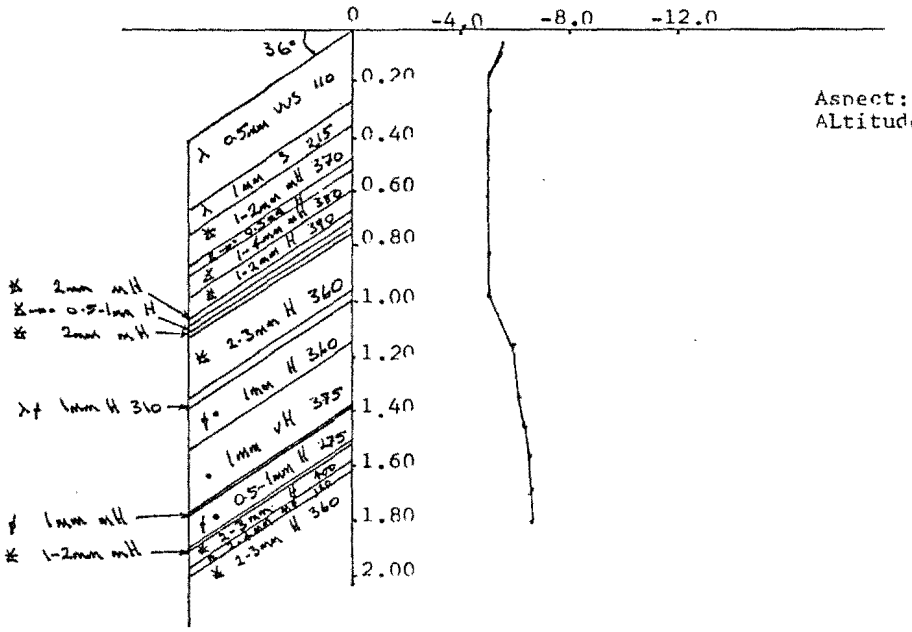

Aspect: E
ALtitude: 2310m

CORNICEWALL (11/9/81)

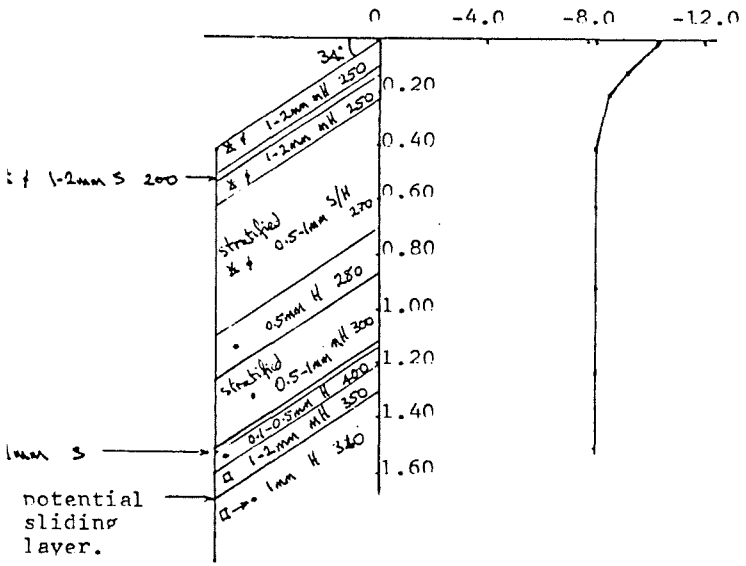

Aspect: SE
Altitude: 2310m

CORNICEWALL (14/9/81)

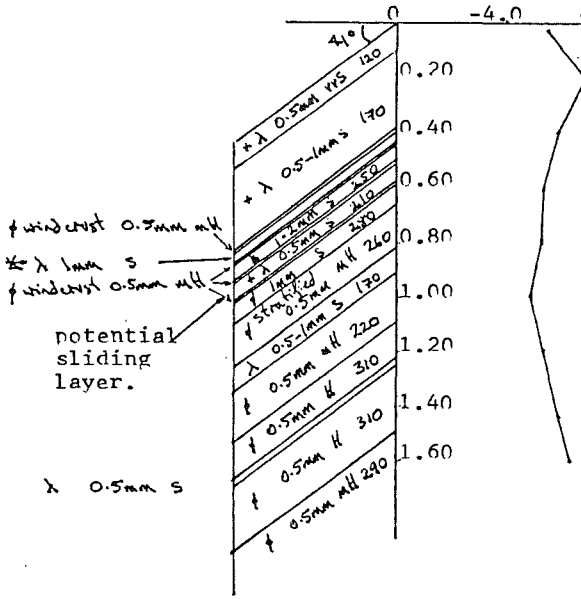

Aspect: SE
Altitude: 2310m
On 15 September part of a cornice fell about 50m from this pit and triggered an avalanche that slid to a depth of 0.60m.

NOSEDIVE FRACTURE (13/9/81)

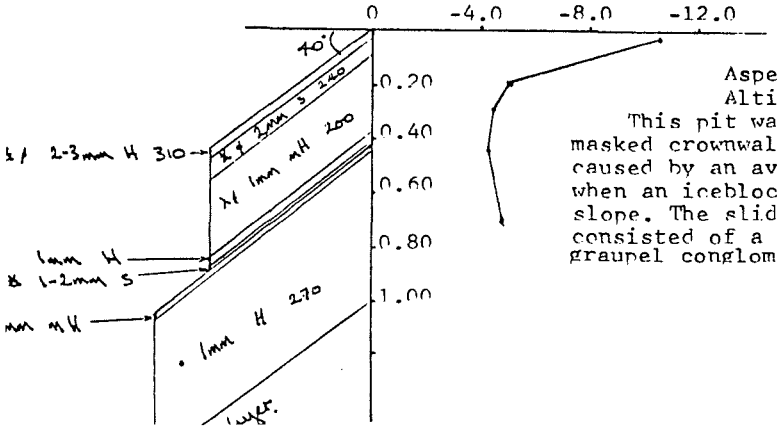

Aspect: S
Altitude: 2160m
This pit was dug 1m above a masked crownwall which had been caused by an avalanche occurring when an iceblock fell onto the slope. The sliding layer at 0.43m consisted of a mixture of graupel conglomerates and needles.

MURCHISON HEADWALL(15/9/81)

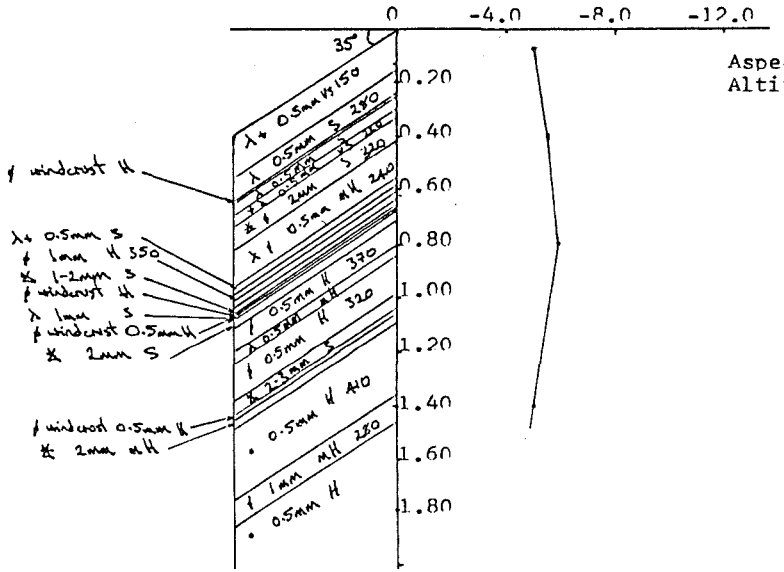

Aspect: E
Altitude:2310m

CORNICEWALL (14/9/81)

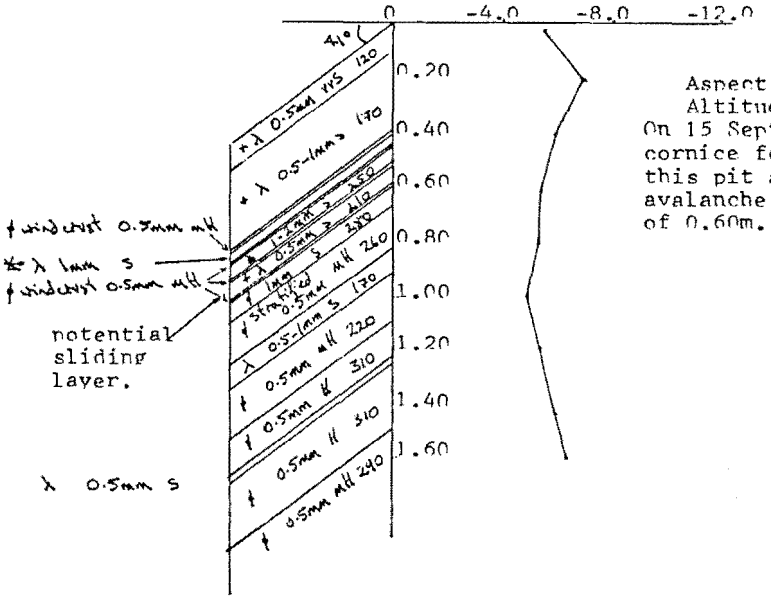

Aspect: SE
Altitude: 2310m
On 15 September part of a cornice fell about 50m from this pit and triggered an avalanche that slid to a depth of 0.60m.

CORNICEWALL (11/9/81)

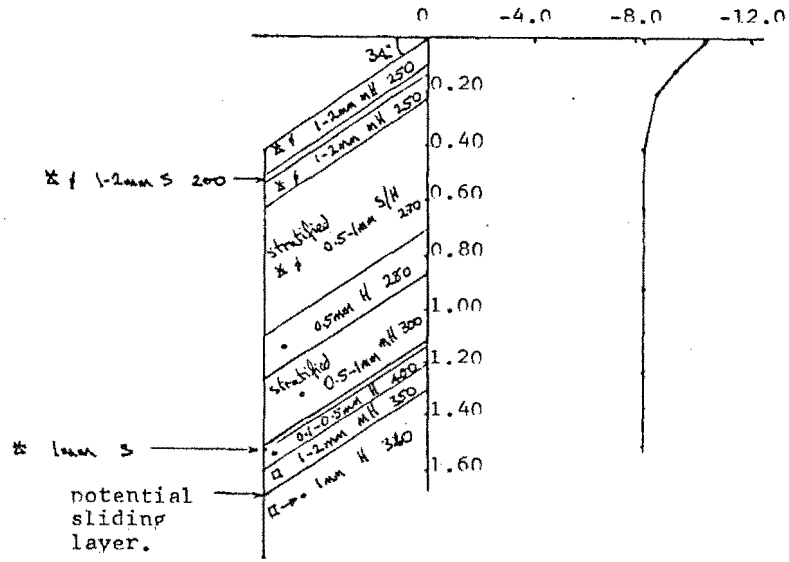

Aspect: SE
Altitude: 2310m

MURCHISON HEADWALL(15/9/81)

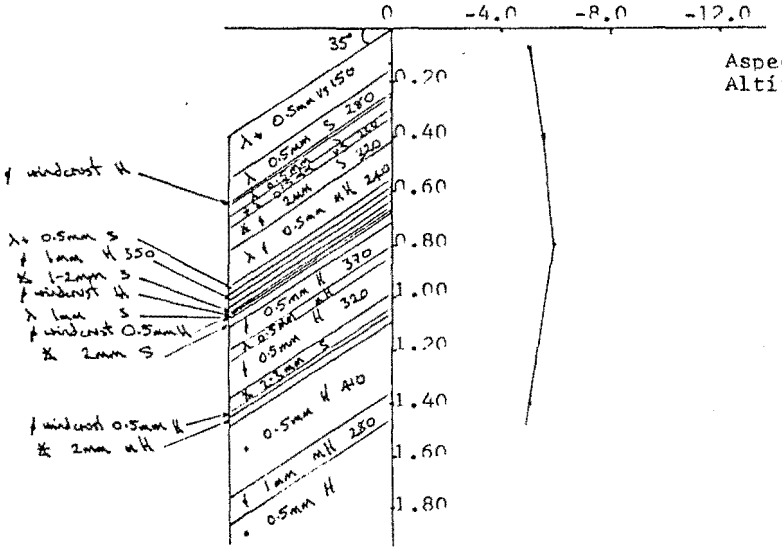

Aspect: E
Altitude:2310m

NOSEDIVE FRACTURE (13/9/81)

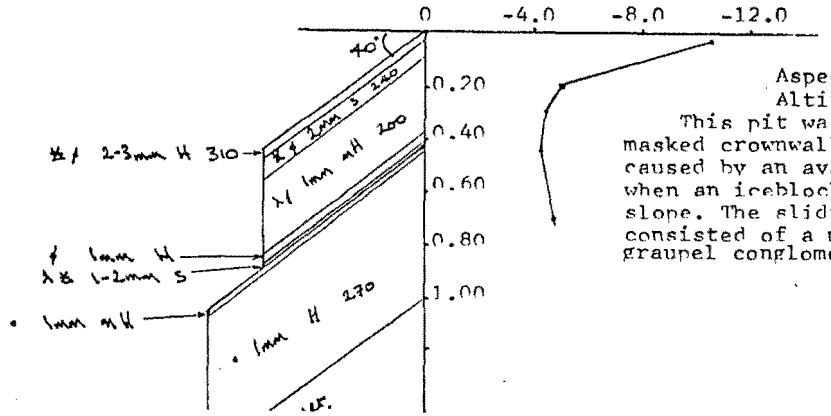

Aspect: S
Altitude: 2160m
This pit was dug 1m above a masked crownwall which had been caused by an avalanche occurring when an iceblock fell onto the slope. The sliding layer at 0.43m consisted of a mixture of graupel conglomerates and needles

MURCHISON HEADWALL (28/9/81)

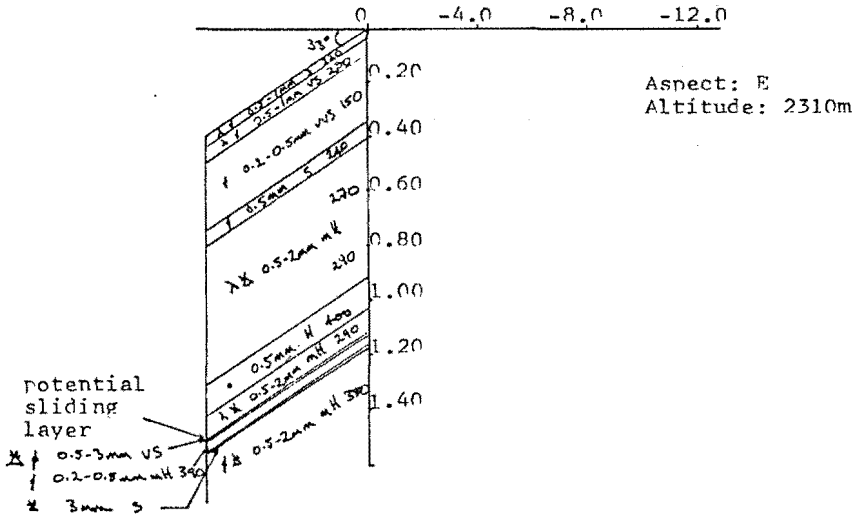

Aspect: E
Altitude: 2310m

NOSEDIVE (10/6/82)

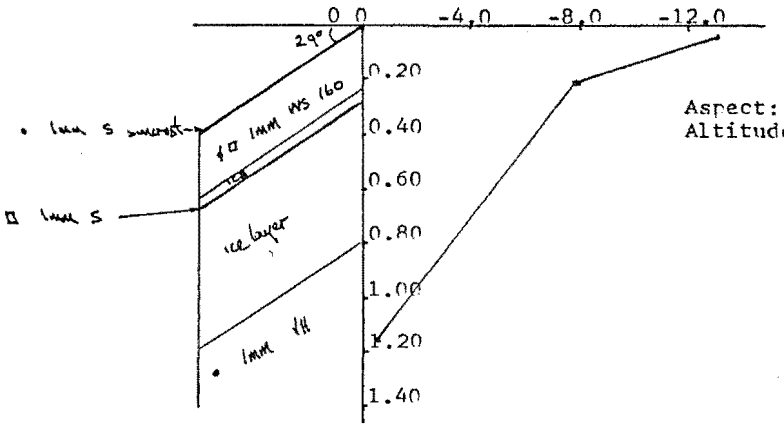

Aspect: S
Altitude: 2160m

CORNICEWALL (29/9/81)

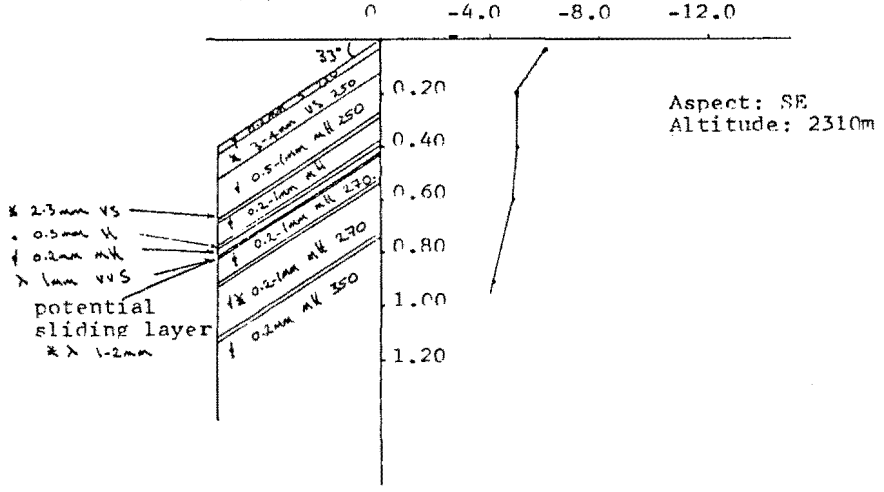

Aspect: SE
Altitude: 2310m

NOSEDIVE FRACTURE (23/6/82)

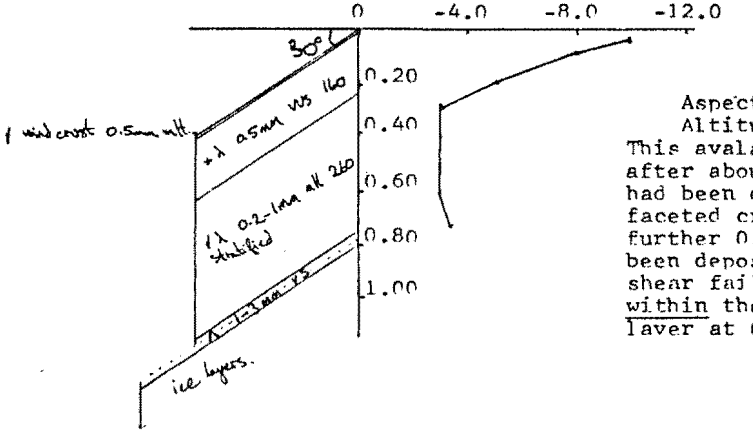

Aspect: S
Altitude: 2160m
This avalanche had occurred after about 0.30m of snow had been deposited above the faceted crystals, and then a further 0.47m of snow had been deposited. The basal shear failure had occurred within the recrystallised layer at 0.77m.

ABLE (4/7/82)

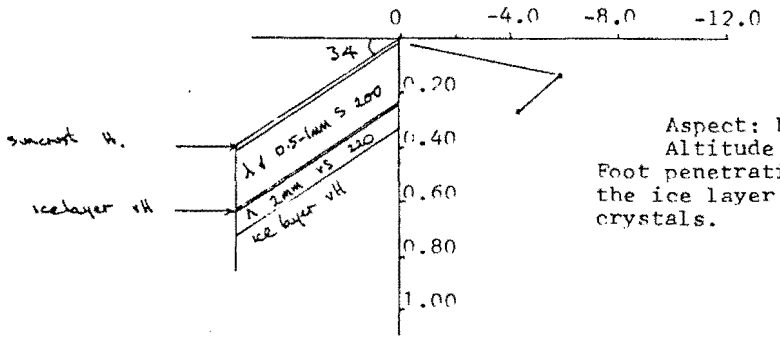

Aspect: N
Altitude: 2530m
Foot penetration was collapsing the ice layer above the faceted crystals.

HOCHSTETTER DOM FRACTURE (26/6/82)

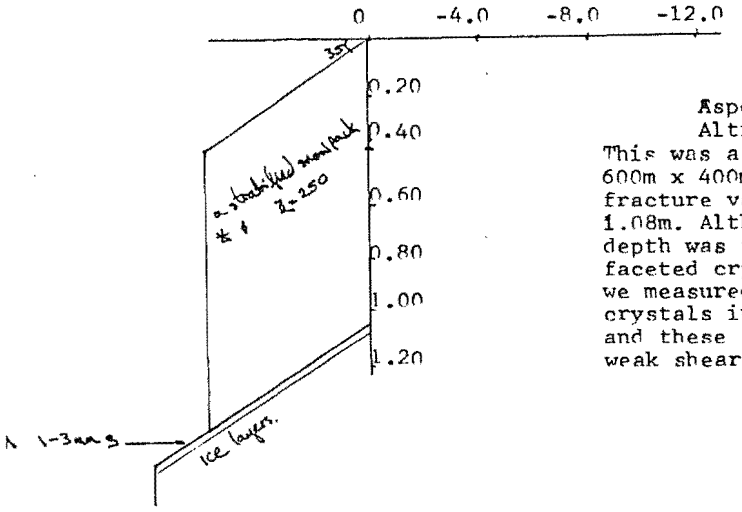

Aspect: S
Altitude: 2500m
This was a large fracture (about 600m x 400m) and the depth of fracture varied from 0.90m to 1.08m. Although the fracture depth was to the top of the faceted crystals, some pits that we measured did not have these crystals in the stratigraphy, and these columns did not have a weak shear plane.

CORNICEWALL FRACTURE (13/7/82)

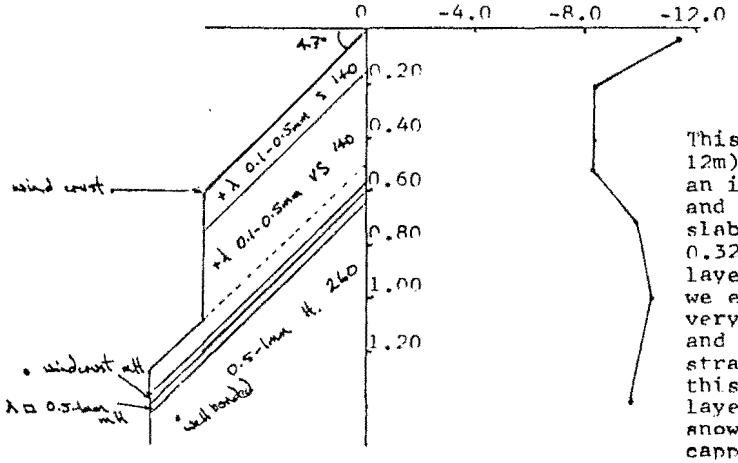

Aspect: SE
Altitude: 2310m
This small fracture (16m x 12m) was ski released to an initial depth of 0.23m and then this released a slab that varied from 0.54-0.32m in depth. The shear layer in the profile that we examined was within the very soft layer at 0.54m and we did not observe a stratigraphic change at this level. The shear layer was newly deposited snow consisting of columns, capped columns, stellars, plates and needles. Large variations of basal shear strength were also measured across the slope (see Conway and Abrahamson 1983).

NOSEDIVE (3/7/82)

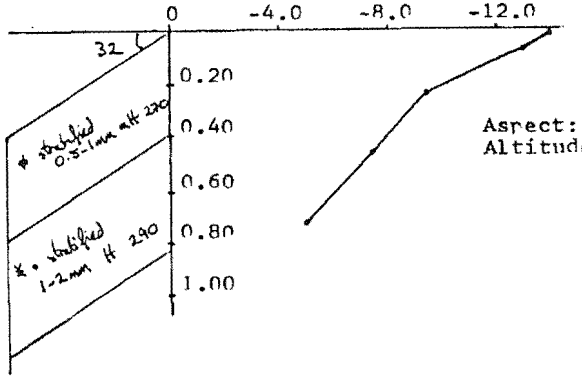

Asrect: S
Altitude: 2160m

CORNICEWALL (20/7/82)

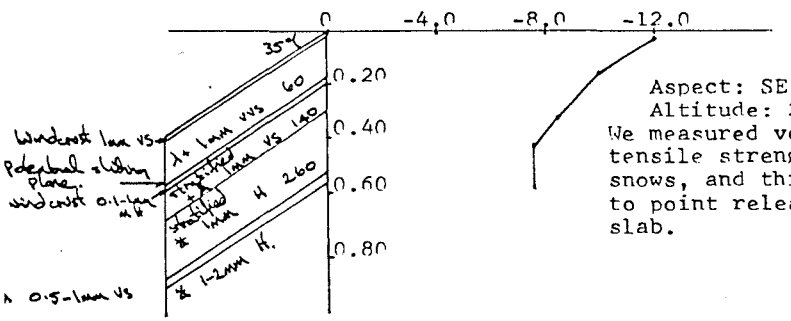

Aspect: SE
Altitude: 2310m
We measured very low shear and tensile strengths in the surface snows, and this snow was tending to point release rather than slab.

CORNICEWALL (15/7/82)

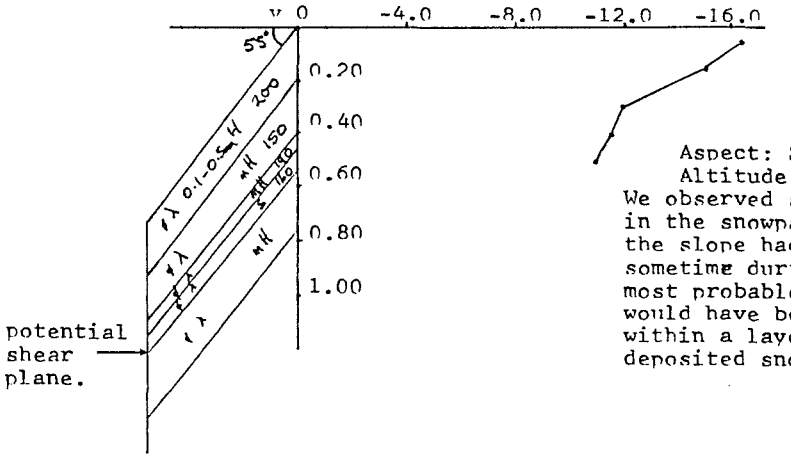

Aspect: SE
Altitude: 2310m
We observed some local cracks in the snowpack, and possibly the slope had avalanched sometime during the storm. The most probable sliding plane would have been at 0.54m within a layer of soft, newly deposited snow.

NOSEDIVE (6/8/82)

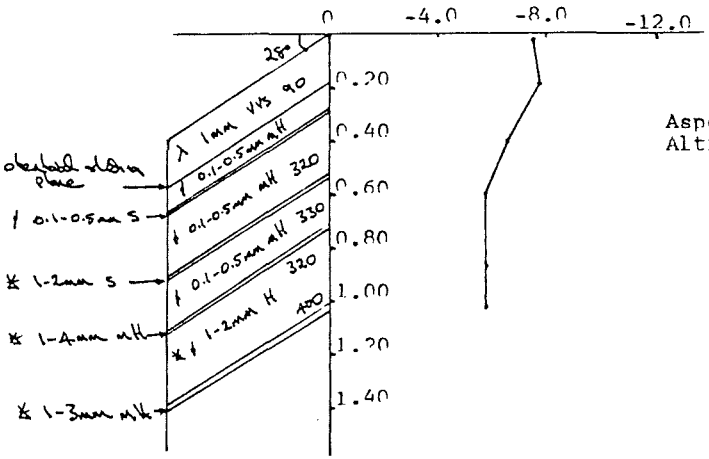

Aspect: S
Altitude: 2160m

CORNICEWALL (19/7/82) FRACTURE.

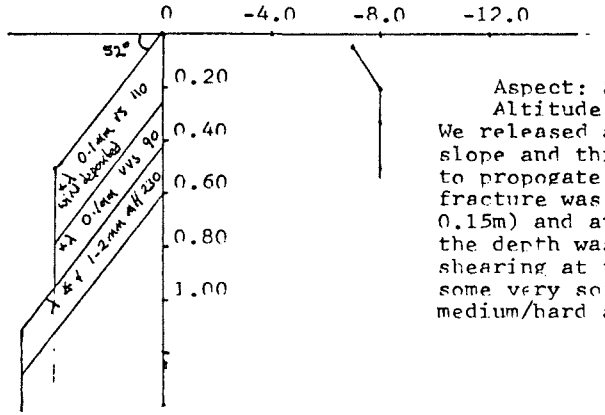

Aspect: SE
Altitude: 2310m
We released a cornice on top of th slope and this caused a small slat to propogate. The depth of this fracture was very variable (0.47-0.15m) and at the pit described, the depth was 0.42m. The slab was shearing at the boundary between some very soft new snow and some medium/hard and well bonded snow.

CORNICEWALL (11/8/82)

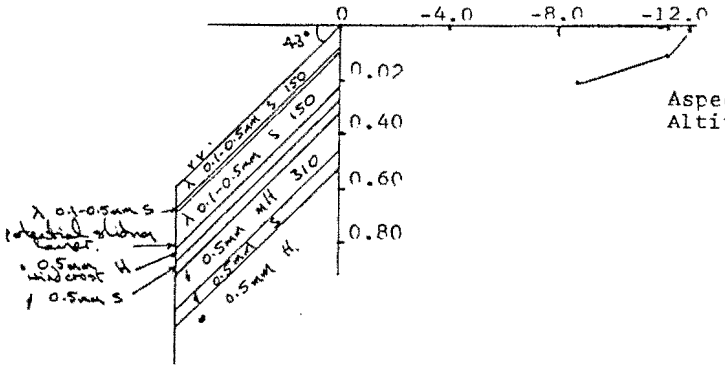

Aspect: SE
Altitude: 2310m

CORNICEWALL (6/9/82)

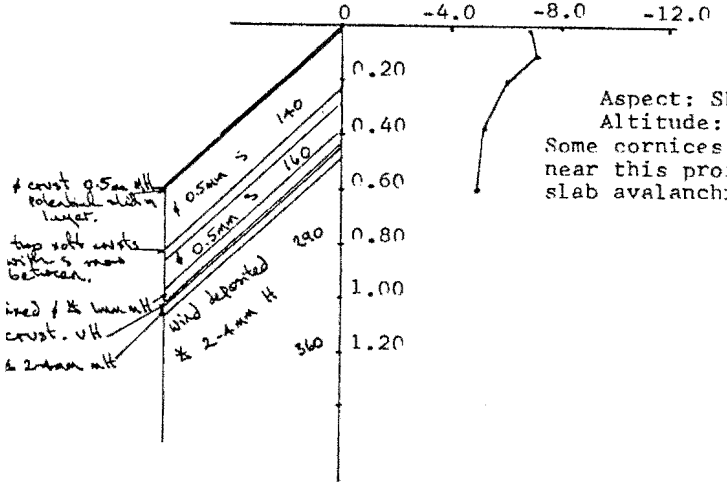

Aspect: SE
Altitude: 2310m
Some cornices that we ski released near this profile did not cause slab avalanching.

HOCHSTETTER DOM FRACTURE (7/9/82)

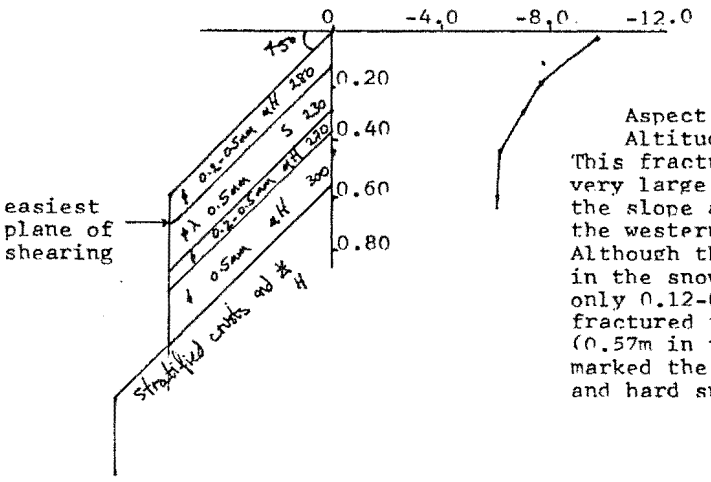

Aspect: S
Altitude: 2270m
This fracture was triggered by a very large iceblock falling onto the slope and we dug this pit on the western extremity of the crown. Although the plane of easiest shear in the snowpack was at a depth of only 0.12-0.18m, the avalanche had fractured to a depth of 0.57-0.84m (0.57m in this profile). This depth marked the beginning of some crusts and hard snow layers.

HOCHSTETTER DOM (9/9/82)

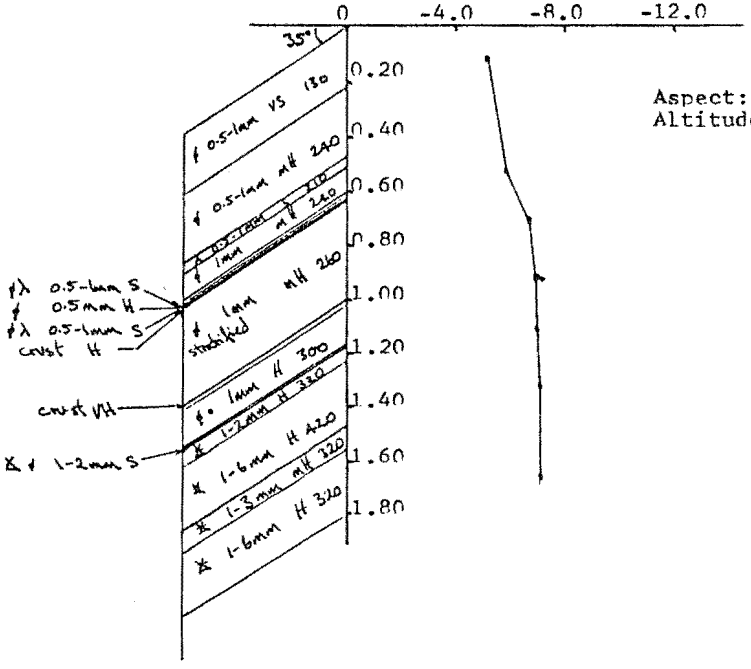

Aspect: S
Altitude: 2310m

CORNICEWALL FRACTURE (19/9/82)

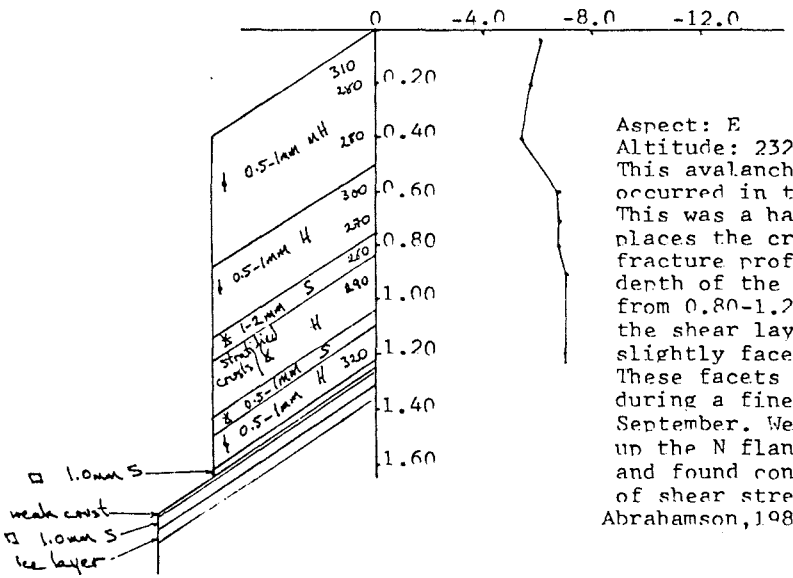

Aspect: E
Altitude: 2320m
This avalanche was one of many that occurred in the area at this time. This was a hardslab and in some places the crown had a double fracture profile. We measured the depth of the main fracture to vary from 0.80-1.25m, and in this profile the shear layer consisted of some slightly faceted crystals at 1.24m. These facets would have developed during a fine period between 14-16 September. We dug a series of pits up the N flank of the avalanche and found considerable variations of shear strength.(see Conway and Abrahamson,1983b).

TASMAN SADDLE SNOW STUDIES, 1981

INSITU TESTS OF LARGE VOLUMES OF SNOW

FINAL REPORT, PART 1, for the Mountain Safety Council - M. Conway
J. Abrahamson

April 1982

INTRODUCTION

Most field strength tests of snow have involved small sample sizes which show large scatter in strength values and consistently high strength values (Sommerfeld (1974)). It is thought that volumes about $1m^3$ may be considered infinite (Sommerfeld (1974)) in terms of flaws, and statistical analysis has been used to extrapolate small sample volumes to large sample volumes. Traditional strength theories which talk about fibre like behaviour are summarised by Sommerfeld (1980), recognising the series-element theories and the parallel element theories, and he indicates that snow fracture behaviour can be described by a combination of these models of failure.

Centrifugal tensile testers have been reported by Keeler and Weeks (1967); Keeler (1969); Martinelli (1971) using sample volumes of $0.5 \times 10^{-3}\ m^3$. This test is not only limited by the small size, but also by difficulties of obtaining an undisturbed sample, and insitu tests are not possible. Perla (1969) undercut cantilever beams of snow in snowpit walls, presuming tensile failure in the top "fibres" of the beam. Although a large undisturbed sample was used, it was difficult to ascertain effects of bending and shear in the beam. A portable constant strain rate tensile testing machine was developed by McCabe & Smith (1978) in which a $3.2 \times 10^{-3}\ m^3$ sample was frozen on to two end plates and strained. Again, insitu tests were not possible. McClung (1979) left some large boxes with removable sides and a movable cart incorporated, in the vicinity of starting zones during storms. After collection the boxes were tilted by lifting one end over a time varying from 1-8 minutes, resulting in a tensile type fracture.

The Roch shear frame tester has been used extensively since Roch (1966) developed it to measure shear frame indices at avalanche fracture profiles. Perla (1980) summarises this work, and again, statistical analysis has been used to rationalise the high indices for small sample volumes ($100cm^2$ Area). Sommerfeld and King (1979) recommend a correction factor of 0.52 based on the Daniels' strength of snow (Daniels (1945)). La Chapelle and Ferguson (1980) developed a wedge that was driven in behind a column of snow, and from this derived a wedge number - an estimate of the layer-parallel component of the applied force over an area of about $0.25m^2$. Personal experience with the wedge has indicated its limited use in soft compressible snows, where the force applied by the wedge is not uniform over the area of fracture.

The present work has evolved from the need for further insitu field tests of snow, and the emphasis is on a large undisturbed sample in a failure mechanism simulating the slab avalanche situation.

SHEAR TESTING

A large Roch type tester was built (Fig. 1) with an area of $0.09m^2$.

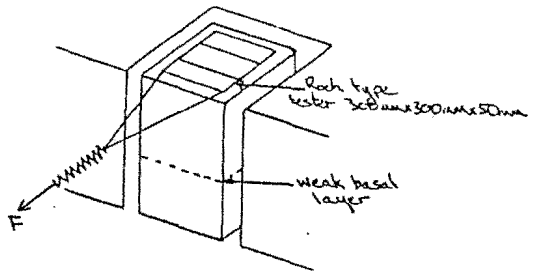

Fig. 1. Shear tests of large volumes of snow

The tester is pushed in flush with the snow surface on a slope. A column is dug out around the tester thus isolating the column from effects of side-shear, compression and downhill tension, to a depth greater than the suspected fracture plane. Placing the tester before isolating the column reduces disturbance of the sample. Slope-parallel tension is applied with a calibrated spring until failure occurs somewhere down the column and the fracture surface area and depth to fracture are measured. Slab density and slope angle measurements make it possible to compute the gravity component parallel to the slope and the sum of this and force to failure gives an indication of shear strength. The test may be repeated down the column below the first fracture.

TENSILE TESTING

A column is isolated on three sides as shown in Fig. 2.

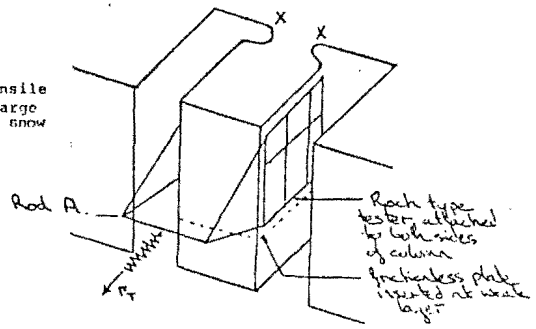

Fig. 2. Tensile tests of large volumes of snow

Two large Roch type testers (area = $0.09m^2$) are placed on each side of the column and are linked to the Rod A to which a calibrated spring balance is attached. A rounded scoop is used at the tensile end X - X to shape the fracture zone. This provided relief of stress concentrations in that zone, and secondly, reduced the pull required to fracture the sample to a force manageable by one person.

A stiff and essentially frictionless plate made from stainless steel (Fig. 3) is slid up the failure plane previously located by the shear test

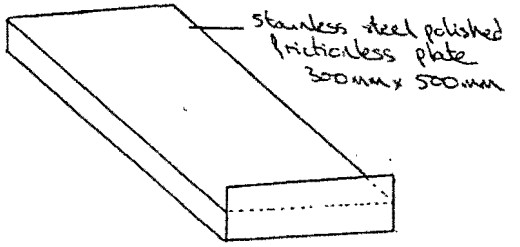

Fig. 3. Frictionless plate for tensile tests

as above. A force is applied until failure occurs. This, together with measurements of slab density, slope angle, area of fracture, enable the computation of the tensile strength.

COLLAPSE TESTING

A 300mm x 300mm plate, roughened on its underside was devised to fit on top of a column after the shear frame had been placed and the column isolated on all four sides (see Fig. 4).

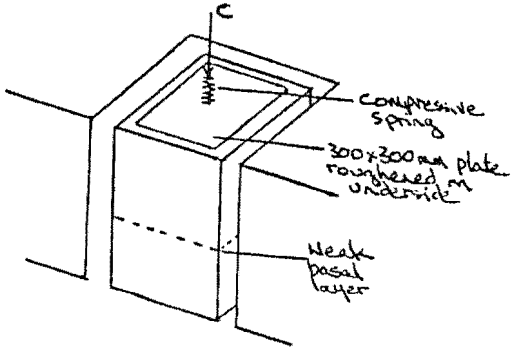

Fig. 4. Compressive collapse testing

A calibrated compressive spring was used to apply a force on the column before the shear tests described earlier were made. In all cases, the normal force was removed while the shear tests were made.

RESULTS OF TESTS

1. Snow Variability

It was noted by Perla (1978) that wind-deposited snow can vary up to 10% in density and on lee slopes, under cornices or other projections, significant variation in wind deposition and wind directions can be observed during storms. This makes lee slopes difficult to ascertain from a geographical standpoint.

Considerable variation of depth of failure planes within small areas on a slope were observed on many slopes this winter at the Tasman neve region. One such case observed was on the locally named Cornice Wall 11/9/81, where fracture planes varied from 105cm to 107cm to 112cm in snow pits dug beside each other. Another case on the Murchison headwall (28/9/81) shows considerable variation in shear strength characteristics. The shear plane varied from 106cm to 114cm with the average at 112cm. Shear strength measurements are summarised in Table 1. Relative locations are marked on Fig. 5.

In cases where the strength:stress ratio is less than 1, the column sheared before the tensile part of the column could be totally isolated. Cases where the shear strength is greater than the number marked indicate that the column did not shear at the 112cm plane before failure around the tester in the snows above.

TABLE 1

Location	σ N/m^2	σ/σ^1
Pit 2	<1110	<1.0
3	<1110	<1.0
4	<1110	<1.0
6	<1110	<1.0
5	>1732	>1.56
8	>1367	>1.23
9	>1340	>1.20

σ = measured shear strength N/m^2
= $\rho g h^1 \sin\theta + F/A$

σ^1 = shear stress in an infinite slab N/m^2
= $\rho g h \sin\theta$

ρ = slab density Kg/m^3

h = depth to fracture plane m

h^1 = depth of snow above fracture when the shear tests were conducted

θ = slope angle

F = slope parallel force applied on Roch tester to failure, N

A = area of plane over which the force is applied, m^2

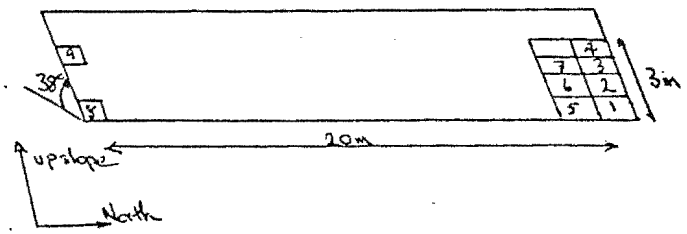

Fig. 5. Location of snowpits, Murchison Headwall 28/9/81

The sliding plane consisted of clusters of graupel up to 3mm diameter. Note that although this slope did not avalanche, avalanches were observed on similar aspects although steeper slopes and many slides were masked by new snowfall.

2. Shear tests and Compressive tests

Gravitational shear stress on a slope is computed, with the assumption that the snow slab is infinite in all directions from:

$\sigma^1 = \rho g h \sin\theta$

ρ = slab density Kg/m^3

θ = slope angle, ^{o}

h = depth to fracture, m

Measured shear strength is computed from

$\sigma = (\rho g h^1 \sin\theta + F/A)\ N/m^2$

F = slope parallel force applied to fracture, N

A = surface area of fracture plane

h^1 = depth of snow above fracture plane when the shear tests were conducted, m

A. Table 2 tabulates some results taken from the Cornice Wall (16/9/81) where slope angle was 28^o. Sampling was within an area of $25m^2$. No compressive forces were applied to the column.

TABLE 2

h(cm)	σ N/m^2	σ/σ^1
30	789	2.52
34	1140	3.64
36	984	3.14
32	1025	3.27
34	780	2.49

The mean shear strength is 944 N/m^2 with a standard deviation of 156 N/m^2 (i.e. 16.5% of the mean).

B. It was found on the Murchison Headwall (17/9/81) that small compressions (about 150 N/m^2) applied perpendicularly on the column prior to shear testing produced a significant reduction in shear strength of the column. It was also possible to observe a clear fracture plane after the collapse. Shear tests prior to compression would often not fail at this plane, or would not fail in a strictly shearing manner, and an irregular failure plane would often be observed. A summary of results from 17/9/81 are shown in Table 3. All pits were dug within an area of $25m^2$ with a slope angle of 35^o, failure plane at 24cm. The sliding plane consisted of needles under a thin crust.

TABLE 3

Before compressions*		After compressions	
σ N/m^2	σ/σ^1	σ N/m^2	σ/σ^1
>1350	>4.25	382	1.20
>1100	>3.46	144	0.45
>1502	>4.72	604	1.90
>1250	>3.93	708	2.23
mean >1300		980	3.08
SD = 169		579	1.82
		mean = 566	
		SD = 285	

* denotes that the fracture was not clear with the applied shear force.

Cases where the index $\sigma/\sigma^1 < 1$ indicate possible effects normal loading has on shear strength, since some of the upper part of the column had been removed prior to the test.

C. Tests on the Cornice Wall (23/9/81) slope angle 44^o are summarised in Table 4. The top 7cm of snow was sluffing off and the main fracture after compression was at 26cm depth. The sliding plane consisted of new snow, 1mm diameter on top of a windcrust.

TABLE 4

Before compressions		After compressions	
σ N/m^2	σ/σ^1	σ N/m^2	σ/σ^1
>1030	>2.54	540	1.33
> 938	>2.32	670	1.65
> 635	>1.57	250	0.61
mean > 870		356	0.88
SD = 207		mean = 454	
		SD = 187	

D. Cornice Wall (26/9/81). Slope angle of 33^o. Settlement sounds were heard over the slope as tests were being conducted, and from skiers crossing the slope. See Table 5.

TABLE 5

hcm	σ N/m^2	σ/σ^1
* 91	978	1.00
*122	<1078	<1.00
#110	< 977	<1.00
	mean = 1011	

* denotes columns settled with small perpendicular force ($\sim$140 N/m^2)
# denotes column settled under its own weight

E. Nose Dive (29/9/81). Before compressions, the shear strength at the 45cm layer was greater than 1675 N/m^2 (strength index $\sigma/\sigma^1 > 2.85$). A large compression (in the order of 2000 N/m^2) caused a failure plane at 45cm (2mm conglomorates of graupel on a rain crust, slope angle 33^o) and the resultant residual shear stress in two tests was 787 N/m^2 ($\sigma/\sigma^1 = 1.34$) and 749 N/m^2 ($\sigma/\sigma^1 = 1.27$). Note in this case the slope-parallel component of the force was about 1100 N/m^2 so this shear stress may have influenced the results. This is unlikely to have been the case in tests previously mentioned where the compressive forces were much lower.

F. Cornice Wall (12/10/81). A sliding plane at 38cm was defined using the shear tests indicating a shear strength of about 1400 N/m^2. The layer consisted of some needles tending towards equitemperature metamorphism, mixed with some 1mm graupel. Very high compressive forces (in the order of 3000 N/m^2) were required to promote a shear type fracture, which again indicates that the slope-parallel component of the downward compression was promoting the fracture, rather than the normal component causing collapse and subsequent shear strength loss.

3. Tensile Tests

Initial tensile tests were made by inserting the frictionless plate up a shear plane (previously defined by the shear tests) on a column isolated on three sides, and slowly sawcutting the remaining side of the column until the downward component of gravity acting on the mass of snow caused failure (Fig. 6).

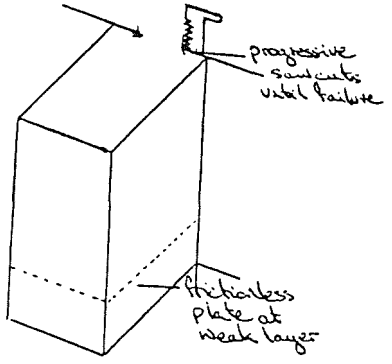

The area left after failure was measured together with slope angle and slab density. This technique was abandoned when

(i) it was thought that the sawcut may be inducing stress concentrations.

(ii) for many snows, the area left after fracture was small (less than 10mm width) and the errors in calculation of tensile strength high.

The technique described previously was developed where a rounded cut was made to reduce the area, and a slope-parallel force applied to the column, and the tensile is calculated from:

$$\sigma_\tau = \frac{g}{A} (W\sin\Theta + \rho V\sin\Theta + F_\tau)$$

σ_τ = tensile strength N/m^2
A = area left after fracture m^2
W = mass of the two Roch testers inserted at the sides of the column Kg
F_τ = mass reading on scale used to apply force to failure Kg
ρ = slab density Kg/m^3
V = slab volume m^3
Θ = slope angle ^{o}

Typical loading times for the tensile tests were of the order of 5-15 seconds.

(i) Tests on Cornice Wall (12/10/81) sliding plane at 38cm, slope angle of 43^o. From two tests, the tensile strength of the slab was 2980 N/m^2 and 2890 N/m^2; mean 2935 N/m^2. On this slab, the shear strength was computed to be about 1400 N/m^2 (see F. of shear test data).

(ii) Cornice Wall (14/10/81). Sliding plane at about 24cm, slope angle 38^o. A summary of four tests is shown below:

	σ_τ N/m^2 at 24cm
Test 1	5222
Test 2	5003
Test 3	8109
Test 4	3210
Mean	5386 SD = 2027 N/m^2

4. Tensile and Shear Properties Summarised

A summary of snowpit shear strengths and tensile strengths is shown below. The tensile tests are those done using the progressive sawcut technique and using the gravitational force of the snow alone to promote failure.

TABLE 6

Date	Location	Slab Density Kg/m^3	Slope Angle θ	Depth of Weak Layer cm	Shear Strength N/m^2 Before Compression σ	σ_1/σ	After Compression σ	σ_2/σ^1	Tensile Strength of Slab N/m^2
16/9/81	Cornice Wall	200	28	33	944	3.34	-	-	1342
17/9/81	Murchison Headwall	236	35	24	>1300	4.09	566	1.78	3450
21/9/81	Murchison Headwall	90	30	17	189	2.52	-	-	84
23/9/81	Cornice Wall	160	44	26	> 870	2.14	454	1.12	1965
26/9/81	Cornice Wall	200	33	108	-	-	<1011	<1.0	-
29/9/81	Nosedive	240	33	45	>1675	2.84	768	1.30	2670
12/10/81	Cornice Wall	224	43	38	1400	2.33	1400	2.33	2935

5. Note on other tests

(i) Side shear

Some preliminary tests were made to find the effects of sideshear in pinning a slab to a slope. These were done by inserting the frictionless plate and cutting out three sides of a column (Fig. 7).

Fig. 7. Sideshear tests

A progressive saw cut was made up the remaining side until the downslope component of mass of snow caused a failure. Typically the area left after failure was small (in the order of (h x .01) m^2 where h is depth of insertion) and difficult to measure accurately. It was noted that the failure was always at 45° to the sawcut, suggesting either a combination of bending/sideshear or a tensile/sideshear mode of fracture as occurs on the flank surface of an avalanche.

(ii) Tensile experiments with a dial gauge

Experiments were made by placing a mechanical dial gauge across the necked area during tensile tests as shown in Fig. 8, and the length of the neck (x) varied to determine sample volume effects.

Fig. 8. Tensile tests with strain gauge

Mechanical contact for the dial gauge were made at points A and A^1 and some difficulty with creep of these contacts (100mm x 100mm) within the snow was experienced.

Preliminary experiments showed that some strain can be observed on application of tensile force, and an increase of length x did appear to increase the measurable creep (see Table 7).

Table 7, Cornice Wall 14/10/81, shows total strain at failure.

TABLE 7

Length x mm	Total Strain mm	Tensile Strength N/m^{-2}
40	.043	8640
130	.064	3575

Note that the time control was not good in these experiments and more experiments are required before firm conclusions can be made.

(iii) Slope-parallel compressive failure measurements

A type of failure expected in the toe of an avalanche was simulated by sliding the frictionless plate in at the expected failure plane of a block of snow shaped as in Fig. 9.

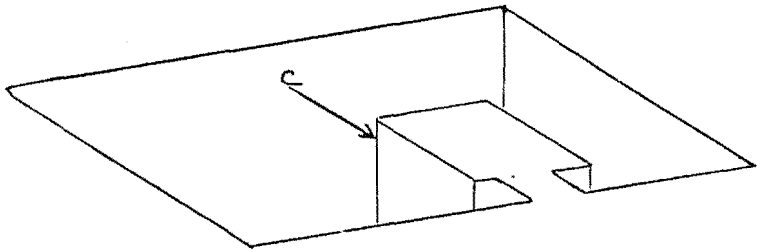

Fig. 9. Downslope compressive failure tests

A compressive force C was applied over the upper end of the column until a compressive failure occurred at the necked region. A few experiments carried out in this manner suggest that it is possible to measure the effect of the compressive region of an avalanche zone in pinning the slab to a slope. For example, on the Cornice Wall (15/10/81) compressive forces applied to a slab were of the order of 5,500 N/m^2 to failure.

6. Downslope measurements of creep rates

Sommerfeld (1975, 1979) (see Fig. 10) measured strain rates on a slope just prior to avalanching and indicates the potential of this sort of measurement for avalanche forecasting. It is thought that in some cases the onset of tertiary (accelerated) creep in a snow slab may be some time before the fracture, thus giving an adequate warning. In order to investigate this further, some strain gauge equipment was wired to a

Tasman data logger, but was not sufficiently sensitive to measure downslope movement during the 1981 winter. This type of measurement will be developed during the 1982 winter.

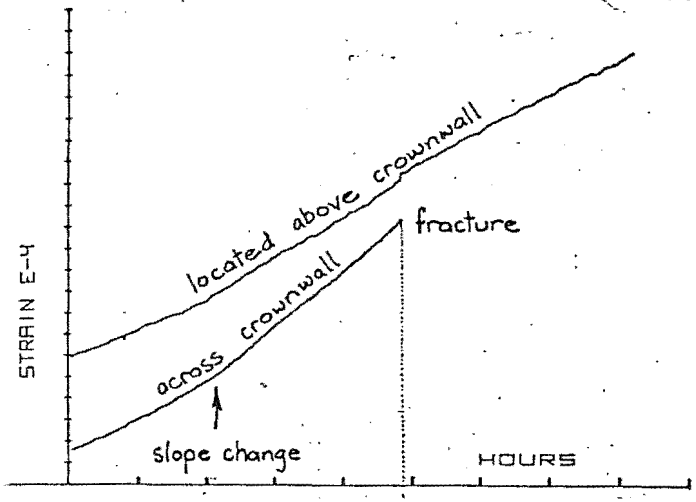

Fig. 10. Strain in units of 10^{-4} vs time in hours on 25/1/77 (from Sommerfeld (1979))

7. Snow testing Apparatus

A semi-portable snow tester has been built in an attempt to study naturally deposited snow under various loading characteristics. The apparatus is capable of shear tests as well as tensile tests of snow volumes up to 300mm x 300mm x 600mm, and is mounted on a pair of skis (see Figs. 11 and 12).

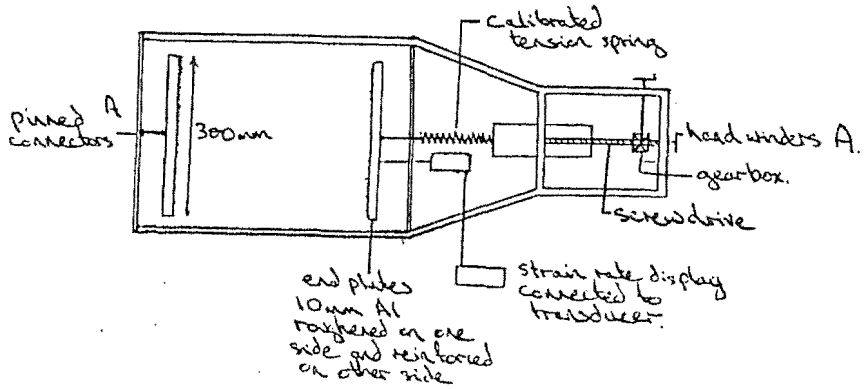

Fig. 11. Tensile tester

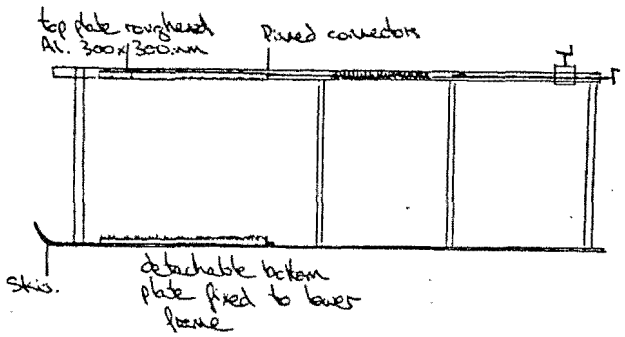

Fig. 12. Shear tests - section AA of Fig. 11

(i) Tensile Tests

A stainless steel sampler is used for collecting a snow sample which is placed on the frictionless base of the tester. Two end plates of 10mm thick aluminium, roughened on one side and strengthened with 10mm box section stainless steel on the other, are heated in a solar heater and then frozen on to the sample (Salm (1971)). The end plates are attached to the frame and tension spring with pinned connectors, and the load applied through a calibrated spring. Rates of load application may be varied using a gearbox and the manual winding mechanism. Movement of the end plate is measured through a transducer, and a strain rate readout is displayed. Two sets of end plates have been constructed, one 300 x 300mm and the other set 300 x 50mm. Sample length can also be easily varied.

(ii) Shear Tests

A sample is placed between the base plate (300 x 300mm) and top plate (300 x 300mm) and set into the tester. The base plate is fixed to the frame of the tester, and a pinned connection is made between the top plate and the calibrated spring. Again loading rates can be varied using the manual winder and gearbox.

Two typical tensile type tests are graphed in Graphs I and II and in many other tests problems were encountered in temperatures higher than $-5^{o}C$ where end plate freezing was slow or not sufficient.

Further problems encountered were:

(i) transducer sensitivity in measuring very low strain rates. The measuring techniques have been modified to try to overcome this problem. (Instead of a pulley and circular potentiometer, we are now using a linear drive potentiometer).

(ii) apparatus portability limits its use to easily accessible snows.

(iii) Sampling of snows without disturbing the sample. This has been largely overcome by using the snow sampler (Fig. 13) although testing of very soft snows (density less than 120 Kg/m^3) is difficult without sample disturbance. Variation within a snow pack over small areas (2 m^2) has already been mentioned, making closely reproducible results on natural snows unlikely.

DISCUSSION OF RESULTS

None of the measurements collected over the 1981 winter were on avalanche fracture line profiles, although on the Murchison Headwall (17/9/81) slides on steeper adjacent slopes had occurred and the headwall was considered to be only marginally safe for travel. On the Cornice Wall (23/9/81) the data was collected during a storm and on the Cornice Wall (26/9/81) settling noises were heard as the tests were being made. More measurements of tensile and shear properties are required on fracture line profiles before an estimate of a stability index could be made using these parameters.

The speed of fracture in an avalanche is uncertain (Gubler (1978), Sommerfeld (1980)). Effects of rates of loading for fractures have been studied in a number of laboratory tests (McClung (1977), McClung (1979), Narita (1980)) and loading rates have been shown to be critical in determining the maximum material strength. For example, a fast brittle type fracture will tend to rupture at a lower load than a slower more ductile type fracture. Rates of the tensile and shear tests described in this paper are in the order of 10 to 30 seconds to failure, which suggests the failure is both elastic and plastic (Gubler (1978)).

1. Shear tests

Traditional shear frame tests where a small tester ($0.01m^2$) is placed in the weak layer, have been found to be strongly dependent on (i) size of frame (ii) operator variability in loading rates and shear frame alignment (Perla (1980)). Perla (1977) found that a $0.1m^2$ area frame indicated 64% of the strengths of the $0.01m^2$ frame. He summarised shear strength to load tests of over 80 cases on fracture line profiles, and found the mean index to be 1.66 (standard deviation 0.98). Table 6 contains a summary of results on the stable snows tested during the 1981 winter on the Tasman glacier using the technique described earlier.

The advantages of using this technique over the traditional technique are:

(i) sample disturbance is minimised.

(ii) the sliding plane is easily located and placement of the frame exactly in the correct layer is not a problem.

(iii) the normal loading on the sample is generally retained.

(iv) A detailed analysis of snow pit stratigraphy above the fracture plane is not necessary since the weakest layer is easily defined. The parameters required to determine the stability index include slab density, slope angle, depth to fracture as well as the force required for the fracture and the surface area of the fracture.

Preliminary data indicate that these tests will be useful in terms of stability evaluation.

2. Shear perturbations as a result of compressions

Prior to a perpendicular compression, many fracture planes were not well defined, and shear planes would often exhibit an irregular surface (Fig. 13).

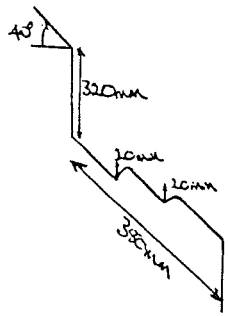

Fig. 13. Profile of an irregular sliding surface before compression, Nosedive 13/9/81

In many cases, a small perpendicular compression would define a fracture plane, and as shown the resulting shear strength would be reduced by about 0.5 the value before the perturbation. In a few cases (e.g. Murchison Headwall 28/9/81 and Cornice Wall 26/9/81) columns of snow visibly settled as they were being isolated from the surrounding snow-pack.

McClung (1977) finds that when some snows are sheared, the shear stress reaches a peak after a relatively short displacement (which he calls a "cohesive" component of shear) and then drops until a residual stress value ("frictional" component of shear) is reached at larger displacements. A possible effect of a normal compression which is strain limited, could be to overcome the cohesive component of the shear. It should be noted that in many of the columns studied, the slope-parallel component of the perpendicular force applied was well below that expected to promote shear. Basset (1978) indicates that a reduction in the void or packing ratio either by continued deformation resulting in closer packed non random assemblages, or by particle disintegration results in a lower frictional resistance than the original random state. Particle disintegration and hence a reduction of the void ratio seems to be a likely mechanism for reducing the shear strength in the above tests, and it is interesting to note that the compressions were most effective in low density snows consisting of needles and/or stellar crystals.

In the snows tested containing large graupel clusters (up to 3mm diam), the shear properties were not altered appreciably by the compressions. The relatively indestructible nature of the balls compared with the low density needle-like crystals would not be conducive to large reductions of void ratio. No snows containing layers of temperature gradient crystals were tested but collapse of such crystals has been recorded (Bradley (1970), Bradley, Brown and Williams (1977)) and such a collapse would also involve a large reduction of the void ratio and subsequent

loss of shear strength. Basset (1978) also notes that the reduction in volume, if free water is available, would give rise to excess water in the shear zones, hence lubricating the shear plane.

Many avalanche release models have been developed to study the effect of bed surface weakness (Perla and La Chapelle (1970), Brown et al (1973), Lang et al (1973), Lang and Brown (1975)). The model developed by Perla and La Chapelle (1970) predicts failure in the tensile zone when the slab is unable to sustain basal stress, and the two modes of failure reinforce one another until the slab fails catastrophically. Perla (1980) uses equations from the Perla and La Chapelle model to note that a shear loss of 50% of the shear strength over a distance of ten times the slab thickness would increase the maximum principal tensile stress by a factor of five.

3. Effects of normal loading

In several cases, after parts of the upper layers of a column had been removed, it was noted that the shear strength measured was less than the shear stress expected by gravity prior to removal (for example, test 2 on Table 3 and test 3 on Table 4).

This behaviour may show an increasing shear strength with increasing normal loading (which has been reported by McClung (1977)). Another possibility is the disturbance and consequent weakening of the weak layer by the snow removal.

4. Tensile tests

The tensile tests described above have several advantages over traditional tests:

(i) the sample disturbance is minimal and the test involves the slab above the weak layer, and hence closely resembles the avalanche situation.

(ii) the large sample volumes result in a more representative sample.

(iii) sample disturbance is minimised.

From Table 6 it is seen that the tensile strength is in most cases larger than the shear strength below the slab. The average tensile strength was twice the shear strength, although in one case the slab tensile strength was about half the shear strength (Murchison Headwall 21/9/81).

5. Surface sluffing

Loose snow avalanches start in cohesionless surface layers of snow and is a rotational type of failure. A snow layer 17cm depth (ρ = 90 Kg(m^3) on the Murchison Headwall (21/9/81) was measured to have a shear strength of 189 N/m^2, a shear strength to gravity shear stress ratio of 2.52 and a tensile strength of 84 N/m^2. These very low values of strength may have been the cause of many surface slides as the temperature increased during the day, releasing snow from rocks above the slope which in turn triggered the sluffs. Further studies are required to determine a stability index for loose snow slides.

6. A Stability Index for Snow Slabs

A slab on a slope can be thought of as being pinned to the slope at the basal layer, at the flank walls, at the staunch wall and at the crown wall. Field tests in the compressive zone are difficult and the importance of flank wall pinning is uncertain. Most field stability tests consider the slab as being infinite, and tests involve the shear plane characteristics and the tensile characteristics of the slab above this plane. The present experiments are aimed at:

(i) determining the shear strength and shear stress below the slab.

(ii) determining the variation of shear strength beneath the slab. For example, large areas of reduced shear will produce high tensile stresses in the slab above. The variations of snow properties are critical.

(iii) determining if the shear strength of the layer beneath the slab is reduced by a perpendicular force (say by a skier, new snowfall or bomb-blast loading) and determining the resultant shear strength. If the compression weakening does occur, the force for the compression required and the area of the bed affected becomes critical and should be measured. For example, we could expect a larger area to be affected by a localised compression as the slab becomes stiffer.

(iv) determining the tensile strength of the slab and finding the state of creep of a snow slab and the conditions required to promote tertiary accelerated creep (for example, extra loading, temperature increase). A critical length L for tensile fracture may be calculated by doing a force balance over the infinite slab at the critical condition (when both shear and tensile strengths are balanced by gravity):

$$\sigma_T \times h \times w = (\sigma^1 - \sigma) \times L \times w$$

$$L = \frac{\sigma_T \times h}{(\sigma^1 - \sigma)}$$

h = depth of slab

σ_T = tensile strength of slab

w = width of slab

σ^1 = shear stress due to gravity, in an infinitely extending slab

σ = shear strength $\quad \sigma^1 > \sigma \qquad$ i.e. $\frac{\sigma}{\sigma^1} < 1$

(v) determining the effects of sideshear and compressive forces in the toe region of the slab.

As an example of the simple predictions which may be attempted from these tests, consider the shear strength to shear stress ratio (σ/σ^1) figures in Table 3. Ignoring rate effects and assuming that additional snowfall is equivalent to the vertical compressive force exerted by the experimenter, we can calculate the snowfall necessary to bring about compressive collapse of the shear layer and then also that snowfall necessary to overcome the reduced shear strength. 150 Nm^{-2} was required to collapse the shear layer, so 100 mm of new snow (150 $Kg(m^3)$ will cause the shear

reduction and will add an additional 86 Nm^{-2} shear stress in the slope parallel direction. Using the "conservative" σ/σ^1 figure of 1.20 (since this is the lowest of the figures resulting from tests with full normal loading), the 100 mm snowfall has increased the shear stress to 404 Nm^{-2} which is greater than the shear strength.

From Table 6, the average tensile strength of the slab above the shearing layer was 3450 N/m^2 over a depth of 240mm. Assuming the additional 100mm of snow has a similar tensile strength, the critical length is computed to be:

$$L = \frac{3450\ (240 + 100) \times 10^{-3}}{(404 - 382)}$$

$$= 53 \text{ m. for shear and tensile failure}$$

If say 200mm of snow had fallen, the length required to fracture decreases to 14m, assuming no changes in the shear strength characteristics of the basal layer.

This calculation of a critical length assumes that the snow has to move to overcome the shear strength at the weakest layer, and this movement is only allowed if tensile fracture occurs. Thus the gravity component causing avalanche must overcome both shear strength and tensile strength in their respective locations. A more complete analysis may reveal that loss of shear strength may occur without tensile fracture, but this will require measurements of strains.

In determining how far the loss of shear may occur from a locally weak area, we will have to compare the typical strains necessary to cause loss of shear, with those resulting from tensile stretching and creep.

Other future tests have been planned to determine the extent of a compressive failure of the shear plane along the snow slab by:

(i) shaping a column as shown in Fig. 14.

(ii) compressing region X.

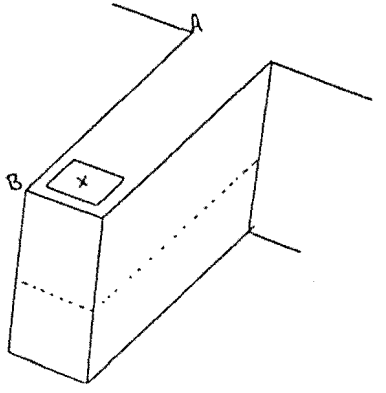

Fig. 14. Techniques for determining effects of compressive perturbations on the basal layers

(iii) isolating a 300mm x 300mm column at this region and completing a shear test as described earlier in this report.

(iv) Repeating progressive shear tests up the column (from B to A) until the shear strength increases to its value before the compressions.

(v) measuring the length of reduced shear.

It would be expected that a hard slab would require a higher compressive force to failure, but would fracture over a large area compared with a soft slab which could be expected to fracture more locally under perhaps a smaller compression.

7. Tensile tests with the snow testing apparatus

Two tensile tests on the tensile test apparatus are graphed in Graphs I and II. Sample B may have fractured prematurely at the end plates, and both samples show an increasing strain rate prior to fracture. The samples were collected from a 10^{o} slope near the Tasman Saddle hut and some stratification and discontinuities were noticed within the samples. More tests are required to determine effects of loading rate on the tensile strength of the sample and the effects of loads on the creep rate of the sample. For example on sample A, after the load was held steady, the strain rate initially decreased but kept increasing. This suggests that at point X marked in Graph I, the sample was already in a stage of tertiary ("runaway") creep.

CONCLUSIONS

Insitu tests of strength of large volumes of snow were developed and preliminary investigations show that these tests may give a useful indication of slope stability. Further tests need to be made on avalanche fracture profiles using the tests developed to find a reliable failure criteria for a slab. Perla and La Chapelle (1970) indicate how critical a loss of shear or compressive support at the base of the slab could be in inducing high boundary stress conditions, and this type of failure could well be a feature of many avalanches. Testing of collapse of the shear layer in relation to skier loading, snowfall loading and explosive shock loading will require further investigation, perhaps using variations of the tests devised during the 1981 season.

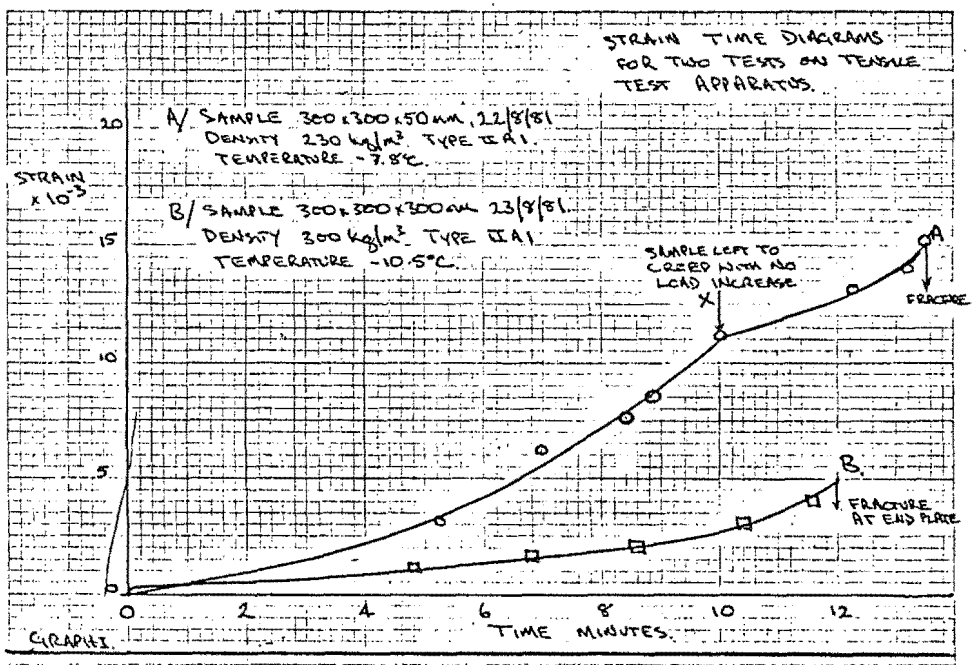

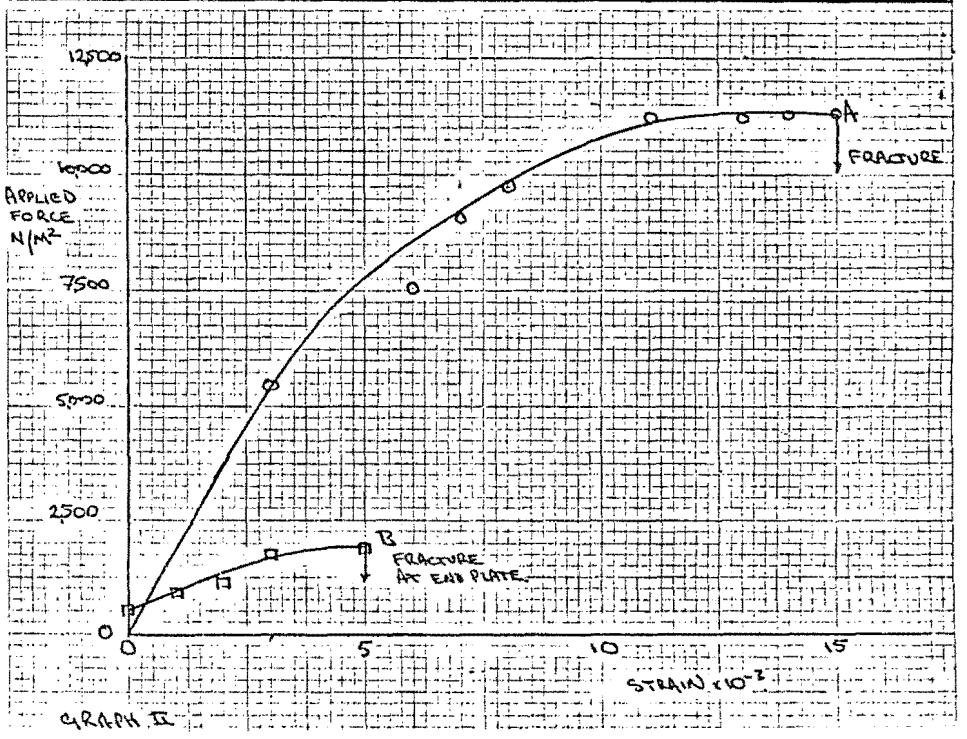

REFERENCES

Basset R.H. (1978) In "Creep of Engineering Materials" (ed. C.D. Pomeroy) Chapter 2. Published Inst. of Mechanical Engineers 1978.

Bradley C.C. (1970) J of Glacial 9 pp253-261.

Bradley C.C., Brown R.L., Williams T. (1977) J of Glacial 18 pp145-147.

Brown R.L. et al (1973) J of Geophys. Res. 78 pp4950-4958.

Daniels H.E. (1945) Proc. of the Royal Soc. of London. Ser. A, Vol.183 No.995 pp450-455.

Gubler H. (1978) J of Glacial 20 pp343-357.

Keeler G.M. (1969) US CREEL Research Report 271.

Keeler G.M., Weeks (1967) US CREEL Research Report 227.

La Chapelle E.R., Ferguson S. (1980) J of Glacial 26 pp506-511.

Lang T.E. et al (1973) J of Geophys. Res. 78 pp339-351.

Lang T.E., Brown R.L. (1975) IAHS-AISH Publ. 114 pp311-320.

Martinelli M. (1971) US Dept. of Ag. Forest Service Research paper RM-64.

McCabe S.L., Smith F.W. (1978) J of Glacial 20 pp433-438.

McClung D.M. (1977) J of Glacial 19 pp101-109.

McClung D.M. (1979) J of Geophys. Res. 84 pp3519-3526.

Narita H. (1980) J of Glacial 26 pp275-282.

Perla R.I. (1969) J of Glacial 8 pp427-440.

Perla R.I. (1977) Can. Geotech. Journal 14 pp206-213.

Perla R.I. (1978) In "Rockslides and Avalanches" (ed. B. Voight) Vol.1 pp731-752. Elsevier, Amsterdam..

Perla R.I. (1980) In "Dynamics of Snow and Ice Masses" (ed. S. Colbeck) Chapt.7, Academic Press, London.

Perla R.I., La Chapelle E.R. (1970) J of Geophys. Res. 75 pp7619-7627.

Roch A. (1966) IAHS- -AISH Publ. 69 pp182-195.

Salm B. (1971) Inst. of Low Temp. Science Series A, No.23 pp1-43.

Sommerfeld R.A. (1974) J of Geophys. Res. 79 pp3353-3356.

Sommerfeld R.A. (1975) IAHS-AISH Publ. 114 pp293-297.

Sommerfeld R.A. (1979) J of Glacial 22 pp402-404.

Sommerfeld R.A. (1980) J of Glacial 26 pp217-223.

Sommerfeld R.A., King (1979) J of Glacial 22 pp547-549.

TASMAN SADDLE SNOW STUDIES, 1981

WEATHER DATA REPORT, WINTER 1981

FINAL REPORT, PART 2, for the Mountain Safety Council

H. Conway
J. Abrahamson

April 1982

Data collected from mid-August to mid-October from Tasman Saddle has been compared with Mt. Cook Village data collected over the same period in an attempt to establish a relationship between weather events at the two sites. If a satisfactory correlation can be found, this would be a valuable tool for avalanche forecasting.

The present data, when plotted for this comparison, in Figs. I, II, exhibit considerable scatter, and some of the possible causes of this scatter are listed below:

(i) Windrun

(a) Incorrect data caused by icing problems on the Lambrecht anenometer (both icing of the chart and of the cups) made for difficulties in assessing wind strength and direction at a particular time. It appears that if precipitation was occurring at a temperature of less than about $-8^{\circ}C$, icing invariably occurred on the anenometer.

(b) Difference of site situations, for example the Tasman Saddle instrument was situated above a 200m cliff with many eddy currents associated with this site. The Tasman saddle location is also very affected by the surrounding mountain topography, and any winds from the West tend to be channelled through the NW direction. Southerly storms funnel up the Tasman glacier and reach the site as a SW storm.

(ii) Temperatures

Most of the data was collected during the Westerly cycle over September and October 1981, but lapse rates could be expected to be different for different types of storms. Further investigation of these characteristics will be made during the 1982 winter.

(iii) Precipitation

This probably incorporates the greatest scatter of the results, perhaps largely due to the nature of the recording site at Tasman Saddle. On days of high winds, snow surface scouring sometimes occurred whereas a relatively high precipitation was recorded in the Village. The difficulty of finding a sheltered and representative site close by to the hut has not yet been solved.

ANALYSIS OF DATA

1. Windrun

The windrun at Tasman Saddle over the twenty-four hour period from 8.30 a.m. - 8.30 a.m. was compared with similar data collected from Mt. Cook Village. A regression analysis was made using 43 comparisons, and the result plotted on Graph I. The regression line determined from this is:

Wind (Tasman Saddle) = 145 + 0.77 x Wind (Village)

Where Wind (Tasman Saddle) = Wind run over a 24 hr period measured in Nautical miles

Wind (Village) = Wind run over a 24 hr period measured in Kilometers

The residual standard deviation above and below the line was 127.

Further data is required to determine a change in the correlation with changing wind direction.

2. Temperature

Minimum temperatures at Tasman Saddle and about Mt. Cook Village are compared (Graph II) and the regression line determined to be:

$$T_{Tas\ Saddle} = -9.8 + 0.7 \times T\ Village$$

Temperatures are in degrees centigrade
The residual standard deviation was ± 3.1

More data is required to determine the significance of the direction and type of storm or airflow on the lapse rate. However, it is interesting to note that the above regression line indicates that for warm conditions the temperature difference between sites is high compared with cold conditions.

3. Precipitation

No satisfactory correlation has been possible with data collected from the 1981 season. As previously mentioned, scatter is probably a function of the exposure of the sites at which the measurements are being conducted.

CONCLUSIONS

Reasonable correlations between Tasman Saddle and Mt. Cook Village have been found for windrun and minimum temperature, but no correlation could be found for precipitation. Since this is of primary importance for aiding avalanche forecasting from the Village, a special effort will be made this (1982) winter to:

(i) ensure data is accurate

(ii) try and establish a measuring stake that is less subject to wind erosion from the site used during the 1981 season.

It is also thought to be of primary importance to establish relationships between the snow fall at Tasman Saddle and the snow fall at the various avalanche paths in the area, and this too will be attempted.

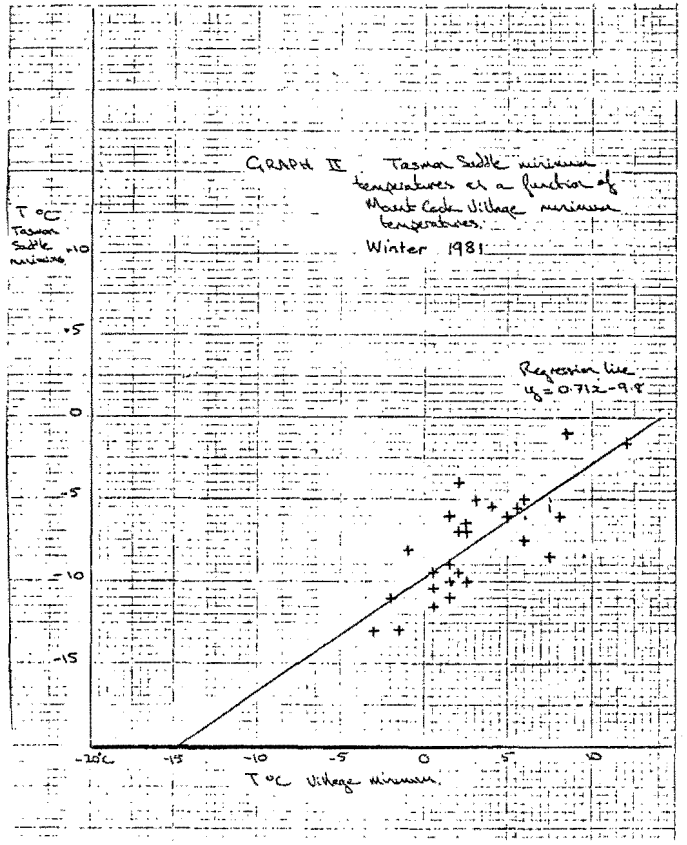

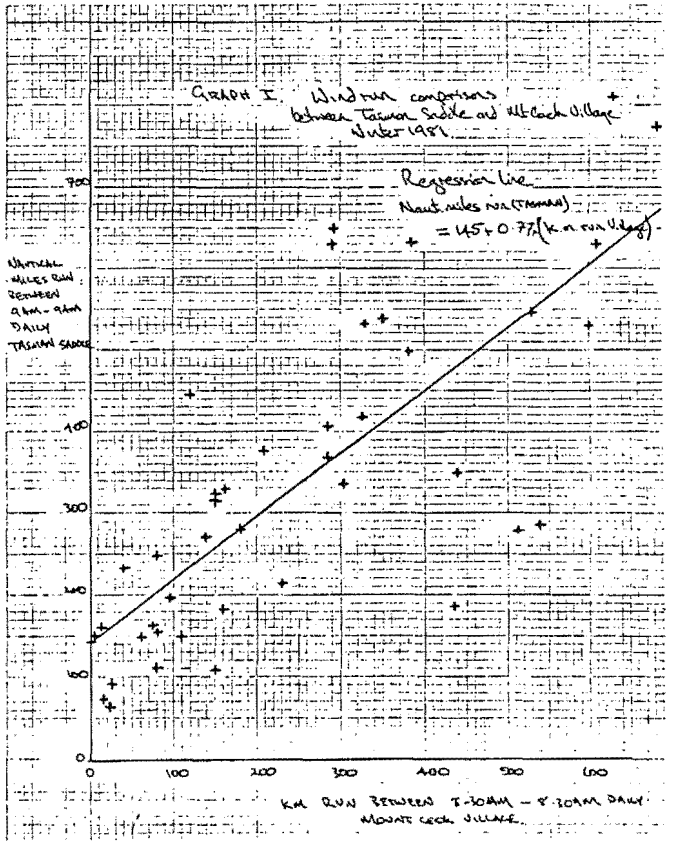

TASMAN SADDLE SNOW STUDIES, 1981

AIR PERMEABILITY AS A MEASURE OF SNOW STRUCTURE

FINAL REPORT, PART 3, for the Mountain Safety Council - H. Conway
J. Abrahamson

May 1982

INTRODUCTION

Shimizu (1970) developed a correlation between the air permeability of snow, crystal size, crystal type and density, for fine grained snow through various stages of metamorphism.

$$B = \frac{7.7 \times 10^{-5} \, d_o^{\,2} \exp(-7.5\rho_s^*)}{\mu} \qquad \ldots\ldots(1)$$

B is the air permeability for fine grained snow $m^4 N^{-1} S^{-1}$

d_o is the crystal diameter, m

ρ_s^* is the specific gravity of the snow

μ is the air viscosity, N S m^{-2}

Martinelli (1971) found that air permeability helped clarify some of the scatter in the tensile strength, density relationship of snow. He suggests there is an optimum texture, or permeability of a snow of a particular density at which the tensile strength is a maximum (Fig. 1).

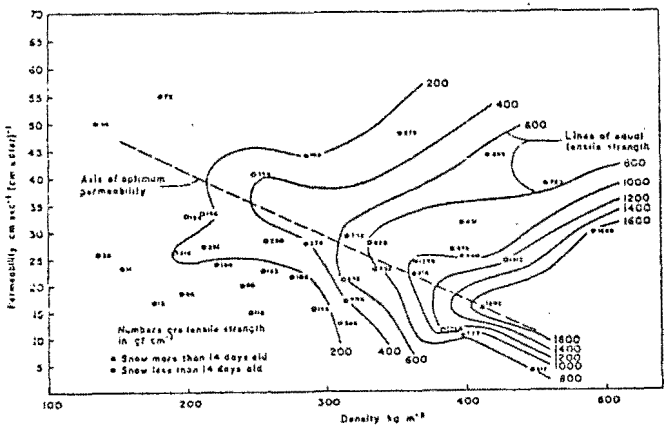

Fig. 1. Tensile strength as a function of air permeability; snow age not limited to 14 days or younger. (from Martinelli (1971)).

Kry (1975) concludes after tests with homogeneous snows under uniaxial compression that the viscoelastic properties of the sample are strongly related to its stress history. He found that as the sample was densified, the elastic properties increased almost linearly and the viscous properties exponentially. Gubler (1978) concludes that tensile strength of snow is a function of snow texture rather than density. There are two major classes of statistical strength theories: series-element theories and parallel-element theories.

Sommerfeld (1980) summarises these theories and applies them to snow failure, suggesting that shearing type failure exhibits parallel-element type characteristics while tensile tests indicate that both theories may be applicable depending on loading rates.

Measurements by Narita (1980) with samples under uniaxial tension at varying deformation rates show the change in deformation mode from brittle to ductile as the strain rate was changed from high to low rates. During the ductile deformations, he observed small cracks across the sample at right angles to the direction of deformation.

A snow slope that has not yet failed in tension, could be expected to exist in a stage of creep, the stage of creep being characterised by the change in snow structure down a slope. As the snow changes from a horizonal, unstressed condition to a region of tension further down a slope, grain bond elongation and small cracks as observed by Narita (1980) could be expected. In the compression zone of a slab, bonds would be expected to initially exhibit bending characteristics and a less aligned type of structure may develop.

Preliminary studies with a portable air permeability device were made in 1981 on slopes around the upper Tasman glacier 2100m asℓ) to see if air permeability might indicate structure changes which occur down a slope. At a later stage these indications may be related to stability strength indices.

THE AIR PERMEABILITY DEVICE

This consisted of (see Fig. 2):

(i) A tank with volume of 4ℓ which was pressurised by a hand pump. The tank had a pressure gauge and a rapidly activated on/off valve.

(ii) A sampling head which could be removed from the device to sample a 0.312ℓ sample of snow. The head had a 1.1mm diam. orifice at the base through which pressurised air flowed from the tank, governed by a flow rate, tank pressure relationship (see Appendix I). A Dwyer manometer (type Dwyer Mk II) with a range 0-80mm water was attached to the side of the sampling head to measure the pressure drop over the sample.

The sampling head was made from perspex tubing to minimise heating from radiation, and a rubber O ring was used at the base of the sample to reduce edge effects. Some glass fibre baffles were used at the base of the sampling head to:

(a) disperse the flow laterally before the sample;

(b) to stop venturi effects past the manometer probe which is located directly beneath the sample.

The overall dimensions of the permeometer (excluding the pump) were 500mm x 350mm x 300mm and the weight 6.2 kg.

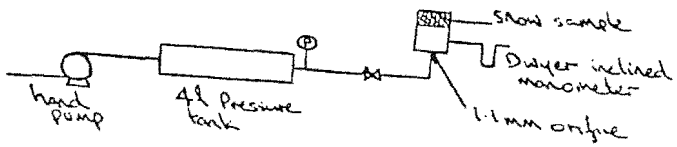

Fig. 2. Schematic drawing of the Permeometer.

EXPERIMENTAL PROCEDURE

Most of the experiments described in this report were made on the upper Tasman glacier (2,100m) in the Mount Cook National Park. This is a region of high snowfall where storm cycles may typically deposit 0.3 - 1.5m of snow with a density variation of 80-250 Kg/m^3. Winter snow pack temperatures may vary from -2°C to -25°C. The region is noted for considerable wind strength and most snowfalls are associated with wind. The area has a glacial base. Most tests were made on a region locally known as the Cornice Wall. Samples taken were cylindrical in shape, and most samples were taken with their axis perpendicular to the snow surface so that the test airflow was perpendicular to the snow surface. Some experiments were made with sampling slope-parallel (up the slope) and slope parallel (across the slope), to determine changes in those directions.

D'Arcy's law states for low velocities (in the laminar flow region) that the rate of flow of a fluid through a bed of particles is directly proportional to the pressure gradient causing the flow. Thus if a volumetric flow rate Q flows through a sample of cross-sectional area A and length L under a pressure difference ΔP between the ends, then

$$Q/_A = \frac{B\Delta P}{L} \quad \text{where B is a constant ("fluid permeability")}$$

A typical plot of flow rate and pressure drop is shown in Graph AII.

Sampling was done down a potential avalanche slope with special efforts being made to sample the same snow layer down the slope to eliminate variability of age, crystal size and type and snow density. The winds associated with snow deposition in the area make this difficult, and some variation of these parameters was noted. Measurements of crystal size and type were made with a 10x hand lens and grid, densities with a Taylor-La Chapelle density kit and snow temperature, slope profile and angle and an estimate of snow age were recorded at each site.

One sample (Cornice Wall 18/9/81, site 3) was retested several times to investigate the effects of the air flow through the sample on permeability, and a regression analysis on this sample was made to determine the variability of air permeability with flow rate (see Graphs AII and AIII).

EXPERIMENTAL PROBLEMS

One of the principle problems in the initial tests when a stainless steel sampling head was being used, was the absorption of radiation from the sun causing free water to form at the sampler walls and to percolate down the sampling head and into the air lines. This had three different effects:

(i) icing on the gauze holding the sample in place and an unusually high pressure drop;

(ii) free water across the orifice reduced the flow rate for a given pressure ratio and resulted in an unusually low pressure drop over the sample for a given pressure ratio. Popping noises were heard in these cases where water restricted flow through the orifice;

(iii) gaps appearing next to the sampler walls presumably provided an enhanced wall bypass of air and a lower pressure drop not representative of the snow.

Radiation problems were minimised by using a perspex sampling head with a very coarse perspex grid.

Obtaining a uniform and undisturbed sample was easier in large layers (greater than 7cm thick) of more dense snow (greater than 200 kg/m^3) than in layered and/or less dense snow. Perla (1978) suggests a density variation of at least 10% in wind deposited snows, and considerable variability of snow strength parameters was recorded on slopes of the upper Tasman glacier during the 1981 winter. A wide scatter of permeability at the same site is expected and at least three samples were taken at any given site.

RESULTS OF TESTS

A summary of tests done on three different days at various sites is listed in Appendix IV. Velocities have been corrected for altitude and temperature using Graph AI (see Appendix I). Pressure drops measured over the sample have allowed for a lag time inherent in the apparatus (see Appendix II).

1. Effects of Flowrate on Air Permeability

Using data from the Cornice Wall (18/9/81) at site 2 (see Appendix IV, Part 2) a regression analysis was made using the flow velocity and the air permeability (Graph AIII). The regression line calculated was:

$$B = -0.17 \times 10^{-4}\, u + 8.65 \times 10^{-5}$$

B = Air permeability $m^4\, N^{-1}\, s^{-1}$
u = Air velocity mm/sec

Comparing the ratio of the line variance to the residual variance with the tables value of F, the slope of the line was not found to be significantly different from zero (0.10 level).

To check that the flow through the snow was laminar, a calculation was made of the characteristic Reynolds number of the flow, and the magnitude of the turbulent contribution to pressure drop. We used the Ergun equation (Bird, Stewart and Lightfoot (1960)). The calculation (see Appendix III) indicates that the air permeability B should drop by 8% for flow rates increasing from 5 to 10 cm sec^{-1} and this is confirmed in the experimental data. (The regression line indicates a 12% reduction). The Ergun equation also indicates that the measured air permeability was about 9% low at a flow rate of 50 mm s^{-1} when compared to flows where the flow is strictly laminar, and 16% low at the higher velocity (100 mm s^{-1}).

2. Effects of Sample Area

Results from a comparison of sampling using two different sampling areas are listed in Part 5 of Appendix III. A t-test used to compare the mean air permeabilities indicated a significant difference. There are two possible reasons for a high air permeability for the large area compared with the smaller sample area:

(i) The very high flowrates through the small sample may result in the pore flow being more turbulent than the flow through the large sample. In the small sample this is expected to lower B by 22% (calculated using the Ergun equation) for an average increase of air velocity from 8 to 26 cm s^{-1}. This compares well with the 27% reduction observed.

(ii) A small sample size could be expected to contain fewer flaws than a larger sample, giving a smaller B. There was one suspected

(iii) Edge effects around the circumference of the sampler could be of importance. For example, if we consider these wall effects as a crack around the circumference, then for a given pressure drop across the sample, the flow will be the sum of flows through the crack and snow.

$$Q \text{ total} = Q \text{ crack} + Q \text{ snow}$$

$$= (\pi DC + \frac{\pi D^2}{4} B)\ \Delta P$$

where C = Crack permeability per unit length
D = Sampling head diameter
ΔP = Pressure drop over the sample of snow

thus the effective measured Bmeas is related to the true B by:

$$Bmeas = \frac{4\ Q \text{ total}}{\pi D^2\ \Delta P} = \left(\frac{4C}{D} + B\right)$$

If C remains constant at different D, then B will increase for lower D i.e. smaller samplers. It appears that this wall leakage was not large.

3. Effects of Sampling in the X, Y, Z directions

Samples on the Cornice Wall (13/10/81) were taken at three different sites in three different directions. (Fig. 3, see also Appendix IV, Parts 3 and 4).

The Table below gives mean permeabilities.

Table 1. Mean Permeabilities on Cornice Wall 13/10/81

Site	Direction		X	Y	Z	Density/kg m^{-3}
	Distance/m	Angle				
1	0	20^o	7.6	7.6	5.7	270
2	40	43^o	11.0	12.6	8.3	240
3	110	30^o	18.9	21.3	16.9	270

a : Units of $10^{-5}\ m^4\ N^{-1}\ s^{-1}$

The standard deviation of a single observation was $1.15 \times 10^{-5}\ m^4\ N^{-1}\ s^{-1}$, but the standard deviations of the above means were reduced to approximately 0.4, as they were taken from at least 9 measurements.

At site 1, to test between sampling directions X and Y, the difference between the means was calculated, and compared with the pooled error standard deviation for the difference. The t value obtained was not significant compared with the appropriate table value. On the other hand, a similar t test done between the Z and X direction permeabilities showed a significant difference.

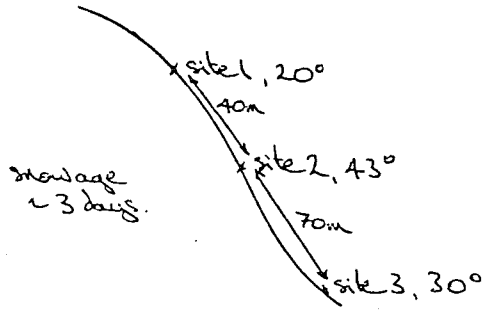

Fig. 3. Location of Sites on Cornice Wall 13/10/81

t values for all sites are summarised below:

Site	texp (X-Y)	$t_{.01}$	texp (X-Z)	$t_{.01}$
1	0.256	2.48	7.25	2.42
2	5.97	2.9	10.69	2.54
3	2.93	2.9	2.85	2.54

From this table, and from the mean permeabilities, the values of Bz are consistently significantly lower than those in the X and Y directions, suggesting less void space running through the sample in this direction. The similarity of the values of Bx and By in most cases, suggests the B values we are measuring could be a function of how the snow is layered, say during deposition (see Fig. 4).

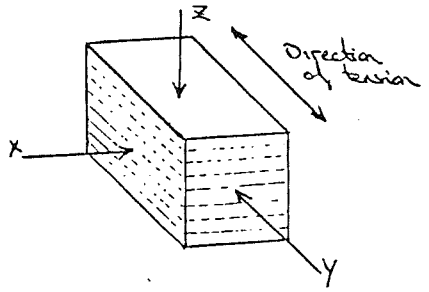

Fig. 4. Showing possible Snow Layering during Deposition

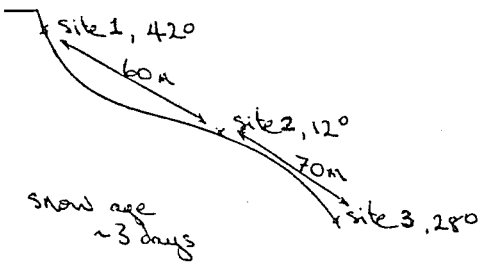

Fig. 5. Location of Sites on Cornice Wall 18/9/81

4. Effects of Downslope Position (sampling in Z direction)

A. Samples on the Cornice Wall (18/9/81) were sampled in the Z direction at various positions down a slope (Appendix V , Part 1) (see Fig. 5) and the mean Z direction permeabilities are presented in Table 2.

Table 2. Mean Permeabilities on Cornice Wall 18/9/81

Site	Distance/m	Angle	Mean Permeability	Order of Measurement	Density/kg m^{-3}
1	0	42^{o}	8.6	3	180
2	50	12^{o}	4.6	1	210
3	120	28^{o}	7.1	2	210
3	120	28^{o}	7.35 (retest after 1h)	4	210

Units of 10^{-5} m^{4} N^{-1} s^{-1}

An analysis of the variation due to change of site was made, and a table of the analysis is shown below:

Source of Variation	Sum of Squares	Degrees of Freedom	Mean Square
Sites	89.6	2	44.8
Error	12.4	39	0.32
Total	102.0		

	F experimental	F table .01
⟶	141	5.2

The experimental F is much larger than the tabled F values, so the mean B values differ significantly down the slope. If the values of B do indicate a change of snow structure due to differences of creep down the slope, it could be expected that site 1 would be in tension and exhibit

a high B compared with site 2, where the snow could be expected to be compressed from the slab above it. Similarly, the permeability B at site 3 could be expected to be greater than that at site 1 (see Fig. 5). This trend is followed in the data.

B. The permeabilities measured on the Cornice Wall (13/10/81) and shown summarised in Table 1 (Z direction) (Appendix IV, Part 3) were analysed in a similar manner. A high F ratio was also found (367, cf $F_{.01}$ (2,39) = 5.2) so that we can also conclude here that changes of site was associated with significant changes in permeability.

This slope differs in topography from that of the Cornice Wall (18/9/81) (Fig. 5), and if the change of B values down the slope do reflect the change of creep down the slope, then the increasing values of B down the slope would suggest increasing creep down the slope. It was thought that site 3 could be in the compression zone of the slab, although this is not indicated by the trend in permeability.

DISCUSSION OF RESULTS

It should be noted that neither of these slopes avalanched within the next few days after the permeability tests, and neither were thought to be at a critical level of stability when the tests were made. The failure model for a slab avalanche outlined by Perla and La Chapelle (1970) suggests that when the ratio of load shear stress to shear strength increases and spreads over a critical load area, high tensile and shear stresses are induced at the boundary of the slab (Perla (1980)). If the boundary stresses are induced rapidly, a brittle fracture could be expected, but if they are induced slowly, the snow at the upper boundary of the potential avalanche would be expected to exhibit signs of creep. Sommerfeld (1979) placed strain gauges on a known avalanche path and recorded an increasing tensile strain rate for four hours preceding a naturally released avalanche. This evidence suggests that the snows around the crown wall were creeping in the final accelerating stage of creep. Other work with seismic geophones (St. Lawrence and Williams (1976), St. Lawrence and Williams (1977)) note seismic spikes associated with slab instability which they associate with internal fractures.

The present work with air permeability suggests that permeability may be useful as an indication of structural differences in the snow. For example, the change of permeability with simple orientation to the air flow suggests that a layering of crystals has occurred as the snow has been deposited. The large differences in permeability observed between snows taken at different sites, but with similar densities and taken from the same layer (and presumably deposited at the same time), indicates structural differences not correlated with density or age. Insufficient data is available to determine whether differential creep down the slope can be measured with the permeability device. It is possible that changes of permeability on the Cornice Wall (18/9/81) between site 1 and site 2 (see Fig. 5) is a function of the more turbulent nature of the wind deposition at site 1 (under the cornice) compared with that at site 2.

The change of permeability with sample size could be a function of the sampler, but it is also likely that changes in snow structure indicating impending fracture may not be evenly distributed. Small cracks may link into larger local defects, and these are likely to be missed by sampling for permeability.

Martinelli (1971) measured permeabilities ranging from 7.2×6^{-5} to 313×10^{-5} m^{4} N^{-1} s^{-1} at very low velocities (0.01 - 0.21 mm s^{-1}) and Shimizu (1970) records a variation of permeability from 3×10^{-5} to 50×10^{-5} m^{4} N^{-1} s^{-1} at

flow velocities of 50 - 100 mm s^{-1}. The Ergun equation suggests, that since the flow rates being used are not strictly laminar, the measured values of B could be up to 16% too high which would marginally reduce the range of air permeability to 3.8 - 16.8 x 10^{-5} m^4 N^{-1} s^{-1}.

It is of interest to compare the permeability predicted by Shimizu (eqn. 1), taking a 0.5 mm grain size, and 1.65 x 10^{-5} Pa s for air viscosity at -10°C. For specific gravity 0.26 (Table 1), an air permeability of 16 x 10^{-5} m^4 N^{-1} s^{-1} is calculated which is in the middle of our range (cf 7.6 to 21.3 x 10^{-5} in Table 1). For a specific gravity of 0.210, a larger air permeability 24 x 10^{-5} is calculated, compared with a lower permeability found by us (Table 2, 4.6 to 8.6 x 10^{-5}). An explanation of this difference could be the different ages of the two snow layers; Martinelli (1971) also found a range of permeabilities for a given density, and noted that snows above the dotted line in Fig. 1 are largely older snows and those below largely younger.

CONCLUSIONS

Changes in air permeability down two slopes with samples of similar density, age, crystal size and type, indicate that this parameter changes significantly and describes structure more sensitively than the other parameters.

The difficulty of determining the origin of the texture changes in the snow pack suggests that more work should be done to investigate the use of permeability as one stability index for some types of slab avalanche.

REFERENCES

Bird, Stewart and Lightfoot (1960) In "Transport Phenomena" Published John Wiley and Sons, New York.
Gubler, H. (1978) J. of Glacial 20, 329-341.
Liepmann, H.W. (1961) J. of Fluid Mech. 10, 65.
Kry (1975) J. of Glacial 14, 479-500.
Martinelli, M. (1971) USDA Forest Service Research Paper RM-64.
Narita, H. (1980) J. of Glacial 26, 275-282.
Perla, R.I. and La Chapelle, E.R. (1970) J. Geophys. Res. 75, 7619-7627.
Perla, R.I. (1978) In "Rockslides and Avalanches" (ed. Voight) Pub. Elsvier, Amsterdam.
Perla, R.I. (1980) In "Dynamics of Snow and Ice Masses" (ed. Colbeck, S.) Pub. Academic Press, London.
Shimizu, H. (1970) Contrib. from the Inst. of Low Temp. Science, Series A, No. 22, p1-32.
Sommerfeld, R.A. (1979) J. of Glacial 22, 402-404.
Sommerfeld, R.A. (1980) J. of Glacial 26, 217-223.
St. Lawrence, W.F. and Williams, T.R. (1976) J. of Glacial 17, 521-526.
St. Lawrence, W.F. and Bradley, C.C. (1977) J. of Glacial 19, 411-417.

APPENDIX I

FLUID FLOW THROUGH A NOZZLE AND ALTITUDE CORRECTIONS

Leipmann (1961) develops a mass flow rate equation for flow through an orifice which may be considered as a Laval nozzle with corrections for a sharp edge.

$$\dot{m} = \Gamma \rho_1 W A \qquad \text{——— A1}$$

$\dot{m}$ = mass flow rate, Kg/s

Γ = a dimensionless factor depending on the specific heat of fluid and including a correction for the sharp edged nature of the orifice. Experimentally, for air under the above conditions Γ $Re \rightarrow \infty = 0.575$.

ρ_1 = density of upstream gas, Kg/m^3

W = characteristic velocity = $(RT_1/M)^{\frac{1}{2}}$, m/s

A = nozzle area, m^2

So for volumetric flow of air under downstream conditions,

$$\frac{\dot{m}}{\rho_2} = 0.575\ A\ \frac{\rho_1}{\rho_2} \left(\frac{RT_1}{M}\right)^{\frac{1}{2}} \qquad \text{——— A2}$$

ρ_2 = density of downstream gas, Kg/m^3

R = gas constant (8.31 J/mole ^oK)

T_1 = upstream gas temperature ^oK

M = molecular mass of fluid Kg/mole (0.29 Kg/mole, air)

$$\rho = \frac{NM}{V} = \frac{PM}{RT}$$

So substituting in A2

$$\frac{\dot{m}}{\rho_2} = 0.575A \left(\frac{R}{MT_1}\right)^{\frac{1}{2}} \frac{P_1}{P_2}\ T_2 \qquad \text{——— A3}$$

where P_1 = upstream gas pressure

P_2 = downstream gas pressure

T_2 = downstream gas temperature

Assuming no temperature change over the nozzle, i.e. $T_1 = T_2 = T$,

$$\frac{\dot{m}}{\rho_2} = 0.575A \left(\frac{R}{M}\right)^{\frac{1}{2}} \frac{P_1}{P_2}\ T^{\frac{1}{2}} \qquad \text{——— A4}$$

where T = gas temperature

The air permeability device was calibrated at sea level using a gas meter, and this calibration is shown in Graph AI.

One calculation is shown using equation A4 to determine the theoretical mass flow rate:

Using $P_{1/P_2} = 3$

$A = \frac{\pi(1.1)^2}{4} \times 10^{-6}\ m^2$ since nozzle diam is 1.1mm

$R = 8.31$ J/mole ^oK

$M = 0.029$ Kg/mole for air

$T = 288^oK$

$$\frac{\dot{m}}{\rho_2} = 0.575 \times \frac{\pi(1.1)^2}{4} \times 10^{-6} \times \left(\frac{8.31}{.029}\right)^{\frac{1}{2}} \times 3 \times (288)^{\frac{1}{2}}$$

$= 28.3$ ℓ/min

which corresponds closely to the measured flow rate of 27.2 ℓ/min under those conditions.

Since the flow rate is dependent on the ratio of the upstream pressure to the downstream gas pressure and the gas temperature, Graph AI can be used to determine the volumetric flow rate at different altitudes. Most tests were made at Tasman Saddle (altitude 2100m) where the atmospheric pressure (P_2) is approximately 79 kPa (since pressure decreases with altitude at 0.1 mb/m). The absolute upstream pressure (P_1) is determined from

$$P_1 = (P \text{ gauge} + 79) \text{ kPa}$$

and the air temperature measured, thus enabling the volumetric flow rate to be read from Graph AI.

Measurements at Mt. Hutt (1680m asl) use a downstream pressure of 83 kPa.

APPENDIX II

LAG TIME IN READING MANOMETER

Experimental evidence indicated a lag time of 2s between the orifice pressure drop reading and the associated pressure drop reading over the sample. This was found by comparing the steady state pressure drop readings with a steady supply of compressed air in the laboratory, with the transient pressure drop readings observed when the instrument was supplied with air from its tank.

It was thought that most of the lag time originated from the base of the sampling head and baffles which are necessary to disperse the air through the sample and to stop a venturi effect past the end of the Dwyer manometer sampling probe.

To ensure that lag from the viscous drag in the manometer was minimised, some calculations were made with regard to critical dampening of the manometer.

From Bird, Stewart and Lightfoot (1960), for critical dampening of a manometer

$$Rcr = \left(\frac{6 \mu^2 L}{g \rho^2} \right)^{\frac{1}{4}}$$

where μ = manometer fluid viscosity

L = manometer length

ρ = manometer fluid density

Rcr = critical manometer tube radius

for the Dwyer gauge

$$\frac{\mu}{\rho} = 57 \times 10^{-6} \ m^2/sec \text{ at } 0^{\circ}C$$

$$L = 15cm$$

$$Rcr = 4 \times 10^{-3} m$$

which is in good agreement with the actual manometer tube ratios, and so we expect an optimum response for this manometer, with a period of $R^2\rho/3\mu = 0.09s$, i.e. $3 \times 0.09 = 0.27s$ was required for a 5% approach to steady state. Thus since the overall lag time was about 2s, the manometer did not limit the speed of measurements. The major lag was probably in the filling of the gas manifold volume below the snow sample.

APPENDIX III

CALCULATION OF THE VARIATION OF B DUE TO NON LAMINAR FLOW THROUGH THE SAMPLE

Using the general behaviour of the Ergun equation (Bird, Stewart and Lightfoot (1960)) and considering that

$$B \propto G/\Delta P$$

so $$B^{-1} \propto \Delta P/G \propto \frac{150(1-\varepsilon)\mu + 1.75G}{D_p}$$

Using conditions from the Cornice Wall (18/9/81) site 3 (see Appendix IV, Part 2)

D_p = particle size = 0.5mm

ε = void ratio = 0.8 (from Shimizu (1970))

μ = air viscosity

G = mass flow rate = ρair (5-10cm sec^{-1})

so $$B^{-1} \propto 1.08 + 2.1 \times 10^{-2}\mu$$

$$\propto 1.185 \text{ (at 5cm sec}^{-1}\text{) to 1.29 (at 10cm/sec)}$$

i.e. B diminishes by $\left(\frac{\frac{1}{1.185} - \frac{1}{1.29}}{\frac{1}{1.185}} \right)$ with flow rate variation, or 8%

Compared with flows that are strictly laminar, the measured B is

$\frac{1.08}{1.185}$ or 9% low at flow of 50mm s^{-1}

and $\frac{1.08}{1.29}$ or 16% low at a flow of 100mm s^{-1}

APPENDIX IV

RESULTS OF AIR PERMEABILITY TESTS

1. Cornice Wall 18/9/81. Between sites.

Site 1: slope angle = 42° snow temperature -6.2°C
ρ = 180 kg/m^3 snow type: windblown 0.5mm ϕ λ

Site 2: slope angle = 12° snow temperature -2.8°C
ρ = 210 kg/m^3 snow type: windblown 0.5mm ϕ λ

Site 3: slope angle = 28° snow temperature -5.9°C
ρ = 210 kg/m^3 snow type: windblown 0.5mm ϕ λ

Tests were made using the sampler 90mm diameter and 49mm deep over a range of flow rates. Several samples were taken at each site, and the air permeability B determined from the D'Arcy equation. Sampling was made in the Z direction (i.e. normal to the snow surface).

SITE 1

μ mm s^{-1}	ΔP mm H_2O	B x 10^{-5} m^4 N^{-1} s^{-1}
98.2	59	8.2
98.2	54	8.9
81.2	46	8.6
81.2	44	9.0
66.8	42	7.8
66.8	36	9.1
52.9	32	8.1
52.9	29	8.9

$\bar{B}$ = 8.58 x 10^{-5}

σ_{n-1} = 0.49 x 10^{-5}

SITE 2

μ mm s^{-1}	ΔP mm H_2O	B x 10^{-5} m^4 N^{-1} s^{-1}
98.2	100	4.8
98.2	110	4.4
98.2	98	4.9
98.2	100	4.8
81.2	90	4.4
81.2	90	4.4
81.2	80	5.0
81.2	90	4.4
66.8	75	4.4
66.8	70	4.7
66.8	78	4.2
52.9	60	4.3
52.9	50	5.2
52.9	58	4.5

$\bar{B}$ = 4.6 x 10^{-5}

σ_{n-1} = 0.8 x 10^{-5}

SITE 3

μ mm s^{-1}	ΔP mm H_2O	B x 10^{-5} m^4 N^{-1} s^{-1}
98.2	78	6.2
98.2	65	7.4
98.2	68	7.1
98.2	72	6.7
98.2	70	6.9
81.2	67	5.9
81.2	53	7.5
81.2	55	7.2
81.2	60	6.6
81.2	58	6.9
66.8	50	6.7
66.8	43	7.6
66.8	42	7.8
66.8	46	7.1
66.8	42	7.8
52.9	40	6.5
52.9	33	7.9
52.9	34	7.6
52.9	36	7.2
52.9	35	7.4

$\bar{B}$ = 7.1 x 10^{-5}

σ_{n-1} = 0.55 x 10^{-5}

2. Cornice Wall 18/9/81. Retesting the same sample from site 3 (see Fig. 5)

μ mm s^{-1}	ΔP mm H_2O	B x 10^{-5} m^4 N^{-1} s^{-1}
98.2	70	6.9
98.2	69	7.0
98.2	70	6.9
98.2	70	6.9
98.2	68	7.1
81.2	58	6.9
81.2	52	7.6
81.2	58	6.9
81.2	59	6.7
81.2	50	8.0
66.8	42	7.8
66.8	40	8.2
66.8	44	7.4
66.8	44	7.4
52.6	35	7.4
52.6	33	7.8
52.6	33	7.8
52.6	34	7.6

$\bar{B}$ = 7.35 x 10^{-5}

σ_{n-1} = 0.45 x 10^{-5}

3. Cornice Wall 13/10/81. Between sites.

Site 1: slope angle = 20^{o} snow temperature $-5.2^{o}C$
ρ = 270 kg/m^3 snow type: windblown 0.5mm E.T. crystals

Site 2: slope angle = 43^{o} snow temperature $-7.0^{o}C$
ρ = 240 kg/m^3 snow type: windblown 0.5mm E.T. crystals

Site 3: slope angle = 30^{o} snow temperature $-5.5^{o}C$
ρ = 270 kg/m^3 snow type: windblown 0.5mm E.T. crystals

Sampling was made in the Z direction.

SITE 1

μ mm s^{-1}	ΔP mm H_2O	B x 10^{-5} m^4 N^{-1} s^{-1}
98.2	85	5.7
98.2	85	5.7
98.2	90	5.3
98.2	75	6.4
98.2	90	5.3
98.2	90	5.3
81.2	70	5.7
81.2	72	5.5
81.2	76	5.2
81.2	62	6.4
81.2	74	5.4
81.2	76	5.2
66.8	55	6.0
66.8	55	6.0
66.8	60	5.5
66.8	47	7.0
66.8	58	5.6
66.8	60	5.5

$\bar{B} = 5.7 \times 10^{-5}$

$\sigma_{n-1} = 0.49 \times 10^{-5}$

SITE 2

μ mm s^{-1}	ΔP mm H_2O	B x 10^{-5} m^4 N^{-1} s^{-1}
98.2	68	7.1
98.2	60	8.0
98.2	55	8.7
98.2	60	8.0
81.2	55	7.2
81.2	47	8.5
81.2	44	9.0
81.2	48	8.3
66.8	41	8.0
66.8	37	8.8
66.8	35	9.4
66.8	38	8.6

SITE 3

μ mm s^{-1}	ΔP mm H_2O	B x 10^{-5} m^4 N^{-1} s^{-1}
98.2	30	16
98.2	35	13.7
98.2	27	17.8
98.2	27	17.8
81.2	25	15.9
81.2	28	14.2
81.2	22	18.1
81.2	22	18.1
66.8	19	17.2
66.8	22	14.9
66.8	17	19.3
66.8	17	19.3

$\bar{B} = 16.86 \times 10^{-5}$

$\sigma_{n-1} = 1.89 \times 10^{-5}$

4. Cornice Wall 13/10/81. Tests at each site using the sample oriented in the X direction (slope-parallel and up the slope) and in the Y direction (slope-parallel and across the slope).

SITE 1, X DIRECTION

μ mm s^{-1}	ΔP mm H_2O	B x 10^{-5} m^4 N^{-1} s^{-1}
98.2	60	8.0
98.2	63	7.6
98.2	80	6.0
98.2	70	6.9
98.2	73	6.6
98.2	63	7.6
81.2	47	8.5
81.2	48	8.3
81.2	68	5.9
81.2	55	7.2
81.2	60	6.6
81.2	47	8.5
66.8	37	8.8
66.8	38	8.6
66.8	52	6.3
66.8	42	7.8
66.8	40	8.2
66.8	37	8.8

$\bar{B} = 7.57 \times 10^{-5}$

$\sigma_{n-1} = 0.98 \times 10^{-5}$

SITE 1, Y DIRECTION

μ mm s^{-1}	ΔP mm H_2O	B x 10^{-5} m^4 N^{-1} s^{-1}
98.2	68	7.1
98.2	65	7.4
98.2	66	7.3
81.2	52	7.7
81.2	50	8.0
81.2	50	8.0
66.8	41	8.0
66.8	39	8.4
66.8	49	6.7

$\bar{B} = 7.62 \times 10^{-5}$

$\sigma_{n-1} = 0.54 \times 10^{-5}$

SITE 2, X DIRECTION

μ mm s^{-1}	ΔP mm H_2O	B x 10^{-5} m^4 N^{-1} s^{-1}
98.2	43	11.2
98.2	47	10.2
98.2	45	10.7
81.2	35	11.4
81.2	38	10.5
81.2	36	11.1
66.8	28	11.7
66.8	30	10.9
66.8	29	11.3

$\bar{B} = 11.0 \times 10^{-5}$

$\sigma_{n-1} = 0.47 \times 10^{-5}$

SITE 2, Y DIRECTION

μ mm s^{-1}	ΔP mm H_2O	B x 10^{-5} m^4 N^{-1} s^{-1}
98.2	40	12.0
98.2	39	12.3
98.2	40	12.0
81.2	32	12.4
81.2	32	12.4
81.2	33	12.1
66.8	24	13.6
66.8	24	13.6
66.8	25	13.1

$\bar{B} = 12.6 \times 10^{-5}$

$\sigma_{n-1} = 0.65 \times 10^{-5}$

SITE 3, X DIRECTION

μ mm s^{-1}	ΔP mm H_2O	B x 10^{-5} m^4 N^{-1} s^{-1}
98.2	23	20.1
98.2	25	19.2
98.2	29	16.6
81.2	19	20.9
81.2	20	19.9
81.2	24	16.6
66.8	15	21.8
66.8	18	18.2
66.8	19	17.2

$\bar{B} = 18.94 \times 10^{-5}$

$\sigma_{n-1} = 1.90 \times 10^{-5}$

SITE 3, Y DIRECTION

μ mm s^{-1}	ΔP mm H_2O	B x 10^{-5} m^4 N^{-1} s^{-1}
98.2	22	21.9
98.2	25	19.2
98.2	22	21.9
81.2	18	22.1
81.2	20	19.9
81.2	18	22.1
66.8	15	21.8
66.8	17	19.3
66.8	14	23.4

$\bar{B} = 21.3 \times 10^{-5}$

$\sigma_{n-1} = 1.46 \times 10^{-5}$

5. Sampling at Mt. Hutt, November 1981. Tests were made on snow of average density 450 kg/m^3, snow temperature 0°C, slope angle 32°, snow type: 1mm primary particles agglomerated in agglomerates up to 10mm, melt freeze crystals.

Tests were at the same same using two samplers of different sizes in an attempt to determine size effects on air permeability. The results are set out below:

MT. HUTT, Sample Diameter = 53.5mm

μ mm s^{-1}	ΔP mm H_2O	B x 10^{-5} m^4 N^{-1} s^{-1}
341	17	10.1
341	12	14.3
341	13	12.4
301	14	10.8
301	10	15.1
301	10	15.1
260	11	11.9
260	8.5	15.4
260	8.5	15.4
223	9	12.6
223	7	16.0
223	7	16.0
185	7	13.4
185	5	18.7
185	5	18.7

$\bar{B} = 14.4 \times 10^{-5}$

$\sigma_{n-1} = 2.55 \times 10^{-5}$

MT. HUTT, Sample Diameter = 90mm

μ mm s^{-1}	ΔP mm H_2O	B x 10^{-5} m^4 N^{-1} s^{-1}
92	3.1	14.6
92	2.1	22.0
92	2.8	16.2
92	2.1	22.0
78.6	2.5	15.4
78.6	1.7	22.6
78.6	2.2	17.6
78.6	1.6	24.0
65.6	2.0	16.0
65.6	1.4	23.0
65.6	1.8	17.9
65.6	1.3	24.7

$\bar{B} = 19.67 \times 10^{-5}$

$\sigma_{n-1} = 3.71 \times 10^{-5}$

Appendix : SUMMARY OF MEASUREMENTS OF SNOW PROPERTIES.

Local names have been used to describe the location of the various slopes, and the aspects and elevations are:

Nosedive: SE, 2150m

Cornicewall: E, 2310m

Murchison headwall: E, 2300m

Hochstetter Dom shoulder: SE, 2550m

Densities are measured in kg/m^3; tensile and shear strengths are measured in N/m^2. ET crystals are equitemperature type crystals (equilibrium form); and TG (or faceted) type crystals are the temperature gradient type crystals (kinetic growth form) as per Sommerfeld and LaChapelle (1970) and Colbeck (1983).

1) DATE: 13 September 1981

Location:Nosedive - No good shear surfaces

Bed surface angle=40°, Slab density=250kg/m^3, Slab depth=.28m, mainly 1mm diam ET crystals

Tensile strengths: 1920, 1820, 2200N/m^2 - spatial distance not recorded

2) DATE: 14 September 1981

Location:Cornicewall - No good shear surfaces

Bed surface angle=41°, Slab density=190kg/m^3, Slab depth=.55m, mainly rimed needles and broken stellar crystals

Tensile strengths: 2450, 1240, 2760N/m^2 - spatial distance not recorded

3) DATE: 15 September 1981

Location:Murchison headwall - no good shear surfaces

Bed surface angle=35°, Slab density=260kg/m^3, Slab depth=.70, wind stratified crusts and early ET crystals Tensile strength: 4880N/m^2

4) DATE: 16 September 1981

Location: Cornicewall - no fracture but a shear layer at .3-.36m depth.

Bed surface angle=28° Slab density=215kg/m^3, Slab depth=.30-.36m

Tensile strengths:4333, 1350, 740, 1590, 958, 1470N/m^2

Shear strength of surface snow (density-230kg/m^3, temp.=-5°C): 604, 574, 60, 356, 231N/m^2

Basal shear strengths (and depths): 534N/m^2 (.30m), 1140N/m^2 (.34m), 780N/m^2 (.34m), 984N/m^2 (.36m), 1025N/m^2 (.32m), the sliding layer consisted of soft, partly metamorphosed, new snow, .5mm diam.

5) DATE: 17 September 1981

Location: Murchison headwall - no good shear layers until a compressive force was applied perpendicular to the slab

Bed surface angle=35°,Slab density=236kg/m^3, Slab depth=.21-.24m

Tensile strength:3450N/m^2

Shear strength of surface snow: 473, 398, 192, 372, 556, 376, 366N/m^2,

Before the compressions, there was no sliding at the .21-.24m level, but after compressions - basal shear strengths (and depths):382(.24) 144(.21m), 708(.23m), 980(.24m), 579(.24m), 1048(.23m). The shear layer consisted of needle crystals under a crust.

6) DATE: 21 September 1981

Location:Murchison headwall - surface sluffing and loose slides were occurring on adjacent slopes

Bed surface angle=30°, Slab density 90kg/m^3, Slab depth=.17m

Tensile strengths:76, 93N/m^2

Shear strength of surface snow (density=90kg/m^3): 0-114N/m^2(6 tests) No good shear layers deeper in the snow-pack

7) DATE: 23 September 1981

Location:Cornicewall - no good shear layers until a compressive force was applied perpendicular to the slab

Bed surface angle: 44°, Slab density=160kg/m^3, Slab

depth=.26m

Tensile strengths:1590, 2340N/m^2

Shear strength of surface snow: <155, 203, <155, <155, 172, <155, <155, 170N/m^2

Before the compressions there was no sliding at the .26m level. After compressions - basal shear strengths: 540, 670, 250, 356N/m^2 at .26m - a soft layer of 1mm, partly metamorphosed, clusters.

8) DATE: 26 September 1981

Location:Cornicewall - settling occurring on the slope, and a small surface slab was released when a cornice was kicked onto the slope.

Bed surface angle: 33°, Slab density=80kg/m^3), slab depth=.19m

The equipment was not sensitive enough to test this weak snow - new snow on top of clustered graupel crystals.

9) DATE: 28 September 1981

Location: Murchison headwall - some weak layers but no avalanche

Bed surface angle: 30°, Slab density=200kg/m^3), Slab depth=1.11-1.15m

Tensile strength: 6340N/m^2

Basal shear strengths and depths:<1110, <1110, >1650, <1110, >1300, >1340, the slab was wind stratified and the shear layer consisted of cohesionless 2mm clustered crystals.

10) DATE: 29 September 1981

Location: Nosedive - a heavily wind affected slope, and no good shear layers

Bed surface angle: 33°, Slab density= 245kg/m^3, Slab depth=.43m

Tensile strengths: 2540, 2800N/m^2 at .43m

11) Date: 12 October 1981

Location: Cornicewall - wind packed snow

Bed surface angle: 43°, Slab density=224kg/m^3,

Tensile strengths: 2980, 2890N/m^2

12) DATE: 14 October 1981

Location: Cornicewall

Bed surface angle: 38°, Slab density=225kg/m^3,

Tensile strengths: 5222; 5003; 8109; 3210N/m^2 at .23m

Basal shear strengths: >3220; >3600N/m^2

13) DATE: 10 June 1982

Location: Nosedive

Bed surface angle: 29°, Slab density=160kg/m^3, A surface sun-crust overlay .24m of very soft, partly metamorphosed, 1mm diam crystals. Beneath this there was an ice layer, with some poorly developed faceted crystals on top of the ice.

Tensile strengths:270, 470N/m^2 at .15m

Surface snow shear strengths:380, 380, 380N/m^2

Shear strengths at .24m:1320, 1320N/m^2.

14) DATE: 16 June 1982

Location: Nosedive

Fine cold weather resulted in 1mm faceted crystals developing through the snowpack. Density=190, 180kg/m^3, Surface snow shear strengths:326, 218, 218, 163, 218N/m^2

15) DATE: 18 June 1982

Location: Nosedive

Fine cold weather continued and 2mm faceted crystals had developed. Density= 190kg/m^3, Surface snow shear strengths:270, 270, 218, 218N/m^2

16) DATE: 23 June 1982

Location: Nosedive - about .78m of new snow overlying the faceted crystals. Most of the slope had avalanched after about .4m of snow had fallen, and the rest of the snowfall had covered the fracture.

Surface snow shear strength(needles and broken stellar crystals of density=165kg/m^3, temp= -7.8°C):325, 325, 163, 325, 325, 325, 325, 272, 325N/m^2.

Slab density=212kg/m^3, Tensile strength: 2320N/m^2 to .78m

Basal shear tests were clustered at two locations:

A) Bed surface angle: 30°, Shear strengths (depths of shear layer are in brackets): >1920(.67m), >1920(.67m), 764(.62m), 1520(.73m), <800(.77m), >2000, 1800(.79m), 1174(.78m).

B) 20m East of above site, bed surface angle: 21-22°, Shear strengths: 1445(.77m), >2000, 770(.78m), 680(.72m), 930(.76m).

17) DATE: 26 June 1982

Location: Hochstetter Dom shoulder - the slope had avalanched about 12 hrs. earlier. Fracture was drifted over and riming had occurred over night. The avalanche was about 400m long and 600m wide, and the sliding layer consisted of 1-3mm faceted crystals. Slab density=250kg/m^3, slope angle=35°

Tensile strengths measured: 14400, 15700N/m^2 to about 1m depth. Basal shear strengths (depths of the shear layer are in brackets): 2420(1.08m), <1380(.98m), 1970(.9m), >2300, <1320(.94m), 2105(1.05m), 1110(.79m), <1400(1.0m), <1320(.94m).

18) DATE: 3 July 1982

Location: Nosedive - wind affected slope

Bed surface angle: 32°, Slab density=280kg/m^3,

Basal shear strength was greater than 1760N/m^2 (6 tests) at .3m

19) DATE: 13 July 1982

Location:Cornicewall - Avalanche ski-released, 30m wide and 20m long. The initial fracture was about 200mm deep and a 2m square section slid locally for about .7m before causing the rest of the snow to fracture. This was a medium- soft slab, and the shear layer consisted of new snow including capped columns, columns, stellars, needles and plate crystals. The fracture occurred within the new snow.

Slab density=140kg/m^3, Bed surface angle=47°

Tensile strengths measured=660, 1430, 1130N/m^2

Total no. of basal shear measurements=18 No. censored measurements=9 (marked by *)

Distance between samples (across-slope)=.89m

Basal shear strength and (slab depth) in spatial arrangement across-slope: 458*(.53m), 788(.53m), 373*(.46m), 429*(.43m), 539(.38m), 345*(.38m), 508(.38m), 316*(.38m), 1075(.32m), 889(.33m), 713(.33m), 1339(.33m), 1422(.35m), 1620(.5m), 199*(.54m), 401*(.54m), 249*(.54m), 285*(.54m).

1x Averaged shear=549, SD.=345, SD.red.factor=1.000

2x Averaged shear=596, SD.=314, SD.red.factor=0.911

3x Averaged shear=622, SD.=301, SD.red.factor=0.873

4x Averaged shear=653, SD.=285, SD.red.factor=0.826

5x Averaged shear=694, SD.=246, SD.red.factor=0.712

6x Averaged shear=709, SD.=232, SD.red.factor=0.673

7x Averaged shear=721, SD.=210, SD.red.factor=0.610

8x Averaged shear=728, SD.=187, SD.red.factor=0.543

Scale of fluctuation between basal shear measurements= 1.84m

Slab depth averaging

1x Averaged depth=0.43 SD.=.09 SD.red.factor=1.000

2x Averaged depth=0.43 SD.=.08 SD.red.factor=0.949

3x Averaged depth=0.42 SD.=.08 SD.red.factor=0.878

4x Averaged depth=0.41 SD.=.07 SD.red.factor=0.826

5x Averaged depth=0.41 SD.=.06 SD.red.factor=0.696

6x Averaged depth=0.40 SD.=.05 SD.red.factor=0.580

7x Averaged depth=0.40 SD.=.04 SD.red.factor=0.486

8x Averaged depth=0.39 SD.=.04 SD.red.factor=0.407

Scale of fluctuation between slab depth measurements=1.03m

20) DATE: 15 July 1982

Location: Cornicewall - jumping on the slope produced cracks up to 2-3m long, but no slope failure.

Basal shear strengths and slab depths in brackets - (bed surface angle: 55°, spacing between samples=.8m):<620(.45m), <760(.54m), 1612(.95m), 1790(1.10m), 1855(.94m), >3000N/m^2

Basal shear strengths (3m from previous site, angle: 45°): <1780(1.47m), <1820(1.5m).

21) DATE: 19 July 1982

Location: Cornicewall - jumping on the cornice above the slope produced a cornice failure over about 4m. This caused a sluff on the slope below. Surface snow consisted of very very soft new snow of density= 100.

Basal shear strengths (depth of layer and bed surface angle are included in brackets with each measurement): 450(.41m,48°), 468(.47m,52°), 264(.28m,47°), 110(.15m,48°), 225(.15m,52°), 700(.5m,58°), 815(.15m,47°), 330(.15m,47°), 380(.15,47°).

22) DATE: 20 July 1982

Location: Cornicewall - some surface slabbing occurred when the surface crust increased in thickness. Slab density=60kg/m^3, tensile strength:213, 260, 482N/m^2.

Basal shear strengths(depth and angle in brackets): 101(.11m,35°), 221(.22m,41°), 120(.18m,38°), 135(.19m,35°). Measurements were spaced about 6m apart.

23) DATE: 22 July 1982

Location: Cornicewall - wind affected slope - two sites 10m apart were tested.

A) Some very very soft new snow, density=60kg/m^3, bed surface angle=40°

Tensile strengths:94, 132N/m^2,

Surface shear strengths: ‹10N/m^2 (3 tests)

B) Snow much more consolidated, density=120kg/m^3,

Tensile strengths:305, 310N/m^2

24) DATE: 3 August 1982

Location: Cornicewall

Bed surface angle=44°, density=200kg/m^3, Tensile strength:4210N/m^2

Sideshear strengths:1250, 2670N/m^2 - we are unsure how successful these measurements are because of possible bending of the sample.

25) DATE: 6 August 1982

Location: Nosedive - some very, very soft partly metamorphosed new snow on the surface. Density=100kg/m^3, vv soft, 1mm diam, partly metamorphosed new snow. Surface shear strengths;163, 163, 196, 196N/m^2 Shear strength at 1m was greater than 2700N/m^2

26) DATE: 11 August 1982

Location: Cornicewall - no good shear layers in the lower snowpack.

Surface snow density=150kg/m^3, shear strengths: 272, 272, 544, 108, 327N/m^2.

27) DATE: 6 September 1982

Location: Cornicewall - a thin wind crust overlying soft wind blown, .5mm partly metamorphosed snow. Snow density=140kg/m^3, angle=43-55°, Surface shear strengths:544, 1090, ‹70, 490, 330N/m^2.

28) DATE: 7 September 1982

Location: Hochstetter Dom shoulder - a large iceblock triggered a variable depth slab about 12hrs. before the tests. Although the fracture depth varied from .57-.84m along the section of the crown measured, the depth of the easiest shear was about .5m above this layer(.1-.3m).

Basal shear measurements are listed below:

No.1 ‹310 at .16m; ›2420 at .67m: bed angle=45°

No.2 490 at .16m; ›2400 at .73m; bed angle=45° (3m across-slope from no.1)

No.3 ‹232 at .12m; ›2400 at .74m; bed angle=45° (directly above no.2)

No.4 1790 at .14m; ›2420 at .67m; bed angle=45° (3m across-slope from no.2)

No.5 ‹370 at .19m; ›2400 at .70m; bed angle=40° (5m across-slope from no.4)

No.6 ‹560 at .30m; ›2800 at .84m; bed angle=45° (8m across-slope from no.5)

No.7 960 at .10m; ›2300 at .57m; bed angle=45° (7m across-slope from no.6)

29) DATE: 9 September 1982

Location: Hochstetter Dom shoulder - some wind affected snow

Surface snow was vs, density=130kg/m^3, .5-1mm early ET, bed angle=34°.

Surface shear strengths:675, 450, 436, 762N/m^2

Measurements also made deeper in the snow pack - slab density=205kg/m^3, bed angle=34°, Distance between measurements=7m

Basal shear strengths (depths of the shear layer in brackets): 1050(.62m), >1700(.62m), 2080(.97m), >2500(1.13m).

30) DATE: 19 September 1982

Location: Cornicewall - a high snowfall and wind transport of snow (1-2m slab) deposited on top of some faceted crystals (up to 40mm thick, 1mm facets), resulted in this slope avalanching naturally. The measurements were made about 15 hours after the avalanche had occurred. Slab density=290kg/m^3, bed surface angle=34°, estimate of tensile strength=3000-8000N/m^2

Total no. of basal shear measurements=19 No. censored measurements=5 (denoted by *) Distance between samples= .7m

Sequential basal shear strength (slab depth in brackets):2096(.8m), 2145(.8m), 2084(.8m), 1590(.8m), 2892(.8m), 1257*(.88m), 993*(.9m), 2169(.9m), 3253(.9m), 2319(1.0m), 1685(.99m), 2130(1.08m), 2207(.99m), 1870(1.01m), 3650(1.01m), 1369*(1.01m), 796*(.93m), 1830(1.03m), 1135*(1.03m).

Basal shear strength averaging

1x Averaged shear= 1840 SD.=722 SD.red.factor=1.000
2x Averaged shear= 1921 SD.=550 SD.red.factor=0.763
3x Averaged shear= 1961 SD.=410 SD.red.factor=0.568
4x Averaged shear= 1999 SD.=314 SD.red.factor=0.435
5x Averaged shear= 2042 SD.=197 SD.red.factor=0.273
6x Averaged shear= 2037 SD.=172 SD.red.factor=0.238
7x Averaged shear= 2042 SD.=163 SD.red.factor=0.226
8x Averaged shear= 2057 SD.=150 SD.red.factor=0.208

Scale of fluctuation between basal shear measurements= 0.21m

Slab depth averaging

1x Averaged depth=0.93 SD.=.10 SD.red.factor=1.000
2x Averaged depth=0.93 SD.=.09 SD.red.factor=0.944
3x Averaged depth=0.93 SD.=.09 SD.red.factor=0.903
4x Averaged depth=0.93 SD.=.08 SD.red.factor=0.435
5x Averaged depth=0.94 SD.=.08 SD.red.factor=0.834
6x Averaged depth=0.94 SD.=.07 SD.red.factor=0.781
7x Averaged depth=0.94 SD.=.07 SD.red.factor=0.730
8x Averaged depth=0.94 SD.=.06 SD.red.factor=0.679

Scale of fluctuation between slab depth measurements=2.26m

31) DATE: 5 October 1982

Location: Cornicewall - a wind affected slope and many ripples and dunes on the surface.

Slab density=220kg/m^3, bed angle=34°, No.1 Basal shear strength <430 at .36m; No.2 No good shear layers in the pack (.8m from no.1); No further good shear layers

32) DATE: 5 August 1983

Location: Hochstetter Dom shoulder - .5mm partly metamorphosed crystals at the surface layers. Density=180kg/m^3, angle=27°.

Surface shear strengths:760, 440, 330, 330N/m^2 (.7m spacing of pits). No good shear layers in the lower snowpack.

33) DATE: 5 August 1983

Location: Nosedive - some vs .5-1mm partly metamorphosed snow at the surface (density=180kg/m^3), and the lower snowpack was wind stratified with no good shear layers.

Surface shear strengths:760, 440, 440, 540N/m^2

34) DATE: 10 August 1983

Location: Cornicewall - extensive jumping on the slope produced only small local failures. Blocks about 2m square slid a short distance. Sliding layer consisted of .5-1.5mm graupel (temp.= -5.0°C)

Slab density=280kg/m^3, bed surface angle=35-50°, Estimate

of tensile strength:3000-8000N/m^2

Total no. of basal shear measurements=11, No. censored measurements=5 (denoted by *), Distance between samples= .75

Sequential basal shear strength slab depth in brackets): 2016(.77m), 1589(.67m), 1332(.52m), 988*(.43m), 578*(.25m), 1098(.37m), 870*(.31m), 742*(.31m), 1095(.31m), 1106*(.34m), 1519(.41m)

Basal shear strength averaging

1x Averaged shear= 1111 SD.=397 SD.red.factor=1.000
2x Averaged shear= 1077 SD.=297 SD.red.factor=0.749
3x Averaged shear= 1050 SD.=237 SD.red.factor=0.596
4x Averaged shear= 1025 SD.=187 SD.red.factor=0.471
5x Averaged shear= 1015 SD.=148 SD.red.factor=0.372
6x Averaged shear= 1019 SD.=136 SD.red.factor=0.342
7x Averaged shear= 1020 SD.=106 SD.red.factor=0.266
8x Averaged shear= 1039 SD.=76 SD.red.factor=0.191

Scale of fluctuation between basal shear measurements= 0.19m

Slab depth averaging

1x Averaged depth=0.43 SD.=.16 SD.red.factor=1.000
2x Averaged depth=0.41 SD.=.14 SD.red.factor=0.869
3x Averaged depth=0.40 SD.=.12 SD.red.factor=0.734
4x Averaged depth=0.39 SD.=.10 SD.red.factor=0.471
5x Averaged depth=0.38 SD.=.08 SD.red.factor=0.487
6x Averaged depth=0.38 SD.=.07 SD.red.factor=0.433
7x Averaged depth=0.38 SD.=.06 SD.red.factor=0.376
8x Averaged depth=0.39 SD.=.05 SD.red.factor=0.308

Scale of fluctuation between slab depth measurements=0.5m

35) DATE: 14 August 1983

Location: Murchison Headwall - considerable variation of snow depth deposition at this site, 2m spacing between pits.

Bed surface angle=32°, Slab density=225kg/m^3,

Surface snow shear strengths: 435, 109, 762, 708N/m^2.

Basal shear strengths:363 (at .18m), 766 (at .16m).

36) DATE: 28 August 1983

Location: Murchison Headwall - slope had fractured sometime near the end of the storm which had finished four days prior to the tests. A drifted over crownwall.

Bed surface angle=32°

Site A: Surface shear strength:1633N/m^2, at .77m shear strength=2828N/m^2 (sliding layer consisted of faceted recrystallised snow at -6.4°C)

Site B: (60m across slope from A) Surface shear strength: 1633N/m^2, at the fracture depth (.72m), there was no good shear.

37) DATE: 15 September 1983

Location: Nosedive - a fracture which had probably occurred on 13 September and had since drifted over. The avalanche had slid on a 1-2mm graupel layer (temp.=-4.8°C), and we suspected subsequent metamorphism to have occurred since we found no good shear layers.

38) DATE: 17 September 1983

Location: Hochstetter Dom shoulder - no shear layers in the snowpack, but we noted considerable variability in the snow depth stratigraphy. The surface snow consisted of alternate erosional/depositional bands about 8m wavelength.

39) Date: 22 September 1983

Location: Cornicewall - loose slides occurred when skiing the slope, but when we reached a position about 40m down slope from the ridge crest, a crack propagated about 15m and that section of the slope slid locally about 4m. The sliding layer consisted of very soft graupel (1-3mm diam) varying in depth from the surface from .13m to .66m(near the ridge crest).

Surface snow density:50kg/m^3, Surface snow shear strengths:220, 160, 160, 160N/m^2.

40) DATE: 24 September 1983

Location: Cornicewall - this slope was relt to be marginally safe. A hard slab and the short length of slope was thought to be helping hold the slope together.

Bed surface angle:36-38°, Slab density= 260kg/m^3, -

consisted of 1-4mm wind stratified clusters of crystals sliding on a 10-20mm thick layer of 1-2mm graupel. We made several basal shear strength measurements both across slope, and down slope. The average spacing between pits was .6m.

Basal shear strength across-slope:1600(.74), 1464(.72m), 1633(.69m), <1100(.7m), <1082(.69m), 1575(.69m).

Basal shear strength down-slope: 1285(.7m), 1174(.63m), <940(.66m), <990(.69m), <960(.67m), 1290(.69m), <1082(.69m).

Note that 2m below the ridge crest, there were no good shear layers (the snow was wind affected). However 10m down from the crest, the basal shear strength was 1690N/m^2(.75m), and this was 30m above the series of pit listed above.

41) DATE: 26 September 1983

Location: Nosedive

Some surface snow tests - new snow density=90kg/m^3, temp.=-6.9°C (at .1m)

Surface snow shear strengths:436, 436, 436, 430, 430, 545, 380, 380N/m^2.

42) DATE: 4 July 1984

Location: Cornicewall - a medium-hard slab of wind deposited snow overlay some soft snow on a short slope (about 30m). Extensive jumping would not release the slab. Slab density= 300kg/m^3, bed surface angle=32-47°, weakest shear plane depth=.35-.52m. Estimate of tensile strength= 3500-8000N/m^3

Of a total of 22 pits over an area of about 6m by 6m, only at four locations did the basal shear strength exceed the downslope gravitational weight. (ie. less than 980N/m^3).

43) DATE: 4 July 1984

Location: Hochstetter Dom Shoulder - a medium (class 3) avalanche had released naturally after the previous snowfall. The slab consisted of .37-.73m of wind- deposited snow overlying a layer of very soft graupel conglomerates (1-4mm diam.). The slab density was 320kg/m^3, and the bed surface angle 32°.Not only was the slab depth variable, but we noted the thickness of the shear layer was also very variable.

At one zone, we measured a strength/stress ratio of less than one over a distance of 4m (6 measurements less than 1160N/m^2), and at others, the strength/stress ratio was high (too high to be measured by our tests). At places where the column would not shear, we often could not find the weak layer in the stratigraphic section.

44) DATE: 28 July 1984

Location: Cornicewall - a slab which was easily ski-released and fractured at the top of a convex roll. The fracture was about 30m long and 60m wide, and stopped in a gully at the northen end. Probably the southern flank was close to a position where skiers had disturbed the snow prior to the storm. The slab consisted of varying amounts of wind deposited snow and it overlay some very-very soft snow which had been recrystallised and faceted (1-2mm diam.). Slab density=340kg/m^3, bed suface angle= 32-40° (steeper below)

Estimate of tensile strength=2000-8000N/m^2.

The basal shear strength measurements all were less than the downslope gravitational load (which ranged from 328-1024 N/m^2 depending on snow depth and angle). The depth of the slab varied from .03m (at the trigger point) to 0.58m in the gully.

Some shear strength measurements made on the surface snows before the subsequent burial of the weak layer (on 27 July 1984) were:653, 327, 490, 991, 218, 327, 272, 762, 545N/m^2 (snow density=170 kg/m^3).

45) DATE: 1 August 1984

Location: Cornicewall - a small slab (12.5m wide and 7m long) ski released near the middle of the crownwall. The crown fractured along the top of a convexity on the slope. The slope was complex and the northen flank ran into a gully. The fracture stopped propagating across the slope when the slab thinned due to lack of accummulation. The slab consisted of rounded, wind affected partly metamorphosed snow, and this

was shearing on some very-very soft new snow (1mm diam. partly rimed capped columns, columns, dendrites, needles at temp.=-8.2°). The avalanche required more energy for its release compared with the avalanche of 28 July 1984.

Slab density= 180kg/m^3, bed surface angle= 35-56°, Estimate of slab tensile strength: 1200-3200 N/m^2

Total no. of measurements= 19, No. censored measurements= 9 (denoted by *), Distance between samples= .7

Sequential basal shear strength (depth in brackets): 497(.15m), 259(.16m), 280(.19m), 74*(.16m), 175*(.16m), 251*(.16m), 205*(.16m), 158*(.16m), 424(.2m), 190*(.2m), 288(.12m), 110*(.18m), 235*(.2m), 618(.18m), 599(.2m), 620(.24m), 220*(.19m), 394(.25m), 384(.24m).

Basal shear strength averaging

1x Averaged shear=271 SD.=158 SD.red.factor=1.000
2x Averaged shear=280 SD.=124 SD.red.factor=0.785
3x Averaged shear=283 SD.=110 SD.red.factor=0.697
4x Averaged shear=286 SD.=103 SD.red.factor=0.655
5x Averaged shear=287 SD.=96 SD.red.factor=0.611
6x Averaged shear=287 SD.=89 SD.red.factor=0.562
7x Averaged shear=284 SD.=79 SD.red.factor=0.500
8x Averaged shear=283 SD.=70 SD.red.factor=0.446

Scale of fluctuation between basal shear measurements=.97m

Slab depth averaging

1x Averaged depth=0.18 SD.=.03 SD.red.factor=1.000
2x Averaged depth=0.18 SD.=.03 SD.red.factor=0.810
3x Averaged depth=0.18 SD.=.02 SD.red.factor=0.669
4x Averaged depth=0.18 SD.=.02 SD.red.factor=0.655
5x Averaged depth=0.18 SD.=.02 SD.red.factor=0.576
6x Averaged depth=0.18 SD.=.02 SD.red.factor=0.511
7x Averaged depth=0.18 SD.=.02 SD.red.factor=0.473
8x Averaged depth=0.18 SD.=.01 SD.red.factor=0.422

Scale of fluctuation between slab depth measurements=0.872m

46) DATE: 25 August 1984

Location: Nosedive - three out of four shear tests did indicated no good shear layers (pits were spaced .7m apart). One test showed a shear strength of 985N/m^2 at .21m depth. The slab consisted of partly metamorphosed wind deposited snow (density=220kg/m^3), and this overlay a soft 3mm diam. graupel layer at a temp.-6.0°C.

47) DATE: 26 August 1984

Location: Murchison headwall - no good shear layers were found during four shear tests. The stratigraphy suggested a weakness at about .22m (loose soft 4mm diam. graupel layer at a temp.-6.2°C.

48) DATE: 28 August 1984

Location: Cornicewall - a small fracture (12m wide and about 10m long), required jumping on skis to release (snowing and blowing at the time). The slope had been mainly wind loaded with heavily rimed and rounded snow crystals, and this was sliding on some low density snow which also contained surface hoar from previous fine weather. After the initial avalanche and these tests, we released a further section of the slope (about 5m further north).

Slab density=260kg/m^3, bed surface angle= 45-49°, Estimate of tensile strength = 2000-8000 N/m^2.

Total no. of shear measurements= 20, No. censored measurements= 7 (denoted by *) Distance between samples= .6m

Sequential basal shear strength (depth in brackets): 1006(.15m), 670(.15m), 430(.14m), 574(.14m), 574(.14m), 760(.17m), 488(.18m), 890(.21m), 782(.21m), 273*(.35m), 431*(.3m), 219*(.26m), 730(.28m), 1263(.3m), 999(.3m), 374*(.3m), 402*(.29m), 311*(.32m), 344*(.39m), 930(.37m).

Basal shear strength averaging

1x Averaged shear=559 SD.=273 SD.red.factor=1.000
2x Averaged shear=566 SD.=210 SD.red.factor=0.769
3x Averaged shear=575 SD.=179 SD.red.factor=0.656
4x Averaged shear=591 SD.=141 SD.red.factor=0.517
5x Averaged shear=606 SD.=92 SD.red.factor=0.338
6x Averaged shear=618 SD.=52 SD.red.factor=0.190

7x Averaged shear=621 SD.=38 SD.red.factor=0.141

8x Averaged shear=616 SD.=44 SD.red.factor=0.163

Scale of fluctuation between basal shear measurements= 0.11m

Slab depth averaging

1x Averaged depth=0.25 SD.=.08 SD.red.factor=1.000

2x Averaged depth=0.25 SD.=.08 SD.red.factor=0.945

3x Averaged depth=0.25 SD.=.07 SD.red.factor=0.884

4x Averaged depth=0.25 SD.=.07 SD.red.factor=0.517

5x Averaged depth=0.25 SD.=.07 SD.red.factor=0.793

6x Averaged depth=0.25 SD.=.06 SD.red.factor=0.746

7x Averaged depth=0.25 SD.=.06 SD.red.factor=0.697

8x Averaged depth=0.25 SD.=.05 SD.red.factor=0.641

Scale of fluctuation between slab depth measurements=1.72m

49) DATE: 30 August 1984

Location: Cornicewall

Some shear tests in new snow (2mm needle crystals) at the surface. Snow density=140 kg/m^3, temp. at .05m = -1.8°.

Shear strengths: 435, 408, 327, 327, 517, 327, 354, 354N/m^2

At a location about 100m away from the above, surface shear strength measurements: 435, 380, 490, 272, 327, 380, 272, 354, 272, 327N/m^2.

50) DATE: 17 September 1984

Location: Hochstetter Dom shoulder - a large fracture about 600m across the shoulder of the Dom. It had occurred some time during the storm of 10-14 September. The slab was hard, consisting of a thick rain crust and stratified graupel layers, while the weak layer consisted of a loose layer of 3mm graupel. Sometimes it was difficult to find the shear layer and probably both the time between the measurements and the event as well as the warm temperatures (about -3.8°C at the weak layer), would have caused metamorphic strengthening of the snow pack.

Average slab density=360N/m^2, bed surface angles measured= 30-40°,

Four basal shear strength measurements were made at an average spacing of 4m: >2600 (depth=.64m), <1930 (depth=.85m), >3357 (depth=.94m), 3000 (depth=.87m).

51) DATE: 17 September 1984

Location: Nosedive - some surface snow just beginning to become faceted (0.1-0.2mm diam.).

Snow density=200kg/m^3, temp.=-6.6°, Surface shear: 436, 327, 436, 327N/m^2.

52) DATE: 24 September 1985

Location: Cornicewall - 15 tensile tests made at 0.8m spacing across the slope.

Snow density=180kg/m^3, Slope angle: 16-21°

Tensile strengths (slab depth in brackets): 2620(.22m), 2203(.22m), 5077(.23m), 2989(.22m), 2337(.22m), 3366(.19m), 4161(.18m), 2318(.22m), 1935(.22m), 2379(.22m), 2053(.22m), 2089(.23m), 2345(.21m), 4234(.23m), 3428(.25m).

Mean tensile strength:2776±30%, Mean slab depth:.22±.016m,

Basal tensile strength averaging

1x Averaged tensile=2776 SD.=834 SD.red.factor=1.000

2x Averaged tensile=2812 SD.=698 SD.red.factor=0.837

3x Averaged tensile=2826 SD.=552 SD.red.factor=0.662

4x Averaged tensile=2793 SD.=470 SD.red.factor=0.563

5x Averaged tensile=2775 SD.=428 SD.red.factor=0.513

6x Averaged tensile=2784 SD.=378 SD.red.factor=0.454

7x Averaged tensile=2792 SD.=308 SD.red.factor=0.369

8x Averaged tensile=2791 SD.=236 SD.red.factor=0.283

Scale of fluctuation between tensile measurements=0.448m

Slab depth averaging

1x Averaged depth=0.22 SD.=.02 SD.red.factor=1.000

2x Averaged depth=0.22 SD.=.01 SD.red.factor=0.799

3x Averaged depth=0.22 SD.=.01 SD.red.factor=0.653

4x Averaged depth=0.22 SD.=.01 SD.red.factor=0.563

5x Averaged depth=0.22 SD.=.01 SD.red.factor=0.488

6x Averaged depth=0.21 SD.=.01 SD.red.factor=0.401

7x Averaged depth=0.21 SD.=.01 SD.red.factor=0.341
8x Averaged depth=0.21 SD.=.00 SD.red.factor=0.282
Scale of fluctuation between slab depth measurements=0.445m